



City Research Online

City, University of London Institutional Repository

Citation: Kosilo, M. (2017). The contribution of the luminance and opponent chromatic post-receptoral mechanisms to visual working memory. (Unpublished Doctoral thesis, City, University of London)

This is the accepted version of the paper.

This version of the publication may differ from the final published version.

Permanent repository link: <https://openaccess.city.ac.uk/id/eprint/19357/>

Link to published version:

Copyright: City Research Online aims to make research outputs of City, University of London available to a wider audience. Copyright and Moral Rights remain with the author(s) and/or copyright holders. URLs from City Research Online may be freely distributed and linked to.

Reuse: Copies of full items can be used for personal research or study, educational, or not-for-profit purposes without prior permission or charge. Provided that the authors, title and full bibliographic details are credited, a hyperlink and/or URL is given for the original metadata page and the content is not changed in any way.

City Research Online:

<http://openaccess.city.ac.uk/>

publications@city.ac.uk

The contribution of the luminance and
opponent chromatic post-receptoral
mechanisms to visual working memory

Maciej Kosiński



School of Arts and Social Sciences

Department of Psychology

City, University of London

This thesis is submitted for the degree of PhD in Psychology

October 2017

Table of Contents

Table of Contents	3
List of Figures	9
List of Tables	13
Acknowledgments	15
Abstract	19
Chapter 1: General Introduction.....	21
1. Working memory and the prefrontal cortex (PFC).....	26
1.1. Summary: working memory and the prefrontal cortex (PFC).....	31
2. The role of top-down signals in working memory.....	32
2.1. Summary: The role of top-down signals in working memory	34
3. Beyond the prefrontal cortex.....	36
3.1. Sensory areas and perceptual processing contributing to working memory.	36
3.2. Interactions between perception and visual working memory: impact on theoretical approaches and significance.....	41
3.3. Summary: common mechanisms of perception and visual working memory	45
4. Chromatic and achromatic shape processing: from the retina to the cortex	46
4.1. The retina – anatomy and functional organisation	47
4.2. Lateral Geniculate Nucleus (LGN) – anatomy and functional organisation	55
4.3. Cortex – anatomy and functional organisation.....	58
4.4. Separation of visual channels.....	60
5. Chromatic and achromatic visual channels in perception	63
5.1. The role of luminance in facilitating perception via top-down signalling	67
5.2. Summary: differential contribution of luminance and chromatic signals to perception	70
5.3. The potential role of luminance signals in working memory: top-down benefits, noise reduction.....	70
6. Conclusion and the main hypothesis.....	72
Chapter 2: General methods and colourimetry.....	75
7. Colour spaces	76
7.1. The CIE 1931 colour space	76
7.2. Physiologically meaningful colour spaces	79
7.2.1. LMS-cone excitation space	79
7.2.2. Cone-opponent colour space: the Derrington-Krauskopf-Lennie (DKL) space.....	80
7.2.3. Use of DKL colour space to stimulate cone-opponent and luminance mechanisms.....	82
7.2.4. Summary.....	85
7.3. Observer’s isoluminance – heterochromatic flicker photometry (HCFP).	85
7.4. Display calibration & gamma correction procedures.....	86

7.4.1.	Calibration	86
7.4.2.	Verification procedures	89
7.5.	Re-calibration	91
7.6.	Stimuli & on-line DKL conversions	92
8.	Psychophysics – overview of methods used to estimate threshold.....	93
8.1.1.	Detection and discrimination thresholds	93
8.1.2.	Adjustment methods	95
8.1.3.	Method of constant stimuli	96
8.1.4.	Adaptive procedures	96
	Chapter 3: The contribution of luminance signals to visual working memory performance – a study using EEG	101
9.	Investigating visual working memory using EEG	104
9.1.	Use of ERP components to study visual working memory.....	106
9.1.1.	Visual component P1	106
9.1.2.	N1	110
9.1.3.	P1 and N1 as gain control mechanism.....	113
9.1.4.	P3 component	113
9.1.5.	Slow wave	116
9.2.	Predicted ERP modulations.....	117
9.3.	Studies on perception/working memory interaction using the ERP technique.....	118
10.	General summary and hypothesis	121
11.	Methods	122
11.1.	Participants	122
11.2.	Procedure.....	122
11.2.1.	Working memory measurements: digit span and letter-number test.	124
11.2.2.	Observer’s isoluminance: Heterochromatic Flicker Photometry test	125
11.2.3.	Same/different shape discrimination threshold.....	125
11.3.	Main WM experiment	127
11.3.1.	Delayed match-to-sample task.....	127
11.4.	EEG data acquisition.....	130
11.5.	Pre-processing and analysis	130
11.6.	Note on ERP amplitude and latency extraction	134
12.	Behavioural results	136
12.1.	Vision tests	136
12.2.	Working memory tests.....	137
12.3.	Threshold measurements	137
12.4.	Accuracy	139
12.4.1.	Match.....	140
12.4.2.	Mismatch.....	141

12.5.	Reaction times.....	143
12.6.	Comparison with mixed signals stimuli	144
13.	Event-related potential (ERP) results.....	146
13.1.	Encoding stage	146
13.1.1.	P1 Amplitude (Oz, O1, O2; 80-160 ms).....	146
13.2.	Low contrast.....	147
13.3.	High contrast.....	148
13.3.1.	Latency.....	150
13.4.	N1 Amplitude (Oz, O1, O2; 130-300 ms).....	150
13.5.	Latency	151
13.6.	P1 and N1 interactions with behavioural performance	152
13.7.	P3a Amplitude (C1, C2, Cz; 200-400 ms).....	154
13.8.	Low contrast.....	155
13.9.	High contrast.....	155
13.10.	Latency	156
13.10.1.	P3b Amplitude (P3, P4, Pz; 200-500ms)	157
13.10.2.	Latency.....	159
14.	ERPs – maintenance stage	161
14.1.	Stimuli offset peak (700-900 ms)	161
14.2.	Slow wave (1000-1600 ms) – occipital (electrodes O1, O2, and Oz).....	161
14.3.	Slow wave (1000-1600ms) – frontal (electrodes F3, F4, and Fz).	163
15.	ERPs – retrieval stage.....	164
15.1.	P1 Amplitude (Oz, O1, O2; 80 ms-160 ms).....	164
15.1.1.	Latency.....	169
15.2.	N1 Amplitude (Oz O1 O2; 130 ms – 300 ms).....	169
15.2.1.	Low contrast	171
15.2.2.	High contrast	171
15.2.3.	Latency.....	172
15.3.	P3a Amplitude (C1, C2, Cz; 200 – 400 ms)	172
15.3.1.	Latency.....	173
15.4.	P3b Amplitude (P3, P4, Pz; 200 – 500 ms)	173
15.4.1.	Latency.....	175
15.4.2.	Low contrast	175
15.4.3.	High contrast	175
16.	Discussion	176
16.1.	Overall behaviour findings	176
16.2.	Match/mismatch effects.....	177
16.2.1.	Contrast effects	178

16.2.2.	Lack of correlation between digit span and letter-number tests and delayed match-to-sample task	178
16.3.	ERP effects.....	179
16.3.1.	Perceptual effects.....	179
16.3.2.	ERP modulations related to working memory load.....	182
16.4.	What mechanism underlies luminance advantage?	185
16.5.	Further directions and general shortcomings.....	186
16.6.	Summary	187
	Chapter 4: Psychophysical experiments on visual working memory.....	191
17.	Psychophysical measurements and sensory perception.	193
17.1.	Insights into visual perception	193
17.2.	Studying memory and cognition with psychophysics	194
17.3.	Summary: studying memory and cognition with psychophysics	197
18.	Current experiment: visual working memory thresholds.....	199
18.1.	Summary – visual working memory threshold experiment.....	202
19.	Experiment 1: working memory thresholds	203
19.1.	Methods.....	203
19.1.1.	Participants.....	203
19.1.2.	DKL colour space & stimuli	203
19.1.3.	Threshold normalisation.....	206
19.1.4.	Procedure	206
19.1.5.	Analysis.....	210
20.	Results.....	211
21.	Control experiments	213
22.	Experiment 2 – shape detection thresholds.....	214
22.1.	Methods.....	214
22.2.	Results.....	215
23.	Experiment 3: Same/different shape discrimination thresholds.....	217
23.1.	Methods.....	217
23.2.	Results.....	217
24.	Discussion	219
	Chapter 5: A pilot study of luminance processing and visual working memory in schizophrenia.....	227
25.	Cognitive deficits in schizophrenia.....	230
25.1.	Perceptual and sensory deficits in schizophrenia	231
25.2.	Interaction between visual perception and working memory in schizophrenia.....	234
25.3.	Luminance processing in schizophrenia: relevance to working memory performance.....	236
25.4.	Investigating luminance – processing in schizophrenia in the context of magnocellular theory and its criticism.....	240
25.5.	Top-down accounts of perceptual deficits in schizophrenia and the potential role of luminance signals.....	242

25.6.	Summary and aims.....	243
26.	Methods.....	246
26.1.	Participants	246
26.2.	Procedure.....	248
26.3.	Averaged thresholds and Weber contrasts.....	249
26.4.	Task design	250
26.5.	EEG data acquisition, pre-processing and analysis	251
26.6.	Vision tests and behavioural data analysis	254
27.	Behavioural results	255
27.1.	Vision tests	255
27.2.	Accuracy	257
27.2.1.	Between-subject effects.....	257
27.2.2.	Within-subject effects	257
27.3.	Reaction times.....	260
27.3.1.	Between-subject effects.....	260
27.3.2.	Within-subject effects	261
28.	Event-related potential (ERP) results.....	262
28.1.	Encoding stage	263
28.1.1.	P1 Amplitude (Oz, O1, O2; 80-160 ms).....	263
28.1.2.	Low contrast	263
28.1.3.	High contrast	264
28.1.4.	Latency.....	265
28.2.	N1 Amplitude (Oz, O1, O2; 130-300 ms).....	265
28.2.1.	Low contrast	267
28.2.2.	High contrast	268
28.2.3.	Latency.....	268
28.3.	P3a Amplitude (C1, C2, Cz; 200-400 ms).....	269
28.3.1.	Latency.....	269
28.4.	P3b Amplitude (P3, P4, Pz; 200-500 ms).....	270
28.4.1.	Control group.....	271
28.4.2.	Patient group	272
28.4.3.	Latency.....	272
29.	Maintenance stage	273
29.1.	Slow wave (1000-1600 ms) – occipital (O1, O2, Oz).	273
30.	Retrieval stage	275
30.1.	P1 Amplitude (Oz O1 O2; 80-160 ms)	275
30.2.	Latency	275
30.3.	N1 Amplitude (Oz O1 O2; 130 ms – 300 ms).....	276
30.3.1.	Latency.....	276

30.4.	P3aAmplitude (C1, C2, Cz; 200-400 ms).....	277
30.4.1.	Latency.....	278
30.4.2.	Control group.....	278
30.4.3.	Patient group	278
30.5.	P3b Amplitude (P3, P4, Pz; 200-500 ms).....	279
30.5.1.	Latency.....	280
31.	Discussion	282
	Chapter 6: General discussion	292
32.	The underlying mechanism(s) behind the luminance advantage in visual working memory	296
32.1.	Is luminance advantage mediated by a top-down or bottom-up mechanism?.....	296
32.2.	Contribution of luminance signals to memory-probe comparison	301
32.3.	Comparison between WM representation and currently-perceived stimuli – insights from WM literature.	301
32.4.	Insights from perceptual comparison studies.....	303
33.	Summary and implications for future research	309
	Conclusion.....	311
	References	313

List of Figures

FIGURE 1 EXAMPLE OF MEMORY FIELDS IN ACTION.	27
FIGURE 2 FOCUS OF ACTIVATION DURING A WM TASK LOCATED IN THE PFC.	29
FIGURE 3 STRUCTURE OF THE MAMMALIAN RETINA BY SANTIAGO RAMON Y CAJAL (1900).....	47
FIGURE 4 SCAN OF THE RETINA BELONGING TO THE AUTHOR OF THIS THESIS, SHOWCASING THE LAYERED STRUCTURE. IMAGE: DR IRENE CTORI.	48
FIGURE 5 A) NORMALISED RESPONSITIVITY SPECTRA OF HUMAN CONE CELLS: SHORT, MEDIUM AND LONG CONES. B) APPROXIMATION OF COLOUR SPECTRUM VISIBLE TO THE HUMAN EYE. C) ISAAC NEWTON’S (1642 – 1726/27) DESCRIPTION OF THE COLOUR SPECTRUM, BASED ON OBSERVATION OF WHITE LIGHT SHINED THROUGH A PRISM AND DECOMPOSED AS AN EFFECT.....	49
FIGURE 6 CONNECTIVITY IN THE PRIMATE RETINA..	54
FIGURE 7 LAYERING OF THE LATERAL GENICULATE NUCLEUS (LGN).....	56
FIGURE 8 VISUAL PATHWAYS FROM THE RETINA THROUGH THE LGN TO THE V1.....	59
FIGURE 9 THE CIE 1931 RGB COLOUR MATCHING FUNCTIONS.....	77
FIGURE 10 CIE CHROMATICITY DIAGRAM.....	78
FIGURE 11 THE DKL COLOUR SPACE.	82
FIGURE 12 A GENERAL OUTLINE OF CALIBRATION AND VERIFICATION PROCEDURE STEPS.....	88
FIGURE 13 AN EXAMPLE OF THE SPECTRAL POWER DISTRIBUTION (SPD) OF THE DISPLAY USED IN THE EXPERIMENTS.	89
FIGURE 14 TRIAL OUTLINE OF THE MATCH-TO-SAMPLE TASK USED TO MEASURE DISCRIMINATION THRESHOLD.	126
FIGURE 15 DELAYED MATCH-TO-SAMPLE TASK.	128
FIGURE 16 RESULTS FROM ACUITYPLUS TESTS AND THE CAD TEST.	136
FIGURE 17 RESULTS OF THE WM TESTS..	137
FIGURE 18 MEAN PROPORTION OF CORRECT RESPONSES FOR S-CONE, L – M AND LUMINANCE STIMULI AT THREE LEVELS OF WM LOAD	139
FIGURE 19 MEAN PROPORTION OF CORRECT RESPONSES FOR S-CONE, L – M AND LUMINANCE STIMULI AT 3 LEVELS OF WM LOAD.....	140
FIGURE 20 A) PROPORTION OF CORRECT RESPONSES FOR S-CONE, L – M AND LUMINANCE STIMULI AT 3 WM LOADS SHOWN SEPARATELY FOR THE MATCH AND MISMATCH PROBES.....	142
FIGURE 21 MEAN OF MEDIAN REACTION TIMES FOR S-CONE, L – M AND LUMINANCE STIMULI AT THREE LEVELS OF WM LOAD	143
FIGURE 22 LINE PLOT SHOWING ACCURACY IN RESPONSE TO S-CONE, L – M, MIXED SIGNALS AND LUMINANCE-DEFINED SHAPES AT THREE WM LOAD LEVELS, IN RESPONSE TO MATCH OR MISMATCH PROBE.....	145
FIGURE 23 LOCAL PEAK AMPLITUDES OF COMPONENT P1 FOR S-CONE L – M AND LUMINANCE STIMULI, AT THREE LEVELS OF LOAD FOR LOW AND HIGH CONTRAST.	146
FIGURE 24 GRAND AVERAGE WAVEFORM AT ELECTRODE O1 DURING ENCODING LOW CONTRAST LUMINANCE-DEFINED SHAPES, AT THREE LEVELS OF WM LOAD.	147
FIGURE 25 GRAND AVERAGE WAVEFORM AT ELECTRODE O1 DURING ENCODING HIGH CONTRAST LUMINANCE-DEFINED SHAPES, AT THREE LEVELS OF WM LOAD.....	148
FIGURE 26 AVERAGED WAVEFORMS AT ELECTRODE O1 DURING WM ENCODING OF LUMINANCE, L – M AND S-CONE DKL DIRECTIONS, PRESENTED AT LOW CONTRAST AND HIGH CONTRAST.	149

FIGURE 27 LOCAL PEAK AMPLITUDES OF COMPONENT N1 FOR EACH DKL DIRECTION, AT THREE LEVELS OF LOAD FOR LOW AND HIGH CONTRAST, AVERAGED OVER ELECTRODES O1, O2 AND OZ..	151
FIGURE 28 GRAND AVERAGE WAVEFORM AT ELECTRODE C1 DURING ENCODING HIGH CONTRAST LUMINANCE-DEFINED, L – M AND S-CONE SHAPES AT LOAD 3.....	156
FIGURE 29 P3B AMPLITUDE AT ELECTRODES P3, P4 AND Pz, AT LOW AND HIGH CONTRAST FOR LUMINANCE, L – M AND S-CONE.	158
FIGURE 30 P3B WAVEFORMS AT ELECTRODE P3 AT THREE LEVELS OF WM LOAD, FOR S-CONE, L – M AND LUMINANCE. .	159
FIGURE 31 GRAND AVERAGE WAVEFORM AT ELECTRODE O1 DURING MAINTENANCE AT THREE LEVELS OF WM LOAD.	162
FIGURE 32 GRAND AVERAGE WAVEFORM AT ELECTRODE F3 DURING MAINTENANCE AT THREE LEVELS OF WM LOAD.	163
FIGURE 33 GRAND AVERAGE WAVEFORM AT ELECTRODE O1 DURING RETRIEVAL OF LOW CONTRAST LUMINANCE-DEFINED SHAPES, AT THREE LEVELS OF WM LOAD.	165
FIGURE 34 GRAND AVERAGE WAVEFORM AT ELECTRODE O1 DURING RETRIEVAL OF HIGH CONTRAST LUMINANCE-DEFINED SHAPES, AT THREE LEVELS OF WM LOAD.	166
FIGURE 35 CORRELATION BETWEEN THE P1 COMPONENT AT ELECTRODE O1 (FOR LOAD 3) AND OVERALL TASK ACCURACY.	168
FIGURE 36 GRAND AVERAGE WAVEFORM AT ELECTRODE O1 DURING RETRIEVAL OF HIGH CONTRAST LUMINANCE-DEFINED SHAPES, AT THREE LEVELS OF WM LOAD.	170
FIGURE 37 GRAND AVERAGE WAVEFORM AT ELECTRODE Cz DURING RETRIEVAL AT THREE LEVELS OF WM LOAD. DKL CONDITIONS AND CONTRAST LEVELS WERE COLLAPSED TO HIGHLIGHT THE MAIN EFFECT OF WM LOAD.	173
FIGURE 38 GRAND AVERAGE WAVEFORM AT ELECTRODE Pz DURING RETRIEVAL AT THREE LEVELS OF WM LOAD. DKL CONDITIONS AND CONTRAST LEVELS WERE COLLAPSED TO HIGHLIGHT THE MAIN EFFECT OF WM LOAD..	174
FIGURE 39 TWO INTERVAL FORCED-CHOICE PROCEDURE (2IFC) USED TO MEASURE STIMULUS DETECTION THRESHOLDS....	208
FIGURE 40 MULTIPLES OF DETECTION THRESHOLDS PLOTTED FOR 4 DKL CONDITIONS, AT 3 LEVELS OF WM LOAD.....	211
FIGURE 41 WM THRESHOLDS AT LOAD 3, FOR EACH DKL CONDITION. RED LINES ARE MEAN WM THRESHOLDS ACROSS OBSERVERS,.....	212
FIGURE 42 RESULTS OF MODEL FITS FOR THE 2IFC DETECTION THRESHOLD TASK.....	216
FIGURE 43 COMPARISON OF SLOPES OF THE PSYCHOMETRIC FUNCTION FOR DIFFERENT POST-RECEPTORAL MECHANISMS FITTED TO DATA DERIVED FROM SHAPE DISCRIMINATION TASK	218
FIGURE 44 RESULTS FROM A DELAYED MATCH-TO-SAMPLE TASK WITH FIXED STIMULUS CONTRAST FROM THE PREVIOUS EXPERIMENT	220
FIGURE 45 TOP: TITLE PAGE OF BLEULER’S 1911 ARTICLE ON DEMENTIA PRAECOX, WHERE HE REFERRED TO THE DISORDER AS “GROUP OF SCHIZOPHRENIAS”. AND A TITLE PAGE OF THE 1912’S TRANSLATION OF KRAEPELIN’S “LEHRBUCH DER PSYCHIATRIE”, ORIGINALLY PUBLISHED IN 1899.....	228
FIGURE 46 RESULTS OF THE VISION TESTS FOR PATIENTS AND CONTROLS SHOWN IN BOX PLOTS..	256
FIGURE 47 OVERALL MEAN ACCURACY FOR CONTROL AND PATIENT GROUP AND CONTROL/PATIENT GROUP MEAN ACCURACY SHOWN AT WM LOAD 1 AND LOAD 3, SEPARATELY FOR DKL DIRECTIONS	257
FIGURE 48 ACCURACY AT LOAD 1 AND LOAD 3 FOR MATCHING AND MISMATCHING MEMORY PROBE, SHOWN FOR EACH DKL DIRECTION AND CONTROL/PATIENT GROUP SEPARATELY..	259
FIGURE 49 OVERALL MATCH & MISMATCH ACCURACY (PATIENTS + CONTROLS) FOR THE DIFFERENT DKL DIRECTIONS AT LOW AND HIGH WM LOAD.	260
FIGURE 50 OVERALL REACTION TIMES FOR CONTROL AND PATIENT GROUP AND CONTROL/PATIENT GROUP REACTION TIMES ARE SHOWN AT WM LOAD 1 AND LOAD 3, SEPARATELY FOR DKL DIRECTIONS.	260
FIGURE 51 REACTION TIMES FOR S-CONE, L – M AND LUMINANCE CONDITIONS.	261
FIGURE 52 OVERALL MATCH & MISMATCH REACTION TIMES (PATIENTS + CONTROLS) AND RTs FOR DIFFERENT DKL DIRECTIONS AT LOW AND HIGH WM LOAD FOR MATCH AND MISMATCH.	261

FIGURE 53 COMPARISON BETWEEN THE NUMBER OF TRIALS FOR PATIENTS AND CONTROLS.	262
FIGURE 54 ERP WAVEFORMS DURING THE ENCODING OF LOW CONTRAST LUMINANCE SHAPES FOR CONTROL GROUP AND SCHIZOPHRENIA GROUP.....	263
FIGURE 55 ERP WAVEFORMS DURING THE ENCODING OF HIGH CONTRAST LUMINANCE SHAPES ARE SHOWN FOR CONTROL GROUP AND SCHIZOPHRENIA GROUP.....	264
FIGURE 56 ERP WAVEFORMS DURING ENCODING OF S-CONE, L – M AND LUMINANCE SHAPES.....	266
FIGURE 57 N1 AMPLITUDE IN RESPONSE TO DIFFERENT DKL DIRECTIONS AT LOW CONTRAST LEVEL FOR CONTROL AND SCHIZOPHRENIA GROUP.....	267
FIGURE 58 N1 COMPONENT LATENCIES FOR CONTROL AND SCHIZOPHRENIA GROUP, FOR THE THREE DKL DIRECTIONS.....	268
FIGURE 59 N1 COMPONENT LATENCIES FOR CONTROL AND SCHIZOPHRENIA GROUP DURING ENCODING LUMINANCE-DEFINED SHAPES.	269
FIGURE 60 P3B AMPLITUDE IN RESPONSE TO S-CONE, L – M AND LUMINANCE SHAPES.	270
FIGURE 61 ERP WAVEFORMS DURING ENCODING OF S-CONE, L – M AND LUMINANCE SHAPES.....	270
FIGURE 62 P3B AMPLITUDES AT ELECTRODE O1, O2 AND Oz, AT TWO LEVELS OF LOAD, FOR EACH DKL DIRECTION.....	272
FIGURE 63 LATE, SLOW WAVE FOR CONTROLS AND PATIENTS PRESENTED AT LOW CONTRAST, AT ELECTRODE Oz.....	273
FIGURE 64 SLOW WAVE FOR THE PATIENT GROUP, PRESENTED AT LOW AND HIGH CONTRAST, FOR SEPARATE DKL DIRECTIONS AND LOAD LEVELS.	274
FIGURE 65 ERP WAVEFORMS COLLAPSED ACROSS LOAD CONTRASTING PATIENT AND CONTROL LUMINANCE DATA AT RETRIEVAL AT LOW AND HIGH LEVELS OF CONTRAST.....	275
FIGURE 66 WAVEFORMS COLLAPSED ACROSS WM LOAD, ELECTRODE LOCATION & CONTRAST TO SHOW DIFFERENCES BETWEEN DKL DIRECTIONS, FOR CONTROLS AND PATIENTS SEPARATELY.	276
FIGURE 67 ERP WAVEFORMS COLLAPSED ACROSS CONTRAS LEVELS, WM LOAD AND ELECTRODE LOCATIONS (C1, C2 & Cz), PRESENTED AT EACH DKL DIRECTION SEPARATELY	277
FIGURE 68 WAVEFORMS COLLAPSED ACROSS DKL DIRECTIONS, LOAD AND CONTRAST LEVELS AT ELECTRODE Pz FOR CONTROLS AND PATIENTS	279
FIGURE 69 P3B AMPLITUDE DURING RETRIEVAL FOR 3 DKL DIRECTIONS, AT LOAD 1 AND LOAD 3.	280
FIGURE 70 WAVEFORMS COLLAPSED ACROSS GROUPS AND ELECTRODES AND PRESENTED AT LOW AND HIGH CONTRAST SEPARATELY, FOR EACH DKL DIRECTION	281

List of Tables

TABLE 1 THE THREE CARDINAL AXES IN DKL COLOUR SPACE.....	81
TABLE 2 PSYCHOPHYSICAL MECHANISMS OF INTEREST AND THEIR CORRESPONDING DKL COORDINATES.	84
TABLE 3 SUMMARY OF TESTS COMPLETED BY ALL PARTICIPANTS.	123
TABLE 4 EXPERIMENTAL CONDITIONS.....	130
TABLE 5 P1 AMPLITUDE AT ENCODING STAGE FOR LUMINANCE CONDITION AND N1 AMPLITUDE AT ENCODING FOR TWO ISOLUMINANT CONDITIONS CORRELATED WITH OVERALL TASK ACCURACY.....	153
TABLE 6 P1 AMPLITUDE AT ENCODING STAGE FOR LUMINANCE CONDITION AND N1 AMPLITUDE AT ENCODING FOR TWO ISOLUMINANT CONDITIONS CORRELATED WITH TASK ACCURACY AT HIGH CONTRAST.....	154
TABLE 7 PEARSON CORRELATION COEFFICIENTS AND P VALUES FOR P1 AMPLITUDE AT RETRIEVAL STAGE WITH OVERALL ACCURACY.....	167
TABLE 8 PEARSON CORRELATION COEFFICIENTS AND P VALUES FOR A CORRELATION BETWEEN P1 AMPLITUDE AT RETRIEVAL STAGE FOR MISMATCHING PROBES AND ACCURACY FOR MISMATCHING PROBE AT THREE WM LOADS.....	167
TABLE 9 PEARSON CORRELATION COEFFICIENTS AND P VALUES FOR P1 AMPLITUDE AT RETRIEVAL STAGE FOR MATCHING PROBES WITH ACCURACY FOR MATCHING PROBE AT THREE WM LOADS.....	168
TABLE 10 PSYCHOPHYSICAL MECHANISMS OF INTEREST AND THEIR CORRESPONDING DKL COORDINATES.	205
TABLE 11 SUMMARY OF EXPERIMENTAL CONDITIONS.....	207
TABLE 12 WEBER CONTRASTS FOR ACHROMATIC AND CHROMATIC MECHANISMS FOR EACH CONDITION, DERIVED FROM L, M AND S CONTRASTS.	223
TABLE 13 CODING OF EDUCATIONAL LEVEL AND A SUMMARY OF AGE/QUALIFICATIONS FOR CONTROL AND SCHIZOPHRENIA GROUP.	247
TABLE 14 INDIVIDUAL DISCRIMINATION THRESHOLDS FOR ALL DKL DIRECTIONS OBTAINED IN THE PREVIOUS EXPERIMENT..	250
TABLE 15 WEBER CONTRAST VALUES FOR ALL POST-RECEPTORAL MECHANISMS TESTED IN THE EXPERIMENT, BASED ON AVERAGED THRESHOLDS.....	250
TABLE 16 CONDITIONS IN THE CURRENT STUDY.....	251
TABLE 17 ANALYZED ERP COMPONENTS, ELECTRODE SITES AND TIME INTERVALS USED TO DEFINE AND EXTRACT COMPONENTS.	253

Acknowledgments

It is impossible to face all the challenges that the PhD brings on one's own. Although I have been told that earning a doctorate is a long journey, there were times where I felt like all I was doing was falling – slowly, but inevitably – rather than walking towards the goal. I am indebted to many people who (knowingly or not) have helped me to get where I am now.

I would like to thank Dr Corinna Haenschel, my supervisor, for the opportunity, support, and patience; Dr Jasna Martinovic, for her expertise, and for getting me on this path in the first place; Dr Elliott Freeman, my 2nd supervisor, and Dr Ben J. Jennings, for all their help; my old University of Aberdeen friends and faculty, for making science fun before I started my PhD; thanks to all the doctorate students and postdocs from our department (and beyond), for keeping it that way, and for creating the community I felt so good to be part of (and for all the Jägerbombs); to the City, University of London faculty and staff, for having me here and helping me out along the way; thanks to Emily and Pete, for all the spare parts and help in the lab; to everyone who I shared the EEG lab with (especially Laila and Matthew – I learned a lot from you); to Jenny, Neelam, Shinal and Saim, for their help in running the patient study; to the Polish science blogging community, for broadening my interests; to the “twitter people”, for company, laughs, and advice; to the Antisocial Grumpy Club, for the friendship and gossip; to Paula, for the email you sent me on the 3/11/2015; to my Princess Bubblegum, for all the spaceship adventures; to Megan, for being a true Walrus to me; to Klaus Schmiegel, for general support; to my coinhabitant friends: Ania and Jadzia (and Kota, too) for all the warmth and non-blended soups; to Michał Wawrzyński, my high school Polish teacher, for cultivating my critical thinking; to Żółwik, Ilona, Kasia, Szymon, Gelu, Asuka, Francuz, Gizmo, Ziół, and other friends from old times, who are (or were) always there; to my brother, Marcin, the best brother I could ever ask for; to my dad, Tadeusz, for believing in me and supporting me (*dziękuję, tatuś*); and to Aga, for the companionship, patience, love, and the cuddles (when I needed them the most) – *dziękuję*.

Finally, I want to give my thanks – and dedicate this thesis – to my mom, Krystyna. I know you would be proud, and it hurts me I cannot share this moment with you.

Będę zawsze za Tobę tęsknił.

Mamie

Abstract

Visual Working Memory (visual WM) is an ability to encode and temporarily maintain visual information. There is some evidence that early perceptual processes make an important contribution to successful WM performance. However, perceptual contributions to WM are not yet fully understood.

In vision, signals originating from three classes of photoreceptors in the retina (L, M and S-cones) are combined into three distinct mechanisms, which form the fundamentals of visual perception. These mechanisms are the two opponent chromatic mechanisms (L – M and S – (L + M)) and an achromatic, luminance mechanism (L + M). Vision science has been long concerned with properties of these mechanisms and how they contribute to the perception of the world.

Despite this, there was little interest to date in how these mechanisms contribute to creating memory representations, i.e. after the visual stimulus has disappeared from the visual field. In a series of experiments presented in this thesis, a differential contribution of three post-receptoral mechanisms to visual WM was investigated. It was hypothesised that luminance signals will prove to be more efficient in their contribution to WM encoding, maintenance and retrieval than opponent chromatic signals. This was investigated using a variety of methodologies, from psychophysical measurements and behavioural responses to recordings of neural activity using electroencephalography (EEG).

Results of the experiments have shown that indeed, remembering abstract shapes designed to excite the luminance mechanism contributed to better WM performance comparing to remembering shapes designed to excite the opponent chromatic mechanisms. EEG recordings have shown that this luminance benefit starts already during WM encoding, although later WM stages are likely to benefit as well. The findings demonstrate that luminance signals provide an advantage over opponent chromatic mechanisms in working memory processing.

Chapter 1

General Introduction

The term *working memory* (WM) became established in the scientific literature in the early 1960s (Miller, Galanter, & Pribram, 1960; Pribram, Ahumada, Hartog, & Roos, 1964). It refers to a short-term storage system that temporarily maintains information for immediate use. The important aspect of the WM definition is its emphasis on goal-directed behaviour. Short-term storage of any information that may be no longer present in the environment is the basis for carrying out complex tasks, such as learning, comprehension, reasoning or operating in a visual world (Baddeley & Hitch, 1974; Logie, 2011; Phillips, 1974).

A decade later, two independent lines of research delivered ideas that still influence our current understanding of WM (Postle, 2006). Electrophysiological recordings in primates looked at neural activity in the dorsolateral prefrontal cortex (dorsolateral PFC) while subjects were engaged in memory task (Fuster, 1973; Fuster & Alexander, 1971; Niki, 1974). This required primates to remember presented stimulus and retain it over time. It was demonstrated that neurons in the PFC continued to fire after the stimulus was no longer present in the visual field. This was taken as an evidence for sustained memory-related activity. These early findings helped to direct the focus of electrophysiological WM research on the prefrontal areas in the brain.

Almost in parallel to the animal research, there was another development in a different field that would later prove to be extremely influential across disciplines. Baddeley and Hitch (1974) offered a comprehensive WM model based on research from the field of human cognitive psychology. The model described

WM as a multi-component system. According to it, WM consists of two separate and largely independent storage systems. The phonological loop is responsible for storing auditory and/or phonological information, while the visuospatial sketchpad deals with visual information. Both storage systems were governed by a central executive system. Its primary role is to control and manage information stored in both buffers.

Another influential WM model was later developed by Cowan (1995, 2001, 2005, 2008). He postulated that WM is a system that forms part of long-term memory and is not, therefore, a separate construct – a view similar to the one proposed by Anders and Kintsch (1995). According to Cowan’s model, what is regarded as WM “representation” is simply information held in long-term memory that has been temporary re-activated. He proposed that this re-activating, cognitive “force” is attention.

Attention can be defined as the ability to select and focus on a piece of information in the environment¹. This definition was extended to highlight that one can focus attention towards internally (mentally) represented stimuli (Itti, Rees & Tsotsos, 2005). Thus, Cowan proposed that the focus of attention can reactivate representations stored in long-term memory and thus make them available for manipulation and immediate usage. While Cowan postulated that there is theoretically no limit to how many long-term memory representations one can hold, the focus of attention is a capacity-limited process. In other words, an individual can reactivate only a number of such representations at a time, thus explaining the limited nature of working memory. Cowan estimated the capacity of focus of attention to be around four “chunks of information”.

An important, although not always spelt-out aspect of working memory is that it involves differed processing stages. Definitions of working memory (e.g.

¹ The definition provided here is constrained to this circumstance, while purposefully avoiding being too specific. Defining attention might seem to be straightforward at a first glance, however it is problematic due to the complex nature of this faculty. This problem was recognised from the field’s earliest days (Tsotsos, Itti & Rees, 2005). For example, Groos (1896) recognised that different definitions of attention “diverge in the most disturbing manner” (Groos, 1896; Tsotsos, Itti & Rees, 2005), while others simply stated that attention was “in disarray” (Pillsbury, 1908) or even “chaotic” (Spearman, 1937). This is in stark contrast with the definition provided by the founder of psychology, William James, who famously began his definition by stating that “Everyone knows what attention is” (James, 1890).

Baddeley & Hitch, 1974; Woodman & Vogel, 2005) implicitly assume that prior to retrieval of information, the information that has been remembered (encoded), needs to be maintained over a period of time. In other words, working memory can be conceptualised as a cognitive ability that is comprised of encoding, maintenance and retrieval/recall. The relative importance of each stage has been explicitly addressed using task designs that allow to clearly separate them temporally (Bays, Marshall, & Husain, 2011; Haenschel, Bittner, Haertling, Rotarska-Jagiela, Maurer, Singer, & Linden, 2007; Woodman & Vogel, 2005). For example, Woodman & Vogel (2005) used a modified change-detection paradigm. In this paradigm, participants are required to encode visual stimuli, followed by a maintenance period, and are subsequently presented with a test array.

Participants retrieve remembered stimuli in order to judge whether the probe is the same as or different than the stimuli presented previously. Using a similar paradigm, Bays et al. (2011) showed that working memory capacity may depend on separate limits imposed during encoding and maintenance. More specifically, the encoding limit constraints transfer of information into memory, while the maintenance limit affects the precision with which the stimuli can be retained over time. Furthermore, another study (Haenschel et al., 2007) showed that different WM stages might be selectively affected in conditions with reported working memory deficits, such as schizophrenia. These examples highlight the importance of defining working memory not as a uniform cognitive ability, but rather a construct that can, and should be, divided into separate processing stages. These three stages will be referred to throughout this thesis as the encoding, maintenance, and retrieval (or recall).

One of the important, however implicit implications of this model was defining WM as an independent cognitive system, separate from other faculties, such as perception. This corresponds to a traditional view that perceptual information is *transferred* to memory and is not considered an integrated part of it (Magnussen, 2000; Squire & Kendell, 1999).

While already influential in its own field, it was not until the early 1990's that Baddeley and Hitch' model began to have an impact on neurophysiological

research. Goldman-Rakic (1989, 1990) proposed that delay-period activity in PFC recorded in behaving animals corresponds to storage buffers described in Baddeley and Hitch multi-component model. An interesting and highly influential consequence of this idea was that working memory was a general phenomenon that could be demonstrated across species. Postle (2006) sees Goldman-Rakic's work as an important milestone that brought cognitive psychology and electrophysiological WM research together. Such an integrated approach proved to be productive: for example, Goldman-Rakic proposed that the division between the object ("*what*") and spatial location of the object ("*where*") seen in the visual system could also hold for visual working memory (Wilson, O'Scalaidhe, & Goldman-Rakic, 1993). The neuroscientific, as well as cognitive and psychological research that followed, has since supported this notion (see Postle, 2006 for references).

It is interesting that Goldman-Rakic and colleagues' proposal described above (Wilson et al., 1993) was one of the first indications that the rules governing the visual system (and thus, visual perception) can be also applied to working memory, a supposedly separate construct. Although visual working memory and perception have continued to be regarded and researched largely separately from visual perception, it seems that such conceptual separation can no longer be sustained (Pasternak & Greenlee, 2005). It is now acknowledged that the role of a perceptual system extends from "mere" encoding of stimuli to memory storage as well (Pasternak & Greenlee, 2005). In neuroscientific terms, this implies that the sensory areas that process a given stimuli will be also responsible for its storage when the stimuli are no longer available to the senses, a notion that was eventually supported by Harrison and Tong (2009). Harrison and Tong showed that it is possible to decode the contents of working memory from patterns of neural activity recorded from the visual cortex. In terms of factors influencing WM performance, this changing view marks a shift from maintenance stage as a determinant of successful WM performance to early, encoding stages as well. Indeed, researchers now emphasize that working memory research is a dynamic field and recent advances have questioned some of the basic assumptions about this (supposedly simple) cognitive function (Fallon, Zokaei, & Husain, 2016).

Fast-growing research on interactions between perception and WM is a symptom of this new approach (D'Esposito & Postle, 2015; Gao, Gao, Li, Sun, & Shen, 2011; Harrison & Tong, 2009; Lara & Wallis, 2012; Pasternak & Greenlee, 2005; Postle, 2006; Yin et al., 2012).

When talking about interactions between perception and working memory, the encoding stage should be given a special consideration. It is at this stage that perception and working memory are likely to interact, given that the stimulus is still present in the visual field. The general aim of the research presented in this thesis is thus to establish the importance of the encoding stage to WM performance (Haenschel et al., 2007). Furthermore, another goal is to specify the relationship of this early WM stage with perceptual processing, as well as to determine whether the later stages of WM can also benefit from these interactions and impact task performance.

In the following sections, I will describe the evidence that established dorsolateral PFC as a crucial anatomical structure responsible for WM processing. I will then describe how later studies questioned this notion as more evidence pointed to the importance of sensory cortices and – as a consequence – perceptual processing. I will then discuss implications of these findings, mainly how the close interaction between perception and WM affected the way the latter is approached (D'Esposito & Postle, 2015; Postle, 2006).

1. Working memory and the prefrontal cortex (PFC)

A good deal of evidence pointing to frontal cortices as the processing and storage site for working memory came from animal studies using delayed-discrimination tasks (Goldman-Rakic, 1992, 1995; Levy & Goldman-Rakic, 2000; Rodriguez & Paule, 2009). In such experiments, animals are instructed to remember a location of a presented target that is subsequently occluded. After a short delay, primates look for a bait in a number of possible locations. Importantly, this task design ensures that the representation has to be updated on a trial-to-trial basis. Hence, target's location cannot be predicted from the stimulus itself or from its location on a previous trial but has to depend on the memory representation of the target (Goldman-Rakic, 1995).

One of the earliest studies of this kind using electrophysiological recordings were published in the early 70's (Fuster & Alexander 1971; Kubota & Niki, 1971). These showed that during a delay period (i.e. a time when the memory representation was stored "in mind" in the absence of the stimulus) a subset of neurons in the PFC sustained their activation.

With time, new paradigms and more accurate techniques became available, which led to the further advancement of the field. For instance, Funahashi et al. (1989) used an oculomotor paradigm, where monkeys were required to maintain fixation on the target during stimulus presentation and retention. This design ensured that animals maintained their fixation on the display, and hence ensured that the performance depended on the stimulus encoding (successful or not), and not on poor fixation or distractibility.

This paradigm also allowed for more a precise mapping of the neural responses. Targets were shown in a number of locations in the visual field, located around the fixation point at different degrees. Firstly, a subset of neurons in the PFC with response fields matching stimulus locations was identified. Subsequently, their firing rates were recorded during the memory maintenance, i.e. after the stimulus was no longer present in subject's visual field. Funahashi found that neurons in

the PFC demonstrated a prolonged target-related activity in the absence of the target, but only at locations that were earlier identified as preferred by these neurons (see Figure 1 for an example). Such delay-period activity associated with a target previously presented in a specific location is referred to as the *memory field*.

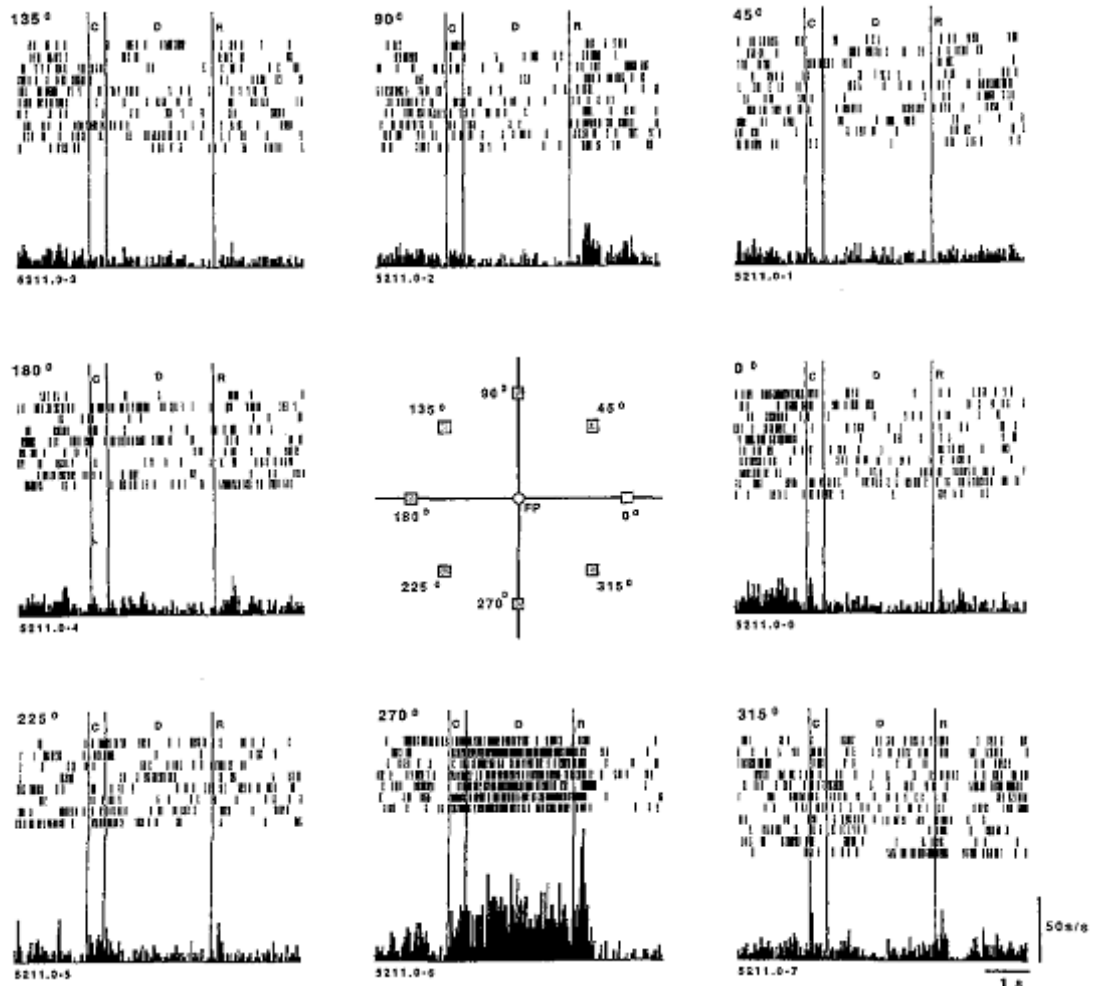


Figure 1 Example of memory fields in action. The target was presented in one of the eight possible locations. In this case, the target appeared at an eccentricity of 270°. On the roster plot in the middle of the bottom row, we can observe an increased spiking of a prefrontal neuron in the absence of the target, during a maintenance stage. Note that the responses of the same neuron do not differ from a baseline if the target was presented at different eccentricities. *Figure from Goldman-Rakic, 1995.*

Subsequent imaging studies suggested that these findings are applicable to human subjects as well. Positron emission tomography (PET) studies (Jonides et al., 1993; Paulesu, Frith, & Frackowiak, 1993; Petrides, Alivisatos, Meyer, & Evans, 1993) demonstrated that frontal areas are engaged during the delay period of

spatial working memory tasks. Although generally, all studies reported activations in the frontal areas, they were not restricted only to these locations. For example, some studies showed activations in Broca's area (i.e. the brain area classically indicated in language processing), in addition to activity in the PFC (Paulesu et al., 1993). This location did not correspond to areas that were previously associated with working memory in primates. It was thought that the differences within human studies and between human and animal studies arise because of a verbal component in these tasks. To address that, McCarthy et al. (1994) attempted to provide a more accurate localisation of working memory processing in humans using a task that would restrict verbal involvement. Their experiments employed magnetic resonance imaging (MRI) rather than PET, which also allowed for a more precise localisation of WM processing. Subjects performed a variation of the delayed – response task: they were presented with an array of stimuli randomly flashed at different locations. Participants had to respond (by raising their finger) if a shape appeared in a location occupied by a stimulus in the previous run. The shape was irrelevant to the task and shapes location would change on every trial, hence minimalizing verbal strategies. The results demonstrated an increase in BOLD signal in the middle frontal gyrus, as can be seen in Figure 2. This activity was maintained during the experimental phase and declined within few seconds after participant's response. It was concluded that these findings are in line with previous human and non-human studies, highlighting the special role of dorsolateral PFC in working memory (McCarthy et al., 1994)

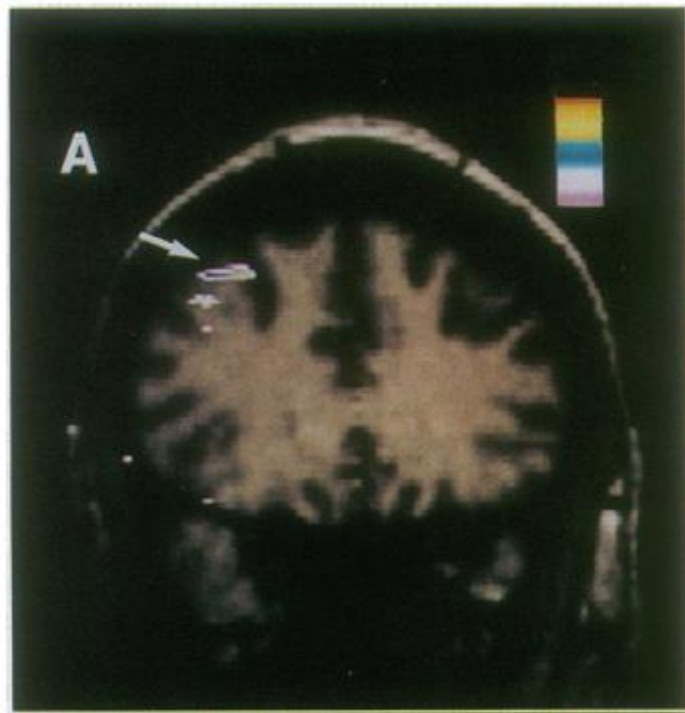


Figure 2 Focus of activation during a WM task located in the PFC. The figure is taken from McCarthy et al. (1994).

Nevertheless, although the prefrontal cortex has been regarded as playing a pivotal role in working memory, it was by far not the only area employed during WM. It was apparent that a distributed network is responsible for WM processing (Goldman-Rakic, 2011; Munk et al., 2002). For example, Linden et al. (2003) identified areas in the frontoparietal network that subserved visual working memory. Specifically, they observed bilateral activations related to storage of a number of items in dorsolateral prefrontal cortex (DLPFC), pre-supplementary motor area (pre-SMA), frontal eye fields (FEF) and intraparietal sulcus. Interestingly, WM-related activations in these particular areas depended on the number of items held in memory: frontal eye fields and intraparietal sulcus were active during storage of a small number of items (two to three), and this activity decreased when a higher number of items were stored. This higher WM load was in turn associated with heightened activity in DLPFC and pre-SMA.

D'Esposito, Postle and Rypma (2000) reviewed fMRI experiments that measured brain activation while participants engaged in delayed discrimination tasks where they had to remember verbal stimuli. Based on the reviewed findings, they

concluded that the activity in the PFC during working memory task is not unitary. During WM, activity in PFC reflects activity associated with different stages of working memory, as well as any non-mnemonic processes that must be employed during these tasks. More specifically, encoding, maintenance and retrieval engage different portions of the PFC to a different extent. For example, while encoding is associated predominantly with the activity in the dorsolateral PFC, maintenance engages ventrolateral as well as dorsolateral PFC. If a manipulation of a stimulus was required in addition to simple maintenance, activation in dorsolateral part could be observed on top of the storage-related activations. When the memorised information has to be accessed to complete a task, dorsolateral PFC is again recruited, although this activation might be reflecting preparation of motor response in addition to processes related to “scanning” memorized information.

Another group of researchers (Pessoa, Gutierrez, Bandettini, & Ungerleider, 2002) took a different approach to show the relevance of activity in different parts of the brain to the task. They compared the activity of correct and incorrect trials during encoding, maintenance and working memory retrieval during a delayed discrimination task. Unlike D’Esposito et al. (2000), a visual rather than verbal stimuli were used. Performance-related activity was mostly demonstrated in the frontal and parietal cortex. The results showed that activity in frontal eye fields and intraparietal sulcus as well as in dorsolateral PFC during memory delay strongly predicted behavioural performance on a trial-by-trial basis. However, performance-related activation during encoding and recall also correlated with performance. Pessoa et al. suggested that variability in behavioural performance occurs due to fluctuations in attention, which can occur at any WM stage, thus explaining the evident correlation between behavioural performance and BOLD activity throughout the task, at encoding, maintenance and retrieval.

Taken together, these studies highlight the importance of frontoparietal network in working memory. It is evident that a big part of the previous research was especially dedicated to these higher-order areas. At the same time, although sensory areas were activated as well, they were not considered crucial to actively

maintain memory representation: activity in these regions was interpreted as related to processing of the stimuli, and not of an active WM storage (Munk et al., 2002; Pessoa et al., 2002). For example, Munk et al. (2002) showed that occipital-temporal areas are recruited predominantly during stimulus encoding. Activity in this areas would return to baseline after the initial stimulus-related activity and could be observed again only during a presentation of a test probe, after the maintenance period. Pessoa et al. (2002) additionally demonstrated that successful behavioural performance in a working memory task could not be predicted from activity in sensory areas during encoding. At the same time, the activation in the frontoparietal network was associated with performance, further supporting the idea that sensory cortices are not involved in the storage of information per se.

1.1. Summary: working memory and the prefrontal cortex (PFC)

To sum up, it was generally agreed that the prefrontal cortex is the main brain structure responsible for short-term memory storage. While the sensory cortices are implicated as well, their role was usually described in the context of processing the stimuli *before* it was “transported” to memory storage. At the same time, research had indicated that the PFC and sensory cortices do not work in separation. Indeed, recent research recognises that working memory involves multiple, coordinated brain areas, with the PFC being only one of them (Christophel, Klink, Spitzer, Roelfsema, & Haynes, 2017). Nevertheless, the role of PFC is implied to be special: sending inputs from the PFC to visual cortex is an important aspect of working memory system (Zanto, Rubens, Thangavel, & Gazzaley, 2011). Such feedback signals occurring between the PFC and the visual cortex – often referred to as top-down signals – will be described in the next section.

2. The role of top-down signals in working memory

The notion of “top-down” processing stems from Gregory’s (1970) theory of perception. According to his theory, visual perception is an active process which is influenced by prior assumptions and knowledge about the world. This is in contrast with Gibson’s (1966) bottom-up account of perception, which states that what we perceive is predominantly stimulus-driven. Both accounts are therefore attempting to establish to what extent our perception relies on information that is present in the environment, versus the information that we already hold. On the neural level, bottom-up processing would refer to processing that goes from the retina “up” the visual hierarchy, through the LGN to sensory cortex, and from there to other brain areas. On the other hand, top-down processing would refer to signals originating in higher-order cortices, such as frontal areas, which propagate back “down” to the sensory cortex. The dorsolateral prefrontal cortex is one candidate for such top-down controller, given its extensive network of reciprocal anatomical connections with other cortical and subcortical regions (Knudsen, 2007; Miller & Cohen, 2001). One of the top-down factors that can influence ongoing perception are predictions, referred to Gregory (1970) as hypotheses. These hypotheses are important to cognition, as they can direct and constrain the incoming information and facilitate its processing (O’Callaghan, Kveraga, Shine, Adams, & Bar, 2017). In terms of perception, it has been shown, for example, that predictions can facilitate recognition of objects (Kveraga, Boshyan, & Bar, 2007; Martinovic, Mordal, & Wuerger, 2011).

Today, the distinction between top-down and bottom-up processing is widely used and is not constrained solely to perception. It can be successfully applied to describe other cognitive functions, such as memory.

One of the top-down factors that have been implicated in a wide range of processes, including memory, is attention. Studies confirmed that attention has a direct effect on memory processing. This was demonstrated by experiments involving repetitive transcranial magnetic stimulation (rTMS) coupled with electroencephalography (EEG) recordings (Zanto et al., 2011). In their study,

Zanto et al. asked human subjects to selectively remember the target feature (motion or colour) while ignoring the distractor (irrelevant feature). Using rTMS over a region in PFC – inferior frontal junction, or IFJ – they hoped to disrupt top-down, attentional modulation of visual processing and working memory encoding. Their results showed that rTMS had an effect on perceptual processing. This was reflected in a decreased amplitude of the EEG signal associated with visual processing (indexed by an event-related component P1) around 100 ms after the stimulus appeared on the screen. Importantly, this decrease in P1 was associated with a decrease in behavioural performance. Zanto et al. suggested that the decrease in both behavioural performance and neural activity was a consequence of disrupted top-down attentional modulation. They hypothesised that top-down signalling (which in their case means selective attention) helps to create a high-fidelity memory representation of the stimulus. Additionally, they speculated that top-down signals from the inferior frontal junction (IFJ) help to update task representations (i.e. maintaining the current task requirement). This agrees with previous studies that also suggested that the activity in the PFC in general, and IFJ in particular, is involved in updating task representations (Brass & Von Cramon, 2004). The finding also agrees with the account that the activity in the PFC interacts with other areas responsible for stimulus or other task-relevant processing (Baddeley 2003, Constantinidis & Wang 2004; Knudsen, 2007). Anatomical connections between the PFC and other brain regions would serve as a neural substrate for such interactions, as mention above (Knudsen, 2007).

This is not a novel view, however. Previous studies on primates have shown that perturbing activity in dorsolateral PFC during a delayed match-to-sample task diminished performance (Fuster, Bauer, & Jervey, 1985). Fuster argued that mutual influences between prefrontal and inferotemporal cortex are taking place through cortico-cortical connections. As a result, both visual discrimination and visual short-term memory depend on the functionality of these interactions.

To date, there are a number of studies suggesting that top-down signals modulate visual processing already at early stages. More specifically, they have been shown

to contribute to greater efficiency of stimulus encoding (Hawkins et al., 1990; Reinitz, 1990). Greater efficiency might also lead to the greater fidelity of mental representation of the stimulus, which is crucial for working memory performance (Zanto & Gazzaley, 2009)². It has also been shown that this top-down control predicts WM performance (Rutman, Clapp, Chadick, & Gazzaley, 2009), thus highlighting the importance of such signals in working memory processing.

2.1. Summary: The role of top-down signals in working memory

The previous section established that multiple brain areas are involved in visual working memory, with the storage located in the prefrontal cortex. Working memory depends on the coordinated activity between these regions, with a special role of top-down inputs from the prefrontal cortex to sensory areas (Knudsen, 2007; Lara & Wallis, 2012). It is interesting to note that the sensory cortex and perception are usually discussed in the context of the PFC and higher cognitive processes (such as attention). Coincidentally, focusing on higher-order cortical areas while “downplaying” the importance of sensory cortices (at least in a sense that they cannot sustain memory representations on their own) is in line with the tendency to view memory and perception as separate constructs (Squire & Kandel, 1999).

However, recent years have seen a certain shift in the way the visual cortex (and, more generally, perception) is viewed in the context of visual working memory.

The evidence for an active involvement of perceptual systems in WM has been accumulating in recent years and is currently enjoying much attention (D’Esposito, 2007; D’Esposito & Postle, 2015; E. Ester, Serences, & Awh, 2010; Harrison & Tong, 2009; Pasternak & Greenlee, 2005). The view that similar

² It is important to note that by fidelity, Gazzaley and others mean how well the target can be distinguished from irrelevant items. The better the fidelity, it is easier to maintain a goal – relevant information while not confusing it with irrelevant information.

mechanisms (and, consequently, similar brain areas and networks) are involved in both encoding *and* storage of information over short periods of time became known as the sensory recruitment hypothesis (Harrison & Tong, 2009; Pasternak & Greenlee, 2005). This is a big departure from a traditional view, in which frontal areas are solely responsible for memory storage. More and more studies provide evidence in support for the sensory recruitment hypothesis (D'Esposito & Postle, 2015). The evidence in its favour spans a range of different methodologies, from single-cell recordings, human neuroimaging, electrophysiology, and psychophysics (Pasternak & Greenlee, 2005). The next section will outline the evidence for the involvement of sensory areas in working memory, with a focus on the visual cortex. This will provide the basis for the notion that working memory and perception are inherently linked, and that they are supported by similar neuro-cognitive mechanisms (Gao et al., 2011; Pasternak & Greenlee, 2005). This will be followed by an account of the importance of these findings and the consequences they have on our approach to visual working memory.

3. Beyond the prefrontal cortex

3.1. Sensory areas and perceptual processing contributing to working memory.

While prefrontal areas were taking most of the spotlight in WM research, reports of an active involvement of visual areas and perception in WM started to appear relatively early (Fuster & Jervey, 1982; Miyashita and Chang, 1988).

Fuster and Jervey (1982) recorded the single unit activity of neurons in the inferotemporal cortex in monkeys during a visual delayed match-to-sample task. Monkeys were presented with a sample colour and, after the delay, required to choose the previously presented one from two alternatives. The results showed colour – dependent increase in firing rates not only during stimulus encoding but also during the retention interval. Fuster and Jervey interpreted this results as evidence for the involvement of a subset of inferotemporal neurons in memory. Importantly, neurons that exhibited such pattern did not appear to be specialised for memory storage. Rather, their participation in memory functions occurred in addition to their visual functions. Miyashita & Chang (1988) extended these findings by showing that neurons in the temporal lobe of a non-human primate are able to sustain the memory of more complex objects as well. After identifying sets of neurons responsive to particular shapes, they showed that these neurons sustained their firing rates during retention interval after the shapes were removed from the visual field. Interestingly, the activity of those neurons, while related to the content of the stimuli, were independent of their size or orientation.

Low-level visual areas have also been implicated in working memory using single-cell recordings in the macaque. For example, one study (Super, Spekreijse, & Lamme, 2001) required macaques to remember objects in a delayed-discrimination task. Remembering objects required subjects to separate them from a background in which they were embedded. Activity in the visual cortex associated with figure-ground segmentation was recorded during encoding, for

both correct and incorrect trials. Super et al. (2001) demonstrated that activity related to this figure-ground separation in the visual cortex was sustained during the maintenance period. Interestingly, this activity was sustained only for correct trials, while it would disappear for incorrect trials.

These findings were further extended by studies showing that activity of populations of neurons, rather than single cells, are also related to working memory (Lee, Simpson, Logothetis, & Rainer, 2005). This can be achieved by recording local field potentials (LFP) and looking at the task-related oscillatory activity. Populations of neurons firing in synchrony create functional networks which can be related to the task at hand (Buzsáki & Draguhn, 2004; Buzsáki & Wang, 2012; Canolty et al., 2006; Whitman, Ward, & Woodward, 2013). For instance, Lee et al. (2005) demonstrated that local field potentials recorded from occipital visual cortex during delayed-discrimination task showed an energy enhancement in the theta band (4 – 8 Hz) during memory maintenance. This pattern was interpreted as an evidence for an active involvement of extrastriate visual cortex in working memory. Another study on non-human primates (Liebe, Hoerzer, Logothetis, & Rainer, 2012) showed evidence for inter-areal communication between prefrontal and sensory areas during a visual short-term memory task. This was evidenced by phase synchronisation in the theta range (defined in this experiment as 3 – 9 Hz) between the areas, i.e. the oscillatory activity in one area was tightly related to activity in the other area. Additionally, single unit activity in these areas was also shown to be related to the ongoing theta oscillations.

Human EEG recordings also point to the crucial role that oscillations originating in sensory cortices seem to be playing in WM. For example, intracranial recordings in humans indicated higher activity in theta frequencies during WM over occipital sites, among other regions (Raghavachari et al., 2001). These findings match the pattern of results derived from non-human studies described above (Lee et al., 2005; Liebe et al., 2012). Other studies also demonstrate a recurrent interaction between prefrontal and occipital cortex, driven by synchronised activity around the theta band (4 – 7 Hz) as well as upper alpha (10

- 12 Hz) between these areas (e.g. Klimesch, Freunberger, Sauseng, & Gruber, 2008; Sarnthein, Petsche, Rappelsberger, Shaw, & Von Stein, 1998; Sauseng, Klimesch, Schabus, & Doppelmayr, 2005).

Another line of evidence for the involvement of sensory cortices in working memory comes from studies using fMRI (Harrison & Tong, 2009). Similarly to single-cell recordings from non-human primates or EEG recordings in humans, fMRI experiments aim to determine whether activity in early visual areas during task performance can be related to WM processing. These experiments would usually employ delayed-discrimination tasks (Greenlee et al., 2000, Pessoa et al., 2002). In particular, results showed that apart from patterns of activity in the PFC, memory-related activity was also elevated in the occipital and parietal cortex.

One of the most compelling evidence for the active involvement of sensory areas in working memory came from a study by Harrison and Tong (2009). They demonstrated that it is possible to decode the contents of working memory from the sensory cortices alone using fMRI decoding methods. This notion has been previously challenged by findings indicating that early visual areas are showing only a weak sustained activity during the maintenance period or none at all (Bisley, Zaksas, Droll, & Pasternak, 2003; Offen, Schluppeck, & Heeger, 2009). In their task, Harrison & Tong applied fMRI decoding methods to try to decode remembered orientation during the maintenance period. They demonstrated that it is possible to do so with high accuracy, despite the fact that overall activity in visual areas is low. This has been shown to be true not only for orientation (Ester et al., 2013, Harrison & Tong, 2009), but contrast as well (Xing, Ledgeway, McGraw, & Schluppeck, 2013). This further supports a notion that early visual cortex stores memory of visual features, and that this observation is not limited to only one specific stimulus features, such as orientation.

It is apparent that, although imaging generally supports the idea of the involvement of sensory cortex in working memory, the results strongly depend on the type of working memory paradigm that is employed. N-back tasks tend to

produce weaker results than delayed-discrimination tasks; in the former case, the activity is observed predominantly in the areas outside the sensory cortices (prefrontal or posterior parietal cortex). Pasternak and Greenlee (2005) propose that one possible explanation is that the memory representations of the target and non-target stimuli are interacting in N-back tasks, making the detection of sensory-specific activation more difficult.

A final line of evidence for the involvement of sensory areas in working memory (and thus for an interaction between perception and working memory processes) can be derived from psychophysical studies³. Over the years, researchers have tested visual memory for single stimulus attributes, such as orientation, contrast, frequency, motion and colour (for a review, see Pasternak & Greenlee, 2005). The rationale behind these studies is that if such features are important for visual perception (being essentially “building blocks of perception”), they should also be important for visual memory (Magnussen, 2000; Magnussen & Greenlee, 1999).

To test this idea, a delayed-discrimination task is usually used. Participants are presented with a stimulus and after a delay required to decide whether a currently presented probe is the same or different to the previously remembered stimulus. Single stimulus dimension (such as orientation) is manipulated to probe the memory for this particular feature. It was demonstrated that the retention of basic stimulus features in visual memory is remarkably stable, even with longer delay periods (Magnussen & Greenlee, 1999).

Interestingly, however, the memory trace for different visual attributes does not decay at the same rate (Pasternak & Greenlee, 2005). For example, attributes such as spatial frequency, size, orientation and speed of motion can be retained for longer periods without a significant decay in precision. This is not the case for luminance contrast, texture or direction of motion, which decay more quickly than other attributes (for a review of studies, see Pasternak & Greenlee, 2005). To account for these findings, Magnussen (2000) proposed that the storage of visual

³ Interestingly, the idea of probing memory using psychophysics is almost as old as the field itself, as pointed out by Magnussen & Greenlee (1999).

attributes is achieved by a system consisting of a series of parallel memory stores which are narrowly tuned to individual stimulus dimensions. A strong support for such parallel, stimulus-selective storage system can be derived from visual masking paradigms. In such tasks, an irrelevant stimulus is presented during working memory encoding (“memory mask”). If the attributes of the mask interfere with the memory of the target, it is concluded that the mask is processed by the same system as the target. On the other hand, if a specific attribute does not seem to interfere with successful encoding, it is concluded that the mask is stored by a different mechanism (Magnussen, Greenlee, Asplund, & Dyrnes, 1991). In one such experiment, Magnussen et al. (1991) showed that delayed discrimination of spatial frequency can be impaired by introducing a mask during a delay period. Importantly, delayed discrimination is most affected if the mask has a different spatial frequency than the memory probe. At the same time, the orientation of the mask proved to be irrelevant to performance. These results suggest that spatial frequency is maintained during the delay period by a similar mechanism that was involved in its encoding.

In summary, it appears that the fidelity of memorised stimulus dimensions closely matches the fidelity achieved during “on-line” perception (i.e. when the stimulus is still present in the visual field). Furthermore, the system responsible for storing these features (Magnussen, 2000) exhibits properties of a narrowly-tuned, spatially localised filters (Magnussen et al., 1991). These findings are taken as an evidence for the contribution of sensory cortical areas to memory storage of basic stimulus dimensions (Pasternak & Greenlee, 2005).

Additional support for the overlap between perception and visual working memory comes from studies demonstrating that vision can be “contaminated” by the contents of memory. In one notable study (Kang, Hong, Blake, & Woodman, 2011) participants viewed patterns of dots moving clockwise or counterclockwise and were required to remember the direction of motion. Subsequently, they were presented with another moving – dot pattern and were required to indicate the direction of the movement. Finally, subjects indicated the direction of the memorised pattern. These findings mimicked the motion repulsion phenomenon

(Hiris & Blake, 1996; Marshak & Sekuler, 1979) which is usually reported only when two motion stimuli are presented simultaneously. In this phenomenon, the direction of motion of one stimulus is distorted by another stimulus. Remarkably, in this study, the *memorized* motion influenced the appearance of perceived motion during the retention period. Later experiments followed this pattern and showed that indeed perception can be distorted (or biased) by the contents of working memory. For example, it has been shown that working memory can bias orientation processing (Scocchia, Cicchini, & Triesch, 2013) and colour appearance (Olkkonen, Allred, Shevell, Singer, & Muckli, 2014). Furthermore, saccade target selection seems to be also influenced by memory contents (Hollingworth et al., 2013). These results suggest that visual features represented in WM can interact with perception, further supporting the notion that these processes might share a common mechanism.

3.2. Interactions between perception and visual working memory: impact on theoretical approaches and significance.

Findings cited in the previous sections opened up a new approach to WM research, one in which working memory and perception share common mechanisms, rather than being two separate systems. This had a considerable impact on theoretical approaches to visual working memory.

For example, Zimmer (2008) argues that the visual WM can be thought of as an emergent property of perceptual processing performed on visual and spatial information. In his view, parts of the environment – such as visual stimuli – are represented by networks which stay activated as long as the stimulus is available. After it is gone (for instance, when the stimulus is removed from the visual field), the activity associated with the stimulus starts to decay, unless it is continuously reactivated by triggers of external or internal origin. While attentional processing could serve as such trigger, it could be also any operation that needs to be performed on the stimulus, such as mental rotation. In Zimmer's view, what we refer to as “working memory” is simply a representation provided by a perceptual

system that is being acted upon by any other cognitive process. Naturally, this implies that the neural networks responsible for working memory are the same as the ones used by perception to represent parts of the environment (in addition to any other networks that are needed to perform additional processing on this representation). In a similar manner to Zimmer's, Postle (2006) also argues for viewing working memory as an emergent property of perceptual processing. According to him, visual working memory functions have evolved from the same systems as those dedicated to sensory and action-related functions and are achieved by coordinated recruitment of those systems.

One of the consequences of localising memory storage to the same networks that are responsible for perceptual encoding is the need to re-evaluate the role of sustained activity in the prefrontal cortex. It is remarkable that the sustained activity has been demonstrated during a variety of working memory tasks, using different methodologies, at different levels (from single-unit recordings to EEG and fMRI) and using human as well as non-human subjects (Lara & Wallis, 2015; Postle, 2006). If it is not related to storage, what is its function?

Perhaps a bit surprisingly, the role of the PFC can be best captured by the classic Baddeley and Hitch' model (1974). As D'Esposito and Postle (2015) point out, the multicomponent model actually distinguished between the storage buffers and a system dedicated to controlling and manipulation of those representations – the central executive. It can be therefore argued that the sustained activity in the prefrontal cortex is simply a neural correlate of the central executive. In more concrete terms, the interpretation of the sustained activity in the prefrontal cortex should not focus on storage per se (Lara & Wallis, 2015), but be considered instead as a reflection of top-down processing of sustained perceptual representations. An obvious candidate for such top-down signal would be attention along with executive functions driving any cognitive processing that needs to be performed to meet task demands (Postle, 2006; Zimmer, 2008). Indeed, the role of attention in working memory has been long acknowledged (for a review, see for example Awh, Vogel, & Oh, 2006 and Lara & Wallis, 2015). Furthermore, it has been also suggested that the prefrontal cortex plays a

modulatory role, i.e. providing other brain areas with top-down signals that shape working memory processing (e.g. Duncan, 2001; Fuster, 2008; Miller & Cohen, 2001; Shallice, 1982). However, new findings suggesting that the same areas that encode stimuli also serve as a memory storage means that to understand working memory, we need to specify the nature of the interactions between the “central executive” (i.e. frontal areas) and sensory areas responsible for perceptual/memory representations more closely than before (Lara & Wallis, 2015). Indeed, current research supports the view that the recurrent interactions between frontal and visual areas are crucial for visual working memory performance (Liebe et al., 2012).

However, not everyone agrees with the view that the PFC (or frontoparietal network in general) is not involved in memory storage at all (Ester, Sprague, & Serences, 2015). This view has been challenged by studies showing that it is possible to decode stimulus-specific activity from the frontoparietal network, suggesting that these areas are indeed involved in working memory storage after all (Ester et al., 2015). While the debate is still ongoing, it is nevertheless evident that the role of sensory cortices should be viewed as an active player in working memory network. Thus, apart from looking at top-down interactions between frontal areas and sensory cortex, there is also a need to focus on the activity in the sensory cortices itself, especially during perceptual encoding (Lara & Wallis, 2015).

One line of research downplays the role of perception-related activity during encoding in working memory. For example, an already mentioned study by Pessoa et al. (2002) showed that frontoparietal activity during encoding predicted correct performance on a working memory task. At the same time, activity in the visual cortex was not crucial to working memory processing. This is not to say that encoding activity in the sensory areas is not important: after all, one would expect that weakly encoded stimuli will lead to worse task performance. However, such effect would not be attributable to worse working memory per se. More specifically, Pessoa et al. demonstrated that if the events were encoded poorly, the subsequent delay activity in the left dorsolateral

prefrontal cortex did not predict successful performance. Furthermore, delay activity could not be distinguished between correct and incorrect trials. On the other hand, for well-encoded trials, activity in the dorsolateral prefrontal cortex during maintenance did predict successful performance (Pessoa et al., 2002). At the same time, activity in the visual cortex for well-encoded stimuli during encoding did not differ between correct and incorrect trials and was not predictive of successful performance. This implies that, although accurate encoding plays role in task performance in the sense that stimuli need to be well perceived to be remembered, it is the frontal (and frontoparietal) activity that can be directly related to working memory processing and task performance. Therefore, the visual cortex does not appear to extend beyond mere perception.

Another line of research gives evidence to the contrary: it views perceptual processing (subserved by sensory cortex) as an important contributor to visual working memory performance in the sense that it is an integrated part of the working memory. For example, Haenschel et al. (2009) compared behavioural performance and neural activation of healthy controls and in patients with schizophrenia using EEG. Schizophrenia negatively affects working memory in affected individuals (Lee & Park, 2005; Silver, Feldman, Bilker, & Gur, 2003). Haenschel et al. showed that successful working memory performance in a delayed match-to-sample task was strongly predicted by evoked theta, alpha and beta activity in neurotypical subjects during early encoding. On the other hand, patients with schizophrenia showed attenuated activity in these frequency bands compared to healthy controls. Another study (Haenschel et al., 2007) recorded EEG as well as a BOLD activity using fMRI from extrastriate visual areas during working memory encoding. Results showed that the activation in these areas in patients was reduced when compared with healthy controls. Furthermore, differences between the groups were most pronounced when subjects had to remember the higher number of stimuli (i.e. at higher working memory loads). In terms of EEG, the early visual component P1 during encoding was reduced for patients, while at the same time its amplitude predicted successful performance in healthy individuals. Together, these findings suggest that: 1) encoding stage of

visual working memory is crucial for working memory and that 2) activity in the extrastriate visual areas during this stage contributes to successful performance.

3.3. Summary: common mechanisms of perception and visual working memory

To summarise, the converging suggests that working memory and perception share common mechanisms. This opens up a new approach in WM research, one in which perception, subserved by activity in the sensory areas, is crucial to working memory performance.

There are at least two research directions that can be taken from here. Firstly, one can investigate in detail the dynamic interactions between frontal and sensory (visual) areas to see how the two give rise to working memory (Lara and Wallis, 2015). On the other hand, one can also investigate how the memory representation is created in the first place – and how top-down signals can influence this process. The assumption is that mechanisms involved will most likely be the same as perception, and therefore subserved by the visual system.

These approaches hold a good promise, considering that a good deal is known about how perceptual representation is created, from the retina to visual cortex and beyond. Therefore, it is sensible to take advantage of the tools used in visual psychophysics and visual neuroscience to investigate whether the rules governing perception are applicable to visual working memory.

To begin, I will first outline how the visual system deals with incoming information to create a perceptual representation of the environment.

4. Chromatic and achromatic shape processing: from the retina to the cortex

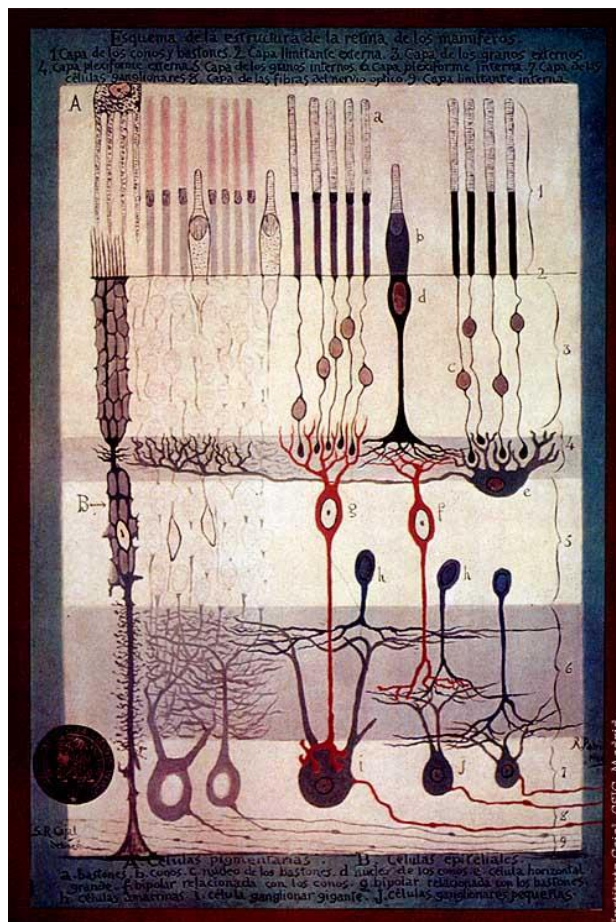
One way to approach visual processing is to model it as a series of progressing stages along which the visual information is carried over from the retina to the cortex. In this chapter, the processing that is carried at each such stage will be described. Computations integrating visual information will be provided, along with the anatomy and physiology that underlie them. This will be done at a single-cell and network level. More specifically, it will be considered how the light reaching the retina is carried and processed in the form of neural signals, from photoreceptors through various retinal cell types, through the optic nerve, lateral geniculate nucleus (LGN) and finally, the cortex. In primates, most of the visual information reaches the cortex via this route (Lennie & Movshon, 2005). This is certainly not the only route; some visual information reaches the striate cortex without the involvement of the LGN, for example via the superior colliculus (Adams, Gattas, Webster & Ungerleider, 2000). Additionally, LGN also projects to extrastriate cortex (Fries, 1981; Bullier & Kennedy, 1983; Lysakowski, Standage & Benevento, 1988). However, such connections are sparse compared to the LGN-cortex (geniculo-extrastriate) route; it is also apparent that these connections alone are not sufficient to activate the cortex appropriately (Lennie & Movshon, 2005; Schiller & Malpeli, 1977; Rodman, Gross & Albright, 1990; Collins, Lyon & Kaas, 2003). Therefore, in this thesis, we will focus solely on the retinogeniculate-striate pathway.

While discussing the flow of visual information, special attention will be given to the processing of luminance and chromatic signals that arise from combinations of cone inputs. The extent to which luminance and chromatic signals are separated (or not) will be discussed. This is a relevant issue as the main question of this thesis is whether luminance and chromatic signals contribute to working memory differently. In the last section of this chapter, I will describe how luminance and chromatic signals contribute to building perceptual representation. The aim of doing so is to show that their contribution is differential, with luminance and chromatic signals being unequally efficient in

sustaining different aspects of perception. This will lay the foundation and provide a rationale for discussing luminance and chromatic signals in a visual working memory, with the assumption that their contribution to memory representations can be also differentiated, just as they are differentiated in perception. We will thus embark on a short anatomical and functional journey through the visual system, starting at the retina, where vision begins.

4.1. The retina – anatomy and functional organisation

The retina is surprisingly simple yet complex part of the central nervous system. The basic framework of neural circuitry and detailed description of the main retinal cells have been already described in the classic work of Ramon y Cajal (1892; see Figure 3 for retina’s anatomy as illustrated by Cajal) and further expanded in the mid-20th century (Polyak, 1941, 1957).



As a first step, we briefly describe the general anatomical organisation of the human retina, before detailing the intricacies of different cell types, connections and computations that they perform. The retina is a layered structure (see Figure 4 for an illustration using the author's retina as an example). The most external layer contains photoreceptors, which absorb light entering the eye and transform them into neural signals. This marks the beginning of visual processing.

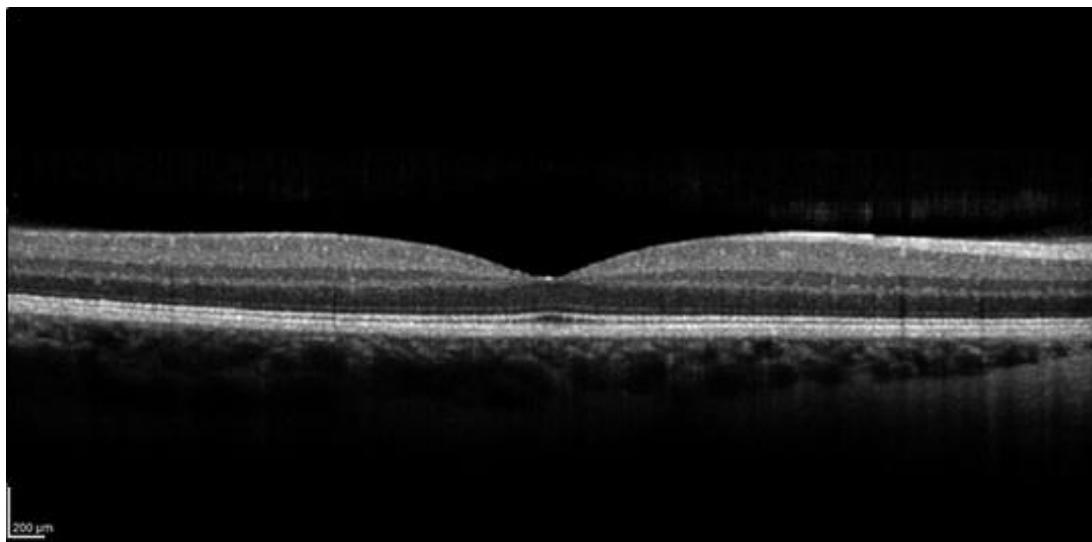


Figure 4 Scan of the retina belonging to the author of this thesis, showcasing the layered structure. Image: Dr Irene Ctori.

Typically, there are three types of photoreceptors – cones – tuned to daylight (photopic) vision. Another class of photoreceptors, rods, are dedicated to night vision. As the focus of this thesis revolves around colour vision and perception under daylight conditions, this chapter will be limited only to cone photoreceptors. Each cone can be described by its probability to respond and absorb light of a specific wavelength. The absorption is determined by opsin, a photosensitive protein. Cones can be divided into three types based on the wavelength at which the cone's absorption reaches maximum (peak absorption wavelength; Smith & Pokorny, 1975). S-cones, or short-wavelength cones, have their absorption peaks in short wavelengths (around 420 nm). M and L cones respond to the middle (~531 nm) and long (~558 nm) wavelengths, respectively (see Figure 5 for illustration of cone sensitivities and their absorption peaks). The probability of absorbing photons by a specific cone, therefore, changes with the wavelength.

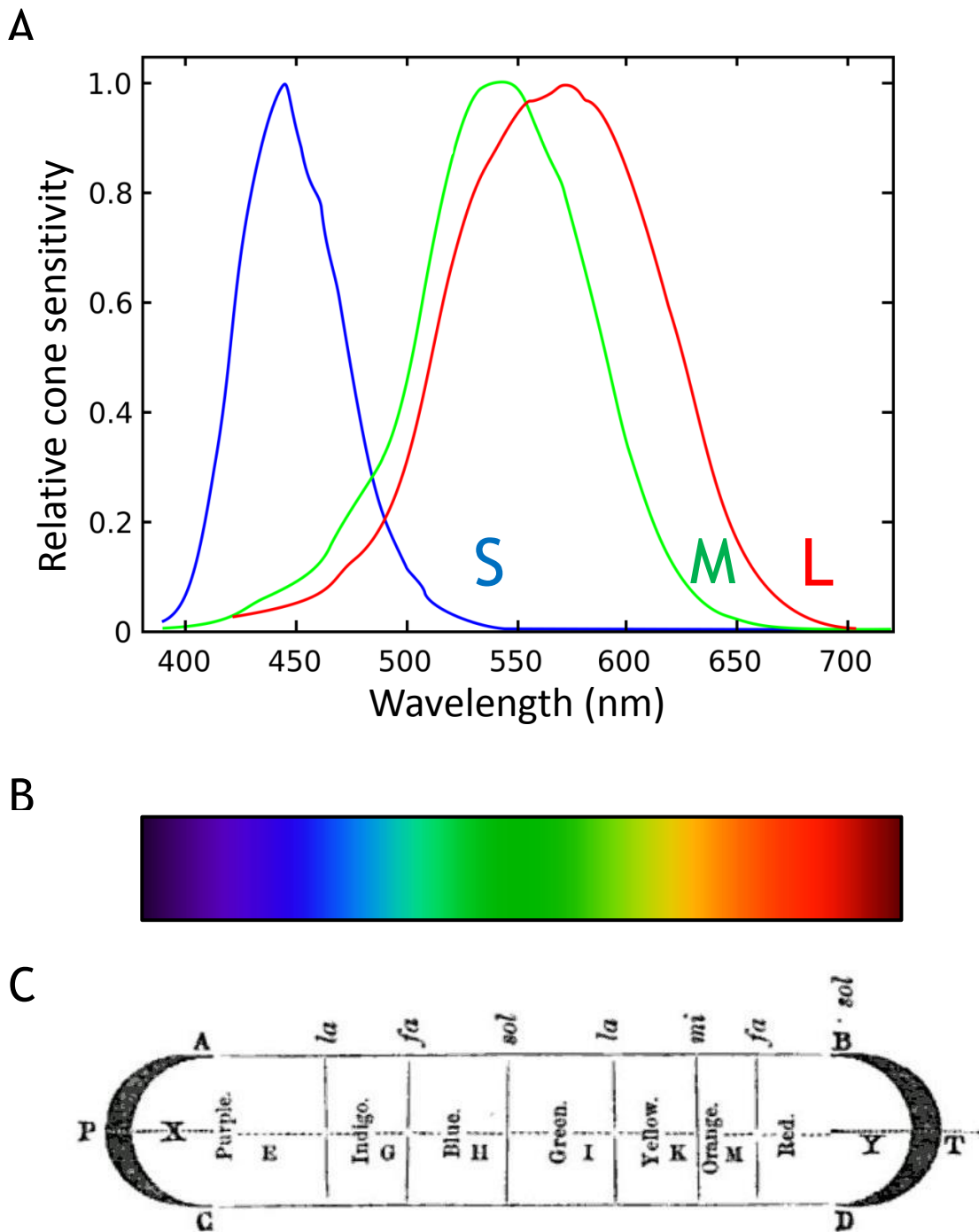


Figure 5 A) Normalised responsivity spectra of human cone cells: short, medium and long cones (Image: Vanessaekowitz at Wikipedia, modified). B) Approximation of colour spectrum visible to the human eye. C) Isaac Newton's (1642 - 1726/27) description of the colour spectrum, based on observation of white light shined through a prism and decomposed as an effect. In Brewster & Newton, 1855.

Absorbed light is converted into electrical signals via photochemical reaction (transduction; Jindrova, 1998). The resulting signal is dependent on the amount of light (photons) absorbed, but the information about the wavelength of the

light is lost at this point. Rushton (1972) referred to this phenomenon as the principle of univariance. As a result, the only information that is available at this point is the photon count and thus information about the chromaticity is ambiguous. For example, a change in photon count in a given cone type could mean that the wavelength has changed to its peak wavelength; however, it could be also due to an increase in overall light intensity, without the actual wavelength change.

To recompute the wavelength information, additional operations need to be performed. Young (1802) and von Helmholtz (1852) already recognised that such additional step beyond the photoreceptors would be necessary. It is now clear that to achieve this, the visual system takes advantage of differences in wavelength sensitivity in different cone type, weighing their excitation against each other. Summing excitations of the three cone types, information about the (achromatic) light intensity – or luminance – can be computed. Chromatic information can be worked out by working out differences between excitations of various cell types.

The way the signals are combined by these cells gives rise to three perceptual channels, otherwise referred to as post-receptoral mechanisms. There are two opponent-chromatic and one achromatic channel (Lennie & D’Zmura, 1988). The first cone-opponent channel, referred to as the red-green channel, computes the difference between excitation of L and M cones (and thus can be referred to as [L – M] channel). The blue-yellow component, on the other hand, is computed by subtracting the difference between L and M signals from the S signal (S – [L+M] channel). The intensity of perceived light is computed by adding signals from L and M cones (L+M, or luminance channel) (see e.g. Krauskopf et al., 1982)⁴.

Interestingly, there was a general agreement in psychophysics that colour vision is driven by these three fundamental mechanisms, even though the physiological

⁴ Note that referencing an end product of the colour processing at this stage is misleading, as colour perception requires inputs from all channels (Stockman & Brainard, 2010) and a relationship between retinal inputs and the perception of colour is not that simple (Derrington et al., 1984; Valberg, 2001; Webster, 2009). Therefore, red-green and blue-yellow terminology is not entirely correct, though such naming convention is still widely encountered in the literature.

data on the spectral sensitivities of cones was still not available in the 1960s (Grindley, 1960; Lennie & Movshon, 2005). Nevertheless, with the advancement of physiological recording techniques and insights from single-neuron recordings in primates (e.g. Wiesel & Hubel, 1966), researchers could finally tap into the physiological basis of mechanisms inferred from psychophysics. I will begin by describing the underlying physiology and move to the description of psychophysical channels later in this chapter's section.

Computations giving rise to the colour-opponent channels are carried out at the post-receptoral stages of the visual hierarchy and are mediated by retinal intermediate (bipolar, horizontal and amacrine) cells and by ganglion cells (Dowling, 1968). The latter are located in the innermost layer of the retina and are the last "stop" before the visual information is carried outside the retina through their extended axons. Bipolar cells take their input from photoreceptors and output to ganglion cells, forming an excitatory pathway. Inhibitory signals are provided by the two types of interneurons. Horizontal cells are adding inhibitory responses to connections between photoreceptors and bipolar cells. Amacrine cells, on the other hand, are dealing with connections between bipolar and ganglion cells (Dacey, 2000; Werblin & Dowling, 1969).

First insights into colour-opponent computations and a confirmation of the existence of three mechanisms/channels were inferred from the recordings of neurons in the lateral geniculate nucleus (LGN) of a monkey (De Valois, Abramov & Jacobs, 1966; de Valois, Smith, Karoly & Kitai, 1958; Wiesel & Hubel, 1966). Neurons in the LGN were easier to record at that time; however, it soon became apparent that the properties of the LGN neurons correspond to cell properties of the ganglion cells. Ganglion cells themselves, in turn, corresponded to the properties of bipolar cells (Gouras, 1968). In other words, our understanding of the role of the retinal neurons in colour-opponent computations was inferred back-to-front. For this reason, the pathway from the ganglion cell to the LGN is defined by the LGN layer to which the ganglion cell is projecting to. Ganglion midget cells receive inputs from L and M cones and connect to the parvocellular layer of the LGN, and is thus called a P-pathway, or

parvocellular pathway. The pathway takes its name from the relatively small size of cells in that layer (from the Latin *parvus*, meaning *small, little*). Parasol ganglion cells also receive L and M cone inputs, but project to magnocellular layers and is thus referred to as the M-pathway (or magnocellular pathway). Cells in this LGN layer are bigger than parvocellular cells, hence the name (from the Latin *magnus*, meaning *large, big*). Later, the existence of the third pathway was confirmed (Henry & Yoshioka, 1994; Martin et al., 1997; Chatterje & Callaway, 2003; Hendry & Reid, 2000). This third pathway receives inputs from S-cones; their signals are processed by a distinct cell type (i.e. not parasol or midget cell type), namely small bistratified ganglion cells. These cells would project to koniocellular layers of the LGN.

Opponency of ganglion cells (Gouras 1968; de Monasterio & Gouras, 1975; de Monasterio et al., 1975; de Monasterio 1978) and neurons in the LGN to which these cells are projecting (DeValois et al., 1966; Derrington & Lennie, 1984) was revealed by studying responses of these neurons in monkeys to lights of different spectral content. Neurons that were excited by one portion of the spectrum and inhibited by another were a direct evidence for this – hence, they were referred to as spectrally opponent neurons. Ganglion cells are also referred to more generally as ON/OFF cells, as they respond with increased firing rates to an increase in activation of a given cone type and decreased firing in response to decrease in activation in another cone type (De Monasterio et al., 1975; Dacey & Lee, 1994). Central to understanding those mechanisms is the notion of receptive fields and their center-surround structure. The receptive field of a cell refers to the retinal area that is “covered” by this cell. Projections from a number of cones converge in a ganglion cell, and thus that cell is excited or inhibited by the activity of these cones. The receptive field of a ganglion cell is usually divided into a center and surround. Center and surround of the receptive field have opposite signs; hence, there are receptive fields with center-ON/surround-OFF, or center-OFF/surround-ON.

Simply demonstrating the opponency in itself tells us little about the underlying machinery that enables antagonistic interactions between these neurons. This

was revealed by further physiological studies (see Figure 6 for an illustration of the circuitry in a primate retina).

In the intermediate layers, a bipolar cell receives inputs exclusively from S-cone photoreceptors. The bipolar cell then projects to the small bistratified ganglion cell (recognised by Dacey, 1993), providing an ON signal. The bistratified cell is also connected to diffuse bipolar cells, which connect non-selectively to L and M cones and thus provide an opponent signal. This allows contrasting the S signal with L and M signals, forming the basis of a blue-yellow opponent channel ($S - [L - M]$). Small bistratified ganglion cells project to the koniocellular layers of the LGN.

Another type of ganglion cells – midget cells – receive inputs from L and M cones and forms the red-green ($L - M$) opponent channel. In the intermediate layers, midget bipolar cell receives input from a single M or L cone and carries it to a single midget ganglion cell (Kolb & Dekorver, 1991; Calkins et al., 1994).

Therefore, a single midget ganglion cell receives an exclusive single-cone input (sometimes referred to as a “private line”); this single input constitutes an ON/OFF centre of the receptive field. A consequence of such arrangement is that the ganglion cell gets a pure L or M signal. Interestingly, surround inputs are not specific. According to a cone type mixed hypothesis (Paulus & Kroger-Paulus, 1983; Lennie et al., 1991; DeValois & DeValois, 1993; Mullen & Kingdom 1996), the receptive field surround receives input from a random arrangement of L and M cones. Given the pure, single-cone input to the surround, weak surround inputs from a mixture of L and M cones will result in a strong L/M (red-green) opponency.

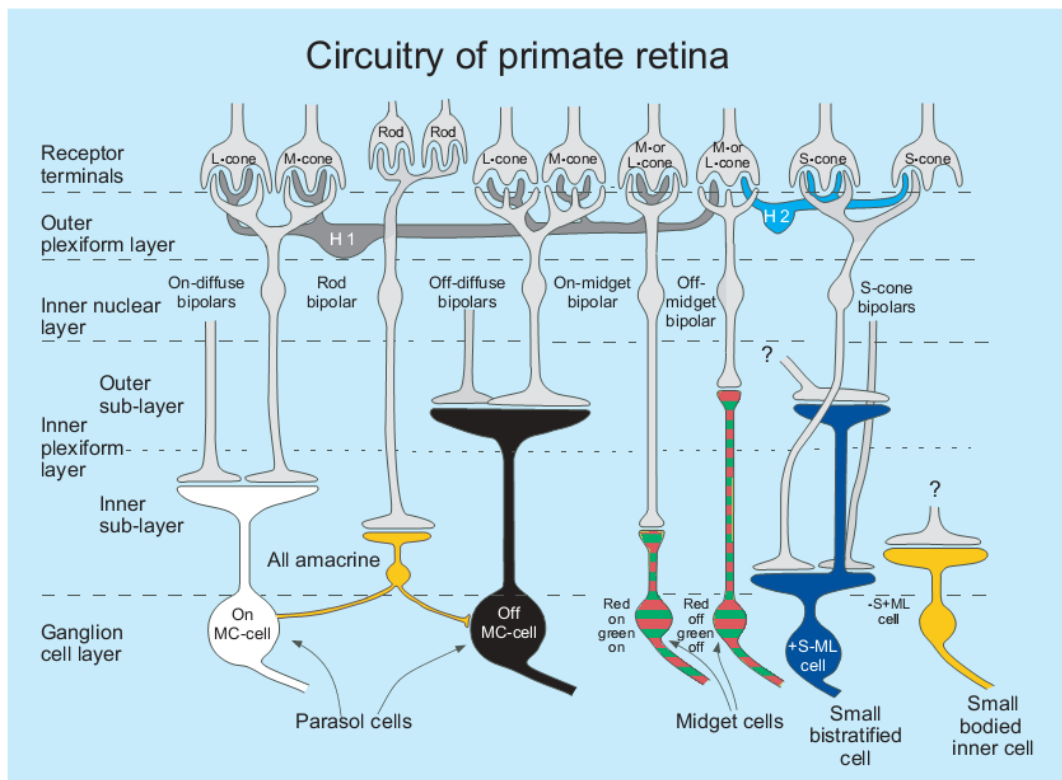


Figure 6 Connectivity in the primate retina. Image: Lee (2004).

Another consequence of this arrangement is that the further away the receptive field is from the fovea (i.e. more peripheral), the opponency becomes weaker. This notion was first inferred from psychophysical observations and confirmed physiologically (Mullen, 1991; Mullen & Kingdom, 1996, Mullen & Kingdom, 1999). It is now evident that peripheral midget ganglion cells show increasingly non-opponent response, essentially summing L and M cone inputs, the way parasol ganglion cells do foveally (see next section). Midget ganglion cells project to parvocellular layers of the LGN.

The next type of ganglion cells – parasol ganglion cells – receive summed signals from L and M cones (through diffuse bipolar cells) and thus form the achromatic luminance channel (L + M). There are two types of parasol ganglion cells: ON and OFF, receiving inputs from ON and OFF diffuse bipolar cells, respectively. Diffuse bipolar cells themselves receive L and M inputs in a non-specific manner (i.e. the input is not cone-specific and can originate from either type). Parasol bipolar cells have a non-opponent center-surround receptive field that is relayed to

parasol ganglion cells; inhibitory signals are (most likely) derived from horizontal cell inputs, which itself connect to both L and M cones. Parasol cells project to the magnocellular layers of the LGN.

4.2. Lateral Geniculate Nucleus (LGN) – anatomy and functional organisation

The next stop along the visual route is the LGN – a bilateral structure located in the thalamus, comprised of six primary layers (see Figure 7 for an illustration of the LGN). Its function is usually described as a “relay station” between the retina and the cortex, which implies it is not a very important structure. One of the reasons why it is regarded as a mere relay station is that cells in the LGN respond analogically to ganglion cells from which it receives its inputs. It has similar receptive fields and exhibits similar colour opponency and achromatic responses (Wiesel & Hubel 1966; Derrington & Lennie, 1984). However, LGN receives inputs propagating back from the cortex, as well as from the brainstem; for these reasons, considering it as a simple relay station is probably a simplification and its primary function is still a matter of ongoing research (Sherman, 2005; Sherman, 2001; Weyand, 2016). Nevertheless, its anatomy and underlying physiology have been extensively studied over the years.

The LGN forms a direct retinotopic map: adjacent ganglion cells representing a portion of the visual field project to a corresponding, adjacent layers in the LGN. The retina located on the ipsilateral side of the LGN projects to layers 1, 4 and 6, while the contralateral retina to layers 2, 3 and 5.

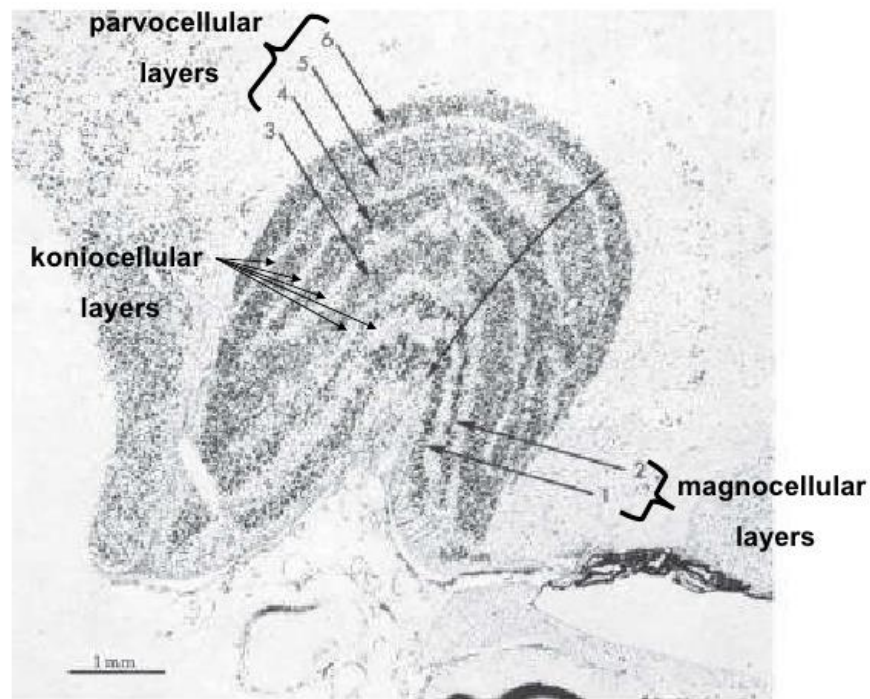


Figure 7 Layering of the lateral geniculate nucleus (LGN)

As mentioned earlier, there are two main layer types, named after their cell sizes. The magnocellular layers, i.e. layers 1 and 2 (comprised of relatively bigger cells) receive inputs from parasol ganglion cells (see the previous section). Parvocellular neurons (smaller cells) in layers 3, 4, 5 and 6 receive inputs from the midget ganglion cells. Later studies (Hendry & Reid, 2000; Szmajda, Grönert & Martin, 2008), revealed the existence of an additional cell type that could be distinguished, situated between the main layers, in their lower sub levels. These are called koniocellular layers, consisting of even smaller cells. They receive input from the small bistratified cells, as described in the previous section.

Magnocellular neurons appear to have larger receptive fields than parvocellular neurons (Derrington & Lennie, 1984; Wiesel & Hubel, 1966); they have a typical ON or OFF-center structure of the receptive field, with L and M cones inputs to both center and surround (Lee, 2008); they do not show a chromatic antagonism. Parvocellular neurons have smaller receptive fields and are chromatically opponent; they receive excitatory/inhibitory input from L and M

cones; thus, P-cells are referred to as red-green colour opponent cells. It is generally assumed that magnocellular cells are a physiological substrate for the psychophysical luminance channel (see next section). Earlier research suggested that neurons in this layer cannot sustain high spatial resolution due to their distribution in the retina and lack of magnocellular cells that would sample from the fovea (Drasdo, 1989). However, later research suggested that the proportion of M-cells in the fovea does not show a large decrease (Grunert et al., 1993). Because of the single-cone input (Polyak, 1941), P-cells are supposed to have higher spatial resolution than M-cells, though experiments suggest that resolution of P and M cells is similar (Derrington & Lennie, 1984; Crook et al., 1988).

There are other differences between M and P cells. Magnocellular neurons are more sensitive to contrast, with a greater contrast gain than P cells at low contrast levels (Kaplan & Shapley, 1982). In terms of temporal resolution, M cells are responsive to higher frequencies than the P cells (Hawken, Shapley & Grosz, 1996). They also appear to differ in terms of visual latencies. Maunsell & Gibson (1992) demonstrated this by lesioning magnocellular layers of the LGN. As a result, response latencies (measured in the striate cortex) were delayed by 7 and 10 ms; a similar lesion in parvocellular layers did not result in a latency shift, suggesting the first few milliseconds can be attributed to inputs incoming from the magnocellular LGN layers.

As mentioned above, in terms of cell responses, neurons in LGN appear to be an “extension” of retinal ganglion cells. As a consequence, the two colour-opponent and the achromatic pathways are still segregated. Complex interactions start to appear only at the cortical level. Contrast sensitivity is however similar for both types of cells at higher contrast levels, as M-cell responses saturate at high contrast (Derrington & Lennie, 1984).

The characteristics of spatial and temporal responses of koniocellular neurons are less understood (Hendry & Reid, 2000). Nevertheless, they are opponent-chromatic and they appear to respond to blue-yellow modulations; as with M and

P cells, koniocellular layers are the target of the small bistratified ganglion cells and thus have analogical response properties, with S-ON centre; opponency is achieved by L and M inputs. They demonstrate low-pass frequency responses, have large receptive fields and slow response latencies (Smithson, 2014; Stockman & Brainard, 2010).

All three main cell types in the LGN provide inputs to the visual cortex, in essence acting as a relay of retinal signals. Since the existence of the third, koniocellular pathway was established relatively recently (Hendry & Reid, 2000; Szmajda, Grünert & Martin, 2008), earlier research focuses exclusively on the parvo and magnocellular layers. In their classic work, Wiesel and Hubel (1966) recognised four neuron types within these layers. Type I and Type II neurons were demonstrating a chromatic opponency. While Type I cells had a center-surround receptive field, Type II neurons did not, as a result being unable to contribute to spatial processing (note that Type II cells were not identified by Derrington & Lennie, 1984).

4.3. Cortex – anatomy and functional organisation

In humans, most of the LGN output goes to the striate cortex (or visual area VI), and in macaque monkey to its equivalent, area 17. VI consists of different layers; LGN inputs mainly to layer 4c and its sublayers (Hubel & Wiesel, 1972). Sublayer 4c α receives inputs primarily from the magnocellular cells in the LGN and 4c β from parvocellular neurons. Koniocellular LGN cells project to the upper layers of the VI, namely to cytochrome blobs (Callaway, 2005; Kaplan, 2012) in layers 1, 2 and 3 (Casagrande, Yazar, Jones & Ding, 2007). See Figure 8 for an illustration of LGN projections to VI layers.

There are also small populations of cells that send signals directly to the area V2 (Bullier & Kennedy, 1983) and V4 (Yukie & Iwai, 1981), completely bypassing the VI. Additionally, there is evidence that koniocellular neurons in the LGN also bypass the VI, projecting into the middle temporal area of the macaque

(Jayakumar et al., 2012). While this is only a small population of neurons, some researchers have speculated that they might be responsible for preserving some visual functions in blindsight, or cortical blindness (Rodman et al., 2001; Vakalopoulos, 2005; Jayakumar, Dreher & Vidyasagar, 2013).

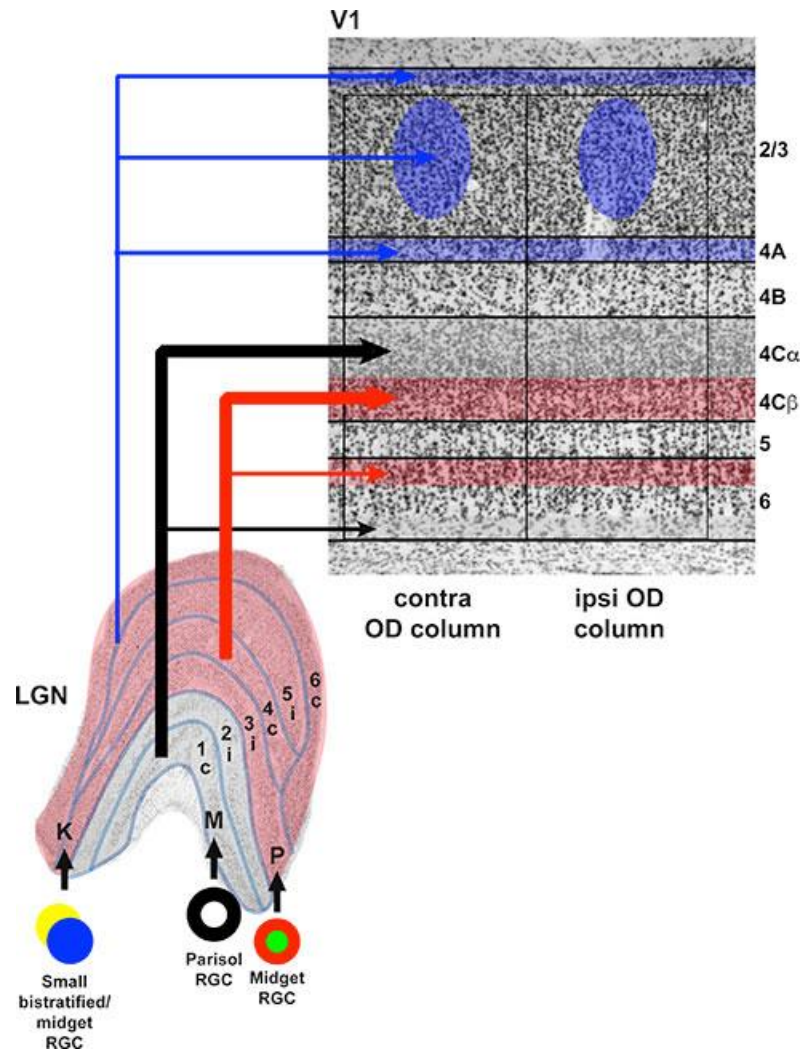


Figure 8 Visual pathways from the retina through the LGN to the V1. Image: Oxford research encyclopaedia.

The fundamentals of what we know about the responses of the striate cortex come from experiments by Hubel & Wiesel (1968), who were the first to comprehensively probe cell responses from the monkey's primary visual areas.

V1 cell responses differ from those of the LGN. They are orientation-selective, are characterised by combining information from both eyes (i.e. their responses are binocular) and they are selective to directional movement (Hubel & Wiesel,

1968). Additionally, depending on the cell, they are selective to particular spatial frequencies and stimulus size (Schiller, Finlay & Wolman, 1976; de Valois, Albrecht & Thorell, 1982). Cells in the first layer of VI are still monocular, but become binocular in layers 2 – 6 (Hubel & Wiesel, 1977). The upper layers project further into extrastriate visual areas: V2, V3 & V4 (Livingstone & Hubel, 1984). Receptive fields of the VI form a topographic map of the visual input.

It has been assumed that cortical responses can arise simply through feed-forward, linear connections from the LGN. Related to this is the psychophysical work (described in more detail in later chapters) that suggested the existence of feature-specific channels; in terms of cortical neuron responses, it was predicted that individual neurons will exhibit properties that would correspond to single features of a given channel. This was largely confirmed in initial work (see Lennie & Movshon, 2005 for references).

4.4. Separation of visual channels

As described in the previous section, magno, parvo and koniocellular pathways can be traced back to distinct classes of ganglion cells, which in turn project mostly in parallel to separate layers of LGN (see review by Kaplan et al., 1990; Lee, Sun & Valberg, 2011).

Visual channels are largely separated at the level of LGN. The additive luminance (L+M) and opponent red-green (L – M) channels appear to be cone-specific. In particular, these two channels seem to lack considerable input from S-cones (Dacey & Lee, 1994; Lee, Martin, & Valberg, 1988; Reid & Shapley, 2002). This was however put into question, as some studies have shown that magnocellular layers of the LGN were responsive to S-cone signals (Chatterjee & Callaway, 2002). However, other studies refuted this claim by showing that S-cone inputs to magnocellular ganglion cells and to parvocellular cells are minimal and negligible (Sun, Smithson, Zaidi, & Lee, 2006a, 2006b). Later studies acknowledged that some midrange ganglion cells (forming the parvocellular pathway) seem to receive detectable S-cone input (Martin & Lee, 2014; Tailby,

Szmajda, Buzás, Lee, & Martin, 2008), although the proportion of these signals is very low. Overall, the available evidence suggests that S-cone signals are visibly separated from parvo and magnocellular cells (Martin & Lee, 2014).

Earlier studies have postulated that the separation between the achromatic and the two chromatic pathways is sustained even in the striate cortex (Bullier & Henry, 1980; Livingstone & Hubel, 1988; Casagrande & Norton, 1991; Casagrande & Kaas, 1994). It has even been suggested that the segregation is maintained beyond primary visual areas (Shipp & Zeki, 1985; Maunsell & Newsome, 1987; DeYoe & Van Essen, 1985, 1988; Livingstone & Hubel, 1988; Zeki, 1993; DeYoe et al., 1994). These findings are in accord with the two-stream hypothesis (Goodale & Milner, 1992), as magno and parvocellular projections seem to feed largely separately to dorsal and ventral stream, respectively (Vidyasagar, Kulikowski, Lipnicki & Dreher, 2002). While parvo and magnocellular pathways do appear to be to some extent segregated, there is also a degree of convergence between the pathways in extrastriate cortex (Maunsell et al., 1990; Ferrera et al., 1992, 1994; Merigan & Maunsell, 1993; Gegenfurtner et al., 1996; Kiper et al., 1997), and even in primary visual areas (Lund et al., 1994; Levitt et al., 1994; Yoshioka et al., 1994; Yabuta & Callaway, 1998). This is derived from physiological studies which demonstrated that particular layers of the cortex are receiving inputs from both pathways. To give a specific example, Yabuta et al. (2001) showed that neurons in area 4B receive excitatory inputs from sublayers $4c\alpha$, a layer that receives direct inputs from magnocellular layers of the LGN. However, at the same time, 4B also receives inputs from layer $4c\beta$, which is a target of P-cells of the LGN. Importantly, 4B has been established earlier as a source of exclusively magnocellular inputs into to the dorsal stream. Thus, 4B becomes an anatomical substrate for M-P pathway convergence in striate areas. Analogically, area 3B of the striate cortex is believed to provide parvocellular inputs to the ventral visual stream. However, this layer also has connections with magnocellular $4c\alpha$ (Sawatari & Callaway, 2000).

The convergence of M and P-inputs has also been investigated functionally. Vidyasagar et al. (2002) recorded responses of neurons in the striate cortex of the

macaque monkeys. The study looked for a characteristic parvo or magnocellular response of a cell in response to a range of stimuli designed to elicit a response characteristic to the pathway in question. Cell's response to chromatic, isoluminant stimuli, which also exhibited a preference for the light of specific wavelength was taken as an indication of a parvocellular response. To test for the typically magnocellular response, low contrast stimuli were used, since parvocellular responses are typically absent when a stimulus with less than 10% contrast is used (Hicks et al., 1983; Shapley, 1990). Furthermore, conduction velocities were also of interest, as M pathway (from the retina to LGN, and also from the LGN to the cortex) responses are faster than those of P pathway (see Dreher et al., 1976; Schiller & Malpeli, 1978 and Bullier & Henry, 1980).

Vidyasagar et al. (2002) found that the majority of cells in the striate cortex demonstrate responses characteristic to either M or P-pathway, suggesting a functional separation between the pathways. However, a large proportion of recorded neurons (26%) exhibited responses consistent with both P and M pathways characteristics. Some of these neurons were located in layer 4 of the striate cortex, which is consistent with anatomical P and M pathways convergent connections with sublayers $4c\alpha$ and $4c\beta$ (see above). It appears then that although parallel nature of the P and M pathway is maintained to some extent in the striate cortex, a convergence is nevertheless present. Vidyasagar et al. (2002) do not exclude the possibility of additional convergence of P and M pathways with koniocellular inputs, though they did not test for this directly. Available evidence seems to be suggesting nevertheless that there is a degree of convergence of P and M pathways with the S-cone pathway (Vidyasagar et al., 2002).

5. Chromatic and achromatic visual channels in perception

As outlined in the previous section, different combinations of cone signals form the basis for colour perception. However, colour is only one of the many attributes of a visual scene. To perceive the world, the higher stages of the visual hierarchy use cone signals – organised into three channels – to compute other aspects of the visual scene, such as lines, edges, depth, motion or texture⁵. Generally speaking, visual streams appear to be (at least to some extent) separated functionally, i.e. they contribute to perception differently. To investigate their differential contributions to perception, researchers used stimuli that were designed to bias visual processing towards the pathway of interest to see to what extent given pathway contributes to the task at hand and how well it can sustain visual perception on its own (De Valois & Kooi, 1991; Livingstone & Hubel, 1987). Thanks to this approach, it was possible to determine that the three channels have different spatial and temporal resolutions. The former is due to a different distribution of cones in the retina: L – M channel is characterised by greater resolution and as L and M cones they are the most numerous types of cones in the retina. However, its response latencies are slower. The S – (L+M) channel is on the other hand characterised by large receptive field and slow latencies (Smithson, 2014; Stockman & Brainard, 2010). The L+M luminance channel is particularly fast in its conductance speeds. The three channels also differ in their sensitivity to contrast levels and spatial frequencies. The magnocellular pathway (which receives predominantly luminance inputs) is most sensitive to low-frequency stimuli and it saturates at higher contrast levels; on the other hand, the parvocellular pathway is sensitive to high-spatial frequencies and does not saturate with increasing contrast (Tootell, Hamilton, & Switkes, 1988; Tootell, Silverman, Hamilton, Switkes, & De Valois, 1988).

⁵ It should be noted that, when talking about perception in this thesis, it is usually implied that we are focusing here on spatial vision specifically. This is due to the fact that the interest of this thesis lies in the memory for visual shapes. Other aspects of perception, such as depth or motion, are not the focus of this thesis.

Neurons in the early visual areas are tuned to respond to particular features of visual input, such as orientation, size, spatial frequency or colour. On the neural level, all these features are represented by different sets of neurons, distributed over visual areas. It is a challenge of the visual system to bring the activity of these neurons together, so objects in the environment are perceived as a whole, rather than a collection of unrelated features. The exact nature of the mechanisms responsible for bringing these features together (or bounding the activity of neurons coding these features) has been a subject of extensive research and is referred to as “the binding problem” (von der Malsburg, 1981, Treisman, 1996). One of the most important information about the visual image comes from edges and contours. This property is derived from low-level aspects of the image, like their luminance and chromaticity, as well as from higher-level properties, such as contrast or texture (Hesse & Georgeson, 2005). Edges are essential to the perception of shapes and it has been long thought that luminance has a special role in edge extraction and – consequently – perception of form (Mullen, Beaudot, & McIlhagga, 2000). This was due to the early studies which showed that colour information is of limited importance in spatial vision (Lu & Fender, 1972; Gregory, 1977; Livingstone & Hubel, 1987, 1988; Gregory & Heard, 1989). Chromatic channels would mainly contribute to the recognition of natural scenes by segregating differently coloured surfaces (Gegenfurtner & Rieger, 2000), or simply act as a “filler” for contours derived from luminance signals (Livingstone & Hubel, 1987, 1988). However, later studies have shown that chromatic channels are able to detect edges as well. This would be subserved by double-opponent cells in V1 (Shapley & Hawken, 2011). These neurons’ receptive field would have a small response to a unified colour shape, but they would produce a larger response at the edge of the figure.

Still, differences in shape processing (in particular, integrating contours) between chromatic and achromatic channels are apparent. For example, although both chromatic and luminance channels appear to be selective for orientation, there are some constraints imposed on the chromatic channels. In particular, chromatic channels appear to be more broadly tuned for orientation than luminance channel (Beaudot & Mullen, 2005). Although the difference between

the channels is not dramatic, Beaudot and Mullen hypothesised that this might be of importance for later stages of perception. This is because form perception relies heavily on orientation discrimination – hence, even small differences in orientation selectivity might translate into impaired form perception at higher stages. Indeed, this was shown to be the case. In their study, Mullen and Beaudot (2002) tested how luminance and chromatic channels perform in a global shape discrimination task. They used stimuli that isolated red green or blue-yellow chromatic mechanisms or achromatic mechanism. In the task, participants were shown two stimuli and asked to discriminate between them, i.e. respond whether they were same or different. The authors showed that the performance was best for the achromatic stimuli, followed by red-green and blue-yellow, which was associated with the worst performance. The authors concluded that the performance for chromatic shapes has shown a mild impairment relative to achromatic shapes; though it was mild, it was evident that chromatic and luminance channels contribute to form perception differently. In terms of contour integration, the performance drops steeply for chromatic channels with the increase of space between figure's elements (Beaudot & Mullen, 2003). Additionally, due to differences in their edge detectors (Mullen et al., 2000), chromatic channels seem to perform worse in contour integration. Therefore, even though colour can support contour extraction on its own and in combination with luminance, it is more restricted in some respects than achromatic channels.

Another line of research suggests that luminance information propagated via magnocellular pathway may significantly contribute to successful binding. Lehky (2000) investigated the amount of feature binding errors subjects produce when viewing isoluminant or non-isoluminant stimuli. Feature binding errors can be produced by a short, simultaneous presentation of two stimuli. An error is produced if a feature of one stimulus is assigned (bound) to the second stimulus. For example, after presenting a yellow letter A with a black letter M, reporting a black letter A is a demonstration of a binding error. Lehky found that, if the stimuli are isoluminant, subjects produce more errors than when the stimuli are non-isoluminant. One of the possible explanations for this observation is the

effect of attention. Why would non-isoluminant inputs be related to attention? Magnocellular input dominates in the dorsal stream (Vidyasagar, Kulikowski, Lipnicki, & Dreher, 2002); dorsal stream leads to the posterior parietal cortex, which was implicated to be involved in attention (Behrmann, Geng, & Shomstein, 2004; Corbetta & Shulman, 2002; Han et al., 2003; Malhotra, Coulthard, & Husain, 2009). Hence, presenting stimuli that provide mostly magnocellular inputs could be a trigger for attention to bind image features. Using isoluminant stimuli might impair the attentional effect, however, leading to more errors. However, Lehky refutes this interpretation by biasing attention towards both classes of stimuli. In these conditions, there were still more errors for the isoluminant stimuli. Lehky concludes that the errors therefore due to abnormalities in form processing and attributes them to processing taking place in the ventral pathway. In particular, Lehky suggests that isoluminant stimuli are poorly defined in the feature map and that it takes time for the system to localise them. Feature binding is a dynamic process that needs to be accomplished before the stimulus disappears from the visual field. It is possible that under isoluminant conditions, this process is less efficient and requires more time, a suggestion that agrees with slow dynamics of feature integration using isoluminant stimuli (Leonards & Singer, 1998).

Another line of research compared performance of luminance and chromatic signals in high-level perception, i.e. object recognition (Martinovic et al., 2011). In their study, Martinovic et al. presented participants with line drawings of either meaningful objects, or non-objects (i.e. scrambled versions of object drawings). The task was to respond which category (object or non-object) the presented image belonged to. The stimuli were designed so that they would contain both chromatic and luminance information, or were impoverished, i.e. the luminance information was absent. The results showed that the inclusion of luminance information resulted in more accurate as well as faster classification of the images as belonging to object category. Interestingly, however, the inclusion of luminance information had no effect on non-object classification speed and accuracy. The authors suggested that luminance information is more efficient in object recognition and is of greater importance for this process than chromatic

information. Later experiments confirmed these findings, showing that object processing benefits from luminance inputs, which may trigger early exploratory eye movements, possibly enhancing the recognition process (Kosilo et al., 2013)

In summary, although luminance and chromatic pathways are capable of coding form and shapes, there are some differences in how they contribute to perception. Aside from such bottom-up contributions, it has been demonstrated that luminance signals can influence top-down processing. The next section will outline how luminance signals contribute to perception via interactions with higher-order cognition.

5.1. The role of luminance in facilitating perception via top-down signalling

Traditionally, visual processing has been regarded as hierarchical, bottom-up process (Hubel & Wiesel, 1959; Kandel, 2014). It has become increasingly clear that vision cannot be seen as a strictly serial (Bullier & Nowak, 1995).

Interestingly, as Bar (2003) points out, anatomical studies have shown that connections between visual areas are not restricted to isolated, bottom-up (ascending) routes. However, these findings were not immediately applied to models of perception (Bar, 2003; Bullier & Nowak, 1995) and researchers largely focused on bottom-up processing. Today, however, top-down influences on visual processing as well as simultaneous horizontal connections within visual areas (Petro, Vizioli, & Muckli, 2014) are acknowledged.

More recent models are looking into the functional role of bottom-up, as well as top-down and horizontal projections (Kafaligonul et al., 2015). Most recent studies focus on the role of these projections in different aspects of object recognition (for example, Wyatte, Jilk, & O'Reilly, 2014), visual attention (Khorsand, Moore, & Soltani, 2015) and various visual phenomena, like masking (Silverstein, 2015).

The important assumption in most of these investigations is that high-level information can be activated rapidly enough to interact with bottom-up

processing. The question remained however how exactly top-down processing can be initiated so early. Bar (2003) emphasized a curious problem, namely that, at least in object recognition, high-level representations are activated even before the sensory input is fully analysed. Object recognition is achieved very rapidly, within 150 – 200 ms after the stimulus onset, meaning that top-down processing must have an earlier start.

To resolve this problem, Bar (2003) proposed a cortical mechanism that would enable the visual system to achieve just that. Bar suggested that such early initiation of top-down processing (and thus its subsequent interactions with bottom-up processing) can be triggered by magnocellular information projected rapidly from sensory to frontal areas.

Bar's (2003) idea was largely inspired by the top-down model of object recognition proposed by Ullman (1995). According to this model, the visual system actively searches for similarities between stored representations and current sensory input. Such process is bi-directional in that both bottom-up and top-down streams explore alternatives for matching an object with a representation simultaneously. Object recognition is achieved successfully when both streams "meet" and a corresponding match is found.

Bar proposed that the visual system extracts a low resolution, a rough outline of a stimulus, which is then projected rapidly to the PFC using "anatomical shortcuts". This low-resolution information is then used in PFC to form expectations about what the input is representing. Such initial guesses, as Bar calls them, are then projected back to inferior temporal cortex (IT). At this point, object representations matching the guesses are activated and integrated with bottom-up processes. As a result, the object recognition is facilitated by top-down processes by limiting the number of possible interpretations of the incoming sensory input.

The candidate for such "anatomical shortcut" would be, according to Bar, the achromatic luminance signals. The achromatic, luminance pathway conveys information very rapidly (Bullier & Nowak, 1995), is quicker than the chromatic

pathways (Laycock, Crewther, & Crewther, 2008) and is sensitive to low contrasts and low spatial frequencies (Maunsell, Nealey, & DePriest, 1990; Shapley, 1990).

Therefore, an anatomical connection that would match this model in terms of speed of projection and information content is the magnocellular pathway to which luminance signals project. Laycock, Crewther and Crewther (2007) reviewed the evidence for higher-order areas providing a sufficiently rapid top-down signal into lower-order areas, which can facilitate recognition. The difference between the arrival of magnocellular and parvocellular inputs into primary visual cortex is termed “magnocellular advantage”, and is reported to be no smaller than 10 ms, with some studies showing the advantage of 20 ms (Laycock et al., 2008). The magnocellular advantage arises from differences in conduction velocities between the two pathways. This advantage would allow for such early top-down facilitation to occur. According to Laycock (2008) and others (Bullier, 2001; Chen et al., 2006), magnocellular projections arrive at V1, and project through the dorsal stream to areas such as V5, and are then “injected back” into V1. There is also evidence for lateral connections to the ventral stream, as well as to frontal cortex. Magnocellular inputs arrive back at V1 before parvocellular projections, and the entire feedforward/feedback loop is completed within 20 ms. In short, this model of visual processing posits that object recognition through the ventral stream is facilitated by feedforward “sweep” through the dorsal stream, which activates parietal as well as frontal regions, and projects back into the V1. This facilitation is possible because of rapid inputs from the magnocellular pathway.

Kveraga et al. (2007) provided support for Bar’s hypothesis. Using stimuli which biased processing towards either magnocellular or parvocellular pathway and investigating the activation of visual areas using fMRI, Kveraga et al. have demonstrated that M-biased stimuli were recognised faster than P-biased stimuli (despite higher recognisability of the P-biased stimuli). Furthermore, M-biased stimuli resulted in greater activation of orbitofrontal cortex than P-biased stimuli. In addition, M-biased stimuli increased the flow of information between middle occipital gyrus to orbitofrontal cortex and fusiform gyrus. Superior object

recognition for stimuli that include luminance information was also demonstrated in other experiments, described earlier (Kosilo et al., 2013; Martinovic, Mordal & Wuerger, 2011).

5.2. Summary: differential contribution of luminance and chromatic signals to perception

As described in the previous section, there is a long tradition of investigating how luminance and chromatic channels contribute to perception, from the lowest to the higher stage of the visual hierarchy. It has been shown that, although both chromatic and achromatic channels are able to sustain vision, there are some differences in the functionality and efficiency of each channel. This is highly relevant to the topic of this thesis.

Visual working memory and perception appear to be sharing common mechanisms, and therefore our aim is to establish how different visual channels contribute not only to on-line perception but also to building working memory representations and sustaining them in the absence of the initial input. Since the mechanisms for both perception and visual working memory are common, we can expect that the contribution of luminance and chromatic channels to working memory will not be the same. Perhaps the relative “luminance advantage” will also translate into the working memory domain.

In the next session, I will return back to visual working memory and speculate how the luminance advantage might manifest itself in this domain. This will be then wrapped up and used to build the main hypothesis.

5.3. The potential role of luminance signals in working memory: top-down benefits, noise reduction

Interestingly, some authors suggested that for successful working memory performance, top-down modulation needs an appropriate “head-start” (Gazzaley, 2011). Such signal would enable the top-down feedback to start sufficiently early

to guide further processing. They also note that without such head-start, WM performance can be diminished as a result, because of increased interference from irrelevant stimuli. This emphasizes the role of preparation and prediction in early stimulus processing. These comments are made in the context of WM tasks where subjects must keep relevant features/stimuli in mind while suppressing distractions. It is interesting that this line of thinking coincides with Bar's comments that high-level representations must be activated even before the stimulus is fully processed on low-level stages of perception. Gazzaley does not really go into depth of how such head-start would be achieved on the neural level. It is implied, however, that this is achieved merely by holding and updating task objectives. It could be argued however that fast signals indicating the presence of target feature would be beneficial as well; therefore, one could hypothesise that such head-start could be achieved by fast luminance projections. This would provide an interesting example of how luminance could benefit WM beyond object recognition, as originally proposed by Bar.

One of the more general mechanisms of how luminance can benefit working memory could be based on noise reduction during encoding a memory representation. A recent view (Bays, Marshall, & Husain, 2011b) poses that noise in neural populations involved in sustaining a memory representation is the primary cause behind errors in working memory (Bays, 2014). According to Bays, substantial accuracy variability in working memory performance as compared with sensory tasks suggests that neural signal must be weak in respect to the noise (i.e. low signal-to-noise ratio). This goes in line with the study by Harrison and Tong (2009) mentioned in the previous section. Even though in their study, Harrison and Tong were able to decode the contents of working memory from activity in the visual cortex, the overall signal was weak. While the stimulus is still in the visual field, the neural activity associated with its processing is strong, while the signal that is decoded from memory is much weaker. Interestingly, the delay-period signal is largely independent of memory load; however, the activity in the areas that demonstrate a transient response to presented stimuli is load-dependent, with neural information in these areas being weaker at higher working memory load (Emrich, Riggall, LaRocque, & Postle, 2013).

6. Conclusion and the main hypothesis

Research on visual working memory has a long tradition in psychology (Baddeley, 2003; Baddeley & Hitch, 1974). Psychological and cognitive models of working memory facilitated neuroscientific research of sustained perceptual representations (Goldman-Rakic, 1995; Levy & Goldman-Rakic, 2000). This led to decades of fruitful research which highlighted the importance of prefrontal brain areas in working memory and which suggested that the short-lived memories are stored in the dorsolateral prefrontal cortex (Levy & Goldman-Rakic, 2000). Although the role of other brain regions has been long appreciated, it is only recently that the evidence accumulated towards conclusion that the same neural mechanisms responsible for encoding and perception of visual stimuli are also used to sustain their representation over time (Harrison & Tong, 2009; Pasternak & Greenlee, 2005), an account sometimes referred to as sensory-recruitment hypothesis (D'Esposito & Postle, 2015; Postle, 2006). As a result, prefrontal cortices are now viewed as a host for control mechanisms over other brain areas engaged in working memory, while the storage is subserved by sensory areas (Lara & Wallis, 2015).

An important consequence of this new approach is that perception and visual working memory can no longer be viewed as separate mechanisms (Gao, Gao, Li, Sun, & Shen, 2011; Postle, 2006; Zimmer, 2008). This opens up new avenues of research: if visual working memory shares neural architecture with perception, it becomes reasonable to investigate whether building a memory representation is governed by analogical processes responsible for building a perceptual representation of the visual world. Classic visual neuroscience research has shown that the building blocks of perception are assembled by three anatomically and functionally defined visual channels (e.g. Livingstone & Hubel, 1988) – two achromatic and one achromatic, luminance channel. Crucially, each channel contributes to low, as well as high-level perception differently, due to their differing spatiotemporal resolutions and other attributes (Clery, Bloj, & Harris, 2013; Cooper, Sun, & Lee, 2012; De Valois, Lakshminarayanan, Nygaard, Schlüssel, & Sladky, 1990; Lee, Sun, & Valberg, 2011; Livingstone & Hubel, 1988;

Mullen & Beaudot, 2002; Shapley, 1990; Tootell, Silverman, Hamilton, Switkes, & De Valois, 1988), with luminance being somewhat superior and more efficient over chromatic channels (Bar, 2003; Kosilo et al., 2013; Kveraga et al., 2007; Martinovic et al., 2011; O'Callaghan et al., 2017). Can this differential contribution of visual channels to perception be extended to working memory domain? In the remaining chapters of this thesis, I will present a series of experiments that attempted to test this idea, and I will argue that the luminance channel has special contributions to working memory processing. I will demonstrate that luminance inputs lead to a better behavioural performance in visual working memory tasks and that this advantage is reflected in neural responses, as measured with electroencephalography.

Chapter 2

General methods and colourimetry

All experiments shared the same experimental setup and were run in the same laboratory. The next section describes details on equipment and experimental methods that were common for all experiments. Particulars specific for a given experiment, if different from the common setup, are detailed in corresponding experimental chapters.

Experiments were implemented in Matlab (Mathworks, Natick, Massachusetts) running on a Dell Precision PC on a calibrated cathode ray tube (CRT) monitor (NEC MultiSync FP2141SB; refresh rate: 109 Hz; resolution: 1264 x 790; see Section 7.4.1 for details on calibration procedure). The use of the CRT monitors is common in vision science due to their good temporal and spatial resolution, good image rendering independent from the viewing angle and low costs (Breinard, 2002). The CRT monitor on which the stimuli were presented was located in an electrically – shielded faraday cage. The CRT was the only source of light during the experiment. The monitor was kept on for least 15 – 30 minutes beforehand to ensure the RGB guns were evenly warmed up before any experiments commenced. Subjects responded using a button box (Cedrus RB – 740, Cedrus Corporation, San Pedro, USA) while seated 57cm from the screen on a comfortable hairdresser’s armchair.

7. Colour spaces

Accurate specification of the stimulus' features, such as chromaticity and luminance, requires the use of appropriate colour space. Colour spaces are systems used to organise and describe colours quantitatively. A range of colour spaces has been developed over the years (Westland, Ripamonti & Cheung, 2012). In this section, I will briefly describe the Commission Internationale de l'Éclairage (CIE) 1931 system, followed by a description of physiologically-meaningful colours spaces: LMS and Derrington-Krauskopf-Lennie (DKL). The latter two systems were developed as an attempt to relate colour specifications to physiological properties of the visual system. In other words, they are meant to serve as a model of how the visual system would react to lights of certain wavelengths. The DKL colour space is used across experiments presented in this thesis and I will describe it in more detail in the following sections. Nevertheless, the CIE and LMS systems are important as most of the routines used for monitor calibration and stimulus generation require conversions between the computer's RGB system and the CIE, LMS and DKL colour spaces.

7.1. The CIE 1931 colour space

The first colour space was developed by the Commission Internationale de l'Éclairage (CIE) in 1931 (for a detailed history of the development of the CIE, see Broadbent, 2004; Wright, 2007). This space is based on the observation that any colour can be matched by a mixture of three primary colours (primaries). The amount of each primary used to match a given colour is referred to as *tristimulus values*. Early colour matching experiments by Wright and Guild (Guild, 1932; Wright, 1929) used a specially constructed split-field, bipartite colourimeter (also called tristimulus colourimeter), designed by Wright (1928). During the experiment, observers looked at a field consisting of two parts, one containing the test colour, and the other one displaying a mixture of the three primaries. Observers were required to adjust the intensities of each primary so that they match the test colour. The tristimulus values were then read out by the experimenter.

Based on these experiments, colour matching functions were described (see Figure 9). Colour matching functions are derived by measuring tristimulus values separately at each wavelength, in tight intervals, within the visible spectrum of light (i.e. 400 – 700 nm). Together, these colour matching functions describe the so-called “standard observer”. Knowing how the tristimulus values change as a function of wavelength allows for the tristimulus values to be calculated for a given light without the need of performing matching by the observers (Westland, Ripamonti & Cheung, 2012).

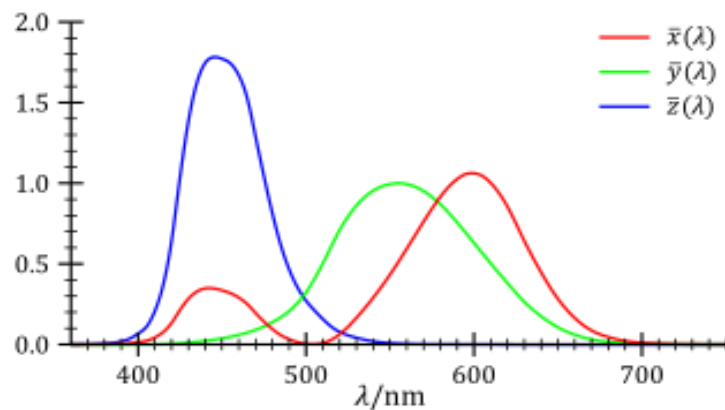


Figure 9 The CIE 1931 RGB colour matching functions. Image by Marco Polo, Wikipedia.

The widely used CIE 1931 system is based on the averaged colour matching functions obtained by Wright and Guild in separate experiments (Guild, 1932; Wright, 1929). The primaries are referred to as X, Y and Z. Importantly, these primaries are normalised mathematically, and thus do not represent real colours, but rather their more saturated versions. Normalising the primaries allows for representing colours using only positive values. Once the XYZ values are known, they can be transformed into two-dimensional coordinates: x and y . This is done by dividing the X and Y by the sum of the tristimulus values. Using this conversion, the CIE colour space can be mapped into a 2D plane (see Figure 10).

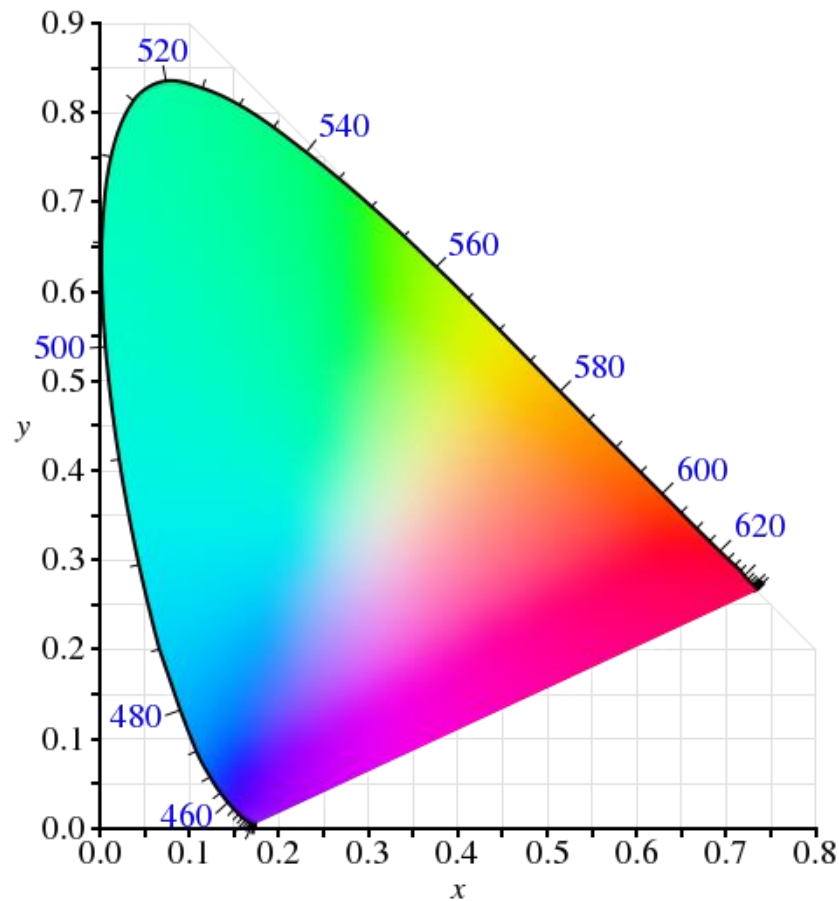


Figure 10 CIE chromaticity diagram (image: BenRG, Wikipedia).

The CIE 1931 system proved to be useful in science and industry by providing means of accurate colour reproduction across devices and displays. However, the CIE system has no direct relation to the physiology and neural computations performed by the visual system. Some attempts have been made to adapt the CIE system in order to improve its formalisation of colour appearance, resulting in the development of the CIELAB and CIECAM02 spaces. Still, all spaces based on the CIE system use values that have no direct physiological meaning (Westland, Ripamonti & Cheung, 2012). For this reason, a different set of physiologically meaningful colour spaces have been developed: cone excitation spaces and cone-opponent spaces (Westland, Ripamonti & Cheung, 2012).

7.2. Physiologically meaningful colour spaces

7.2.1. LMS-cone excitation space

The cone excitation space describes colours in terms of the excitation (i.e. absorption of light quanta) of the three primary retinal photoreceptors. In other words, such space provides a description of colours at the first stage of the visual system. As described in detail in the introduction, cones differ in terms of the probability that a photon of a given wavelength will be absorbed by them. A number of approaches have been used to describe the relationship between the contrast matching functions (described in the previous subsection) and the spectral sensitivities of the cones. One strategy is to use observers who lack some cone classes from birth: dichromats and monochromats. While missing some cone classes, other photoreceptors are spared in these observers since mono and dichromacy are simply a reduction of normal trichromacy. Therefore, instead of isolating a given cone class in a trichromatic observer, colour matching may be performed by observers who have only specific types of cones spared. Such approach has proved to be efficient and has been in use since the 19th century (Young, 1807; Helmholtz, 1866; König & Dieterici, 1886, 1893). Using this approach, Stockman and Sharpe (2000) measured cone spectral sensitivities, otherwise known as cone fundamentals. Knowing the cone fundamentals, it is possible to calculate cone excitation for a given stimulus by integrating the cone fundamentals data with spectral power distribution of the stimulus. In other words, published cone fundamentals allow for calculating cone excitation without the need to measure it directly. While there is a number of cone fundamentals sets to choose from (e.g. DeMarco, Pokorny, & Smith, 1992; Smith & Pokorny, 1975), we are using Stockman and Sharpe (2000) cone fundamentals measured for 2-degree stimuli for colour space conversions (see further subsections).

One of the drawbacks of the LMS colour space is that it is not meant to go beyond the first stage of vision, i.e. light absorption by cones. As mentioned in Chapter 1, the signals from all cone types are combined in subsequent stages,

creating three mechanisms: two chromatic and one achromatic. To describe colours in terms of how they arise from the combined activity of all cone classes, cone-opponent colour spaces may be used, such as the DKL space. Because our hypotheses concern these three visual channels, the DKL space is thus an appropriate choice to define the chromaticity of the stimuli used in our experiments. The next section will describe this colour space in more detail.

7.2.2. Cone-opponent colour space: the Derrington-Krauskopf-Lennie (DKL) space

Derrington-Krauskopf-Lennie colour space (DKL; Derrington, Krauskopf, & Lennie, 1984) describes colours in terms of such post-receptoral mechanisms (combinations of cone excitations). It was based on Macleod and Boynton's chromaticity diagram (MacLeod & Boynton, 1979) and earlier psychophysical research (Krauskopf, Williams, & Heeley, 1982).

The space was developed based on experiments performed on eight macaque monkeys, with the assumption that their spectral sensitivities correspond to those of a human. Derrington et al. presented macaques with gratings with varying chromaticity and luminance, whose coordinates were varied around a three-dimensional space. The responses of the ganglion cells were measured in the lateral geniculate nucleus (LGN) – the relay station between the retina and the cortex (see Chapter 1 for details). By measuring the responses of the ganglion cells, Derrington et al. were able to identify “*best response*” and “*null*” planes in that three-dimensional space for the measured cell. Stimulus changes along the *best response* plane modulated the response of the cell while modulating parameters along the *null plane* would produce no response. Their results confirmed that colour opponency at the level of LGN is served by three cardinal mechanisms: two achromatic and one achromatic, luminance mechanism. Derrington et al. also identified that the cells responsive to the achromatic direction were primarily located in the magnocellular layers, while the chromatic modulations produced responses of cells in the parvocellular layers (Derrington et al., 1984).

In this space, colours are defined as variations along three cardinal axes: achromatic and two chromatic. In the achromatic axis, the excitation of the L, M and S-cone classes is the same (see Table 1). In the red-green axis, the excitation of L and M cones varies while leaving the S-cone constant; hence it is sometimes referred to as “constant S-cone axis” (Kaiser & Boyton, 1996) or “red-green isoluminant” (Brainard, 1996). Along the third axis, the excitation of the S-cone is varied while L and M are held constant. This axis is therefore referred to as “constant L and M axis” (Kaiser & Boyton, 1996) or “S-cone isoluminant axis” (Brainard, 1996).

An important feature of the DKL colour space is that it describes stimuli in terms of its contrast against the background. The background provides a reference, or an adaptation level, against which the stimuli parameters are described. For this reason, the DKL colour space uses arbitrary values relative to the used background.

Table 1 The three cardinal axes in DKL colour space. L, M and S refer to long, middle and short wavelength cone classes, Δ signifies a difference in excitation between the stimulus and the background, BG refers to the background (so that, for example, L_{BG} signifies the L cone excitation of the background).

Cardinal axes in the DKL colour space

Achromatic axis	$\Delta L/L_{BG} = \Delta M/M_{BG} = \Delta S/S_{BG}$
Red-green axis	$\Delta S = 0$
S-cone axis	$\Delta L = \Delta M = 0$

Modulations along the two chromatic axes produce different colour appearances, the L & M axis producing colours in the red-green range (hence Brainard’s “red-green” axis), while the S-cone axis produces colours in the blue-yellow range.

Any point in the DKL colour space is described using the following coordinates: a radius (r), the angle of rotation (ϕ_{DKL} ; also referred to as “DKL direction”), and angle of elevation (θ_{DKL} ; see Figure 11).

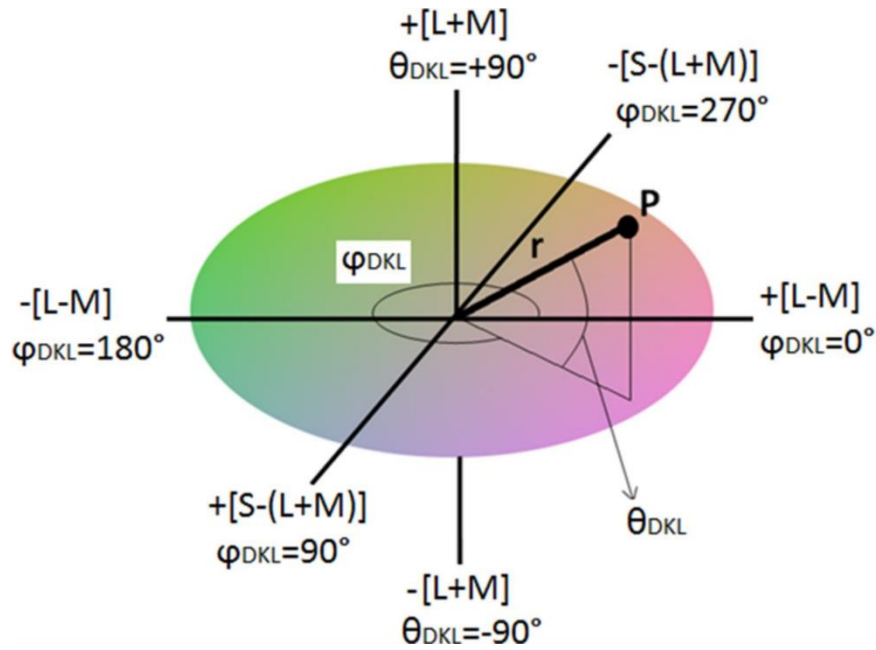


Figure II The DKL colour space. Figure: Jennings & Martinovic (2014). “P” provides an example of a point with the chromaticity of both L – M and S – (L+M) (defined by the appropriate angle of rotation ϕ) as well as a luminance (L + M) component (defined by the angle of elevation θ).

7.2.3. Use of DKL colour space to stimulate cone-opponent and luminance mechanisms

It is important to note however that the colour in itself is not of interest in this thesis, but rather cone mechanisms that happen to produce these colours. The DKL colour space is particularly useful to achieve this goal as it allows to define the stimuli not only in terms of the respective L, M and S-cone modulations (as described above) but can be easily used to create stimuli that will correspond to the hypothetical psychophysical mechanisms. As mentioned in the introduction, psychophysical experiments suggested the existence of three such mechanisms: two cone-opponent, chromatic mechanisms and luminance, achromatic mechanism.

The first mechanism weights the difference between L and M-cone excitations (i.e. “L – M”). The second takes the weighted difference between S-cone and summed L and M-cone excitations (“S – (L+M)”). The luminance sums L and M-cone signals (“L + M”). The luminance elevation must be held constant for the chromatic mechanisms in order to make the stimuli isoluminant. The r parameter can be thought of as reflecting the intensity of the colour stimulus, as

the larger the value, the further away from the white point (background) we move, which corresponds to increased contrast. The angle of rotation determines which particular chromatic mechanism is stimulated. The L – M mechanism is achieved with an angle of 0° (for increment) or 180° (for decrement). The S – (L + M) is achieved with an angle of 270° (increment) or 90° (decrement).

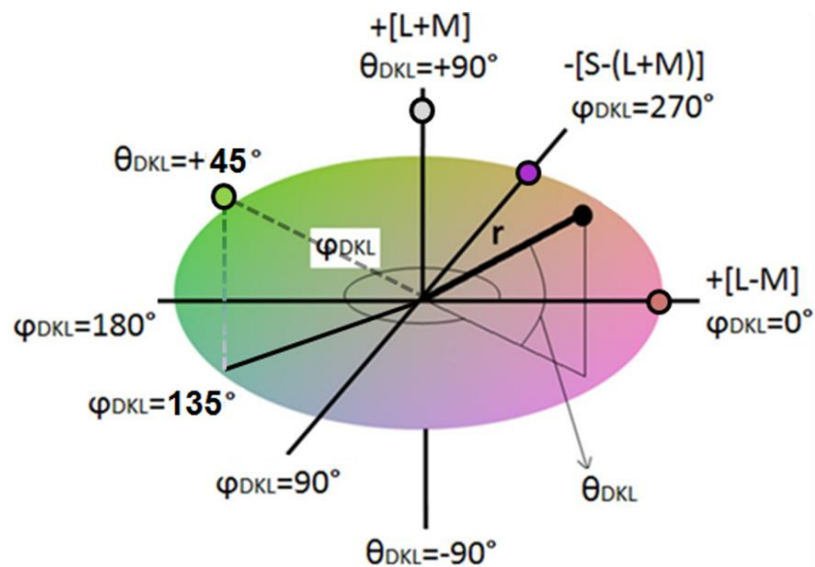
Modulating the elevation stimulates the luminance mechanism (i.e. L + M). In our experiments, elevation value is fixed at 90° (for increment) or -90° (for decrement), as at these angles the achromatic mechanism is isolated. Similarly to chromatic directions, r is used as an index of intensity (contrast).

Throughout the thesis, I will refer to the two chromatic mechanisms as *L – M* and *S-cone isolating* (or *S-cone*). I will refer to the achromatic, luminance mechanisms simply as *luminance*.

It is also possible to engage all three mechanisms simultaneously using appropriate coordinates in the DKL space. In our experiment, we incorporate such a condition where the stimuli are meant to engage both chromatic mechanisms as well as the luminance mechanism. This condition is referred to as *mixed signals* condition. It was mainly used as a control condition to characterise how responses to isoluminant conditions would be affected if they contained a luminance artifact (McIlhagga & Mullen, 1996). Further details and rationale for its use are provided in experimental chapters. Table 2 (column 1 and 2) lists labels used to describe experimental conditions as well as psychophysical mechanisms along with their coordinates in the DKL space.

Table 2 Psychophysical mechanisms of interest and their corresponding DKL coordinates. Only angle and elevation are provided as r is either fixed at individuals' discrimination threshold (Experiment 1, chapter 3) or serves as the dependent variable in threshold experiments (experiment 2 and 3, chapter 4). *The elevation of $L - M$ and S -cone is not 0° , but is determined from the HCFP procedure to adjust for individual's point of isoluminance. Signs in brackets corresponds to the polarity of the angle or luminance elevation (+ for increment and - for decrement). A rough appearance of the stimuli as it could appear on the display is provided, along with a position inside the DKL space (radius r is given only arbitrarily for presentation purposes).

Label	Mechanism	Angle	Elevation	Approx. appearance
Chromatic blue-yellow (S-cone)	$S - (L + M)$	$270 (+)$	x^*	 
Chromatic red-green	$L - M$	$0 (+)$	x^*	 
Achromatic luminance	$L + M$	0	$90 (+)$	 
Mixed signals	$L - M$ & $S - (L + M)$ & $L + M$	$135 (-)$	$45 (+)$	 



Previous studies using DKL colour space tested both increments and decrements (e.g. Martinovic et al., 2011), but as they appeared to produce similar responses, the data were collapsed across increments and decrements. We did not test both increments and decrements of each mechanism to reduce the number of conditions in our experiments. We choose either decrement or increment arbitrary to make the stimuli appearance different across conditions.

7.2.4. Summary

To summarise, the DKL colour space is of particular use to vision scientists aiming to investigate the contribution of the post-receptoral mechanisms to visual perception. Using an appropriate set of coordinates, it is possible to define the chromaticities and luminance of stimuli so that they excite one of the three cardinal mechanisms in isolation or some intermediate mixture of the three. Because of this feature, all experiments presented in this thesis are using the DKL space to define the chromatic and luminance properties of the stimuli.

7.3. Observer's isoluminance – heterochromatic flicker photometry (HCFP).

Individuals differ in terms of the luminous efficiency function (Wyszecki & Stiles, 1982; Wyszecki & Stiles, 2000). As a result, luminance artifact can be present alongside chromatic signals, thus violating the isoluminance of the stimuli.

However, this can be avoided by applying an appropriate correction.

Heterochromatic flicker photometry method (HCFP; Walsh, 1958) is usually used to address this issue by adjusting for individual's point of isoluminance (e.g. Kosilo et al., 2013; Martinovic et al., 2011; Ruppertsberg, Wuerger, & Bertamini, 2003; Wuerger, Ruppertsberg, Malek, Bertamini, & Martinovic, 2011).

HCFP takes advantage of the superior temporal resolution of the luminance channel over opponent-chromatic channels. Experiments on macaque monkeys confirmed that the magnocellular system underlies performance on this task (Lee et al., 1988). The luminance system is able to detect fast temporal changes, such as flickering at high frequencies. In the HCFP procedure, the observer is adjusting

luminance contrast of a flickering stimulus so that the perception of the flicker is minimized. If the perception of the flicker is minimal, so is the luminance difference. Corresponding value provides an isoluminant correction for a given individual.

This technique can be applied to the DKL colour space. The procedure used in our experiments is based on previous studies, with modification (Ruppertsberg, Wuerger, & Bertamini, 2003; Martinovic, Mordal, & Wuerger, 2011; Kosilo et al., 2013; Jennings & Martinovic, 2014). Participant adjusts the luminance elevation for each chromatic direction (L – M and S-cone) using a response pad (CEDRUS RB-740, San Pedro, CA) for a stimulus presented at a fixed radius (r) until the perception of flicker was minimal. In all our experiments, the stimulus is presented in the middle of the screen, flickering at 20Hz against a grey background. Participants did in total 8 to 10 adjustments reliably (after the removal of the outliers) and the average was taken and used as a luminance angle value for the corresponding DKL condition.

7.4. Display calibration & gamma correction procedures

This section provides details on display calibration and further procedures that helped to verify the calibration. An overview of the steps is provided in Figure 12 below.

7.4.1. Calibration

In CRT displays, the voltage is delivered to the cathode ray tube which emits light via red-green-blue (RGB) electron guns. The relationship between the input voltage to the monitor and the resulting output luminous intensity of the display is non-linear. This relationship is described by gamma functions. In order to ensure that the input provided by the user (here, the experimenter) produces a light intensity that is actually desired, one needs to apply the gamma correction. This is done simply by inverting the gamma function so that the input value needed to produce any desired output can be found.

The calibration of the monitor in our laboratory (Figure 12., I) was done using the CRS calibration system (ColourCAL II, Cambridge Research Systems, Ltd., Kent, UK). Before commencing the calibration, the monitor was kept on for at least half an hour to ensure that the RGB guns were warmed up. Subsequently, a white uniform patch was displayed on the screen and the red, green, and blue phosphor guns of the CRT were balanced to adjust the intensity of the white display so that it corresponded to the CIE standard illuminant D65. The standard illuminant is commonly used in colourimetry. It refers to a theoretically defined source of light which spectral power distribution is provided by the International Commission on Illumination (CIE). It is meant to represent a daylight illumination. Its coordinates are defined in the CIE 1931 Colour Space (CIE, 1931; Smith & Guild, 1932; see section 7.1) and are $x=0.31271$, $y=0.32902$. Once the colourimeter readings were satisfyingly close to these values, the monitor calibration procedure commenced (Figure 12, A).

Measurements were performed at 256 voltage input levels in evenly-spaced intervals for each gun (red, green and blue) to ensure sufficient precision. Lookup tables that specify the gamma functions are created based on these measurements and are read automatically by the ViSage system before any stimulus or colour is displayed (using CRS Toolbox functions).

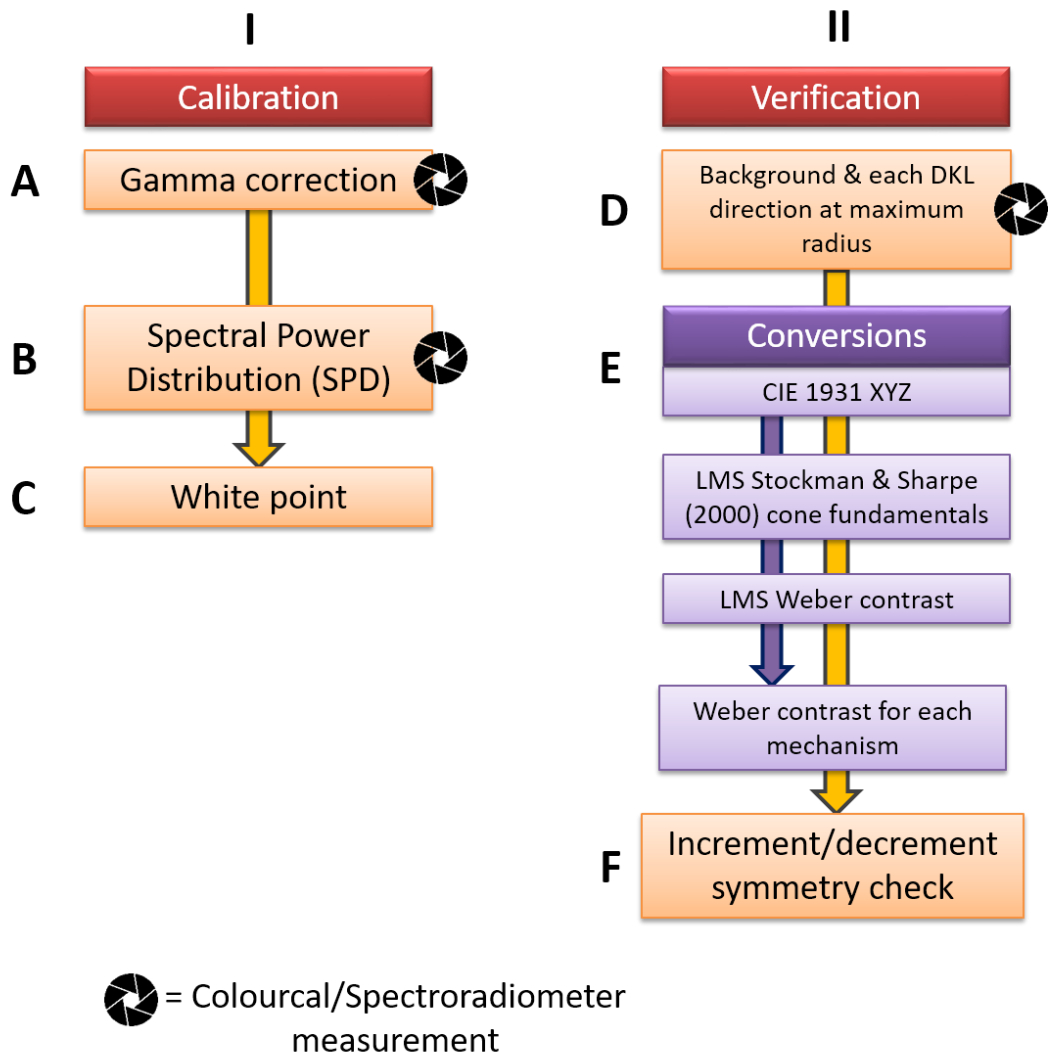


Figure 12 A general outline of calibration and verification procedure steps. Main text provides details on each step.

After calibration was completed, the next step involved specifying the monitor’s gamut (the range of chromaticity the monitor is capable of displaying) and obtaining the coordinates for the “white point” to be used as the background during the experiments. In any colour space, the white point refers to a set of coordinates which define the colour “white”. To obtain the white point, the spectral power distribution of the display must be known first (Figure 12, B). This is done by displaying red, green and blue patches on the screen and measuring their emittance using a spectroradiometer (SpectroCal, Cambridge Research Systems, Ltd., Kent, UK). Combined readings of these three colours give the spectral power distribution (SPD) of the display (see Figure 13 for an example

SPD). The monitor's gamut and the white point was derived using the routines from the CRS Colour Toolbox (Figure 12, C). Device SPD and the white point are saved in separate files and are loaded during the experiment. This ensures that the rendered colours are gamma-corrected, with the background specified by the white point coordinates every time the experiment was run.

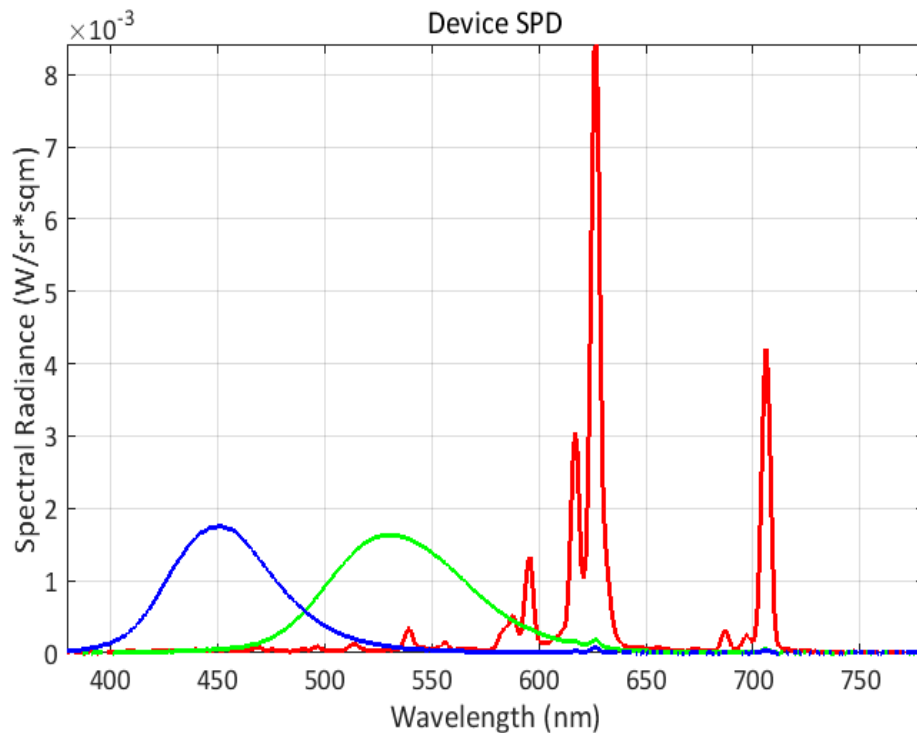


Figure 13 An example of the spectral power distribution (SPD) of the display used in the experiments. Note that the monitor was recalibrated across different experiments.

7.4.2. Verification procedures

The next step verified the accuracy of the calibration (Figure 12., II). We use the DKL colour space which assumes that any two points on a given axis, at the opposing sides of the white point, are symmetrical, i.e. they have the same radius at a given angle and elevation. For any point in the DKL (or any other) colour space, one can estimate the excitation of the L, M and S-cones of an observer, if the observer was looking at a stimulus characterised by the coordinates of that point. Our aim was to ensure that this symmetry is true when moving from DKL coordinates to cone excitations. This can be done by displaying opposing points on the DKL space at a given angle and elevation, measuring their spectra using

the spectroradiometer, and calculating the LMS excitations based on these measurements.

A uniform colour patch was displayed for the three cardinal axes at a maximum radius (at either side of the white point, i.e. increment and decrement) that could be reproduced within the monitor's gamut, as well as for the background (i.e. the white point, with DKL coordinates of 0, 0, 0). Additionally, we have also measured out increment and decrement at an angle of 45 and 135, with an elevation of 45 for the *mixed signals* stimuli class.

Each patch was measured out using the spectroradiometer (Figure 12, D), which gave the coordinates in the CIE 1931 xyY colour space. Spectroradiometer readings were followed by colour space conversion procedures (Figure 12, E). Firstly, CIE coordinates obtained using the spectroradiometer were converted into the LMS colour space, based on the Stockman and Sharpe cone fundamentals (Stockman & Sharpe, 2000). As described in the previous section, LMS space essentially models human colour perception and allows for colours to be expressed in terms of excitation of the three cones of the human eye: long (M), medium (M) and short (S) cones. A particular LMS model that is used here is one based on Stockman & Sharpe's (2000) two-degree cone spectral sensitivities.

To convert between the two colour spaces, a conversion matrix is required. A conversion matrix is calculated based on phosphor spectra of the (calibrated) display and cone sensitivities. This was done using a method described in Golz & MacLeod (2003).

After the LMS excitations are calculated for the maximal radius for each DKL condition, excitation for each cone is then expressed in Weber contrast values; this is done using the following formula:

$$W = \frac{Tc - Bc}{Bc}$$

where W represents Weber contrast, Tc denotes target cone excitation, and Bc denotes the corresponding cone excitation of the background. For example, to calculate Weber contrast for the L cone, c is replaced with a specific cone excitation, so that

$$W = \frac{Tl - Bl}{Bl}$$

where Tl corresponds to L cone excitation of the target and Bl corresponds to the L cone excitation of the background.

Following the calculation of contrast for each cone class, the contrast for each mechanism was calculated according to a formula describing that mechanism (that is, L - M, S - (L+M) and L+M). At this point, we know the cone excitation of each of the three mechanisms, expressed in Weber contrasts, for the maximum radius of the particular DKL direction. Having those, we can finally verify the calibration by calculating the difference between increment and decrement contrasts for each mechanism (Figure 12, F). Contrasts were concluded to be symmetrical if the difference was not greater than 5%. If that was not the case, the RGB guns were adjusted and the calibration procedure was repeated until satisfactory results were obtained. For each calibration used in our experiments, the difference did not exceed 1%.

Note that in the DKL space, the contrasts should scale linearly when moving along a line specified by a certain angle of rotation and elevation. Hence, having measured the contrast for each DKL direction at a given radius, it is possible to work out the contrast of any radius for that direction. We take advantage of this while converting individuals' detection, discrimination and working memory thresholds to contrasts (see experimental chapters for details).

7.5. Re-calibration

The display was re-calibrated between experiments, and in one instance during the experiment due to a technical error. Display use was monitored and the calibration was re-checked (using verification procedures described above) after the display was used for more than 100 hours in total.

The following section describes some of the common details of the experiments presented in this thesis. The individual experimental chapters specify any deviations or additions to procedures described below.

7.6. Stimuli & on-line DKL conversions

102 BORTS (Blurred Outlines of Random Tetris Shapes; Linden et al., 2003) were used for stimuli in the study. The shapes are created by randomly distorting shapes from a *Tetris* video game (Pajitnov, 1984) to obtain a set of non-natural, abstract objects. They were successfully used in previous experiments using similar design (Linden et al., 2003; Haenschel et al., 2007). These formed the default stimulus pool for all experiments. Shapes were presented at varying orientations to increase the number of stimuli that appeared unique.

The stimuli were created off-line and were initially monochromatic. Their chromaticity and orientation were set on-line, during the experiment, before they appeared on the screen. This was done using CRS Toolbox routines, based on procedures used previously (e.g. Kosilo et al., 2013; Martinovic et al., 2011). Current stimulus parameters are determined by the experimental condition in a given trial.

8. Psychophysics – overview of methods used to estimate threshold.

Experiments described in this thesis use psychophysical procedures for threshold estimation. In this section, I will provide a quick overview of various psychophysical methods. I will first define what is meant by detection and discrimination thresholds, along with the tasks used to estimate them.

Subsequently, I will describe different methods of manipulating the stimulus magnitude during different tasks. I will primarily focus on the adaptive QUEST (Watson & Pelli, 1983) since it was used in all experiments. Additionally, experiments described in Chapter 4 also incorporated the method of constant stimuli.

This section is not meant to be an exhaustive overview of all psychophysical methods available but is rather provided to give a quick overview of the procedures used in this thesis and how they are classified in relation to other methods. A detailed description of other methods has been presented elsewhere (e.g. Ehrenstein & Ehrenstein, 1999; Kingdom & Prins, 2012; Pelli & Farell, 1995; Pelli & Farell, 2010). The exact implementation of the methods will be provided in the methods section in the corresponding experimental chapter.

8.1.1. Detection and discrimination thresholds

Detection threshold refers to stimulus magnitude value required for stimulus detection at a given performance level. The threshold is usually defined by the experimenter as a certain percentage derived from observer's performance in a task. For example, a threshold of 75% reflects the observer's ability to detect the stimulus at a specific contrast level correctly 75% of the time.

In other words, the threshold (as well as the associated slope of the psychometric function) can be used as a measure of a relative efficiency with which the perceptual representation of a stimulus is created. They can also be utilised to infer the efficiency of a mechanism responsible for processing certain stimulus. In

that sense, lower threshold reflects better efficiency of the system, since less physical intensity is required to produce a response.

One of the widely used paradigms in estimating detection thresholds is a two-interval forced choice task (2IFC). The observer is presented with two intervals, one empty, and one containing a target. The task is to indicate which of the intervals contains a target. Experimenter manipulates the magnitude of a given stimulus parameter, such as contrast. By doing so, one can describe the relationship between the probability of detecting stimulus (i.e. correctly indicating which interval contained the target in this case) and the magnitude of a parameter of interest (here, contrast). The threshold is defined as stimulus magnitude value at which the observer reaches a certain level of proportion correct above the chance level (50%), for example, 75%. Detection thresholds were used in Experiment 2 (see Chapter 4).

Other widely estimated thresholds are discrimination thresholds. These are often obtained using a standard two-interval forced choice task, or the 2IFC. The observer is presented with two temporally-spaced intervals (i.e. presented one after another), each one containing a stimulus. For example, one interval could contain a Gabor patch oriented to left, while the second one a Gabor oriented to the right. After the presentation, the observer is required to respond, for example, which of the two stimuli was oriented to the left. In another variation of the task, the two-alternative forced choice task (2AFC) the procedures are identical to the 2IFC, except that in the former the two stimuli are presented simultaneously (e.g. on either side of the fixation cross), and not temporally spaced as in the 2IFC (where the stimuli are presented in the middle of the display, and hence viewed foveally). Similarly, as with detection thresholds, one stimulus feature (here, orientation) is adjusted, and the discrimination threshold reflects the magnitude of the difference that allows the observer to tell the two stimuli apart with a certain probability.

Notably, the 2IFC/2AFC tasks (as described above) are usually used to estimate discrimination thresholds for a single stimulus dimension known to the participant (e.g. orientation). There are instances, however, where one wants to

measure discrimination from a range of multiple stimulus dimensions. Another example is when one wants observers to discriminate between two stimuli without specifying what dimension/stimulus feature the observer is supposed to use to make a discrimination. This kind of discrimination threshold can be referred to as “same/different threshold”. The usual task used to measure such thresholds is a same/different task. In this task, participants are presented with two stimuli and are required to respond whether they appear to be same or different. The stimuli might be presented either simultaneously on either side of the fixation cross, or they can be temporally spaced, similarly to the 2IFC task. During the task, a certain stimulus dimension is manipulated, for example, the contrast of the stimuli. Threshold will thus reflect the certain probability of the observer to tell the two stimuli apart at a given contrast level. It is important to note that the discrimination is not based on the contrast per se. The underlying assumption is that this stimulus dimension will affect the individual’s ability to make a same/different judgement. This task is referred to sometimes as a match-to-sample task.

The same/different threshold task is used in Experiment 1 as a control measure (see Chapter 2, “EEG experiment”). This kind of task is appropriate to our experiments: we are using abstract shapes, but we are not interested in which stimulus dimension is used to make a discrimination, but rather, how manipulating colour or luminance contrast will affect the overall ability to tell stimuli apart.

8.1.2. Adjustment methods

Adjustment methods assume full control of the stimulus magnitude to the observer. The observer adjusts the magnitude of the stimuli manually. For example, if the task is measuring contrast detection threshold, the observer is presented with stimuli at certain contrast level. The contrast level is adjusted by the participant himself until it just becomes visible. The observer can be also presented with a standard stimulus and asked to adjust another stimulus so that it either matches the standard or becomes just noticeably different than the

standard. The value associated with observer's choice is recorded to provide an estimate of the threshold. In these experiments, our HCFP procedure uses this method.

8.1.3. Method of constant stimuli

The method of constant stimuli (as well as adaptive methods described in the next section) does not allow observers to make adjustments themselves. Instead, the stimulus magnitude is adjusted from trial to trial. This technique provides a more standardized way of measuring the threshold (Ehrenstein & Ehrenstein, 1999) and is used in designs where observers are "forced" to respond from trial to trial. Because of the nature of such tasks, trials must be somehow sequenced. In the method of constant stimuli, the experimenter generates a list of stimulus intensities. The stimulus intensity on a given trial is randomly chosen from such a predefined list. The aim is to cover stimulus intensities that produce responses ranging from near-chance to near-100% correct (Kingdom & Prins, 2012). Each intensity level is presented multiple times per condition (e.g. 100 times). A psychometric function is then fitted to the data to obtain the threshold, i.e. stimulus value at which the observer achieves, for example, 75% correct level (depending on how the threshold is defined). Psychometric function is simply a function that describes the relationship between the stimulus intensity and the percentage of correct responses.

8.1.4. Adaptive procedures

Another common method of threshold estimation is the adaptive staircase procedure. The stimulus level is determined by the programme from trial to trial and is dependent on observer's performance on previous trials. By itself, the adaptive procedure is not designed to specifically adjust the stimulus intensity downwards by some degree in case of a correct response, and upwards in case of incorrect response. However, this is the way the procedure usually ends up behaving (it can be thought of as an emergent property of this procedure; Kingdom & Prins, 2012).

There is a number of methods used to determine the stimulus intensity on proceeding trials. In the up/down method (Dixon & Mood, 1948), correct response increases stimulus intensity by one step, and in case of an incorrect response, the intensity is decreased by one step. Step size is pre-determined by the experimenter and requires some pilot testing. There are variations of the up/down method. For example, in the transformed up/down method, on the other hand, the “decision” to increase or decrease the intensity is based on a few preceding trials rather than one. For example, one of the commonly applied rules is a 1 up/2 down rule, where the step up is made after one correct response, but to make a step-down, two consecutive incorrect responses are required. In a weighted up/down method, the size of the upward steps is not equal to the size of downward steps.

The threshold in the up/down method can be estimated by averaging intensity levels in the last few trials. Notably, up/down method can be used only to guide the flow of the experiment, and the threshold can be estimated by pooling the responses and fitting a psychometric function to them, as was the case with the method of constant stimuli. Doing so additionally enables to estimate the slope of the psychometric function. Such use of this method is referred to as hybrid adaptive procedure.

A more sophisticated set of methods that allow for a considerable reduction of trial numbers are running-fit methods, otherwise known as the maximum likelihood procedures (Hall, 1968; Taylor & Creelman, 1967). In this family of procedures, some of the parameters of the psychometric function (such as threshold and slope) are selected by the experimenter before the start of the experiment. During the experiment, after every trial, a psychometric function is fitted to the data that was collected so far. The fit is updated as the trials proceed. Estimated threshold value from such fit is then used to update stimulus intensity on proceeding trial. In practice, this means that intensity steps become smaller as the trials proceed – the algorithm essentially “homes-in” on the threshold (Kingdom & Prins, 2012).

The adaptive procedures are considered to be more efficient in comparison to other methods, such as the method of constant stimuli. The main reason for that is that adaptive methods present stimuli at intensities which are more likely to be informative in terms of the threshold value that we try to estimate (or any other parameter of interest). In the method of constant stimuli on the other hand, since the intensities are fixed, one can potentially waste trials by presenting stimuli multiple times at a level which will lead to an incorrect answer 100% of the time.

There is a number of different methods available within adaptive approaches. In The Best PEST method (Pentland, 1980; Taylor & Creelman, 1967), all parameters of the psychometric function are assumed before the experiment, apart from the threshold, which value is updated based on the preceding trials. Another method, called the QUEST procedure (Watson & Pelli, 1979; Watson & Pelli, 1983) is similar to the PEST, however, it takes advantage of the Bayesian approach. The experimenter decides on all parameters of the psychometric function – including the thresholds – before the experiment. This serves as a prior, which is updated as the experiment progresses. The prior serves as a guide to select the intensity of the upcoming trial. This procedure has been recently extended (Watson et al., 2017); the classic QUEST procedure allows for the stimulus intensity to be adjusted only along one stimulus dimension, such as contrast. The new QUEST (QUEST+) procedures have been updated to incorporate more than one stimulus dimension to be handled simultaneously, as well as allowing for more than one response outcomes (e.g. yes/no, correct/incorrect), among other additions.

With both of the adaptive methods, the parameters of the psychometric function can be derived from the function that was fitted by the programme at the end of the experiment. However, this can be also done “off-line”, by pooling the data collected during the experiment and making a new fit. In this sense – just like with the methods of constant stimuli – staircase procedures might be used to guide stimulus selection, rather than being a mean of obtaining parameters of interest.

In all experiments described in this thesis, we use the (original) QUEST procedure for selection of stimulus intensity. Threshold and slope are derived off-

line by fitting the psychometric function to the collected data (Prins & Kingdom, 2009). In experiments described in Chapter 4, we also use the method of constant stimuli to provide some additional control measures. All the details about the parameters and exact implementation of the procedures are provided in the methods section of the corresponding experimental chapters.

Chapter 3

The contribution of luminance signals to visual working memory performance – a study using EEG

As mentioned in the introduction, the main goal of this thesis is to investigate interactions between early perceptual processing and WM. We decided to focus on the contribution of luminance and chromatic mechanisms to WM performance. It was hypothesised that stimuli designed to predominantly engage the luminance mechanism would benefit WM performance.

This was investigated using a well-established paradigm, namely the delayed match-to-sample task (Haenschel et al., 2009; Haenschel et al., 2007; Linden et al., 2003). In this task, participants remember a number of shapes and are subsequently presented with a probe. Participants need to judge whether the probe is same or different from the remembered shapes. Unlike the majority of tasks probing WM (e.g. Bays et al., 2011b; Luck & Vogel, 1997), we are using a design in which stimuli are presented sequentially, one at a time. On each trial, WM load was manipulated by presenting one, two, or three stimuli in succession. The rationale was to probe WM without adding the complexity of having to encode a number of items simultaneously. This has also allowed probing the effects of WM load directly – participants were required to encode a new item while holding the previous one in memory. Thus, we could investigate how the number of items already in memory would affect the neural encoding of a new item (Agam & Sekuler, 2007). Such strategy, therefore, maximises the effect of prior processing on the processing of the current shape (Haenschel et al., 2007).

It was predicted that the luminance advantage would be manifested in a higher proportion of correct responses and faster reaction times for the luminance-defined shapes than for isoluminant stimuli.

Apart from engaging different post-receptoral mechanisms, there was a number of other factors that were manipulated in this study. Firstly, stimuli were presented either at low or high contrast levels. Contributions of post-receptoral mechanisms to stimulus processing tend to overlap at high contrasts during shape processing (Ivanov & Mullen, 2012). Furthermore, with luminance-defined stimuli presented at low contrast, the signal is processed largely through the magnocellular pathway. As mentioned in the introduction (see Chapter 1, Section 4.4), the parvocellular responses are typically absent when a stimuli with less than 10% contrast are used – this is mostly due to magnocellular cells being more sensitive to contrast (Derrington et al., 1984; Hicks, Lee, & Vidyasagar, 1983; Kaplan & Shapley, 1982; Shapley, 1990; Vidyasagar et al., 2002). At high contrast, luminance-defined stimuli would be therefore processed by both magnocellular and parvocellular pathway. To that end, we decided to dissociate between low and high contrast levels in our task, with a prediction that luminance effects will be more pronounced at low contrast.

Furthermore, we also differentiated between match/mismatch (same/different) judgements, i.e. trials where the probe matched the previously presented stimuli or not. The processes behind the comparison between memory representation and incoming stimuli in working memory have sparked relatively little interest (Hyun, Woodman, & Vogel, 2009), though some authors postulate that the memory-percept comparison is a distinct stage that deserves more attention (Yin et al., 2012). The distinction between detecting familiarity or novelty (analogical to our match and mismatch conditions, respectively) is crucial here: the current evidence and theoretical accounts highlight that these two processes are not equivalent (Hyun et al., 2009). For example, Bledowski, Kaiser, Wibral, Yildiz-Erzberger and Rahm (2011) reported that mismatch-dissimilar probes were accurately rejected regardless of memory load. On the other hand, rejecting match probes or similar probes (probes similar to sample) was worse with increasing WM load. For this reason, we decided to investigate how working

memory performance in a delayed match-to-sample task is affected by match/mismatch comparisons.

An important aspect of the delayed match-to-sample task used in this experiment is that it allows to clearly differentiate between working memory stages: the encoding, maintenance and retrieval. Processing at each stage appears to be crucial for performance (e.g. Bays et al., 2011; Haenschel et al., 2007; Woodman & Vogel, 2005). It is worth noting that, given our design, behavioural data alone makes it difficult to determine which working memory stage contributed to task performance, or at which point the hypothesised luminance advantage starts to take effect. The response made at the end of the trial is a result of processes occurring at each stage. Distinguishing between match/mismatch responses is helpful in that respect, as it is only at the retrieval stage that participants are presented with such judgement and there are no other cues that could allow for differentiating between match/mismatch processing at earlier WM stages. Still, relying on behavioural data alone is preventing us from making any stage-specific conclusions about the mechanisms that are likely to underlie performance in our task. In order to investigate WM processing at different stages, we are therefore taking advantage of the millisecond temporal resolution of the electroencephalogram (EEG). In the section below, I will briefly describe this technique and outline studies that used it to investigate visual working memory.

9. Investigating visual working memory using EEG

EEG records electrical potentials of the brain from the scalp and is one of the oldest and one of the most widely used techniques in human imaging (Millet, 2002; La Vaque, 1999). The signal that is recorded by an EEG electrode is a local field potential propagated from its cortical source through the tissue, resulting in a spatiotemporal distortion and smoothing of the signal recorded at the electrode (Buzsáki, Anastassiou, & Koch, 2012). It is generally agreed that the signal originates from postsynaptic potentials of populations of cortical neurons (more specifically, pyramidal cells), firing in synchrony (da Silva, 2009; Holmes & Khazipov, 2007; Jackson & Bolger, 2014; Kandel, Schwartz & Jessell, 2000).

The EEG signal is very rich in information and there is a number of measures that can be derived from it using a variety of signal processing techniques. One of the most widely used measures derived from the EEG signal are event-related potentials, or ERPs (Luck, 2014). ERPs are obtained by time-locking the EEG activity to an event of interest and averaging this activity over a number of trials. As a result of this procedure, variation in the EEG signal should be averaged out, leaving a task-related activity. Averaging EEG signal to extract ERPs during various perceptual and cognitive tasks allows for identifying a specific “signature” related to the processes of interest. It was discovered that some of these signatures – termed ERP components – occur at a variety of tasks and that their amplitudes and latencies (i.e. approximate times at which they appear in the waveform) can be experimentally manipulated (Luck, 2014). Research has sought to identify factors which modulate strength and latency of various ERP components. They span from low-level perceptual, stimulus-dependent factors (such as stimulus contrast level) to factors related to higher cognition (such as object recognition or attention).

In this experiment, we will use this technique as a measure of neural processing during working memory processing. ERPs have been used in the past to infer about neural processing behind cognitive functions, including working memory (e.g. Drew, McCollough, & Vogel, 2006; Luria, Balaban, Awh, & Vogel, 2016; Woodman & Vogel, 2005). One of the advantages of the ERP technique is that it

allows investigating the time course of activations during WM processing (Luu et al., 2014). Furthermore, the millisecond resolution is required to fully understand how working memory processing unfolds with time (Agam et al., 2009). Various labs have shown that event-related potentials sensitive to WM processing are found at various latencies after stimulus presentation; Luu et al. divide them roughly into early (around 200 ms), mid (390 ms) and late latencies (600 – 900 ms; Gevins et al., 1996; Luu et al., 2014). ERPs at early and mid-latencies appear to be reflecting memory maintenance requirements, memory updates and selection of relevant stimuli for maintenance, while later components appear to reflect inhibition of distractors or memory updates (Kiss et al., 1998, 2007; McColough et al., 2007; Yi & Friedman, 2011). However, ERP components that seem to be sensitive to WM are also found earlier than 200 ms (e.g. Agam & Sekuler, 2007; Haenschel et al., 2007).

In our experiment, we aim to identify ERP components that can index the interaction between perception and WM. More specifically, we are interested how these components will be modulated by stimuli engaging luminance or isoluminant mechanisms, and whether any modulation will be also dependent on WM load. Since there is a number of different components that we expect to observe, I will now describe each separately. I will focus on what factors influence their amplitude and latency, with emphasis on perceptual and WM factors. This will be followed by a summary of our predictions regarding how the components will behave in response to luminance/isoluminant stimuli and WM load. We will relate that to specific hypotheses of this thesis.

9.1. Use of ERP components to study visual working memory

9.1.1. Visual component P1

P1 (or P100) is a positive component with an onset of approx. 60 ms – 90 ms after presentation of a visual stimulus. The peak reaches its maximum around 100 ms and 130 ms (Luck, 2014). The component is largest at lateral occipital and parietal sites. This is consistent with studies that attempt to localise the neural generators of this component (Di Russo, Martínez, Sereno, Pitzalis, & Hillyard, 2002). Studies using mathematical modelling paired with fMRI measures suggest that, based on its localisations, the P1 can be divided into two parts. Its early portion (80 – 100 ms) appears to be generated in the dorsal extrastriate cortex in the middle occipital gyrus and its later part (100 ms – 130 ms) is generated in ventral extrastriate cortex of the fusiform gyrus (Di Russo et al., 2002; Martínez et al., 1999; Martínez et al., 2001). However, as Luck (2014) emphasizes, other cortical areas – beyond extrastriate areas – are also likely to contribute to the P1 (Luck, 2014; Foxe & Simpson, 2002). Nevertheless, because of its localisation in the cortex, P1 is responsive to changes in various low-level stimulus properties, which affect both its latency and amplitude (Luck, 2014). For example, component's latency as well as amplitude is modulated by varying contrast levels (Shawkat & Kriss, 2000; Souza, 2007; Elleberg & Hammarrenger, 2001). Higher luminance also elicits higher occipital P1 amplitude (Johannes, Münte, Heinze, & Mangun, 1995). These effects also appear to vary according to spatial frequency of the stimulus. At low contrast, the P1 amplitude in response to low frequency stimuli increases and rapidly saturates (Baseler & Sutter, 1997; Elleberg et al., 2001; Klistorner et al., 1997; Souza et al., 2007). Comparing low versus high contrast responses also reveals longer latency for the former (Luck, 2014).

Elleberg & Hammarrenger (2001) investigated the contribution of the magnocellular and parvocellular pathway to the generation of ERPs. These studies are relevant to our experiment as post-receptoral mechanisms that our stimuli excite map onto those pathways (see Chapter 1 for details).

Using sinusoidal gratings of varying spatial frequency and contrast levels, Elleberg & Hammarrenger (2001) demonstrated that P1 component shows a characteristic magnocellular response pattern. In particular, P1 appeared at low contrasts, increased rapidly in amplitude with increasing contrast and saturated at medium contrasts. This corresponds with the findings that magnocellular cells respond to low contrasts, have high contrast gain and saturate at medium contrasts (Livingstone & Hubel, 1988). With increasing spatial frequency, N1 component becomes more dominant in the waveform, and exhibits characteristic parvocellular response: for intermediate and high frequencies, the contrast-amplitude function appears to be linear, and increases with increasing contrast without saturating (Bach & Ullrich, 1997; Elleberg et al., 2001; Vassilev et al., 1994; Souza, 2007; see next subsection for further description of this component).

Furthermore, Crognale (2002) and Gerth, Delahunt, Crognale, and Werner (2003) showed that isoluminant stimuli do not elicit a clear P1, N1 being the first component that can be readily observed in the averaged waveform. On the other hand, P1 is easily elicited by luminance-defined stimuli and is also followed by N1 component. The fact that isoluminant stimuli designed to engage chromatic pathways do not elicit a P1 supports the notion that P1 reflects magnocellular response pattern (Elleberg & Hammarrenger, 2001).

Some studies indicate that P1 is not responsive to top-down factors. For example, Hillyard & Münte (1984) measured ERP amplitudes in response to target categories. Their results indicated that stimuli matching the category could not be distinguished from non-matching stimuli. However, other studies make the opposite claim, namely that P1 can be modulated by attention and possibly by other high-level factors as well (Linkenkaer-Hansen et al., 1998; Rutman, Clapp, Chadick, & Gazzaley, 2009). Linkenkaer-Hansen et al. demonstrated for example that the P1 amplitude and latency increased for inverted rather than upward and visually degraded face stimuli. At the same time, the precise nature of this modulation is not clearly defined; in other words, amplitude modulation in such tasks could result from low-level factors as well (Rutman et al., 2009)

The relationship between attention and P1 component has been studied extensively (Hillyard, Vogel, & Luck, 1998; Luck, Woodman, & Vogel, 2000). It has been demonstrated that attentional load increases peak latency of this component as well as its amplitude (Fu, Fedota, Greenwood, & Parasuraman, 2010). Furthermore, amplitudes to attended versus unattended locations produce increased amplitudes of component P1 and N1 (Fukuda & Vogel, 2009; Hillyard et al., 1998; Johannes et al., 1995; Mangun, Hillyard & Luck, 1993). As mentioned above, source localisation studies indicated that component P1 has at least two distinct cortical sources; based on the timing of their activation, P1 can be subdivided into early dorsal (80 – 100 ms) and late ventral (100 – 130 ms) portions (Di Russo et al., 2002). This early portion has been suggested to correspond to spatial selection taking place in extrastriate areas, while the later portion to attention-enhanced processing taking place in the ventral stream in object recognition regions (Di Russo, Martínez, & Hillyard, 2003; Martínez et al., 2001).

Another study (Natale, Marzi, Girelli, Pavone, & Pollmann, 2006) supports the notion that the attention effects indexed by the P1 are related to modulation of visual occipital areas by attention, which is in line with previous studies as well (Luck, Heinze, Mangun, & Hillyard, 1990; Luck, 1995). In their study, Natale et al. (2006) presented participants with stimuli that appeared either at a predictable location or at a random one. In the predictable condition, attention would be focused on one possible location. In the unpredictable condition, attention would have to be initially spread over the entire presentation field. When the stimulus finally appeared, attention would be shifted towards that stimulus. Therefore, this task design allowed to dissociate between focused attention and attentional shift. The authors found that the P1 amplitude was larger for stimuli appearing at a predictable location. Natale et al. (2006) interpreted these findings as an evidence that P1 indexes sustained attention, which probably reflects modulation of activity in visual areas achieved via attention (in this sense, this interpretation is congruent with earlier studies, e.g. Luck et al., 1990 and Luck, 1995). These findings are in line with an earlier study (Barcelo, Suwazono, & Knight, 2000) that utilised the P1 component to provide an evidence for the involvement of the

prefrontal cortex in modulating the activity in the extrastriate cortex. In their study, patients with damage to dorsolateral prefrontal cortex showed a reduction in the PI compared to healthy controls during a visual discrimination task. Since the task involved allocation of attention, the authors concluded that the reduction of the component reflects a deficit in attention.

PI component amplitude appears to be also modulated by the perceptual load (Handy & Mangun, 2000). In a spatial cueing paradigm, Handy et al. (2000) showed that PI amplitude (as well as NI) was increased under high perceptual load in response to cued targets. The authors propose that higher PI and NI amplitudes, in this case, reflect an increase in selective processing taking place in the extrastriate visual cortex. Their results provide support for Lavie and Tsal's (1994) model of spatial selection, which states that spatial selection is directly related to perceptual load. If the perceptual load is relatively low, attentional resources are automatically allocated to task-irrelevant information as well. However, under high perceptual load, attentional resources will be focused on the attended, task-relevant target, thus showing an increased spatial selection. Referring back to PI and NI amplitudes in Handy et al.'s (2000) study, high perceptual load led to an increase of PI – NI amplitude because of such increased attentional selection.

Another study has looked at whether PI, in addition to perceptual load, is also modulated by the number of stimuli held in memory (Rose, Schmid, Winzen, Sommer, & Büchel, 2004). In their study, Rose et al. (2004) looked at the influence of WM load on the processing of irrelevant backgrounds. They showed that while the PI was modulated by the visibility of the backgrounds, WM load did not appear to reliably modulate its amplitude. The authors concluded that while the PI is clearly related to early perceptual processing, it is not directly affected by WM.

However, as mentioned earlier, one study (Haenschel et al., 2007) demonstrated that WM load modulates the PI amplitude. The difference between this study and the study of Rose et al. (2004) is that Haenschel et al. (2007) used a delayed match-to-sample task rather than N-back task; the former allows for more direct,

temporal differentiation between WM stages (encoding, maintenance and retrieval). Haenschel et al. (2007) report WM load-related modulation when they looked at the P1 during WM encoding. In their task, the number of to-be-remembered stimuli was varied, and the ERPs were time-locked to the onset of the last stimulus in the memory array.

Their results showed that the amplitude of P1 component was modulated by WM load: the higher the number of items kept in memory, the greater P1 amplitude. Additionally, higher amplitude was correlated with successful performance. In the same study, a cohort of participants with early-onset schizophrenia showed attenuated P1 amplitude in the same task. One of the core features of schizophrenia are cognitive impairments, including working memory (details on how working memory is affected in schizophrenia are provided in Chapter 5). Haenschel et al. hypothesised that, based on the lack of clear P1 component in patients and amplitude modulations in neurotypical population, visual working memory performance depends on the early perceptual stages of processing.

In summary, early component P1 appears to be sensitive to low-level visual properties. At the same time, it can also index higher-level cognition, such as attention and WM. This is in line with evidence that due to top-down influences from parietal and frontal regions, early ERP components, including P1, are likely to reflect processing from cortical areas not constrained to the visual cortex (Foxy & Simpson, 2002).

9.1.2. N1

Component P1 is largely attenuated or absent in response to isoluminant stimuli; however, unlike P1, the N1 component can be reliably elicited by isoluminant chromatic modulation (Crognale, 2002; Gerth et al., 2003).

The N1 peak is the first major negative deflection generated after The P1. The N1 deflection is manifested as a summation of several negative components (subcomponents; Luck, 2014). Even though together they form a characteristic N1 signature, it does not imply that these subcomponents are reflecting the same processes (Luck, 2014). The topography and timing appear to be slightly

different. For example, anterior subcomponent peaks earlier than other subcomponents, around 100 – 150 ms poststimulus. There are also two subcomponents are detectable at posterior electrodes, peaking around 150 – 200 ms, one generated in parietal cortex, and the second in the lateral occipital cortex (e.g. electrodes PO7 and PO8 in Hopf et al., 2013).

The NI amplitude is significantly reduced in response to a stimulus that was preceded by a stimulus presented at the same location (Luck et al., 1990; Luck, 2014), a phenomenon referred to as sensory refractoriness. However, this effect seems to occur only when the stimulus interval is sufficiently short (in Luck et al., 1990 it ranged from 310 to 450 ms). In studies using longer inter-stimulus intervals, any reduction in NI amplitude is less likely to be explained by refraction (Natale et al., 2006).

As mentioned in the previous section, while the PI exhibits a typically magnocellular response, the NI is parvocellular, as it becomes pronounced with high-frequency stimuli and does not saturate with increasing contrast (Elleberg & Hammarrenger, 2001). The NI is also reliably elicited by isoluminant stimuli, both S-cone and L – M (Gerth et al., 2003). NI in response to S-cone is slightly delayed compared to the L – M, though it is nevertheless clearly detectable. The NI also appears to be smaller in response to luminance, achromatic stimuli. As described in the previous section, the NI has been shown to be related to the amount of perceptual load (Handy & Mangun, 2000), with larger NI amplitude in response to cued targets under high perceptual load condition (see the previous section on PI component for more details on this study).

In addition to the above findings showing the perceptual modulation of the NI, there is also evidence that this component is indexing higher-level cognitive processing, such as discrimination, attention and WM. More specifically, the subcomponent localised to anterior sites is believed to reflect discriminative processing (Hopf, Vogel, Woodman, Heinze, & Luck, 2002; Ritter, Simson, Vaughan, & Friedman, 1979; Vogel & Luck, 2000). In their study, Vogel and Luck (2000) examined NI component in response to attended locations under two conditions. Participants had to either discriminate between two classes of stimuli

or to simply respond as quickly as possible without making a discrimination. Posterior NI elicited larger amplitude for the discrimination conditions. Interestingly, the amplitude was equally modulated by discrimination in easy and hard conditions, which suggests that the anterior component is invariant to task demands. Therefore, modulation is not likely to arise from resource-related processing.

This anterior subcomponent also appears to be sensitive to spatial attention (similarly to component P1; see the previous section). This is also the case with posterior NI subcomponents (Hillyard et al., 1998; Mangun, 1995). Although spatial attention modulated component P1 as well (see the previous section), it appears that the two components may reflect different aspects of attention. As mentioned in the previous section, the P1 seems to index facilitation of perceptual processing achieved via attention sustained at the target stimulus (Luck et al., 1990; Luck, 1995; Natale et al., 2006). NI, on the other hand, is more likely to reflect shifting (orienting) attention to targets (Luck et al., 1990; Natale et al., 2006). In the previous section, I described a study by Natale et al. (2006) who used a task that allowed to discriminate between sustained attention and stimulus-driven shifts of attention by using stimuli appearing at predictable or unpredictable locations. While the P1 component in this task was modulated by predictable stimuli, the NI amplitude was larger for stimuli appearing at random location. Since not knowing the location of an upcoming stimuli requires participants to shift their attention, Natale et al. (2006) concluded that NI is indexing exogenous attention orienting. According to the authors, this component would, therefore, reflect activity in frontoparietal attentional areas.

There is some evidence that the NI can be also linked to WM. As already mentioned in the previous section, Rose et al. (2004) looked at the modulation of P1 and NI components in response to task-irrelevant backgrounds under varying WM load. They were able to show that higher WM load resulted in lower NI amplitude.

Another study has demonstrated that NI has a reduced amplitude during the retrieval stage (Pinal et al., 2015). It is suggested that lower amplitude reflects a

reduction of resources allocated to the encoding of a new stimulus since some of these resources have to be used to maintain previously seen stimuli.

In summary, the NI has been shown to be reliably evoked by isoluminant stimuli. While the NI is modulated by purely perceptual factors, it has been shown that it can serve as an index for higher-level cognitive processing as well, including attention and, possibly, WM.

9.1.3. P1 and N1 as gain control mechanism

Despite differences between P1 and N1 components, it has been suggested that both components reflect a gain control mechanism in sensory processing (Hillyard et al., 1998). The gain control mechanism refers to filtering process in which the irrelevant (unattended) stimuli are suppressed, while the relevant (attended) ones are amplified, which is reflected in suppression or enlargement of the sensory evoked responses in animals, respectively (Hernandez-Peon et al. 1956; Hernandez-Peon 1966; Oatman & Anderson 1977). Analogically, the P1 and N1 components recorded from human subjects have been shown to increase in amplitude in response to attended versus unattended stimuli (Hillyard et al., 1998). Consequently, this observation provided a support for the “spotlight” hypothesis of attention, which poses that attended stimuli are processed with increased efficiency (Hawkins et al., 1990; Reinitz, 1990). According to this account, a higher amplitude of these components reflects amplification of neural response (which occurs automatically), thus optimising signal-to-noise ratio. Other researchers have also adopted similar view (Hanslmayr et al., 2007; Klimesch et al., 2004).

9.1.4. P3 component

P3 component has been associated with memory processes at various stages of working memory processing (Bledowski et al., 2006; Kok, 2001). There are two apparently different components that can be observed within its time range (Luck, 2014): P3a, which appears to originate in frontal areas, while the P3b is generated in temporal and parietal areas (Ebmeier et al., 1995; Kirino, Belger,

Goldman-Rakic, & McCarthy, 2000; Polich, 2007). These components may reflect different processes, depending on the task during which the component was observed. For example, perhaps the best known P3 component associated with responses to odd events in a sequence of otherwise repeated tones have been demonstrated in classical oddball tasks (Squires, Squires, & Hillyard, 1975). This particular odd event component is maximal at frontal electrodes if the odd event is not task related. This component is referred to as P3a component, also known as orienting P3. On the other hand, task-relevant odd events are also associated with changes at the parietal sites. This particular component is known as P3b. Confusingly, a lot of papers referring to “component P3” usually mean parietal P3b elicited by an odd event in an oddball task.

An influential theory has been proposed to account for these findings, according to which the P3 component reflects context updating (Donchin, 1981; Polich, 2007). After the stimulus is initially processed and kept in WM, an attention-based system evaluates this representation and compares it with incoming stimuli. First, the incoming stimuli are processed, which evokes the usual sensory potentials (e.g. P1, N1). If a change occurs, however, the WM representation is updated to accommodate new information, a process which evokes the P3⁶. If there is no change, there is no need for a revision of the representation, and the P3 is not elicited following the usual sensory evoked potentials.

Since component P3 consists of two subcomponents, as mentioned above, a further refinement has been put forward to outline the differential contribution of P3a and P3b to context updating processing and their possible neural generators. According to Polich (2003), both subcomponents are driven by attention but serve a different purpose. P3a reflects frontal attention mechanism during the stimulus processing; it arises when sufficient attentional resources are

⁶ As Polich (2007) emphasizes, the updating process reflected by the P3 is related to another component obtained using an oddball task, namely the mismatch negativity (Näätänen, Gaillard, & Mäntysalo, 1978; Näätänen, Paavilainen, Rinne, & Alho, 2007) obtained by subtracting the activity in response to a standard events from activity evoked by odd events. However, Polich (2007) suggests that the underlying process behind the P3 is distinct from the mismatch negativity.

dedicated to the stimulus, which is the case with oddball stimuli. Subsequently, a memory-related processing takes place in temporal and parietal areas, giving rise to the P3b (Polich, 2007). Indeed, the amplitude of the P3b (Bledowski et al., 2006; Kok, 2001; Verleger, 1997) or P3 (Pinal, Zurrón, & Díaz, 2014) has been found to be decreasing with increasing WM load, thus further supporting the view that P3, with its subcomponents, is related to WM.

In addition, Kok (2001) regards the P3, in particular, its subcomponent P3b, as a useful measure of processing capacity. Kok (2001) suggested that increased task demands, including greater demand for attentional resources, disrupt processes underlying the P3b generation, leading to a lower amplitude. This decrease reflects interactions between WM and perception. Furthermore, as Haenschel et al. (2007) suggested, the P3 may play important role in determining successful performance.

Further, it has been suggested that the P3b component is not related to the storage of the information per se, but rather reflects a completion of cognitive operations related to a task-relevant stimulus (Desmedt, Bourguet, Huy, & Delacuvellerie, 1984; Desmedt & Debecker, 1979; Desmedt, 1980; Tomberg & Desmedt, 1998; Verleger, 1988).

As pointed out by Croizé et al. (2004), during the encoding period in a delayed-discrimination task, a “closure” of cognitive operations is not yet achieved, which would be reflected in the decreased amplitude of this component. During the retrieval, however, the P3b component indexes a decision mechanism during stimulus comparison, which also marks an end to the cognitive operations performed on the stimuli (Croizé et al., 2004).

To sum up, looking at the amplitude of P3a and P3b in the current experiment will be used as an index for WM and attentional demands. We hypothesise that the amplitude of this component will decrease with increasing WM load. On the other hand, if the encoding of luminance-defined items is more efficient, then fewer resources would need to be dedicated for their processing due to increased efficiency. Thus, we expect that at higher loads efficient encoding of luminance-defined shapes will result in lower amplitude than for S-cone and L – M stimuli. If

this effect occurs at particular subcomponent (P3a or P3b), it will help to elucidate the mechanism responsible for more efficient luminance processing. This will be possible since they seem to be generated in different cortical areas (more frontal for P3a and temporal/parietal for P3a; see Polich, 2007) and have been suggested to reflect different processes (Polich, 2007).

9.1.5. Slow wave

Previous studies have observed a sustained activity during WM maintenance sensitive to the amount of information stored in WM (Ruchkin, Johnson, Canoune, & Ritter, 1990; Ruchkin, Johnson, Grafman, Canoune, & Ritter, 1992). Additionally, one study (Klaver, Talsma, Wijers, Heinze, & Mulder, 1999) reported that a sustained negative ERP can be observed in a matching to sample task at electrodes contralateral to stimulus presentation. Sometime later, Vogel and colleagues (Vogel & Machizawa, 2004; Vogel, McCollough, & Machizawa, 2005) developed a way to isolate sustained activity during WM maintenance using a bilateral change-detection paradigm. Similarly to Klaver et al. (1999), they observed WM-related activity on the posterior sites contralateral to the presented stimuli. However, they were able to isolate activity purely related to WM storage by subtracting activity from ipsilateral sites, assumed to reflect visual processing. This component was termed contralateral delayed activity, or CDA, and has been since validated as a robust measure of WM and widely used in research hence after (Luria et al., 2016).

In the current study, we are using stimuli presented at the centre of the screen, and thus our design makes it impossible to isolate the CDA wave. Although it is still regarded to reflect some aspects of WM retention-related activity (e.g. Pinal et al., 2014), without wave subtraction it is reasonable to expect that the slow, sustained activity during WM maintenance in our experiment will likely reflect both visual and WM processing. Nevertheless, we expect the slow wave to reflect increased WM load. We also predict that, since the slow wave should reflect both visual and WM effects, there should be no difference between different DKL directions.

In general, a negative slow wave occurring during the delay period is usually recorded over occipital and parietal sites (Barceló, Martín-Loeches, & Rubia, 1997; Bosch, Mecklinger, & Friederici, 2001; Löw et al., 1999; Martin-Loeches, Gomez-Jarabo, & Rubia, 1994; McEvoy, Smith, & Gevins, 1998; Mecklinger & Pfeifer, 1996; Rolke, Heil, Hennighausen, Häussler, & Rösler, 2000; Ruchkin, Johnson, Grafman, Canoune, & Ritter, 1997; Ruchkin, Canoune, Johnson, & Ritter, 1995; Schubotz & Friederici, 1997; as cited in Croizé et al., 2004). At the same time, a negative slow wave recorded at frontal sites is also present, and has been related to the maintenance and manipulation of the remembered stimuli, as well as increased attentional demands (Bosch et al., 2001; Löw et al., 1999; Rämä et al., 1997; Ruchkin et al., 1997; Ruchkin, Johnson, Canoune, & Ritter, 1990). Hence, in the current study, we will analyse waves recorded at both posterior and anterior sites.

It is important to mention that the processes generating P3 are complex and not unitary. Since slow wave can occur during the same time window as the P3, the amplitude of P3 itself might be distorted by this wave and difficult to dissociate (Kok, 2001).

9.2. Predicted ERP modulations

The previous section discussed a number of ERP and their modulation by perceptual and cognitive factors, including working memory. Below, I will outline our predictions regarding how these components will be modulated in our experiment. The general prediction was that EEG responses during WM encoding would show a load-related sensitivity in response to luminance-defined stimuli as early as component P1. Furthermore, it was also predicted that this activity would correlate with accuracy on WM task. We did not expect the P1 to be present in response to isoluminant conditions, in accordance with previous findings (Crognale, 2002; Gerth et al., 2003); therefore, we used N1 as an index of memory-related activity in response to isoluminant stimuli. Unlike with the component P1 in response to luminance, we did not expect to find load-dependent modulation of the N1 for isoluminant conditions

Later components were also of interest during the encoding stage, namely the family of P3 components. As they have been linked to WM processing (Polich, 2007), we also expected to see load-dependent modulation. It was predicted that the amplitude of P3's subcomponents (P3a and P3b) will be sensitive to WM load for each stimuli class (luminance, L – M, and S-cone). If each mechanism equally modulates the P3 amplitude, this would suggest that each mechanism contributes to WM to a similar degree. For the maintenance stage, we looked at the slow, sustained wave which has also been related to WM maintenance (Vogel, McCollough, & Machizawa, 2005). We expected to see load effects at this stage for each post-receptoral mechanism. Similarly to encoding and retrieval, if each mechanism equally modulates the slow wave, this would suggest that each mechanism contributes to WM maintenance to a similar degree.

For retrieval, we looked at the same components as during encoding (P1 and N1) and also correlated their amplitudes with behavioural performance. This was to assess whether the contribution of post-receptoral mechanisms differed depending on the current working memory stage. It was expected that the luminance benefit will manifest itself as early as during encoding, especially in light of findings suggesting that working memory performance depends on processing during this stage (Haenschel et al., 2007).

Notably, there were few studies that addressed the question of the interaction between perception and working memory explicitly. These will be summarised in the next section.

9.3. Studies on perception/working memory interaction using the ERP technique

Certain studies investigated the interaction between visual perception and working memory at early processing stages directly, rather than looking at these two processes separately. In one such study (Agam & Sekuler, 2007) presented participants with a yellow disc in the middle of the screen, which moved in a quasi-random trajectory after the start of the trial. The trajectory was temporarily divided into five segments; after one segment ended, the disc would remain

stationary for a certain time, after which the disc continued the trajectory during the next segment until the whole trajectory was completed over the five segments. Participants' task was to reproduce the trajectory after a delay. The ERPs were time-locked to the onset of each segment. Their results showed that the amplitude of the ERP during segment encoding decreased as the number of segments increased – this can be thought of as an equivalent to increasing working memory load. Importantly, the ERP amplitude correlated with behavioural performance on the task – the larger the amplitude, the better the performance. The amplitude differences between early and later segments (i.e. working memory loads) were significant around the 250 – 370 ms time interval at frontal and frontoparietal electrode sites. Notably, the difference between waveforms was significant earlier, between 180 – 250 ms for central and occipital electrodes. The authors interpret these waveforms as indexing perceptual processing and suggest that perception is affected by working memory load.

These results are similar to the findings described in the preceding section (Haenschel et al., 2007; see Section 9.1.1). Haenschel et al. (2007) also found that the ERP amplitude of the P1 component (measured in the 80 – 160 ms time range) during memory encoding was modulated by increasing working memory load. It was demonstrated that the amplitude increased with increasing load and that this increase correlated with behavioural performance.

The studies described above provide evidence for an early interaction between working memory and perception that occurs during the encoding stage of visual working memory. Furthermore, these studies show that it is possible not only to successfully index these early interactions using the ERP technique, but also that they correlate with behavioural performance. Hence, the ERPs appear to be an adequate measure of perception and working memory interactions that are relevant to performance.

Other studies have also investigated the relationship between perception and working memory, albeit concentrating on later stages of processing. In particular, they focused on the processing accruing during the comparison between perceptual and memory representations, a step crucial to meet the demands of

the match-to-sample tasks (Agam et al., 2009; Yin et al., 2012). Agam et al. (2009) looked at how similarity of the memory representation with the test probe affected ERP waveforms. Participants were presented sequentially with two stimuli, composed of horizontal and vertical gratings, that they were required to remember. Memory presentation was followed by a test/probe stimulus. The task was to judge whether the probe matched one of the previously presented stimuli in terms of gratings' spatial frequency. Prior to the task, experimenters measured spatial frequency discrimination thresholds for each individual, i.e. the magnitude of the spatial frequency difference that led to 79% of correct same/different judgements. Thanks to this, it was possible to manipulate the perceptual similarity of memory stimuli and the probe – probes that were dissimilar to memories stimuli were presented at multitudes of the discrimination thresholds, relative to the average spatial frequency of memory items. The results showed that the difference between the ERPs in response to memory-similar and memory-dissimilar probes appeared at 156 ms after the onset of the memory probe at the posterior recording sites. In contrast, the difference was detectable at anterior recording sites only 50 ms later. The results indicate perceptual signals from the posterior areas contribute to successful memory-probe comparisons, suggesting that the interaction between perception and working memory during later stages starts early after the probe onset.

Another study also looked at ERPs during memory-probe comparison during a delayed match-to-sample task (Yin et al., 2012), in which participants remembered a set of stimuli and had to indicate whether the probe set matched the previously presented one. Although the study did not find significant differences in the behavioural accuracy in responding whether the probe was a match or mismatch, they demonstrated that the change in the probe set (task-relevant or not) produced a distinct negative waveform in the 230 – 340 ms time window. The authors suggested that these ERPs reflect a distinct comparison stage of working memory.

10. General summary and hypothesis

To summarise, the current study investigated interactions between early visual processing and WM. In particular, the aim was to investigate how the three post-receptoral mechanisms (S-cone, L – M, and L+M/Luminance) contribute to WM processing. It was hypothesised that encoding luminance-defined stimuli will result in better WM performance over isoluminant stimuli, which would be manifested in a higher proportion of correct responses and reaction times for these stimuli in a match-to-sample task. Further, the contribution of the three mechanisms to each stage of WM processing – encoding, maintenance and retrieval – was tested. To that end, the EEG was recorded while the participants performed the task to see how the EEG response is modulated by perceptual and working memory-related processing performed by the brain during the task.

We identified a number of early visual ERP components that can be reliably elicited by luminance and isoluminant stimuli – these were both P1 and N1 for luminance, and N1 for isoluminant stimuli. These components are known to be modulated by visual attributes of the stimuli. In our study, we treated them as an index of WM processing as well. Therefore, these components were measured under three WM load levels during encoding. We reasoned that if a given visual component will differ with WM load for a particular class of stimuli (luminance, L – M, or S-cone), this would suggest that the corresponding post-receptoral mechanism interacts with WM processing. To confirm that such load-dependent modulation is indeed related to WM and affects subsequent performance, we correlated the amplitude of the component with behavioural performance.

11. Methods

11.1. Participants

23 participants were recruited for the study through a SONA recruitment system (Sona Systems, Estonia) and word of mouth. One participant had to be excluded as scaled stimuli contrast based on individual discrimination threshold were outside the monitor's gamut. Thus, behavioural data from 22 participants were analysed (18 women and 4 men, median age: 25).

Participants were paid for the time. The exclusion criteria included a history of psychiatric disorders. All participants reported having normal or corrected-to-normal vision. Although colour deficiency was exclusion criteria as well, all participants were screened using Colour Assessment and Diagnosis test (CAD) to confirm this. All individuals passed the test according to the test's criteria.

The study was reviewed by and received ethics clearance through the Department of Psychology Research Ethics Committee, City, University of London.

11.2. Procedure

The experiment consisted of three sessions, each completed on a separate day. Over three days, participants completed approximately 7.5 – 9 hours of testing in total. Table 3 summarises all tests and measurements completed by the participants.

Table 3 Summary of tests completed by all participants. Section numbers where the tests are described in more detail are provided.

Control and baseline measures			Main experiment
Vision tests	WM measures (see section 11.2.1)	Baseline measurements (see section 11.2.2 and 11.2.3)	WM experiment with EEG recording (see section 11.4)
– CAD – AcuityPlus	– Digit Span – Letter-number test	– HCFP – Discrimination threshold experiment	– Delayed match-to-sample WM task

The first session consisted of two parts which took around 1.5 hours to complete. In the first part, participants completed a diagnostic colour test (CAD; Barbur, Rodriguez-Carmona & Harlow, 2006) to ensure their colour vision was within age-appropriate limits. We have also collected data on participant’s acuity and functional contrast sensitivity using the AcuityPlus test (Barbur, Rodriguez-Carmona & Harlow, 2006). We did not reject any participants based on these measurements.

Following the vision tests, participants were invited to the EEG laboratory, where further baseline measurements were conducted (for the experimental setup and display characteristics, see Chapter 2). First, participants completed the digit span and letter-number tests. Later, a same/different discrimination threshold experiment was conducted.

After the experiment, participants were scheduled for further two sessions (on two separate days). Each session lasted approximately two to three hours. Participants completed a delayed match-to-sample WM task while we recorded the EEG (see section 11.3 for details on the task design and section 11.4 for the details of the recording procedure). The task itself (and hence, the EEG recording) lasted approximately 1 hour and 20 minutes, subject to the amount and the length of the breaks.

11.2.1. Working memory measurements: digit span and letter-number test.

Participants completed two standardized measures of WM: digit span and letter-number test. These two tests form part of the Wechsler Intelligence Scale (Wechsler, 1949; Wechsler, 1991). In the current experiment, tests originate from the 3rd edition of the Wechsler Memory Scale (WMS III).

The rationale for conducting these tests was to assess whether performance on our visual WM tasks correlates with standardized WM measures. This might be of importance given that the two tests (administered as part of the full Intelligence Scale assessment and on its own) are one of the most commonly used WM tests by psychologists (Evers et al., 2012; Richardson, 2007; Woods et al., 2011).

The digit span consists of two tasks. In the first one, the digit-forward task, participants are instructed to repeat sequences of numbers after the experimenter. In the digit-backward test, participants repeat different sequences of numbers in a reversed order. The sequence in both tests begins with two items and is further increased as the task progresses until the participant reaches maximum (9 items for digit forward and 8 for digit backward), or until the participant makes two consecutive errors. The number of correct trials is summed across both tests to produce a final score. In the letter-number sequencing test, participants are listening to a series of numbers and letters and are asked to repeat the sequence, but with numbers arranged from lowest to highest and letters in alphabetical order. There are characters per item on the first level, with 4 items per level. The length of the sequence increases by one character on every level. The test is finished after all 25 items are administered across the 6 levels, or if the participant fails to repeat all items at a current level. The number of correctly repeated sequences form a final score (Wechsler, 1997).

11.2.2. Observer's isoluminance: Heterochromatic Flicker Photometry test

We used Heterochromatic Flicker Photometry (HCFP) test to determine observer's individual point of isoluminance. For the design, procedure and rationale of this test, see Chapter 2, Section 7.3.

Participants adjusted the flicker for stimuli chosen randomly from the experimental set. In total, 8 – 10 reliable measurements were recorded (after the outliers were discarded) and averaged to use as an elevation angle for the next task (see next section).

11.2.3. Same/different shape discrimination threshold

The purpose of the baseline threshold experiment was to equate stimulus salience between different directions in DKL colour space. This was done on the basis of same/different discrimination thresholds measured for each condition, for every participant. Thresholds were measured using a 2-interval forced choice task (2IFC), four times for each of the four stimulus types by running four interleaved staircases together. Participants saw two shapes in succession, each one lasting 650 ms and with a 500 ms fixation period in between and responded whether the shapes were same or different with a button press (see Figure 14).

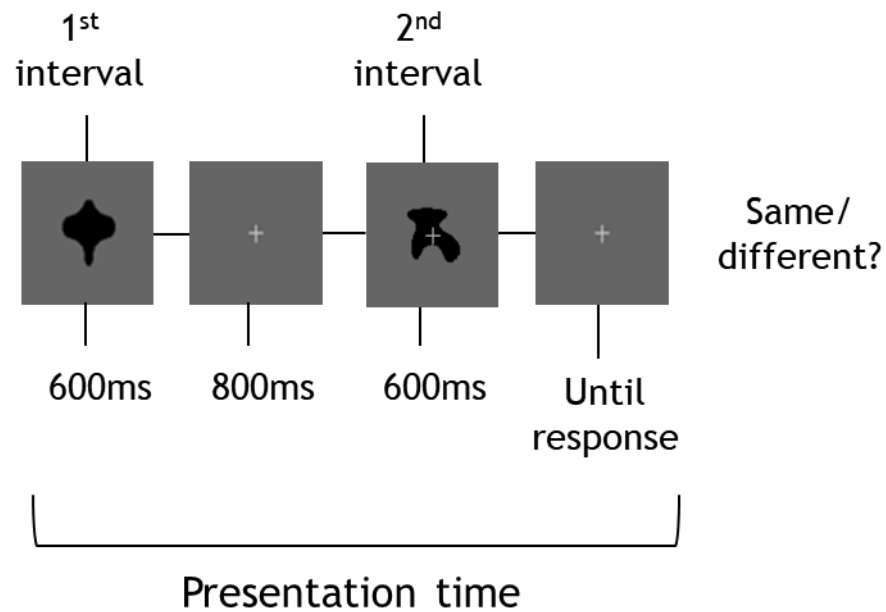


Figure 14 Trial outline of the match-to-sample task used to measure discrimination threshold. In the presented case, the correct response is “different” (or “mismatch”).

Stimulus intensities were controlled using an adaptive staircase procedure ran with the Palamedes toolbox for Matlab (Prins & Kingdom, 2009). Each staircase consisted of 35 trials with auditory feedback. To estimate the colour contrast threshold from the relative frequency of a correct response, a Weibull function was fitted to obtain the threshold contrast (defined as the 75% correct point on the psychometric function). The four threshold measures were averaged to obtain a mean threshold for each participant. For some participants and for some conditions, the thresholds did not converge in a single run; such run was discarded and staircase limits were adjusted for the subsequent runs. As a result, thresholds for some conditions were based on three rather than four runs (but never less than three). Contrasts were then scaled from the threshold for each participant to create equivalent *low contrast* and *high contrast* stimuli: the luminance stimulus was scaled to a radius of 0.07 (low) and 0.14 (high contrast) and then all the other stimuli were scaled using the same scale factor to create a set of equivalent suprathreshold contrasts. A radius of 0.14 was chosen on based on the results of an unpublished, pilot study in a different laboratory (Haenschel, Kosilo & Martinovic, 2012). In their case, the radius of 0.14 enabled to create a high contrast stimulus for the majority of observers whilst staying within the

monitor gamut. A radius of 0.07 was chosen as the pilot study showed that it sustains a still reasonable level of performance in a working memory task.

11.3. Main WM experiment

11.3.1. Delayed match-to-sample task

Participants completed a delayed match-to-sample task with varied working memory load. As outlined in the introduction, this task allows to investigate directly how increasing working memory load affects WM processing since the stimuli are presented sequentially, one at a time (Haenschel et al., 2007; Linden et al., 2003). The stimuli design was described in Chapter 2, Section 7.6.

The WM load was varied by presenting 1, 2 or 3 shapes in succession (see Figure 15). Individual shapes stayed on the screen for 600 ms, with a fixation cross displayed for 800 ms during the inter-stimulus interval in case of load 2 and 3 (encoding stage). After a 1000 ms delay (maintenance stage), a probe stimulus was displayed until a response (retrieval stage). Participants were asked to judge whether the probe matched or mismatched one of the shapes presented at the encoding stage with a button press (match/mismatch or same/different response). All participants completed a practice session before the experiment so that they could familiarise themselves with the task.

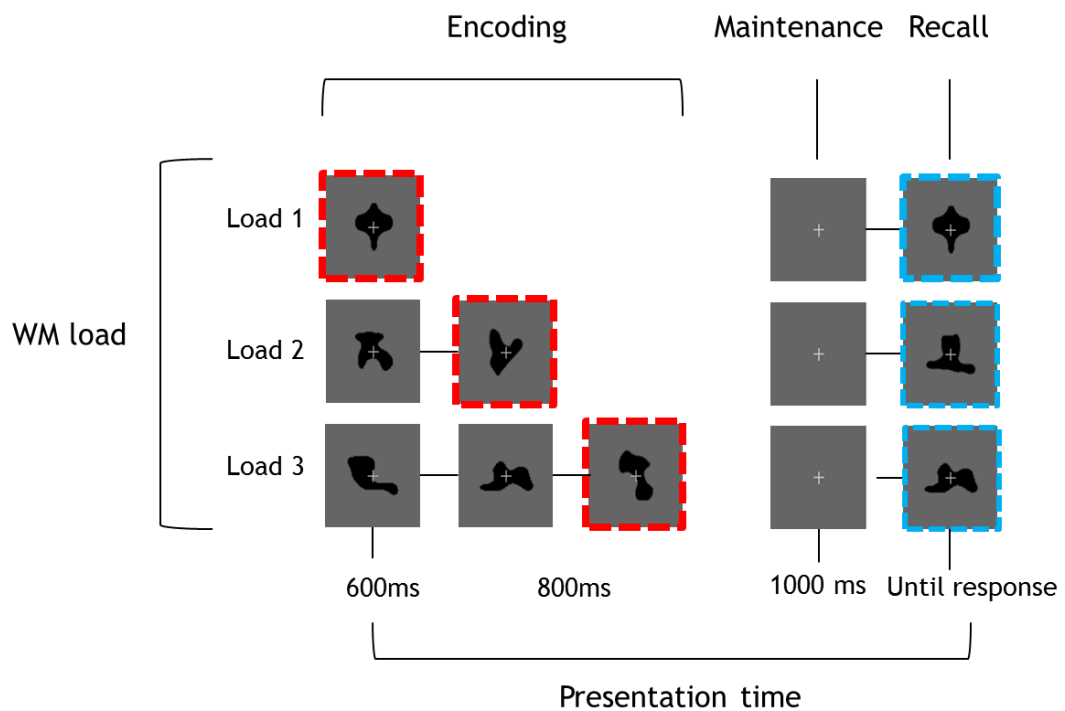


Figure 15 Delayed match-to-sample task. On each trial, WM load was manipulated by presenting one, two, or three stimuli in succession (rows 1 – 3). Red and blue boxes are for illustration purposes only and did not appear on the screen during the task. Red boxes indicate the ultimate shape in the encoding stage – ERP epochs for encoding stage were time-locked to the onset of that stimulus. Blue boxes indicate the probe (i.e. the recall/retrieval stage of working memory). ERP epochs for the retrieval analysis were time-locked to the onset of this stimulus.

There were 4 conditions which determined the DKL coordinates of all of the stimuli on a given trial. There were 2 isoluminant chromatic conditions designed to stimulate the following post-receptoral mechanisms: $S - [L+M]$ (referred to as “S-cone”) and $L - M$. In the achromatic condition, stimuli were luminance-defined, i.e. they were designed to stimulate the luminance mechanism ($L+M$, referred to as “luminance”). Additionally, a “mixed-signals” condition was incorporated, in which all of the above mechanisms were stimulated ($L - M$ and $S - [L+M]$ and $L+M$). As mentioned in Chapter 2 (General Methods), it was mainly used as a control condition to characterise how responses to isoluminant conditions would be affected if they contained a luminance artifact. Stimuli designed to excite chromatic mechanisms with added luminance component have been used previously (Kosilo et al., 2013; Martinovic et al., 2011; McIlhagga & Mullen, 1996). Since it is problematic to compare responses to stimuli combining responses from both chromatic and luminance mechanisms with stimuli that

selectively excite chromatic or luminance mechanisms, the mixed signals condition was not included in the main analysis. A separate analysis for this condition was conducted and is described in Section 12.6.

Overall, there were 24 conditions. These corresponded to 3 WM loads (1, 2 or 3 shapes to be remembered), 2 contrast levels (low or high contrast), and 3 DKL directions (luminance, L – M and S-cone– see Table 1.). For each participant, a randomized condition list was generated beforehand to be loaded during the task.

Behavioural accuracy (i.e. proportion of correct responses) and reaction times were analysed using within-subject, repeated measures ANOVA with factors: contrast level (2 levels: low and high contrast), DKL direction (3 levels: Luminance, isoluminant L – M, isoluminant S-cone), WM load (3 levels: Load 1, Load 2, Load 3) and probe type (2 levels: match or mismatch). Greenhouse-Geisser corrections were applied where necessary. As mentioned above, mixed signals condition was not included in the main analysis.

Participants took part in two EEG sessions recorded on two separate days. Each session consisted of 576 trials (1152 trials overall). This resulted in 48 trials per each of the 24 conditions. Each session was divided into 4 blocks of 144 trials; there were 3 breaks within each block, one after every 36 trials. Each EEG session lasted approx. 3 hours (including practice, EEG preparation and washing the hair after recording).

Table 4 Experimental conditions. Each DKL condition (S-cone, L – M, Mixed signals and luminance) was presented at three WM load levels (1, 2, or 3), at two levels of contrast (low and high contrast). This resulted in 24 conditions overall.

	Load 1	Load 2	Load 3	
DKL condition	1. S cone	9. S cone	17. S cone	Low contrast
	2. L-M	10. L-M	18. L-M	
	3. Luminance	11. Luminance	19. Luminance	
	4. Mixed	12. Mixed	20. Mixed	
DKL condition	5. S cone	13. S cone	21. S cone	High contrast
	6. L-M	14. L-M	22. L-M	
	7. Luminance	15. Luminance	23. Luminance	
	8. Mixed	16. Mixed	24. Mixed	
	Load 1	Load 2	Load 3	

11.4. EEG data acquisition

EEG data were acquired using a 64-electrode ActiCap, with an in-built reference electrode at location FCz. FP7 electrode was placed below participant’s left eye and served as a vertical ocular electrode. Recording and digitization were performed using a BrainAmp amplifier and the BrainVision Recorder software (Brain Products, Munich, Germany). The EEG was recorded at a 1000Hz sampling rate with an on-line bandpass filter between 0.1 and 1000 Hz.

11.5. Pre-processing and analysis

Data were pre-processed using custom-written routines as well as functions derived from EEGLAB (Delorme & Makeig, 2004) and FieldTrip (Oostenveld, Fries, Maris, & Schoffelen, 2011) toolboxes developed for Matlab (Mathworks, Natick, Massachusetts), incorporated into custom scripts.

As there were two separate EEG recording sessions, they were treated separately during first pre-processing steps and only after they would be merged to be

treated as a single dataset. The following steps are based on the recommendations published on EEGLAB wiki page (Miyakoshi, 2017).

Step 1: Data were filtered with a low-pass filter (0.01 Hz) to remove low-frequency drifts.

Step 2: Noisy electrodes were removed. Removal was done based on a visual inspection by the experimenter, aided by inspection of spectral activations and contrasting the activity of all electrodes to identify electrodes with uncommonly large (or low) voltages

Step 3: The data were re-referenced to an average of all electrodes.

Step 4: A crude, visual artifact rejection was applied. The experimenter scanned through the continuous recording, removing periods of “crazy” artifacts (Luck, 2016) and break periods.

Step 5: Independent Component Analysis (ICA; Delorme & Makeig, 2004) using EEGLAB routines was applied to the cleaned, continuous data.

Step 6: Artifact rejection was performed. Experimenter scanned through the ICA components detected in Step 5 and rejected ones that reflected various artifacts. Judgements were made by the experimenter, but SASICA EEGLAB plugin was used to aid the judgement (Chaumon, Bishop, & Busch, 2015).

Step 7: If the ICA yielded unclean components (so that, for example, eye blink components were not readily identifiable), experimenter scanned through component activations to detect and remove periods of data where components appeared to be dependent (i.e. an artifact was reflected in a number of neighbouring components). ICA was performed on these datasets again and step 4 was repeated.

Step 8: Cleaned, single-session datasets were merged together with corresponding sessions and epoched.

Epochs ranging from -100 ms before stimulus onset and to 600 ms were used for analysis of the encoding stage; longer epochs were used for maintenance stage (-100 ms to 1700 ms). For the retrieval stage, shorter epochs were again used (-100 ms to 600 ms). This was done to maximise the number of trials available for

analysis. Extracting longer epochs results in the decreased amount of trials due to artifacts occurring after 600 ms. Epochs of each WM stage were baselined to 100 ms prior to stimulus onset.

Epochs were time-locked to the onset of the last item in the memory array, i.e. single item for load 1, second item from the two presented for load 2 and third item from the three presented for load 3 (see Figure 15).

To improve signal-to-noise ratio, the data were again filtered using a 30Hz high-pass filter for the extraction of peak amplitude measures for the encoding and retrieval stage. Since the mean amplitudes were used for analysis of the maintenance stage, the high-pass filter was unnecessary here, as the noise would be averaged out.

Time intervals and electrodes of interest were based on intervals defined in the previous study by Haenschel et al. (2007). Grand averages plotted against individual participant averages were inspected visually to confirm that the intervals used covered latencies when the peaks could be observed.

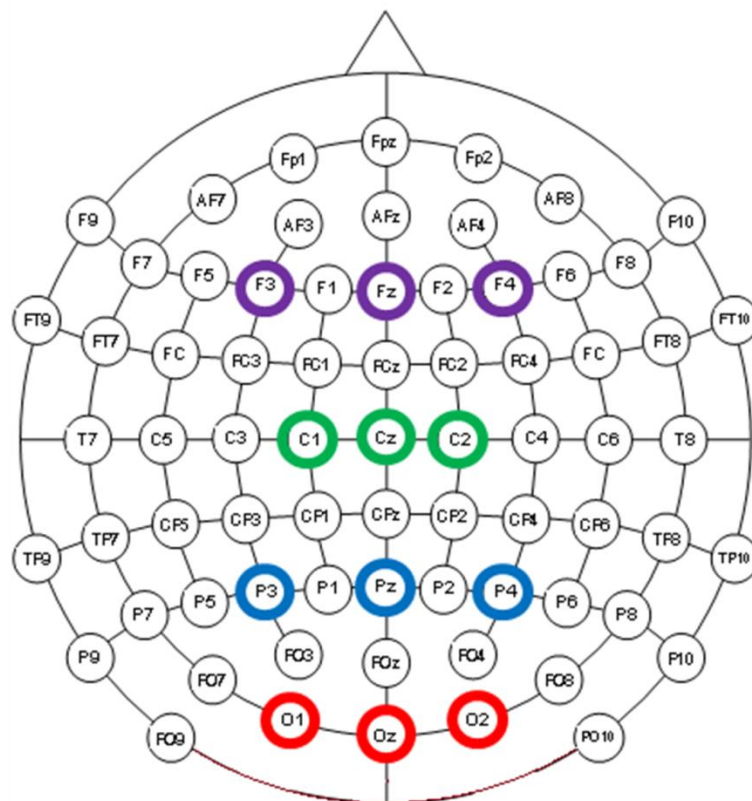
Upon inspection of grand average waveforms, it was evident that for the P3b component (electrodes P3, Pz and P4), ERPs in response to L – M and S-cone shapes are characterised by a longer onset latency than stimuli in Haenschel et al. (2007), exceeding their predefined time range of 200-400 ms. Thus, we decided to extend the interval used in Haenschel et al. (200-400 ms) and 200 and 500 ms time window was used instead.

We additionally analysed data during the maintenance stage. The maintenance stage was defined as a period between the offset of the last to-be-remembered item (at 600 ms after onset of that stimulus) to the onset of a memory probe/start of retrieval stage (at 1600 ms). Visual inspection of this period pointed to a clear negative peak between 700 and 900 ms, as well as a slow positive/negative potential starting at around 1000 ms, continuing throughout the maintenance (ending at the onset of the probe, at 1600 ms after the onset of the first stimulus in a trial). The slow wave during maintenance was analysed at both occipital and frontal sites.

The measured components are summarised in Table 2.

Table 2. Analysed ERP components, electrode sites and time intervals used to define and extract components. The map at the bottom shows electrode setup used in the experiment, with electrodes of interest marked with coloured circles.

ERP component	Time interval	Electrodes	
P1	80 – 160 ms	O1, Oz, O2	○
N1	130 – 300 ms	O1, Oz, O2	○
P3a	200 – 400 ms	C1, Cz, C2	○
P3b	200 – 500 ms	P3, Pz, P4	○
Negative offset peak	700 – 900 ms	O1, Oz, O2	○
Slow wave (occipital)	1000 – 1600 ms	O1, Oz, O2	○
Slow wave (frontal)	1000 – 1600 ms	F3, Fz, F4	○



ERP amplitudes and latencies for each component were analysed using a repeated measures ANOVA with factors: contrast level (low or high) WM load (Load 1, 2 and 3), DKL direction (3 levels: S-cone, L – M and luminance) and electrode location (3 levels, specific to the analysed component; see Table 4).

11.6. Note on ERP amplitude and latency extraction

Traditionally, ERP components are compared on the basis of their peak amplitude, i.e. the maximum amplitude measured in a specified time window (Luck, 2014; Donchin & Heffley, 1978). While still widely used, a number of alternative approaches have been developed over the years, such as mean amplitude. In our analysis, we decided to use traditional approach for two reasons. Firstly, we wanted to replicate the finding of Haenschel et al. who, using both peaks and mean amplitude measures, showed WM modulation of component P1. Secondly, while mean amplitude measure is usually superior to peak amplitude mostly due to better signal-to-noise ratio (see Luck, 2014), one of the drawbacks of using this measure is that it is very sensitive to the choice of measurement window. In the case where the latency of a component varies across conditions, a fixed measurement window can include two different components, affecting its amplitude. Indeed, we have noticed that attempts to measure mean amplitude of component P1 in our experiment resulted in negative amplitudes for Load 3 condition, despite the fact that P1 could be clearly identified when individual data was plotted for inspection. The use of signed area amplitude (Sawaki, Geng & Luck, 2012) can overcome the problem of defining a measurement window. However, this measure is not recommended when the noise levels between groups or conditions are likely to vary (Luck, 2014). Importantly, the same problem arises with peak amplitude measures; however, since mean amplitude was also not an ideal measure in our case, we decided to carry on with peak amplitude measures.

However, other than measuring a maximum voltage within the specified time window, we identified local peaks (local maxima) in the data. These were defined as time points which had a larger amplitude than the two neighbouring peaks.

The minimum peak height was defined as 0, and had to be positive for positive – going components or negative for negative- going components. If these criteria were not met, the local peak was replaced with a maximum peak value in the time window; if that was not successful either, the value was set to 0.

To quantify component latencies, we used the 50% fractional peak latency measure approach (Luck, 2014; Hansen & Hillyard, 1980). In this approach, a local or maximum peak is found; next, the procedure finds the time point (towards the time 0) at which amplitude equals a specified fraction of the local/maximum peak of the waveform – here, 50%. This time point is then used as a measure of onset latency (see Kiesel, Miller, Jolicœur & Brisson, 2008, for a discussion on the efficiency of different onset latency measurement techniques).

12. Behavioural results

12.1. Vision tests

Results of the vision tests are summarised in Figure 16 below. All participants passed the colour vision test and had normal acuity and functional contrast sensitivity. Therefore, no participants were rejected based on these measurements. We correlated each measure with performance on the WM task. There were no significant correlations.

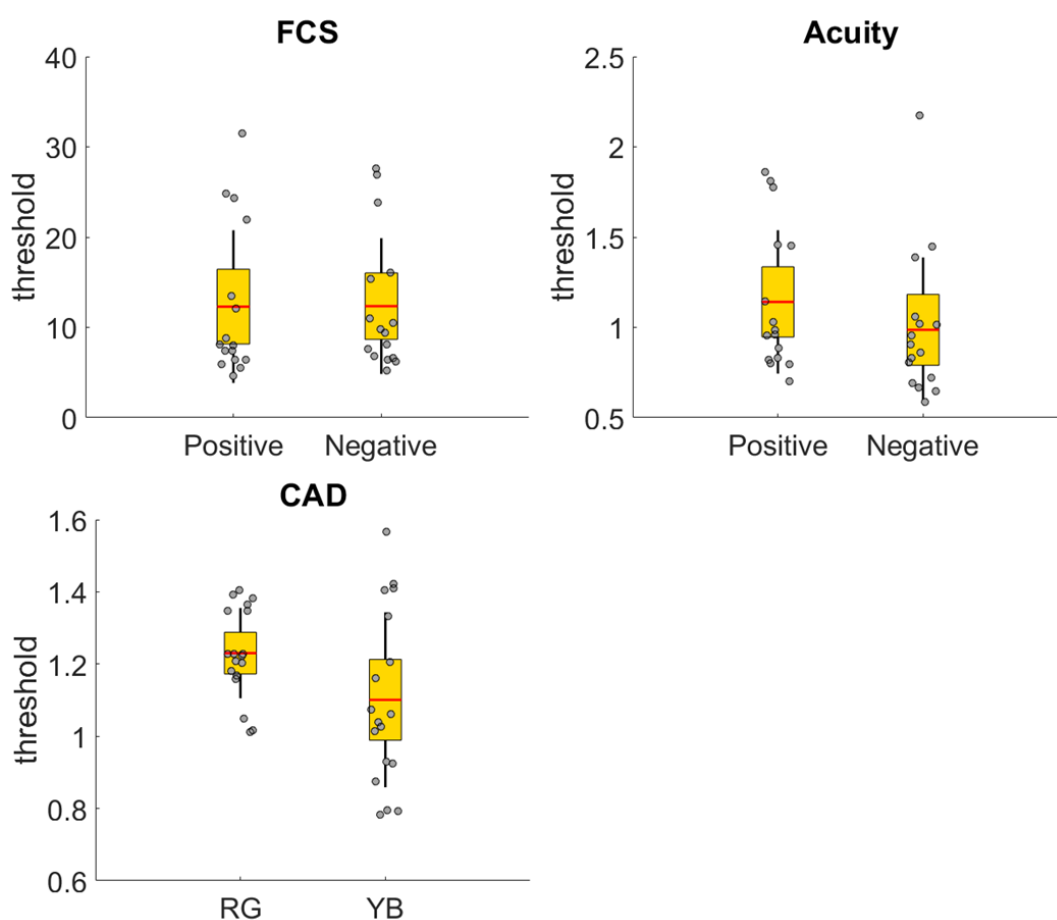


Figure 16 Results from AcuityPlus tests (functional contrast sensitivity: upper left, acuity – upper right) and the CAD test (bottom left). Each dot represents the overall score of one individual on a particular test (indicated on the x-axis). The red line in the middle represents the mean, red shading is the 95% confidence interval, and the blue line is one standard deviation.

12.2. Working memory tests

We correlated the digit span and letter-number tests with performance on the WM task. There were no significant correlations.

Overall results of working memory tests are shown below (see Figure 17).

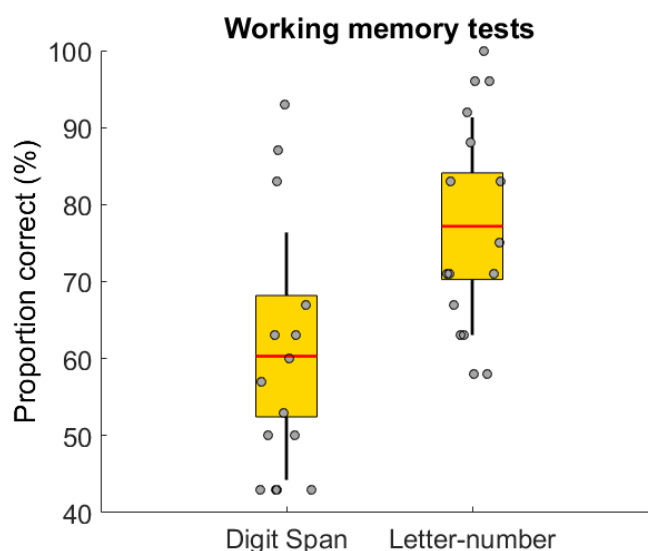


Figure 17 Results of the WM tests. Each dot represents the overall score of one individual on a particular test (indicated on the x-axis). The red line in the middle represents the mean, red shading is the 95% confidence interval, and the blue line is 1 standard deviation.

12.3. Threshold measurements

DKL coordinates (radius, elevation and angle) in which individual same/different discrimination thresholds are expressed are relative to the white point set up for the experiment, and thus are monitor-specific. Therefore, the threshold values were converted into cone excitations expressed in Weber contrasts. During the calibration and verification procedures, Weber contrasts were obtained for each post-receptoral mechanism, measured out from maximum contrast level that could be reproduced on the display (details on the procedure were described in Chapter 2, General Methods). In other words, at this point, the cone excitation of each of the three mechanisms, expressed in Weber contrasts, for the maximum radius of the particular DKL direction is known. Based on this, a scale factor was calculated by dividing Weber contrast of the mechanism by the radius. Using that scale factor we can work out excitations for any radius, since (with fixed

elevation and angle), the radius scales linearly. Thus, using DKL radiuses of the same/different discrimination thresholds and its scaled counterparts and by multiplying them by the scale factor obtained using above method we finally acquired cone excitations for each DKL condition for each participant.

One participant was tested under a different calibration than the rest, and hence scale factors differed for that individual. Further two participants were tested with the same calibration as the other 19 participants during session one, however, session two was run under a different calibration (they were unable to complete the study immediately, and completed the 2nd session after the display was recalibrated for a different experiment). For these participants, we checked whether the contrasts differed in a substantial way between the sessions. This could introduce a bias, making one of the sessions easier or more difficult than the other. For L – M and luminance contrast, the difference was 1 % and 1.3 %, respectively, and for S-cone it was 3.3%. We concluded that these differences were within acceptable levels. For these two participants, we averaged the contrasts between the sessions and used those to summarise contrast levels across all participants and mechanisms. These were as follows: Weber contrasts for discrimination thresholds ranged from 0.04 to 0.14 for S-cone (0.08 on average), from 0.007 to 0.016 for L – M (0.01 on average) and from 0.03 to 0.06 for luminance (0.04 on average). Scaled contrasts used as the *low contrast* combination ranged from 0.12 to 0.29 for S-cone (0.18 on average), while for L – M the contrast went from 0.01 to – 0.04 (0.3 on average). The *high contrast* stimuli ranged from 0.23 to 0.59 for S-cone (0.36 on average) and for L – M the contrast went from – 0.03 to 0.08 (0.05 on average).

Because of the scaling procedure applied, low and high contrast luminance shapes had a fixed value (see Chapter 2). Since three participants were tested on a different calibration, their low and high luminance contrast different slightly from the last set of the participants. Taking these three participants into account, luminance contrasts at threshold ranged from 0.032 to 0.062 (0.044 on average), *low contrast* luminance contrasts ranged from 0.097 to 0.102 (0.097 on average), and *high contrast* luminance contrasts ranged from 0.194 to 0.204 (0.195 on average).

12.4. Accuracy

There was a main effect of visual input ($F(2, 42)=43.3$, $p<.001$, $\eta^2=.67$). Bonferroni post-hoc tests showed that accuracy for luminance-defined stimuli was higher than the performance for both S-cone ($p<.001$) and L – M stimuli ($p<.001$). S-cone accuracy was itself lower than the L – M ($p<.001$). With an increase in WM load, the accuracy decreased ($F(2, 42)=227$, $p<.001$, $\eta^2=.91$; see Figure 2). Bonferroni post-hoc tests confirmed that load 3 was characterised by lower accuracy than load 2 and load 1, and load 2 by lower accuracy than load 1 (all comparisons $p<.001$; see Figure 18).

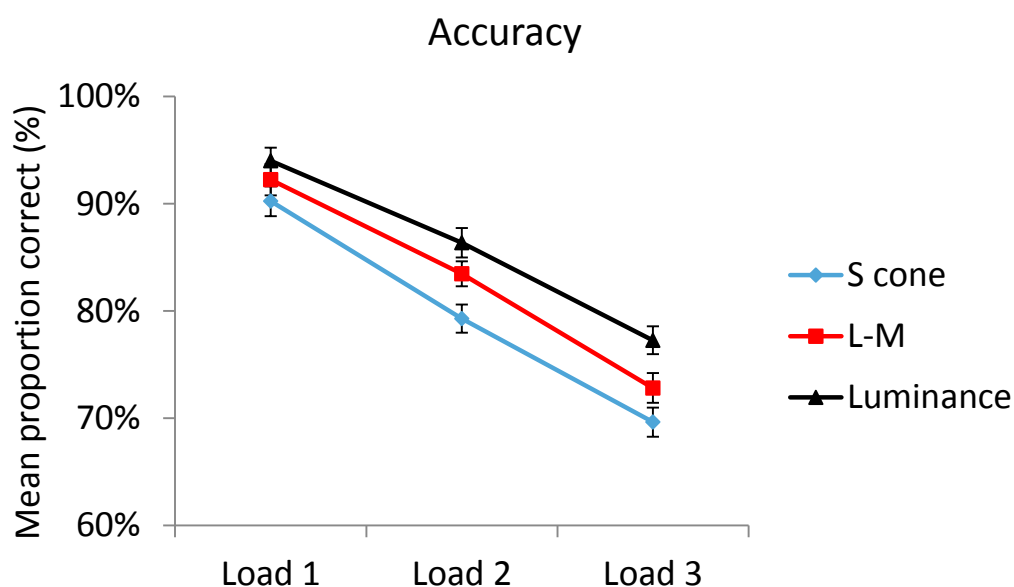


Figure 18 Mean proportion of correct responses for S-cone (blue line), L – M (red) and luminance stimuli (black) at three levels of WM load (error bars: standard error)

Accuracy was also significantly higher in response to high contrast compared to low contrast shapes ($F(1,21)=61.04$, $p<.001$, $\eta^2=.74$). There was a significant interaction between visual input and contrast ($F(2,42)=4.72$, $p=.004$, $\eta^2=.18$; see Figure 19). Bonferroni post-hoc tests showed that, at low contrast, accuracy rate differences between DKL directions were more pronounced than at high contrast. In particular, accuracy for luminance was higher than for both isoluminant conditions ($p<.001$). At the same time, L – M accuracy was itself higher than S-cone ($p=.001$). At high contrast on the other hand, there was no difference

between luminance and L - M ($p=.24$, n.s.), though both conditions elicited higher accuracy than S-cone ($p<.001$).

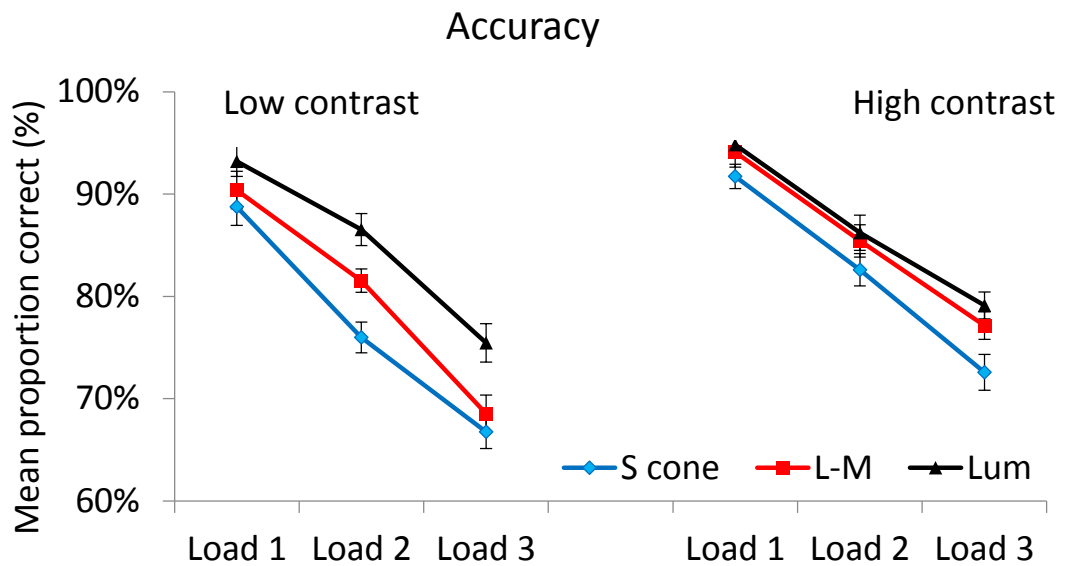


Figure 19 Mean proportion of correct responses for S-cone (blue line), L - M (red) and luminance stimuli (black) at 3 levels of WM load, shown separately for low (left) and high (right) contrast levels (error bars: standard error).

There was a main effect of probe type (match/mismatch; $F(1, 21)=5.07$, $p=.035$, $\eta^2=.19$), with mismatching probes producing a more accurate response. There was also a significant interaction between visual input and the probe type ($F(2,42)=4.19$, $p=.022$, $\eta^2=.17$) and a three-way interaction between visual input, probe type and WM load ($F(4,84)=3.46$, $p=.011$, $\eta^2=.14$). To follow up on these interactions, we conducted an ANOVA for match and mismatch separately with factors: DKL direction, WM load and contrast level. The breakdown of this interaction and illustration of effects described below are depicted in Figure 20.

12.4.1. Match

For the match, accuracy was higher for high than low contrast ($F(1, 21)=21.8$, $p<.001$, $\eta^2=.51$). Accuracy decreased with increasing load ($F(1.55,32.6)=103.0$, $p<.001$, $\eta^2=.83$). There was a main effect of DKL direction ($F(2,42)=7.36$, $p=.002$, $\eta^2=.26$). Post-hoc, Bonferroni corrected tests showed that luminance and L - M were not significantly different ($p=1.0$, n.s.). At the same time, both luminance

($p=.013$) and L – M ($p=.005$) were characterised by higher accuracy than S-cone condition. No interactions were significant.

12.4.2. Mismatch

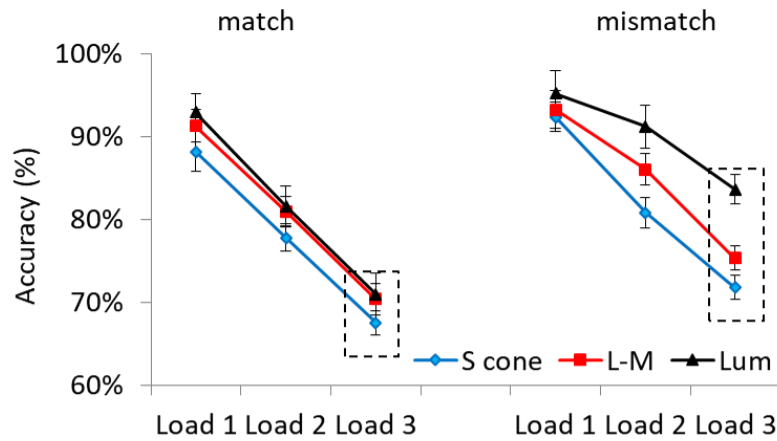
For mismatch, accuracy was also higher for high compared to low contrast ($F(1, 21)=22.6$, $p<.001$, $\eta^2=.52$), and decreased with increasing WM load ($F(1.18, 24.8)=57.1$, $p<.001$, $\eta^2=.73$). Like in the match, there was a main effect of DKL direction ($F(2, 42)=30.5$, $p<.001$, $\eta^2=.59$). This time, however, DKL directions were dissociated in terms of accuracy; according to post-hoc tests, luminance elicited higher performance than both L – M and S-cone (both $p<.001$) and L – M itself was characterised by higher accuracy than S-cone ($p=.002$).

The main effect of load and the main effect of DKL were qualified by an interaction between contrast and load ($F(2, 42)=4.71$, $p=.014$, $\eta^2=.18$) and between contrast and DKL ($F(2, 42)=6.93$, $p=.003$, $\eta^2=.25$; see Figure 20, B). Interestingly, accuracy was higher at high contrast than at low contrast for S-cone and L – M ($p<.001$, as showed by post-hoc, Bonferroni-corrected comparisons). This was not, however, the case for luminance, i.e. performance was not significantly different between low and high contrast for this DKL direction ($p=.869$).

Additionally, better accuracy for high versus low contrast was present for load 1 ($p=.001$) and load 3 ($p<.001$), while the difference was not significant for load 2 ($p=.090$). Of main interest was the interaction between load and DKL direction which, unlike at match, was significant ($F(3, 63.3)=6.2$, $p=.001$, $\eta^2=.23$; see Figure 20 A). Luminance was characterised by better performance than S-cone at all WM loads ($p=.037$, $p<.001$ and $p<.001$ for load 1, 2 and 3, respectively).

Luminance had better accuracy than L – M at load 2 ($p=.009$) and load 3 ($p<.001$) only. L – M demonstrated better accuracy than S-cone only at load 2 ($p=.003$). In other words, at load 2, accuracy differentiates all three DKL directions, with the lowest accuracy for S-cone, intermediate for L – M, and highest for luminance. At highest WM load, the difference between isoluminant conditions disappears, while luminance still elicits better performance. See Figure 20 B for a breakdown of effects at load 3 for low and high contrast and match and mismatch.

A) Behavioural accuracy (N = 22)



B) Accuracy at Load 3

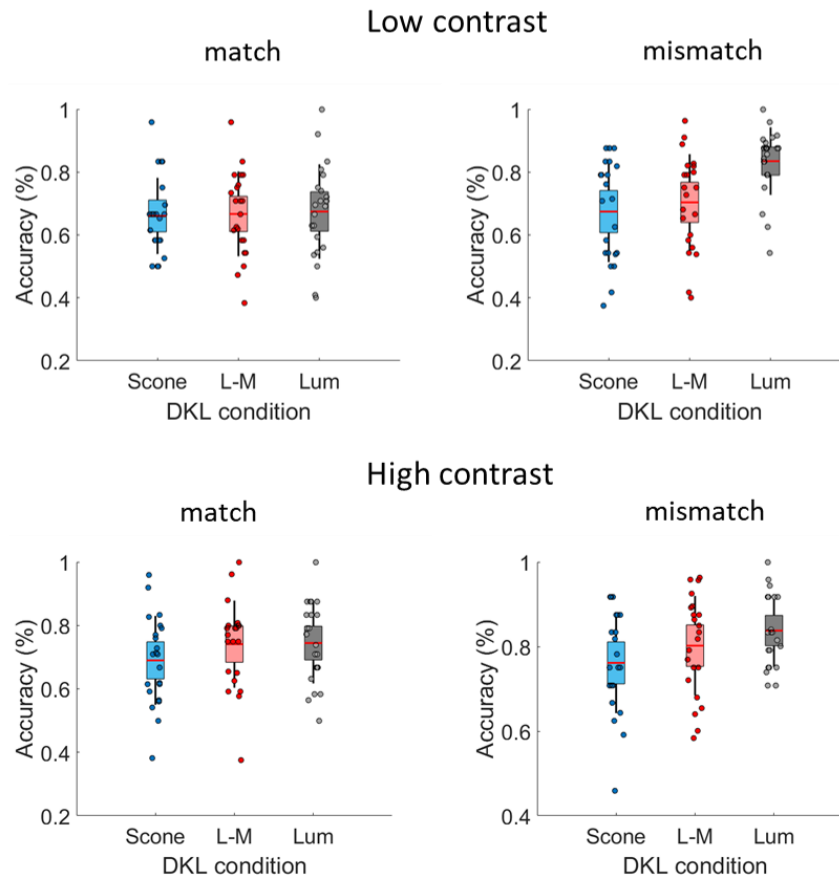


Figure 20 A) Proportion of correct responses for S-cone (blue line), L – M (red) and luminance stimuli (black) at 3 WM loads shown separately for the match (left) and mismatch probes (left). Error bars represent standard error of the mean. Dashed box marks comparison between the DKL directions at WM load 3. B) Box plots with individual data points (each dot is an average of one participant) for the three DKL directions, at WM Load 3, shown separately for low/high contrast and match/mismatch condition. Note the increase in accuracy for luminance at low contrast mismatch condition, and smaller spread and narrower confidence intervals at high contrast. Red lines inside box plots represent the mean, coloured patches are 95% confidence intervals, the black vertical line is one standard deviation.

To summarise participants' performance between match and mismatch, accuracy at different WM loads differentiated between luminance and isoluminant conditions at mismatch. Although the performance dropped for all DKL conditions, luminance remained superior over isoluminant conditions. At match, on the other hand, performance dropped with increasing WM load for luminance and isoluminant stimuli to a similar magnitude. In both cases, performance for S-cone was the lower than other conditions throughout, although for mismatch at highest WM load, L - M performance drops to similar levels as S-cone.

12.5. Reaction times

Figure 21 depicts mean of median reaction times for S-cone, L - M and luminance shapes. There was a main effect of DKL direction ($F(2,42)=24.3$, $p<.001$, $\eta^2=.54$). Bonferroni-corrected post-hoc tests indicated that responses were faster for luminance than S-cone and L - M ($p<.001$). S-cone and L - M did not differ ($p=.222$, n.s.). Reaction time increased with WM load (main effect of load ($F(1.41,29.6)=38.1$, $p<.001$, $\eta^2=.65$).

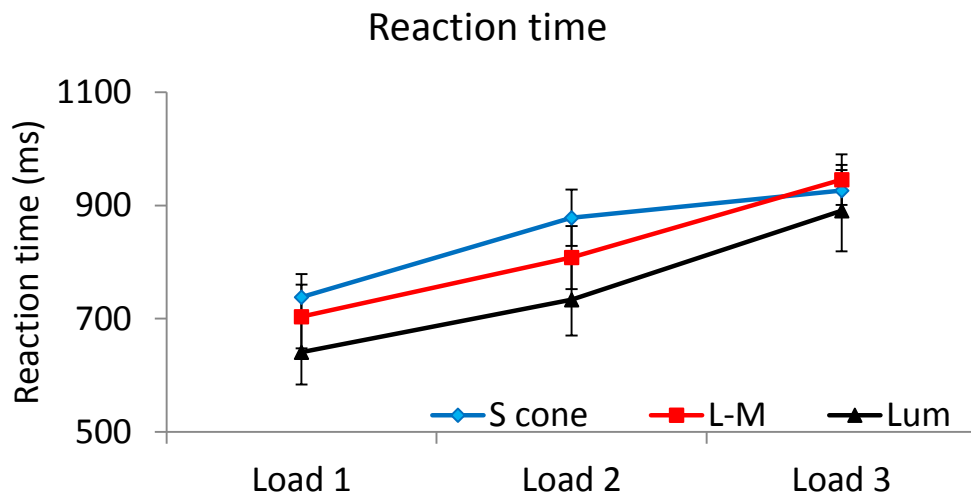


Figure 21 Mean of median reaction times for S-cone (blue line), L - M (red) and luminance stimuli (black) at three levels of WM load (error bars: standard error).

Responses to matching probes were faster than responses to mismatching shapes (the main effect of probe type, $F(1, 21)=10.5$, $p=.004$, $\eta^2=.33$) and faster for high contrast compared to low contrast condition ($F(1,21)=52.65$, $p<.001$, $\eta^2=.65$).

An interaction between WM load and DKL direction was also significant ($F(2.21,46.3)=3.95$, $p=.023$, $\eta^2=.16$). Post-hoc tests showed that responses were faster for luminance shapes than for S-cone and L – M at load 1 ($p<.001$ and $p=.004$ for S-cone and L – M, respectively) and load 2 (both $p<.001$). Responses to L – M shapes were also faster than responses to S-cone at load 1 ($p=.048$) and load 2 ($p=.004$).

At load 3, post-hoc tests did not show significant differences between the three DKL directions.

12.6. Comparison with mixed signals stimuli

As mentioned in the methods section, a “mixed signals” condition was used as a control to investigate how luminance artifact would affect performance in response to isoluminant conditions, if such artifact was present. To that end we conducted an additional ANOVA with factors: contrast level (2 levels: low and high contrast), DKL direction (4 levels: Mixed signals, luminance, isoluminant L – M, isoluminant S-cone), WM load (3 levels: Load 1, Load 2, Load 3) and probe type (2 levels: match or mismatch). Greenhouse-Geisser corrections were applied where necessary.

An interaction between probe type and DKL direction was significant ($F(2.05,43.2)=4.63$, $p=.014$, $\eta^2=.18$), as well as a three-way interaction between probe type, WM load and DKL direction ($F(6, 126)=2.21$, $p=.046$, $\eta^2=.095$; see Figure 22.A). Post-hoc, Bonferroni-corrected tests showed that, for the mismatch condition at high WM load, mixed signals condition performed better than S-cone ($p<.001$) and L – M ($p=.002$), but it also elicits similar performance as luminance-defined shapes ($p=.114$, n.s.).

Further, an interaction between contrast and DKL direction was significant ($F(3, 63)=3.80$, $p=.014$, $\eta^2=.15$; see Figure 22.B). Post-hoc, Bonferroni-corrected tests revealed that at low contrast, mixed signals condition elicited better performance than S-cone ($p<.001$) and L – M ($p=.044$), while it did not reach luminance accuracy level ($p=.005$).

This indicates that a luminance artifact present in otherwise isoluminant stimuli can lead to higher accuracy at low contrasts, as well as in response to mismatch probes at high WM load. The finding that in both cases performance in response to chromatic shapes that contain an additional achromatic component is clearly dissociable from purely isoluminant shapes suggests that our isoluminant stimuli were likely not significantly contaminated by luminance signal. It appears that only a relatively large luminance component (as it was the case with the mixed – signal condition) leads to improvement in performance. In summary, these findings validate the design of the stimuli used in this study.

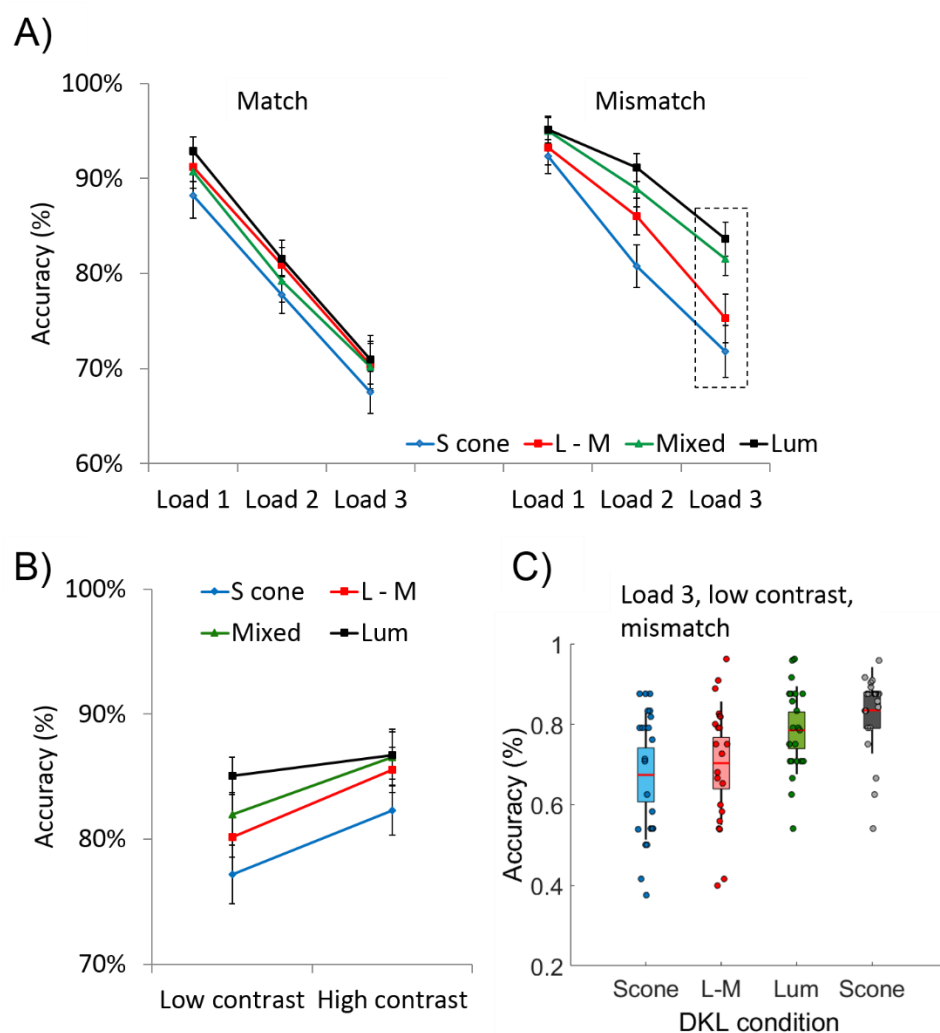


Figure 22 A) Line plot showing accuracy in response to S-cone (blue line), L – M (red line), mixed signals (green line) and luminance-defined shapes (black line) at three WM load levels, in response to match (left) or mismatch probe (right). B) Overall accuracy at low (left) and high contrast (right) in response to four DKL directions. Error bars in A and B represent standard error of the mean. C) Box plots with individual data points (each dot is an average of one participant) for the three DKL directions, at WM Load 3, shown separately for low contrast in response to mismatch probe (see the dashed-line box in A). Red lines inside box plots represent the mean, coloured patches are 95% confidence intervals, the black vertical line is one standard deviation.

13. Event-related potential (ERP) results

13.1. Encoding stage

13.1.1. P1 Amplitude (Oz, O1, O2; 80-160 ms)

Inspection of Grand averaged waveforms (see Figure 26) suggested that the P1 component was reliably elicited only by luminance shapes, which is in accordance with the previous literature (Crognale, 2002; Gerth et al., 2003). In addition, amplitudes in response to high contrast shapes appeared to be larger than for low contrast shapes. We used a repeated measures ANOVA with factors: contrast level (low or high) and DKL direction (3 levels: S-cone, L – M and luminance) to confirm these observations (see Figure 23).

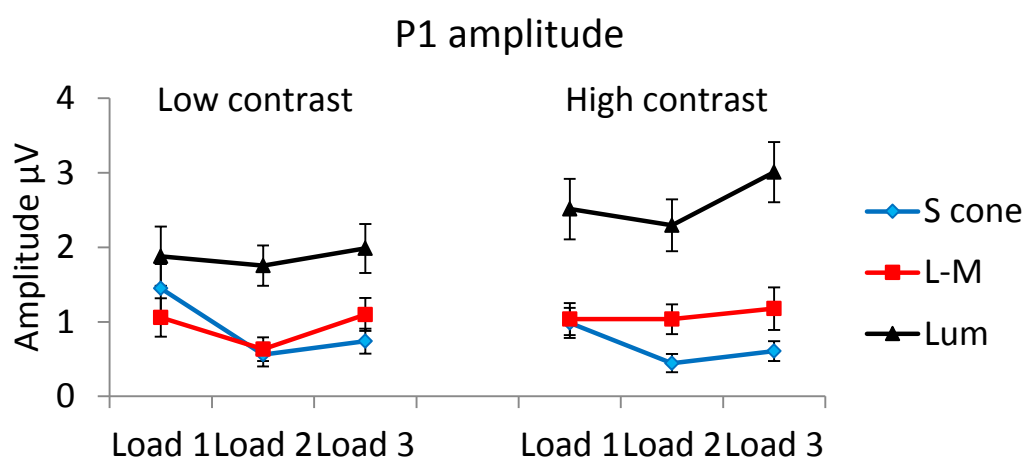


Figure 23 Local peak amplitudes of component P1 for *S-cone* (blue line), *L – M* (red) and *luminance stimuli* (black), at three levels of load for low (left) and high (right) contrast. (error bars: standard error).

There was indeed a main effect of DKL direction ($F(1.17, 24.6)=19.6$, $p<.001$, $\eta^2=.48$), with luminance eliciting higher amplitudes than S-cone ($p=.001$) and L – M ($p<.001$). Additionally, an interaction between contrast level and DKL condition was significant ($F(2, 42)=8.09$, $p=.001$, $\eta^2=.28$). Post hoc tests using the Bonferroni correction showed that luminance was higher than S-cone ($p=.020$) and L – M ($p=.014$) at low contrast as well as at high contrast (both $p<.001$).

There was no difference between amplitudes at low and high contrast for S-cone and L – M. For luminance, amplitudes at high contrast were higher ($p=.001$).

Based on these results, we did not include S-cone and L – M in further analyses.

Two separate ANOVAs with factors WM load (3 levels) and electrodes (3 levels: electrodes O1, O2 and Oz) for each contrast level were conducted.

13.2. Low contrast

There was a main effect of electrode location ($F(1.55, 32.5)=4.27, p=.031, \eta^2=.17$).

Local peak amplitude was lower at electrode Oz than O2 ($p=.005$). See Figure 24 for a grand average of the PI component at low contrast.

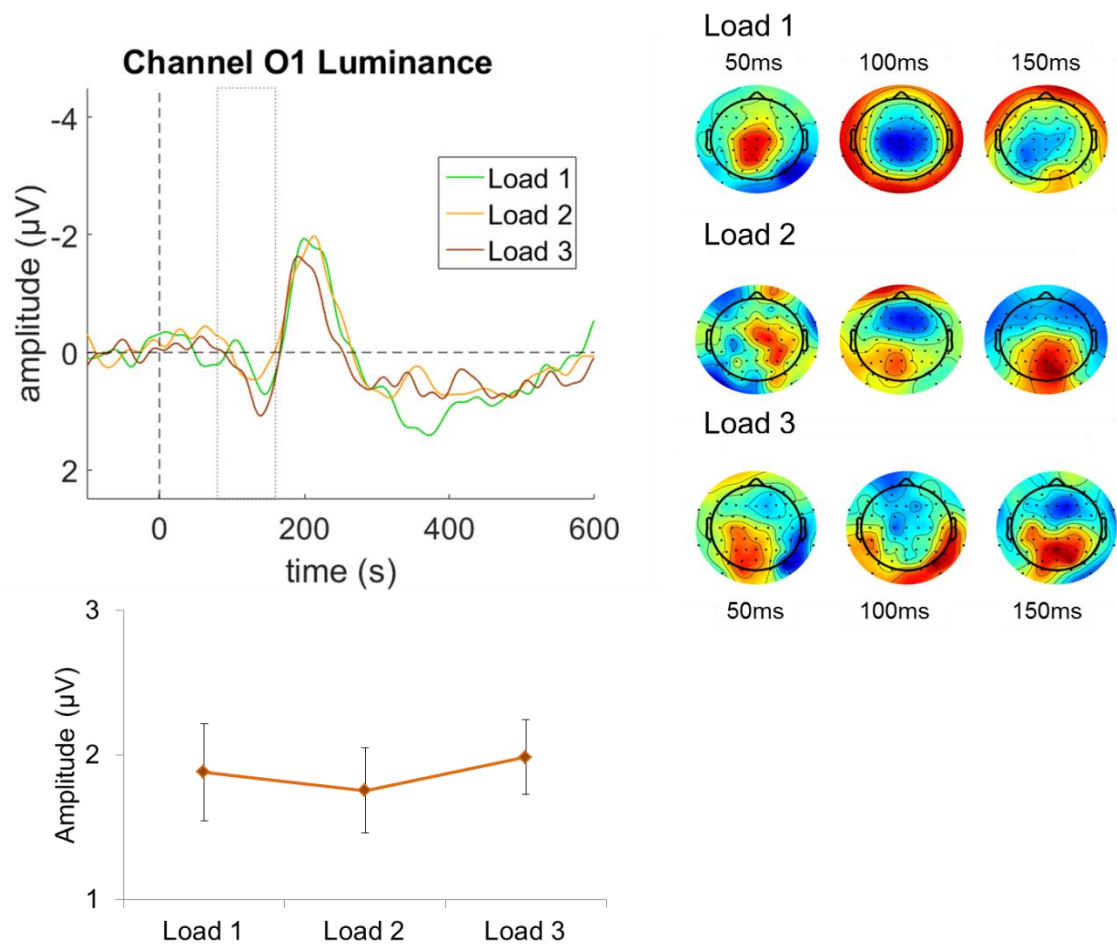


Figure 24 Upper left: Grand average waveform at electrode O1 during encoding low contrast luminance-defined shapes, at three levels of WM load. Gray box marks the time window (80 – 160 ms) from which peak amplitudes were extracted for analysis. Bottom left: average peak amplitude values at three levels of WM load, extracted from 80 – 160 ms time window. Error bars are standard error of the mean. Upper right: corresponding topographic maps at 50, 100 and 150 ms after stimulus onset.

13.3. High contrast

As expected, results demonstrated WM load-related amplitude modulation (main effect of load ($F(2, 42)=3.84, p=.029, \eta^2=.15$). Post-hoc, Bonferroni-corrected tests did not point to significant pairwise comparisons, although inspection of the waveforms and average peak amplitude values (see Figure 25) suggest that amplitudes are the highest at load 3.

There were no significant differences between electrodes ($p=.079, n.s.$) and no electrode by load interaction ($p=.42, n.s.$).

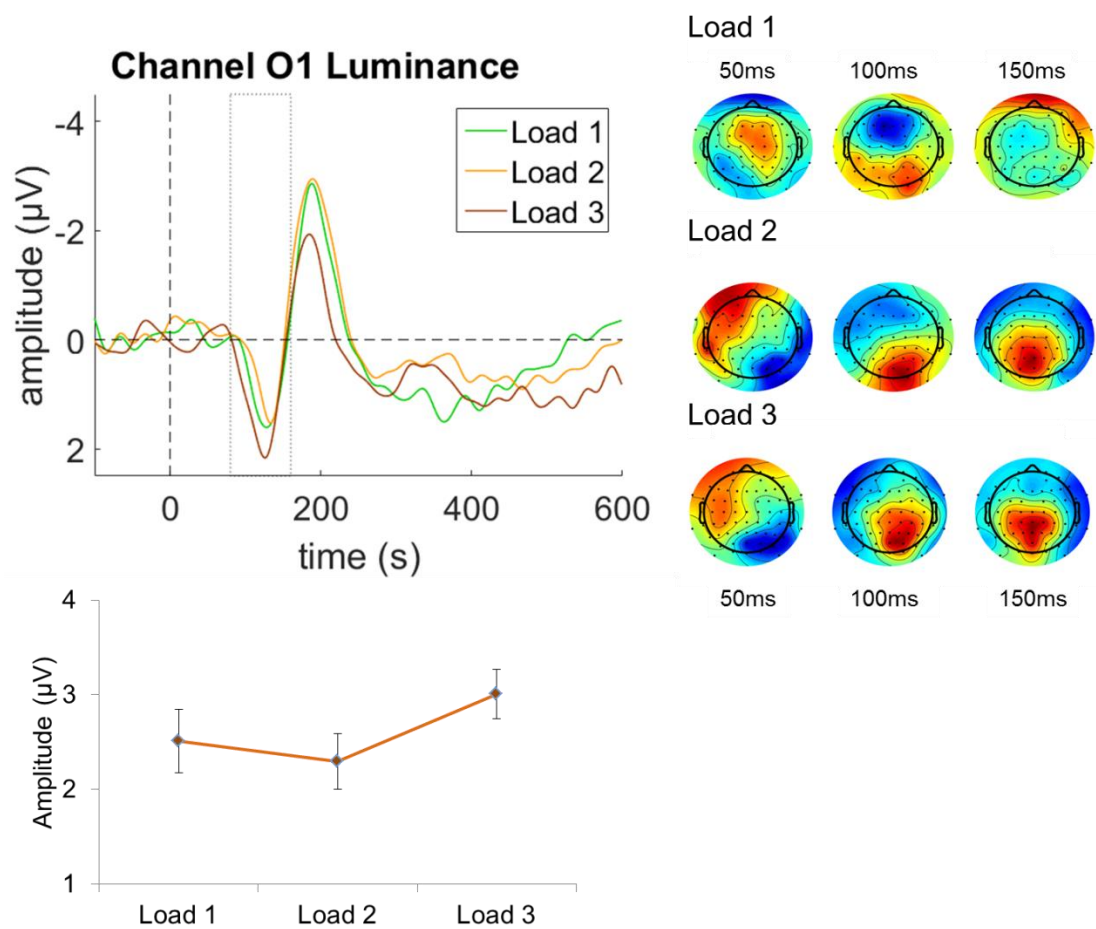


Figure 25 Upper left: Grand average waveform at electrode O1 during encoding high contrast luminance-defined shapes, at three levels of WM load. The grey box marks the time window (80 – 160 ms) from which peak amplitudes were extracted for analysis. Bottom left: average peak amplitude values at three levels of WM load, extracted from 80 – 160 ms time window. Error bars are standard error of the mean. Upper right: corresponding topographic maps at 50, 100 and 150 ms after stimulus onset.

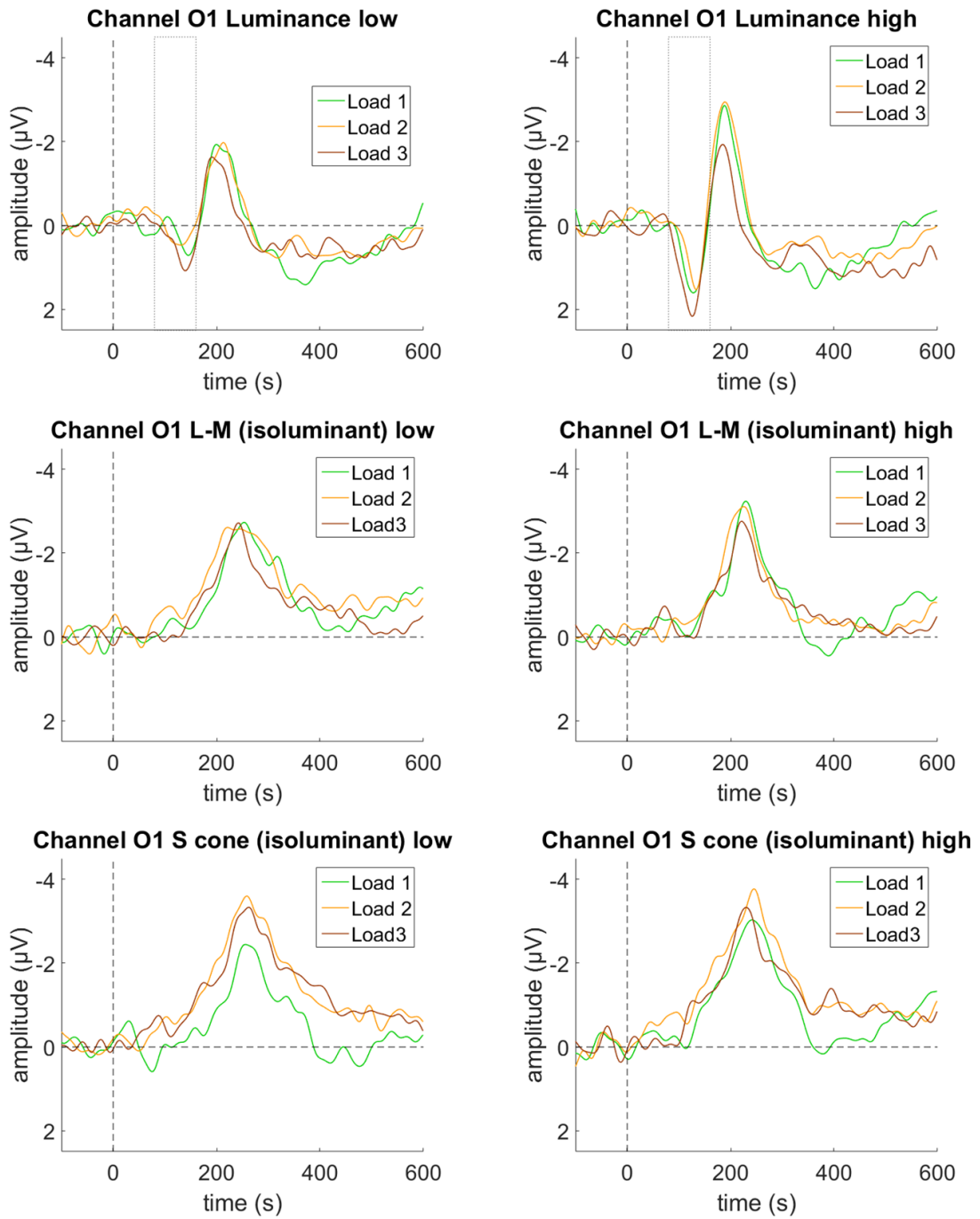


Figure 26 Averaged waveforms at electrode O1 during WM encoding of luminance, L - M and S-cone DKL directions, presented at low contrast (left column) and high contrast (right column). Note a robust PI component for luminance at high contrast and its smaller, though still clear, counterpart in low contrast condition. Isoluminant conditions did not elicit a reliable PI, in accordance with previous findings (Gerth et al., 2003).

13.3.1. Latency

No effects or interactions were significant.

13.4. N1 Amplitude (Oz, O1, O2; 130-300 ms)

Refer to Figure 26 for plotted Grand averaged waveforms. Average peak amplitudes for the component N1 for different conditions are shown in Figure 27. Refer to Figure 26 for Grand averaged waveforms.

There was a main effect of DKL direction ($F(2, 42)=27.8, p<.001, \eta^2=.57$). This effect was qualified by an interaction between electrode location and DKL ($F(2.97, 62.3)=6.31, p=.001, \eta^2=.23$). Post-hoc, Bonferroni-corrected tests showed that luminance elicited less negative amplitudes than both isoluminant conditions at all electrode sites (all $p<.000530$). Additionally, S-cone elicited more negative amplitude than L – M at electrodes O2 ($p=.040$) and Oz ($p=.015$), but this was not the case at electrode O1 ($p=.220, n.s.$).

There was no main effect of load ($F(2, 42)=.758, p=.475, \eta^2=.03, n.s.$), however, an interaction between WM load and DKL was significant ($F(3.58, 75.3)=2.66, p=.045, \eta^2=.11$). Post-hoc, Bonferroni-corrected tests showed that, at every load level, luminance elicited less negative amplitude than both S-cone and L – M (all comparison p – values ranged from $p=.000014$ to $p=.008$). However, only at load 2 did the L – M differed from S-cone, with less negative amplitude for the latter ($p=.006$). At load 1 and load 3, S-cone and L – M did not differ significantly (see Figure 27).

N1 amplitudes for high contrast were larger (more negative) than for low contrast ($F(1, 21)=19.3, p<.001, \eta^2=.48$).

The main effect of electrode location ($F(1.41, 29.7)=5.55, p=.016, \eta^2=.21$) suggested that N1 amplitudes at electrode O1 tended to be less negative than at electrode O2. While post-hoc, Bonferroni-corrected tests did not point to any significant differences, there was a significant quadratic component to this interaction ($F(1, 21)=7.20, p=.014, \eta^2=.25$), which suggested that electrode O2 had more negative amplitude than the other two electrodes.

All factors interacted with each other ($F(8, 168)=2.72$, $p=.008$, $\eta^2=.11$).

This was followed with an ANOVA for each DKL direction separately, with the following factors: contrast, electrode location and WM load. The results showed that, for luminance, a three-way interaction between contrast level, electrode location and load was significant ($F(4, 84)=3.27$, $p=.015$, $\eta^2=.13$). This interaction was followed up with a separate ANOVA for each contrast, with factors electrode location and load. At low contrast, electrode location and load interacted ($F(4, 84)=3.15$, $p=.018$, $\eta^2=.13$). Post-hoc analyses using the Bonferroni correction did not point to any significant pairwise comparisons. At high contrast, there were no main effects or interactions.

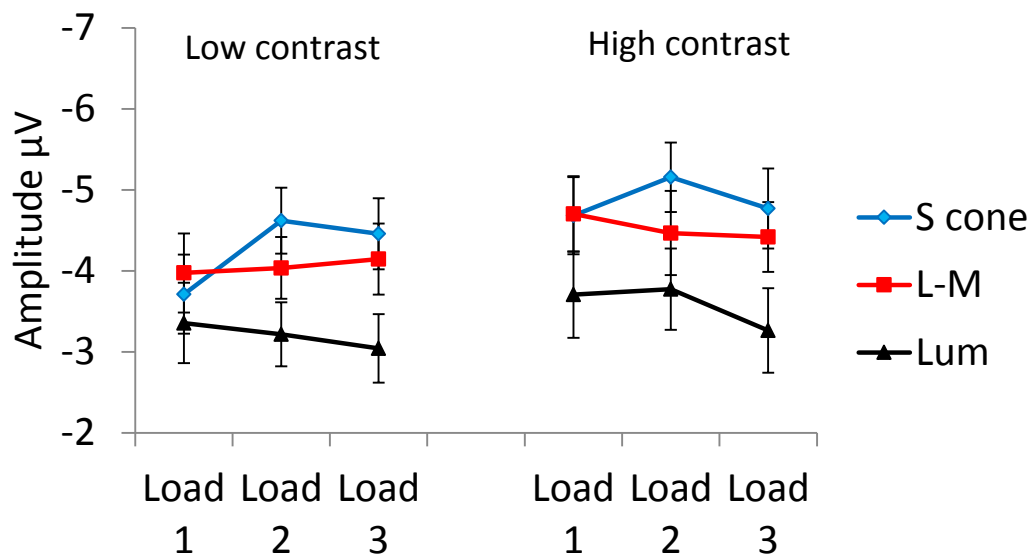


Figure 27 Local peak amplitudes of component NI for each DKL direction, at three levels of load for low and high contrast, averaged over electrodes O1, O2 and Oz. Error bars represent standard error of the mean.

13.5. Latency

There was a main effect of DKL direction $F(2, 30)=9.02$, $p=.001$, $\eta^2=.38$). Overall, amplitudes in response to luminance peaked earlier than for L – M ($p=.002$). In addition, the interaction between electrode location and DKL direction was significant $F(4, 60)=3.78$, $p=.008$, $\eta^2=.20$). Bonferroni-corrected post-hoc tests showed that NI in response to luminance shapes peaked earlier than S-cone ($p=.021$) and L – M ($p=.002$) at electrode O2, as well as at electrode O1 ($p=.018$

and $p=.005$ for comparisons with S-cone and L – M, respectively). At electrode Oz, latencies in response to S-cone peaked earlier than L – M ($p=.040$).

There was a main effect of load $F(2, 30)=4.39$, $p=.021$, $\eta^2=.23$). As shown by post-hoc, Bonferroni-corrected tests, amplitudes in response to load 1 peaked earlier than in response to load 2 ($p=.030$).

Latencies in responses to high contrast shapes were shorter than in response to low contrast shapes $F(1, 15)=25.1$, $p<.001$, $\eta^2=.63$). There was a main effect of electrode location $F(2, 30)=4.29$, $p=.023$, $\eta^2=.22$). All factors interacted with each other $F(8, 120)=2, 76$, $p=.008$, $\eta^2=.15$).

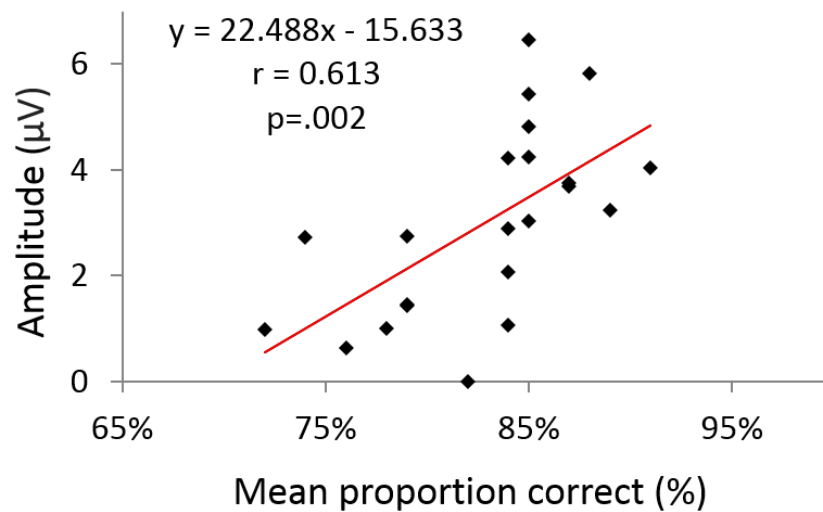
13.6. P1 and N1 interactions with behavioural performance

We have correlated P1 in response to luminance stimuli and N1 amplitude in response to isoluminant conditions (S-cone and L – M) at each electrode and three load levels with overall accuracy (i.e. average accuracy at both contrasts, for each DKL condition). The results indicated that P1 component during the encoding of luminance shapes correlated with performance at load 1 ($r=.480$, $p=.024$), load 2 ($r=.593$, $p=.004$) and load 3 ($r=.613$, $p=.002$; see *Table 5* for details) at electrode OI⁷. There were no correlations between the overall performance in response to N1 amplitudes elicited by both isoluminant conditions.

⁷ Even though there was no clear P1 for S-cone and L – M, we have run the same correlation with values extracted from the same time – window for these two conditions. Not surprisingly, amplitudes did not correlate with overall task accuracy.

Table 5 P1 amplitude at encoding stage for luminance condition and N1 amplitude at encoding for two isoluminant conditions correlation with overall task accuracy. Light green=significant correlations, light blue=non-significant values. The figure below shows the correlation between the P1 component at electrode O1 (for load 3) and overall task accuracy.

	P1 amplitude			N1 amplitude						
	Luminance			Isoluminant: L-M			Isoluminant: S cone			
Overall accuracy	Load 1	Load 2	Load 3	Load 1	Load 2	Load 3	Load 1	Load 2	Load 3	(Pearson's r)
	.480*	.593**	.613**	-0.006	0.169	0.075	-0.039	0.02	0.219	
	0.024	0.004	0.002	0.98	0.453	0.742	0.862	0.929	0.328	(p-value)



Since the amplitude values used for correlation are derived from high contrast luminance waveforms, an additional correlation was performed with accuracy in response to high contrast stimuli only, rather than overall accuracy. Performance correlated with P1 amplitude at load 2 ($r=.488$, $p=.021$) and load 3 ($r=.483$, $p=.023$), but not with load 1 ($r=.199$, $p=.375$, n.s.; see Table 6 for details). As before, the N1 amplitude in response to both isoluminant conditions did not correlate with performance.

Table 6 P1 amplitude at encoding stage for luminance condition and N1 amplitude at encoding for two isoluminant conditions correlation with task accuracy at high contrast, for corresponding DKL condition. Light green=significant correlations, light blue = non-significant values.

	P1 amplitude			N1 amplitude						
	Luminance			Isoluminant: L-M			Isoluminant: S cone			
Accuracy (high contrast)	0.199	.488*	.483*	-0.015	0.1	0.032	0.029	0.184	0.316	(Pearson's r)
	0.375	0.021	0.023	0.948	0.658	0.887	0.899	0.412	0.152	(p-value)
	Load 1	Load 2	Load 3	Load 1	Load 2	Load 3	Load 1	Load 2	Load 3	

13.7. P3a Amplitude (C1, C2, Cz; 200-400 ms)

The main effect of DKL was significant ($F(2, 42)=5.69, p=.006, \eta^2=.21$). Post-hoc tests showed that luminance elicited lower P3a amplitude than L – M ($p=.032$), but not S-cone ($p=.053, n.s.$). S-cone and L – M itself did not differ ($p=1.0$).

The amplitude decreased with increasing load ($F(2, 42)=4.32, p=.020, \eta^2=.17$). Interestingly, inspection of Grand averaged waveforms (see Figure 28) would suggest that P3a amplitude in response to luminance-defined shapes tended to be lower than the isoluminant conditions; however, the interaction between WM load and DKL direction was not significant ($F(4, 84)=1.89, p=.119, \eta^2=.08$).

The overall P3a amplitude was lower for low compared to high contrast stimuli ($F(1, 21)=7.36, p=.013, \eta^2=.26$).

P3a amplitude was highest at lateral electrode sites ($F(2, 42)=109, p<.001, \eta^2=.84$). An interaction between contrast and electrode location ($F(2, 42)=3.45, p=.041, \eta^2=.14$), although post-hoc tests did not account for this interaction.

A separate ANOVA with factors WM load (3 levels), visual input/DKL direction (3 levels: S-cone, L – M and luminance) and electrodes (3 levels: electrodes C1, C2 and Cz) for each contrast level was conducted.

13.8. Low contrast

DKL effect was not significant ($F(2, 42)=3.15$, $p=.053$, $\eta^2=.13$), although luminance appeared to elicit somewhat smaller amplitude than other DKL directions. Test of within-subject contrasts supports this with a marginally significant linear decrease in amplitude from S-cone and L – M to luminance conditions ($F(1, 21)=4.46$, $p=.047$, $\eta^2=.17$).

13.9. High contrast

Luminance elicited smaller amplitude (main effect of DKL: $F(1.47, 31.0)=7.38$, $p=.005$, $\eta^2=.26$) than L – M (Bonferroni-corrected post hoc test, $p<.001$) but not S-cone ($p=.082$, n.s.); S-cone itself did not differ significantly from L – M ($p=1.00$, n.s.). Load 1 elicited larger amplitude than load 3 ($p=.012$), but not load 2 ($p=.09$, n.s.). The interaction between load and DKL direction ($F(4, 84)=2.53$, $p=.046$, $\eta^2=.11$) suggested that at the highest load, luminance had a lower amplitude than S-cone ($p=.020$) and L – M ($p<.001$). Additionally, luminance had a lower amplitude than L – M at load 2 as well ($p=.002$), but not S-cone ($p=.074$, n.s.). There were no significant simple effects at load 1, suggesting waveforms from all conditions were similar across DKL directions.

Waveforms in response to both isoluminant conditions were not by itself modulated by WM load, as shown with post-hoc tests using Bonferroni correction. However, for luminance, Load 1 had significantly higher P3a amplitude than Load 2 ($p=.005$) and load 3 ($p=.004$). Test of within-subject contrasts for the Load by DKL interaction has shown a significant linear effect ($F(1, 21)=8.27$, $p=.030$, $\eta^2=.20$), suggesting that the amplitude tended to decrease with increasing WM load for luminance.

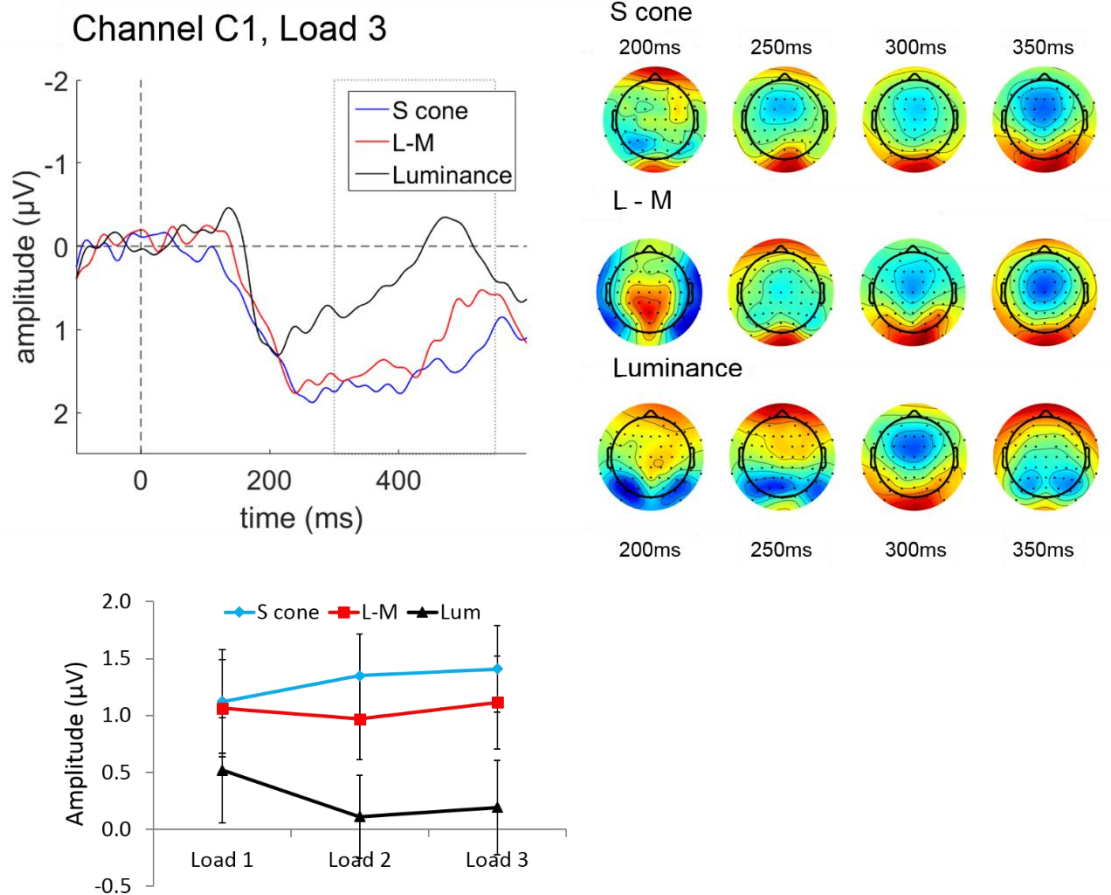


Figure 28 Upper left: Grand average waveform at electrode C1 during encoding high contrast luminance-defined, L - M and S-cone shapes at load 3. The grey box marks the time window (200-400 ms) from which peak amplitudes were extracted for analysis. Bottom left: average peak amplitude values at three levels of WM load for luminance, L - M and S-cone shapes, extracted from 200-400 ms time window. Error bars are standard error of the mean. Upper right: corresponding topographic maps at 200, 250, 300 and 350 ms after stimulus onset.

13.10. Latency

There was a main effect of WM load $F(2, 32)=4.10, p=.026, \eta^2=.20$. While post-hoc, Bonferroni-corrected tests did not point to significant pairwise comparisons, load 1 appeared to elicit somewhat shorter latencies than load 2 and load 3.

There was a main effect of contrast ($F(1, 16)=7.0, p=.018, \eta^2=.30$), qualified by an interaction between contrast and DKL direction ($F(2, 32)=8.08, p=.001, \eta^2=.33$). Post-hoc, Bonferroni-corrected tests showed that latencies in responses to high contrast shapes were shorter than in response to low contrast shapes for S-cone ($p=.017$) and L - M conditions ($p=.001$). However, the latencies did not differ between contrast levels for luminance-defined stimuli ($p=.475, n.s.$).

13.10.1. P3b Amplitude (P3, P4, Pz; 200-500ms)

There was a main effect of DKL $F(2, 42)=18.1, p<.001, \eta^2=.46$), qualified by an interaction between electrode location and DKL ($F(2.7, 56.8)=5.01, p=.005, \eta^2=.19$; see Figure 29). Post hoc tests using Bonferroni correction showed that there were no significant differences between DKL directions at electrode Pz. At electrode P3 and P4, luminance elicited higher amplitudes than both S-cone and L – M luminance (electrode P3: $p<.001$ and $p=.012$ for S-cone and L – M, respectively; electrode P4: $p=.001$ and $p=.002$ for S-cone and L – M, respectively; see Figure 30).

Main effect of load was not significant ($F(1.18, 24.7)=2.61, p=.086, \eta^2=.11$).

Amplitudes were higher for high contrast stimuli ($F(1, 21)=17.7, p<.001, \eta^2=.46$).

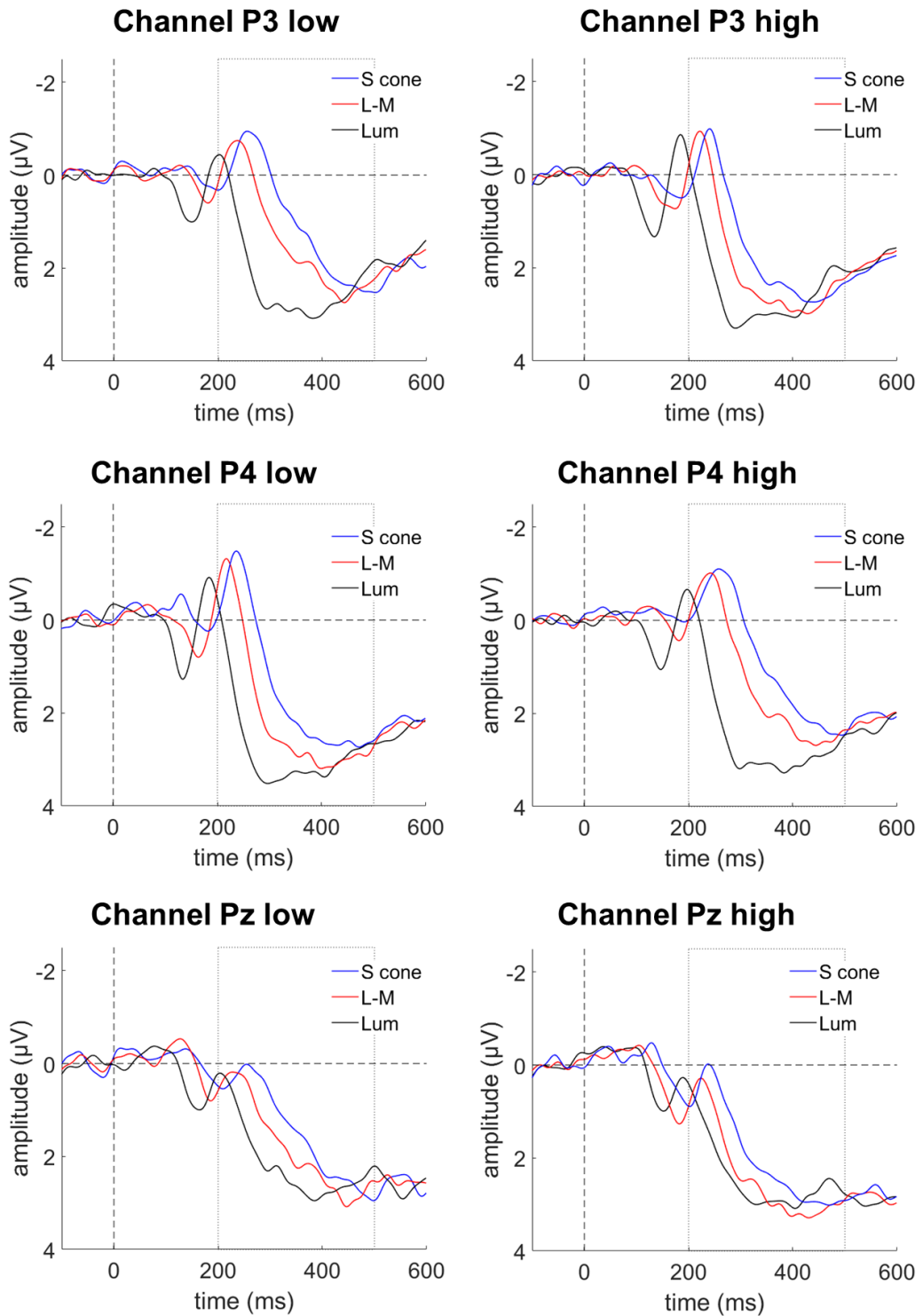


Figure 29 P3b amplitude at electrodes P3, P4 and Pz (rows 1 – 3), at low and high contrast (columns 1 & 2), for luminance (black line), L – M (red) and S-cone (blue). The grey box indicates time window from which the peak amplitudes were extracted for analysis (200 – 500 ms).

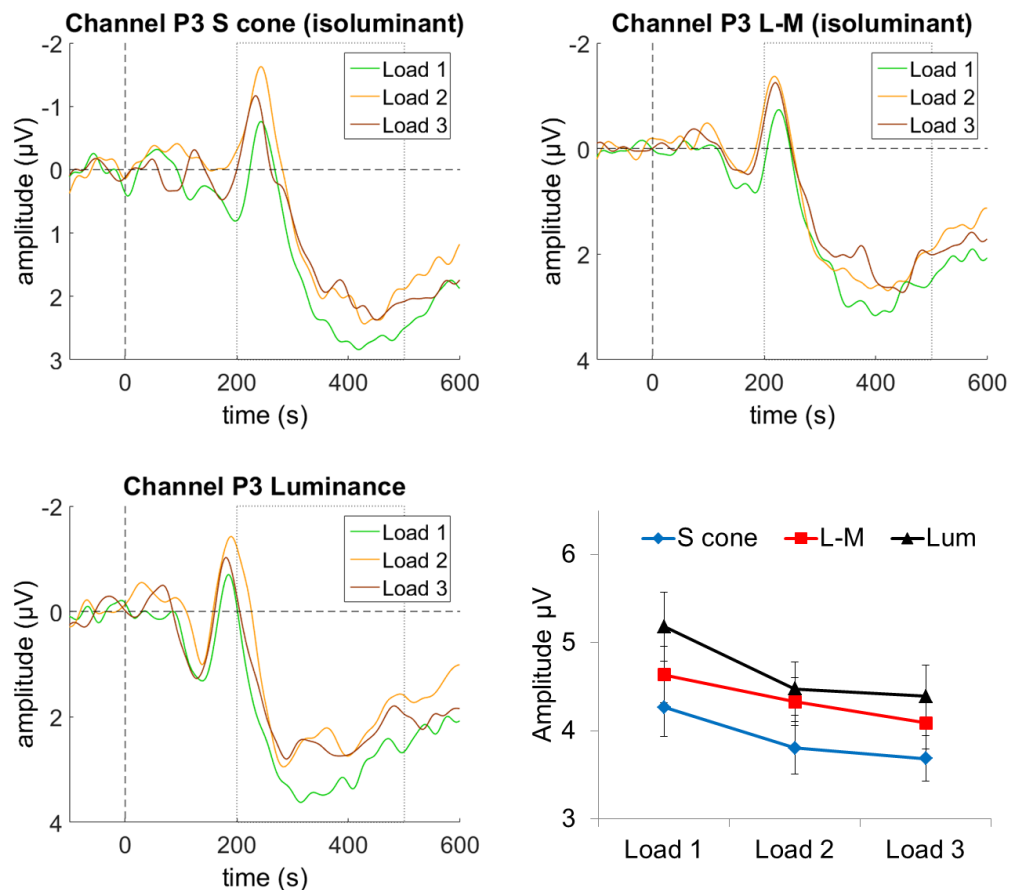


Figure 30 P3b waveforms at electrode P3 at three levels of WM load, for S-cone (upper left), L – M (upper right) and luminance (bottom left). The grey box indicates time window from which the peak amplitudes were extracted for analysis (200 – 500 ms). Average peak amplitude values at three levels of WM load for S-cone (blue line), L – M (red line) and luminance (black line) are shown on the line plot at the bottom-right corner. Error bars are standard error of the mean.

13.10.2. Latency

There was a main effect of DKL direction $F(2, 32)=41.2, p<.001, \eta^2=.72$) and load ($F(2, 32)=6.51, p=.004, \eta^2=.29$), qualified by an interaction between load and DKL direction $F(4, 64)=3.45, p=.013, \eta^2=.18$). Post hoc tests using Bonferroni correction showed that component latencies in response to S-cone shapes varied with WM load. More specifically, P3b latency was shorter at load 1 than at load 2 ($p<.001$) and load 3 ($p=.003$). There was no load modulation for L – M and luminance shapes. There was a main effect of contrast ($F(1, 16)=31.5, p<.001, \eta^2=.66$), qualified by an interaction between contrast and DKL direction $F(2, 32)=3.92, p=.030, \eta^2=.20$).

Post-hoc, Bonferroni-corrected tests showed that latencies in responses to high contrast shapes were shorter than in response to low contrast shapes for S-cone ($p=.001$) and L – M conditions ($P<.001$). However, the latencies did not differ between contrast levels for luminance-defined stimuli ($p=.182$, n.s.).

14. ERPs – maintenance stage

14.1. Stimuli offset peak (700-900 ms)

A negative peak could be observed in the grand average waveforms shortly after stimulus offset (see Figure 31). It is most likely a stimulus offset – evoked potential. The peak is most clearly visible in Luminance data and, analogically to PI, it is less robust or absent in response to isoluminant shapes. It is interesting to note that for luminance shapes, Grand average waveforms seem to be somewhat load – sensitive, with the highest amplitude for load 1 and the lowest for load 3. The same offset peak is not that robust for L – M and S-cone shapes and it does not display similar load – dependence pattern. To confirm these observations, we performed a repeated measures ANOVA with factors: contrast (2 levels: low and high contrast), WM Load (3 levels), DKL direction (3 levels: S-cone, L – M and luminance) and electrode locations (3 levels: O1, O2 and Oz). Local amplitudes were extracted from the 700 – 1000 ms interval, determined subjectively based on grand average waveforms.

There was a main effect of DKL direction $F(1.47, 30.8)=5.12, p=.019, \eta^2=.20$. Pairwise comparisons did not point to significant differences, however, it appeared that luminance tended to elicit larger amplitude than S-cone ($p=.082, n.s.$) and L – M ($p=.066, n.s.$).

An interaction between contrast and electrode location was also significant ($F(2, 42)=6.1, p=.005, \eta^2=.22$), although post-hoc, Bonferroni-corrected tests did not point to significant pairwise comparisons.

14.2. Slow wave (1000-1600 ms) – occipital (electrodes O1, O2, and Oz).

There was a main effect of DKL direction ($F(2, 42)=12.3, p<.001, \eta^2=.37$): luminance elicited lower amplitude than S-cone ($p=.005$) and L – M ($p=.001$). There was a main effect of load ($F(2.39, 29.2)=3.936, p=.044, \eta^2=.16$; see Figure

31). Post-hoc tests suggested that load 3 had a larger amplitude than load 2, although this effect was not significant ($p=.05$, n.s.).

There was a main effect of electrode location ($F(1.52, 31.9)=13.1$, $p<.001$, $\eta^2=.38$), qualified by an interaction between contrast level and electrode location ($F(2, 42)=5.73$, $p=.006$, $\eta^2=.21$). Post-hoc, Bonferroni-corrected tests showed that mean amplitude was larger at channel Oz than O1 at both contrast levels (both $p<.001$), however amplitude at electrode O2 was larger than at electrode O1 only at high contrast ($p=.008$), but not at low contrast ($p=.741$, n.s.).

Channel O1

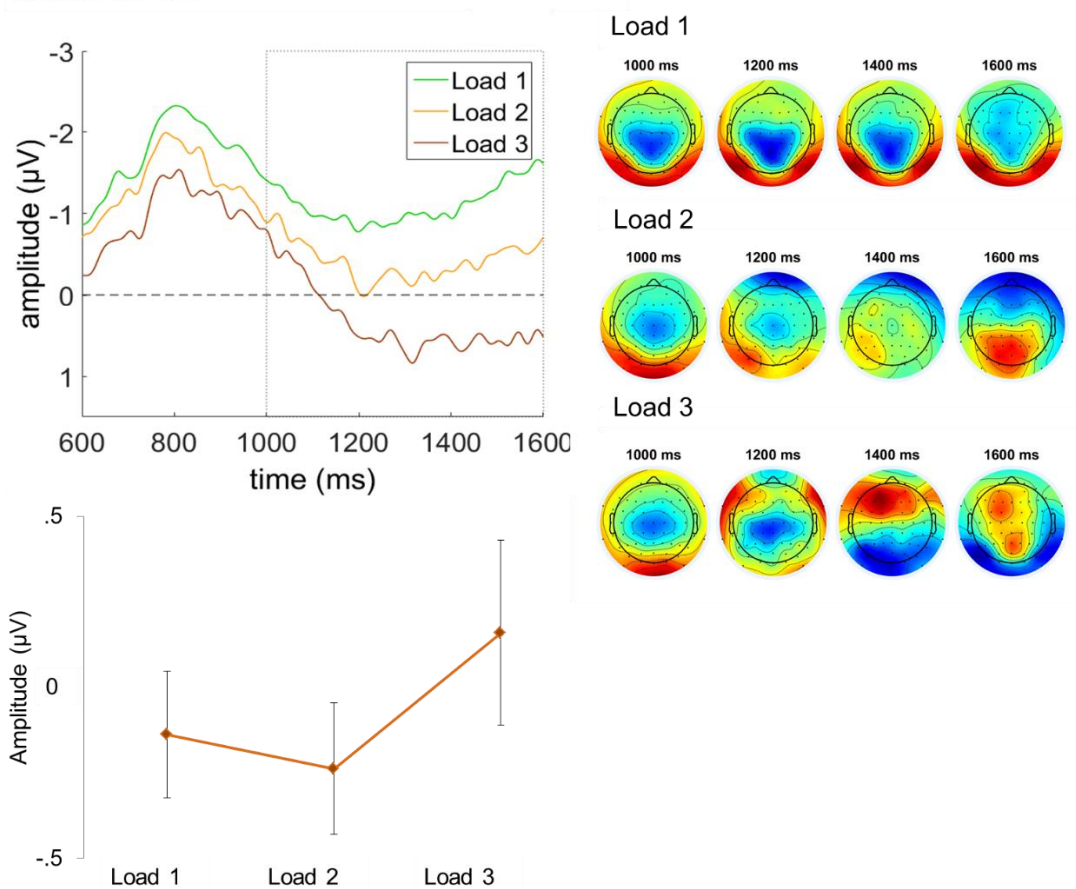


Figure 31 Grand average waveform at electrode O1 during maintenance at three levels of WM load. DKL conditions and contrast levels were collapsed to highlight the main effect of WM load. The grey box marks the time window (1000– 1600 ms) from which mean amplitudes were extracted for analysis. Bottom left: average mean amplitude values at three levels of WM load, extracted from 1000 – 1600 ms time window. Error bars are standard error of the mean. Upper right: corresponding topographic maps at 1000, 1200, 1400 and 1600 ms after the stimulus onset. The last stimulus in the encoding array disappeared at 600 ms mark.

14.3. Slow wave (1000-1600ms) – frontal (electrodes F3, F4, and Fz).

Main effect of DKL ($F(2, 42)=9.88, p<.001, \eta^2=.32$) showed that luminance elicited higher amplitude than S-cone ($p=.014$) and L – M ($p=.003$). There was a main effect of load ($F(2, 42)=4.7 p=.014, \eta^2=.18$); amplitude in response to load 3 was significantly lower than load 2 ($p=.017$; see Figure 32).

There was also a main effect of electrode location ($F(2, 42)=7.50 p=.002, \eta^2=.26$), with an amplitude at electrode Fz being greater than at electrode F4 ($p=.008$).

Channel F3

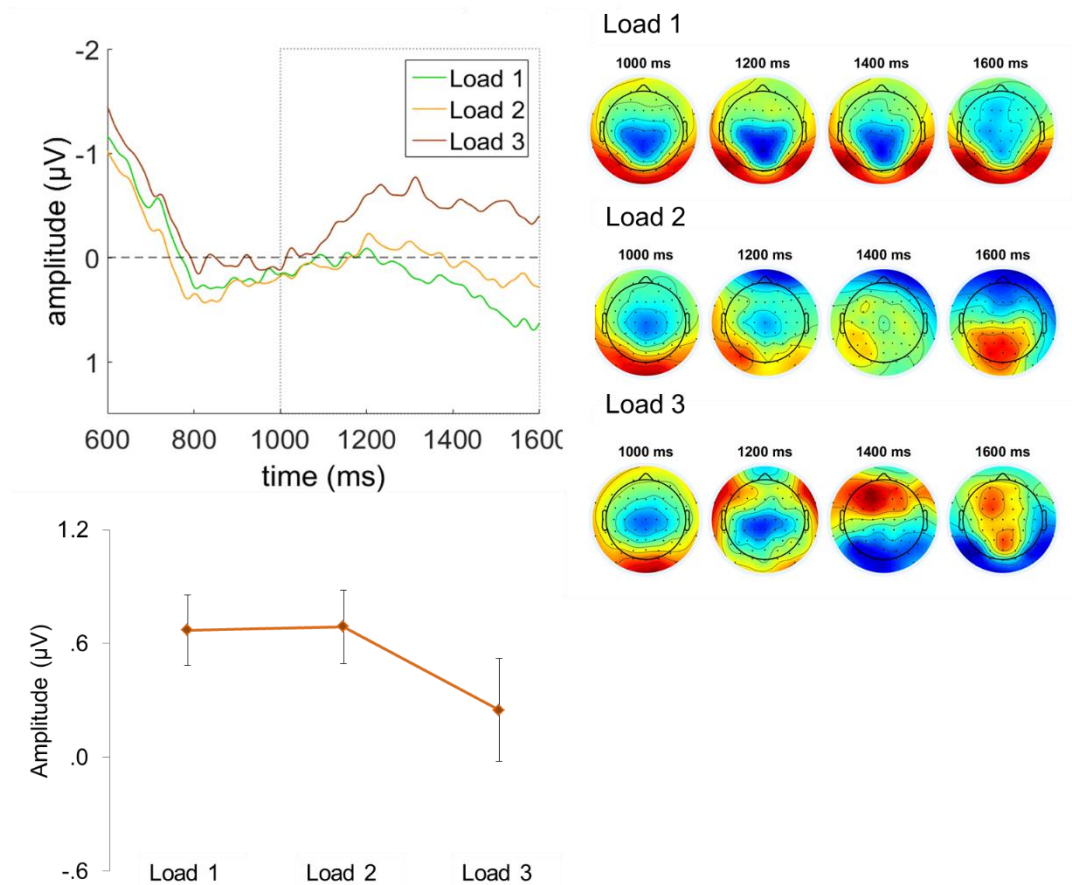


Figure 32 Grand average waveform at electrode F3 during maintenance at three levels of WM load. DKL conditions and contrast levels were collapsed to highlight the main effect of WM load. The grey box marks the time window (1000– 1600 ms) from which mean amplitudes were extracted for analysis. Bottom left: average mean amplitude values at three levels of WM load, extracted from 1000 – 1600 ms time window. Error bars are standard error of the mean. Upper right: corresponding topographic maps at 1000, 1200, 1400 and 1600 ms after the stimulus onset. The last stimulus in the encoding array disappeared at 600 ms mark.

15. ERPs – retrieval stage

15.1. P1 Amplitude (Oz, O1, O2; 80 ms-160 ms)

Similarly to P1 component at encoding, Inspection of Grand averaged waveforms suggested that the P1 component was reliably elicited only by luminance shapes. In addition, amplitudes in response to high contrast shapes appeared to be larger than for low contrast shapes. We used a repeated measures ANOVA with factors: contrast level (low or high) and DKL direction (3 levels: S-cone, L – M and luminance) to confirm these observations (see Figure 23).

There was a main effect of DKL direction ($F(1.07, 22.5)=28.7, p<.001, \eta^2=.58$), with luminance eliciting higher amplitudes than S-cone and L – M (both $p<.001$). High contrast shapes elicited higher amplitude than low contrast shapes ($F(1, 21)=10.7, p=.004, \eta^2=.34$). Additionally, an interaction between contrast level and DKL condition was marginally significant ($F(2, 42)=3.26, p=.048, \eta^2=.13$). Post hoc tests using the Bonferroni correction showed that luminance was higher than S-cone at low contrast as well as at high contrast (all comparisons $p<.001$). There was no difference between amplitudes at low and high contrast for S-cone and L – M. For luminance, amplitudes at high contrast were higher ($p=.004$).

Based on these results, we did not include S-cone and L – M in further analyses. Two separate ANOVAs with factors WM load (3 levels) and electrodes (3 levels: electrodes O1, O2 and Oz) for each contrast level were conducted. There were no significant effects at low contrast (see Figure 33). At high contrast, only the effect of electrode location was significant ($F(1.36, 28.6)=5.38, p=.019, \eta^2=.20$). P1 amplitude was higher at electrode O2 than O1 and Oz. No other effects were significant (see Figure 34).

Channel O1, Luminance low contrast

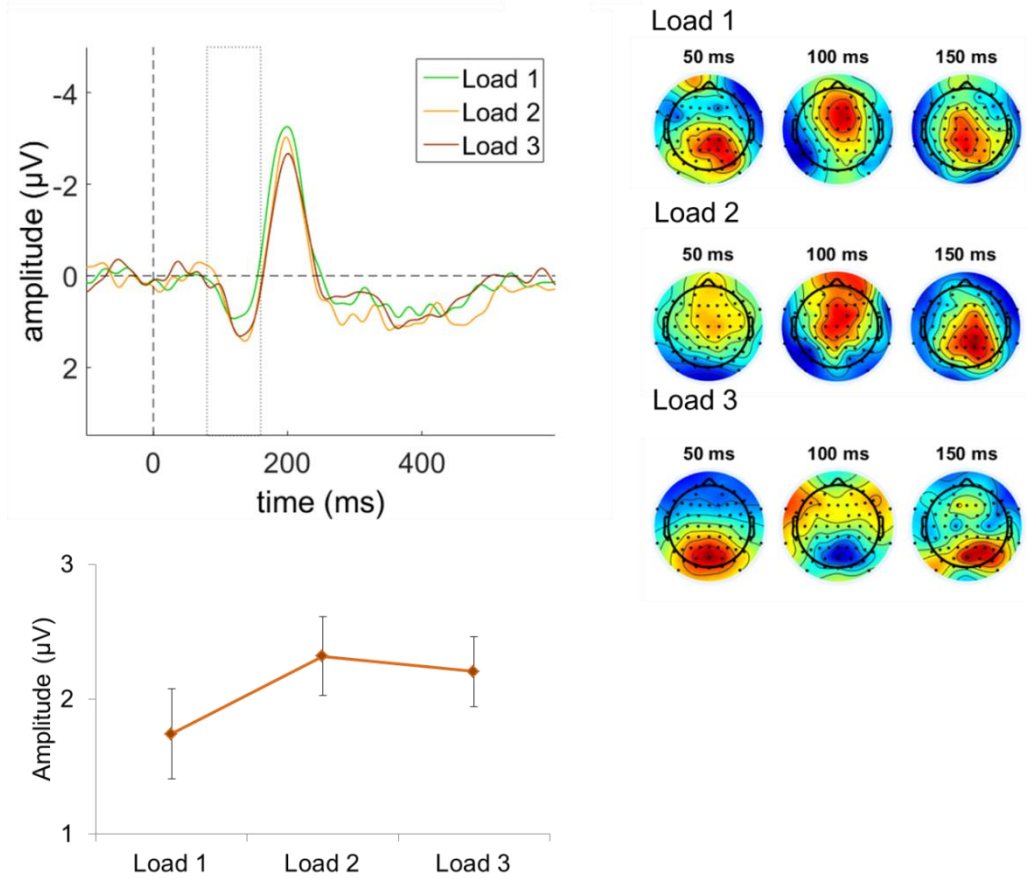


Figure 33 Grand average waveform at electrode O1 during retrieval of low contrast luminance-defined shapes, at three levels of WM load. The grey box marks the time window (80 – 160 ms) from which peak amplitudes were extracted for analysis. Bottom left: average peak amplitude values at three levels of WM load, extracted from 80 – 160 ms time window. Error bars are standard error of the mean. Upper right: corresponding topographic maps at 50, 100 and 150 ms after the onset of the memory probe.

Channel O1, Luminance high contrast

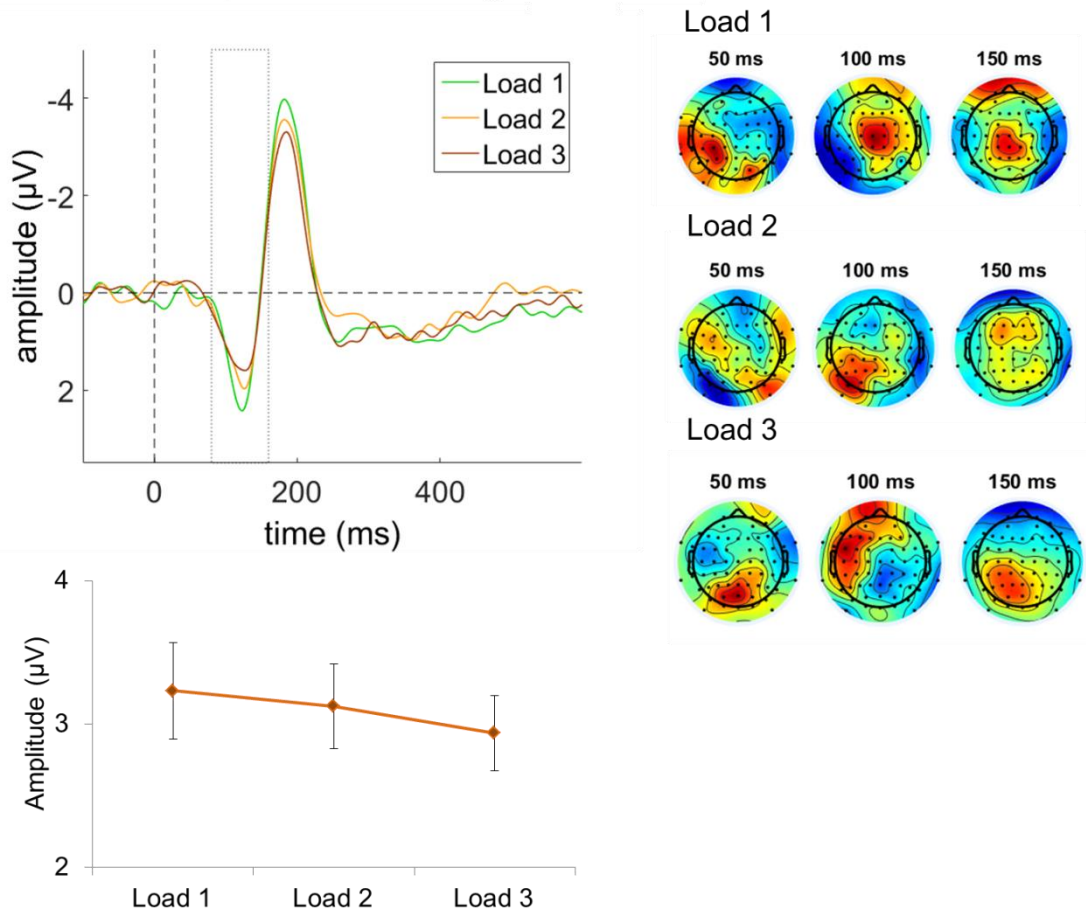


Figure 34 Grand average waveform at electrode O1 during retrieval of high contrast luminance-defined shapes, at three levels of WM load. The grey box marks the time window (80 – 160 ms) from which peak amplitudes were extracted for analysis. Bottom left: average peak amplitude values at three levels of WM load, extracted from 80 – 160 ms time window. Error bars are standard error of the mean. Upper right: corresponding topographic maps at 50, 100 and 150 ms after the onset of the memory probe.

As with encoding, the PI amplitude at retrieval in response to high contrast shapes was correlated with behavioural performance. The amplitude at electrode O1 correlated with overall performance at all loads for electrodes O1 and Oz and for Load 1 and Load 3 for electrode O2 (see *Table 7* for details). Interestingly, when looked at match and mismatch probes separately, PI correlated with accuracy for mismatch probes at all loads and electrodes (see *Table 8* for all p values and correlation coefficients, and *Figure 35* for plotted variable correlations for load 3 at electrode O1), but not for match probes (see *Table 9*). The distinction between match and mismatch is interesting given that, in behavioural results (see *Section 12.4*), luminance benefit was manifested in mismatch condition.

Table 7 Pearson correlation coefficients and p values for P1 amplitude at retrieval stage with overall accuracy. Light green=significant correlations, light blue = non-significant values.

Component P1 amplitude - memory retrieval

	O1			O2			Oz			
	Load 1	Load 2	Load 3	Load 1	Load 2	Load 3	Load 1	Load 2	Load 3	
Overall	.533*	.638**	.617**	.515*	.346	.440*	.501*	.427*	.501*	(Pearson's r)
accuracy	.011	.001	.002	.014	.115	.041	.018	.047	.017	(p-value)

Table 8 Pearson correlation coefficients and p values for P1 amplitude at retrieval stage for mismatching probes with accuracy for mismatching probe at three WM loads. Light green=significant correlations, light blue=non-significant values.

Component P1 amplitude - memory retrieval (mismatch)

	O1			O2			Oz			
	Load 1	Load 2	Load 3	Load 1	Load 2	Load 3	Load 1	Load 2	Load 3	
Load 1	.237			.249			.254			(Pearson's r)
mismatch	.289			.264			.255			(p-value)
Load 2		.495*			.256			.323		(Pearson's r)
mismatch		.019			.250			.142		(p-value)
Load 3			.489*			.500*			.508*	(Pearson's r)
mismatch			.021			.018			.016	(p-value)

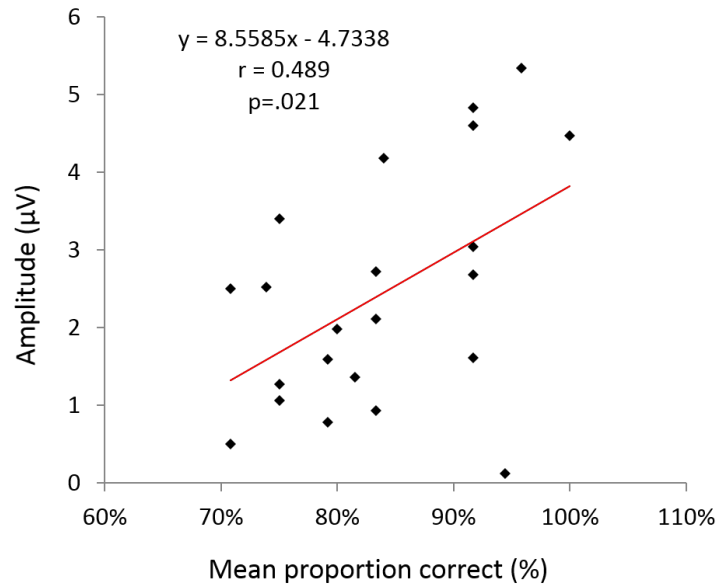


Figure 35 Correlation between the P1 component at electrode O1 (for load 3) and overall task accuracy.

Table 9 Pearson correlation coefficients and p values for P1 amplitude at retrieval stage for matching probes with accuracy for matching probe at three WM loads. Light green=significant correlations, light blue=non-significant values.

Component P1 amplitude - memory retrieval (match)

	O1			O2			Oz			
	Load 1	Load 2	Load 3	Load 1	Load 2	Load 3	Load 1	Load 2	Load 3	
Load 1 match	.229			.286			.283			(Pearson's r)
Load 1 accuracy	.306			.196			.203			(p-value)
Load 2 match		.437*		.096			.197			(Pearson's r)
Load 2 accuracy		.042		.671			.380			(p-value)
Load 3 match			-.099			-.201			-.231	(Pearson's r)
Load 3 accuracy			.663			.370			.302	(p-value)

15.1.1. Latency

Latencies in responses to high contrast shapes were shorter than in response to low contrast shapes $F(1, 16)=34.4$, $p<.001$, $\eta^2=.68$). There were no other significant effects or interactions.

15.2. N1 Amplitude (Oz O1 O2; 130 ms – 300 ms)

High contrast shapes elicited higher amplitudes than low contrast shapes $F(1, 21)=10.6$, $p=.004$, $\eta^2=.33$). There was a main effect of electrode location $F(2, 42)=12.6$, $p<.001$, $\eta^2=.37$). Post-hoc tests using Bonferroni correction showed that amplitudes at electrode Oz were lower than at electrode O1 ($p=.009$) and O2 ($p<.001$).

There was a main effect of DKL direction $F(2, 42)=19.2$, $p<.001$, $\eta^2=.48$). Load and DKL interaction was also significant ($F(4, 84)=3.66$, $p=.008$, $\eta^2=.15$). Post-hoc, Bonferroni-corrected tests indicated that only luminance condition was modulated by WM load (see Figure 36): load 1 elicited more negative amplitude than both load 2 ($p=.009$) and load 3 ($p=.042$). The amplitude of load 2 and 3 did not differ significantly ($p>.05$).

Channel O1, Luminance high contrast

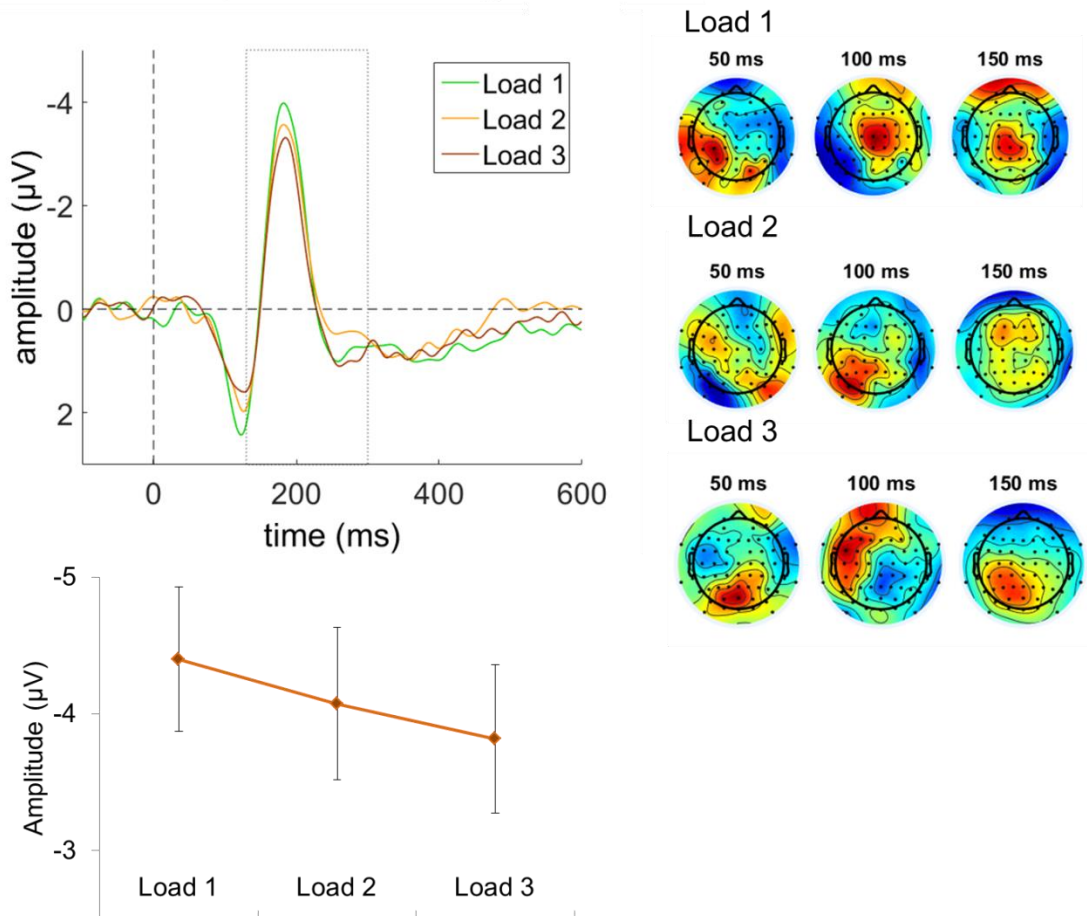


Figure 36 Grand average waveform at electrode O1 during retrieval of high contrast luminance-defined shapes, at three levels of WM load. The grey box marks the time window (130 – 300 ms) from which peak amplitudes were extracted for analysis. Bottom left: average peak amplitude values at three levels of WM load, extracted from 80 – 160 ms time window. Error bars are standard error of the mean. Upper right: corresponding topographic maps at 50, 100 and 150 ms after the onset of the memory probe.

The following interactions (all including DKL direction) were significant: an interaction between DKL direction and electrode location ($F(2.07, 43.5)=5.19$, $p=.009$, $\eta^2=.20$), a three-way interaction between contrast, electrode location and DKL ($F(4, 84)=2.72$, $p=.035$, $\eta^2=.11$), as well as three-way interaction between contrast, load and DKL ($F(4, 84)=3.03$, $p=.022$, $\eta^2=.13$) was significant.

To account for the above interactions, a separate ANOVA with factors WM load (3 levels), visual input/DKL direction (3 levels: S-cone, L – M and luminance) and electrodes (3 levels: electrodes O1, O2 and Oz) was conducted for each contrast level.

15.2.1. Low contrast

For low contrast, there was a main effect of electrode location $F(2, 42)=11.9$, $p<.001$, $\eta^2=.36$), with electrode Oz demonstrating lower amplitude than electrode O1 ($p=.016$) and O2 ($p<.001$). DKL effect was significant $F(2, 42)=21.1$, $p<.001$, $\eta^2=.50$). S-cone elicited the highest amplitude; higher than L - M ($p=.020$) and luminance ($p<.001$). Luminance was also characterised by lower amplitude than L - M ($p=.008$). An interaction between WM load and DKL direction was significant $F(4, 84)=2.79$, $p=.032$, $\eta^2=.12$). This interaction shows that differences between DKL directions were not uniform across WM loads. Luminance had a lower amplitude than S-cone at all WM loads, but it differed from L - M only at load 2. Similarly, S-cone had a higher amplitude than L - M only at load 2 as well, but was not significantly different at load 1 and load 3.

Neither DKL direction was modulated by WM load.

15.2.2. High contrast

DKL conditions differed in terms of local NI amplitude (main effect of DKL: $F(2, 42)=10.9$, $p<.001$, $\eta^2=.34$). Amplitudes differed across electrode locations ($F(2, 42)=12.2$, $p<.001$, $\eta^2=.37$), with an amplitude at electrode Oz significantly lower than at electrode O1 ($p=.008$) and O2 ($p<.001$). There was an interaction between DKL direction and electrode location ($F(2.43, 51)=7.78$, $p=.001$, $\eta^2=.27$) with luminance amplitude being larger at electrode O1 than both S-cone ($p=.032$) and L - M ($p<.017$), electrode O2 ($p<.001$ and $p=.005$ for S-cone and L - M, respectively) and electrode Oz ($p=.001$ and $p=.006$).

There was a significant interaction between WM load and DKL ($F(4, 84)=3.95$, $p=.006$, $\eta^2=.16$). Luminance shapes elicited lower NI amplitudes than S-cone ($p<.001$) and L - M ($p=.029$) at load 3 and load 2 ($p=.009$ and $p=.032$ for S-cone and L - M, respectively). At load 1, there was a significant difference only between luminance and L - M ($p=.003$) but not S-cone ($p=.066$, n.s.). L - M had a lower amplitude than S-cone only at load 3 ($p=.003$).

As with luminance condition, we attempted to run correlations between NI amplitude for isoluminant stimuli and overall performance. Unlike the luminance condition, there were no significant correlations.

15.2.3. Latency

There was a main effect of electrode location ($F(2, 38)=3.79$, $p=.031$, $\eta^2=.17$), with shorter latencies for electrode Oz than O1 ($p=.009$).

There was a main effect of DKL ($F(2, 38)=15.0$, $p<.001$, $\eta^2=.44$) and a significant interaction between electrode location and DKL direction ($F(4, 76)=15.9$, $p<.001$, $\eta^2=.45$). Post-hoc tests using Bonferroni correction showed that differences in latencies between DKL directions were most pronounced at electrodes O1 and O2. More specifically, at electrode O1, luminance had the shortest latencies when compared with S-cone and L – M (both $p<.001$), while S-cone had the longest latencies when compared with L – M and luminance (both $p<.001$). At electrode O2, luminance had shorter latencies than S-cone ($p<.001$) and L – M ($P=.004$). There were no significant differences between DKL conditions at electrode Oz.

In addition, there was a main effect of contrast ($F(1, 19)=60.6$, $p<.001$, $\eta^2=.76$), which indicated that latencies were longer at low compared to high contrast condition. An interaction between contrast and DKL direction was significant ($F(2, 38)=3.57$, $p=.038$, $\eta^2=.16$). Post-hoc, Bonferroni-corrected tests showed that luminance elicited faster latencies than both S-cone ($p=.008$) and L – M ($p=.001$) at high contrast, while at low contrast luminance latencies were shorter only from S-cone ($p<.001$). Additionally, S-cone was characterised by slower latencies than L – M only at low contrast ($p=.023$), but not high contrast.

15.3. P3a Amplitude (C1, C2, Cz; 200 – 400 ms)

The main effect of DKL was not significant ($F(2, 42)=1.57$, $p=.221$, $\eta^2=.069$, n.s.).

P3a was modulated by WM load ($F(2, 42)=5.45$, $p=.008$, $\eta^2=.21$), with load 1 amplitude lower than amplitude for load 2 ($p=.029$).

The amplitude of the P3a component was largest at electrode Cz (main effect of electrode location: $F(2, 42)=28.1$ $p<.001$, $\eta^2=.57$).

Channel Cz

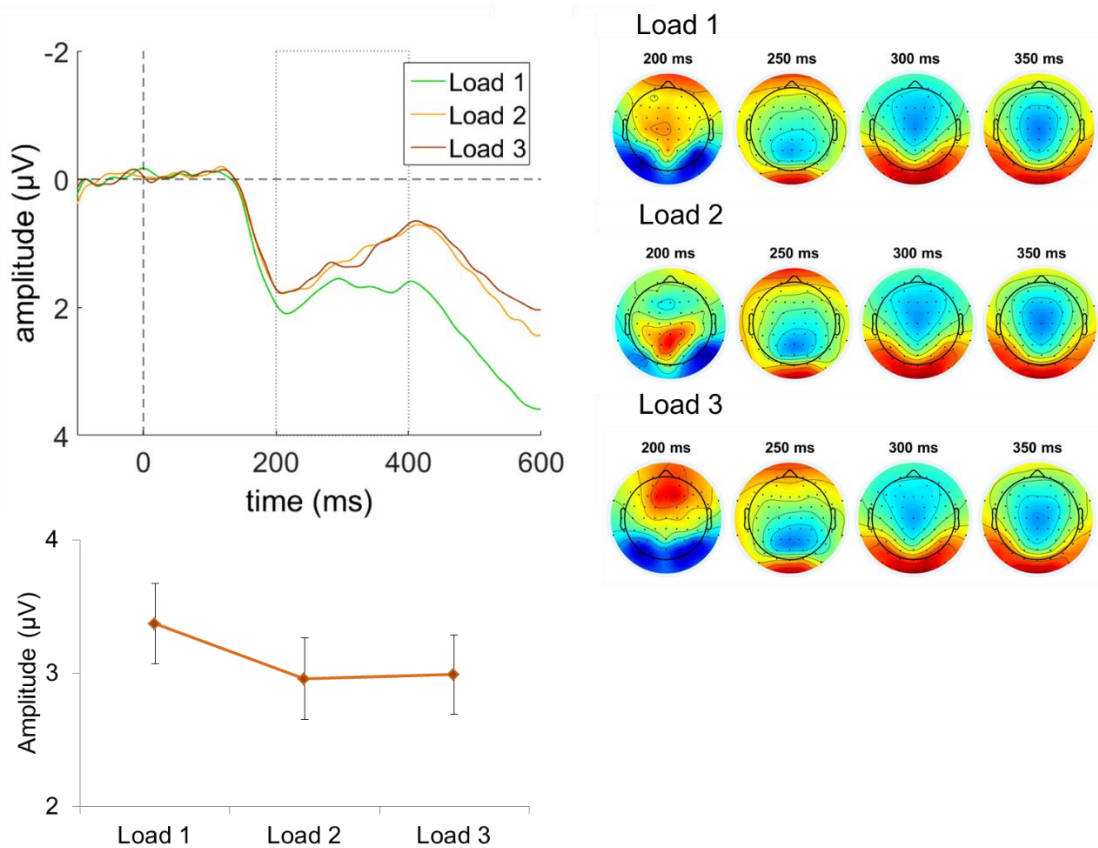


Figure 37 Grand average waveform at electrode Cz during retrieval at three levels of WM load. DKL conditions and contrast levels were collapsed to highlight the main effect of WM load. The grey box marks the time window (200-400 ms) from which peak amplitudes were extracted for analysis. Bottom left: average peak amplitude values at three levels of WM load, extracted from 200-400 ms time window. Error bars are standard error of the mean. Upper right: corresponding topographic maps at 200, 250, 300 and 350 ms after the onset of the memory probe.

15.3.1. Latency

Latencies in responses to high contrast shapes were not significantly different than in response to low contrast shapes $F(1, 16)=.037$, $p=.851$, $\eta^2=.002$, n.s.). No effects or interactions were significant.

15.4. P3b Amplitude (P3, P4, Pz; 200 – 500 ms)

DKL effect was significant $F(2, 42)=16.4$, $p<.001$, $\eta^2=.44$). Post-hoc tests using Bonferroni correction showed that S-cone elicited the lowest amplitude (lower

than L – M at $p=.019$ and luminance at $p<.001$). Amplitude in response to luminance was higher than both S-cone ($p<.001$) and L – M ($p=.011$).

Load effect was significant $F(1.46, 30.7)=5.90$, $p=.012$, $\eta^2=.22$). Post hoc tests showed that amplitude for load 1 was higher than at load 2 ($p=.016$; see Figure 38).

Low contrast amplitudes were lower than high contrast ($F(1, 21)=14.0$, $p=.001$, $\eta^2=.40$). There was a main effect of electrode location $F(2, 42)=7.04$, $p=.002$, $\eta^2=.25$). Post hoc tests using Bonferroni correction showed that amplitude at channel Pz was higher than at channel P3 and P4 (both $p=.015$).

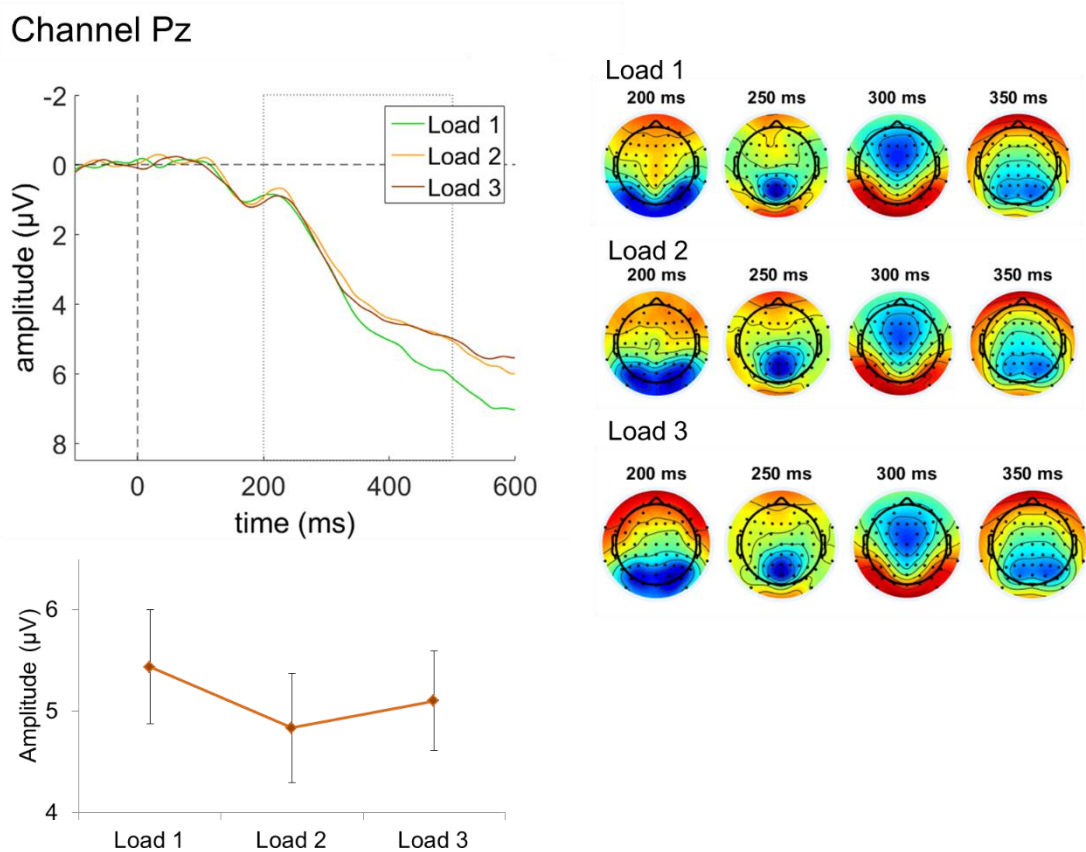


Figure 38 Grand average waveform at electrode Pz during retrieval at three levels of WM load. DKL conditions and contrast levels were collapsed to highlight the main effect of WM load. The grey box marks the time window (200 – 500 ms) from which peak amplitudes were extracted for analysis. Bottom left: average peak amplitude values at three levels of WM load, extracted from 200 – 500 ms time window. Error bars are standard error of the mean. Upper right: corresponding topographic maps at 200, 250, 300 and 350 ms after the onset of the memory probe.

15.4.1. Latency

The main effect of DKL direction was also significant ($F(2, 38)=70.4, p<.001, \eta^2=.79$); luminance peaked earlier than both S-cone and L – M (both $p<.001$). Latencies for S-cone were longer than L – M and luminance (both $p<.001$).

There was a main effect of electrode location ($F(1.25, 23.8)=8.18, p=.006, \eta^2=.30$). Electrode P3 had a longer latency than P4 ($p=.040$) and Pz ($p=.019$).

Latencies in responses to high contrast shapes were shorter than in response to low contrast shapes ($F(1, 19)=65.1, p<.001, \eta^2=.77$). Contrast level interacted with electrode location ($F(2, 38)=6.80, p=.003, \eta^2=.79$), as well as with DKL direction ($F(2, 38)=5.55, p=.008, \eta^2=.23$). A separate repeated measures ANOVA was conducted for latency measures with factors: WM load (3 levels of load) and electrodes (3 levels: electrodes P3, P4 and Pz), separately for each contrast.

15.4.2. Low contrast

There was a main effect of electrode location $F(2, 38)=11, p<.001, \eta^2=.37$.

Amplitudes peaked later at amplitude P3 than P4 ($p=.045$) and Pz ($p=.003$).

Amplitudes at electrode Pz were peaking earlier than at P3 ($p=.003$) and P4

($p=.045$). There was a main effect of DKL direction $F(2, 38)=63.2, p<.001, \eta^2=.77$).

Latencies were the slowest for S-cone condition; component P3b peaked later than for L – M ($p=.033$) and luminance ($p<.001$). Luminance had the shortest latencies, with shorter component peak latency than S-cone and L – M (both $p<.001$).

15.4.3. High contrast

There was a significant main effect of DKL condition ($F(1.38, 27.7)=63.9, p<.001, \eta^2=.76$). P3b in response to luminance peaked earlier than S-cone and L – M (both $p<.001$). Additionally, L – M peaked earlier than S-cone ($p<.001$).

16. Discussion

16.1. Overall behaviour findings

This experiment examined the differential contribution of luminance and isoluminant signals to visual WM encoding and performance. We used stimuli that were defined along different directions in cardinal colour space, in an effort to differentially excite post-receptoral mechanisms of interest. These included 2 isoluminant, chromatic directions (S-cone isolating and L – M), and one luminance, achromatic channel. The stimuli were matched for saliency on the basis of each participant’s discrimination thresholds.

We found that remembering abstract shapes designed to engage the luminance channel resulted in a superior behavioural performance in a delayed match-to-sample task over isoluminant stimuli. This effect was most pronounced when the stimuli were presented at low contrast levels, and when the WM load was high. In terms of reaction times, we observed that responding to luminance stimuli was associated with quicker responses than responding to both isoluminant stimuli types. While we also observed the increase of reaction times with increasing load – most likely reflecting higher task demands – we did not find any special benefit of luminance at higher WM loads, as was the case with the accuracy data.

Demonstrating a superior WM luminance performance supports previous findings, which showed that achromatic signals benefit object recognition (Bar, 2003; Kosilo et al., 2013; Kveraga et al., 2007; Martinovic et al., 2011). In particular, these studies showed that object recognition performance benefits from luminance inputs. Therefore, our experiment extends these findings, showing that the “luminance benefit” is not specific to perception or object recognition, but instead can be demonstrated in other cognitive domains, like working memory. Importantly, the accuracy benefit was most pronounced at higher WM loads, which further suggests that these effects are not purely perceptual, but stem from the interaction between perception and WM. While the performance naturally dropped when participants had to keep more stimuli

in the memory for all DKL directions, the loss of accuracy was not as severe in the luminance condition compared to the isoluminant conditions.

16.2. Match/mismatch effects

Another important finding of this study is that luminance-defined shapes elicited higher accuracy when the memory probe was different than the remembered stimuli (i.e. when the currently perceived probe mismatched remembered stimuli). The behavioural pattern replicates unpublished results from a different lab with a different set of participants (Haenschel, Kosilo & Martinovic, 2012). This finding is important for two reasons. Firstly, it confirms that better behavioural accuracy in response to luminance-defined shapes cannot be explained by differences in stimulus saliency. If the stimuli were not equally salient across DKL directions, we would expect that the decrease in accuracy would be the same for match and mismatch and different WM loads. However, this is not the case in our study, as we have shown that luminance benefits performance over isoluminant stimuli only at higher WM load conditions, and predominantly when the probe mismatched previously presented shapes. Therefore, we argue that the scaling procedure did not introduce a bias towards any stimulus category.

Secondly, this finding is in line with the literature suggesting that the mechanisms behind same/different (or match/mismatch) judgements made between perceptual and memory representations are not equivalent (Engel & Wang, 2011; Hyun et al., 2009; Johnson, Spencer, Luck, & Schöner, 2009). Interestingly, similar conclusions come from research investigating how match/mismatch (or same/different) judgements are achieved for comparisons in purely perceptual domain (i.e. between two sensory representations, rather than between sensory and memory representation; Davelaar, Tian, Weidemann, & Huber, 2011a; Huber, Tian, Curran, O'Reilly, & Woroch, 2008). This further speaks to the view that perception and working memory share the same mechanisms (Pasternak & Greenlee, 2005). Importantly, our results extend these findings by demonstrating the process of comparing mnemonic representation

with currently perceived stimuli benefits from luminance inputs. The implications of this finding will be discussed at length in the General Discussion (Chapter 6). Generally, however, we suggest that differentiating between match and mismatch comparisons in future studies can be beneficial for our understanding of processes contributing to WM performance.

16.2.1. Contrast effects

As expected, we also found that the differences in accuracy between luminance and isoluminant stimuli were more pronounced at lower contrasts. This pattern is consistent with the previous literature (outlined in the Introduction to this chapter), suggesting that contributions of different inputs are better dissociable at lower contrasts; at high contrast levels, the influence of post-receptoral mechanisms tend to overlap more (Ivanov & Mullen, 2012). Using low contrast stimuli also biases the luminance processing to be carried by the magnocellular pathway, since it is more sensitive to contrast (Derrington et al., 1984; Hicks et al., 1983; Kaplan & Shapley, 1982; Shapley, 1990; Vidyasagar et al., 2002). At higher contrast levels, luminance can be processed by both magno and parvocellular pathways. Therefore, this pattern of results implicates the magnocellular pathway in improving WM performance.

16.2.2. Lack of correlation between digit span and letter-number tests and delayed match-to-sample task

We have correlated the digit span and letter-number WM tests with behavioural accuracy on our match-to-sample task. No significant correlations were found. This result might be due to different modalities: digit span and letter-number tests are presented in a verbal/auditory manner, while our delayed match-to-sample task is predominantly visual. Previous studies attempting to correlate performance on tasks that differ in modality also yielded no significant effects. For example, Miller, Price, Okun, Montijo, & Bowers (2009) found that the N-back task performance did not correlate with digit span backwards. The authors

also attribute this to differences in modality, although they also suggest that it might be because the N-back is not a pure measure of working memory.

16.3. ERP effects

Our task design allowed for a clear distinction between WM stages: the encoding, maintenance and retrieval. For each stage, a number of well-defined ERP components were analysed, focusing on those that are related to visual processing and/or WM processing. There were two aspects of each ERP that we were particularly interested in in the context of this thesis. These were: 1) the differences (or similarities) between the ERPs recorded in response to shapes defined along different directions in DKL colour space (S-cone isolating, L – M, and luminance), and 2) changes in amplitude and timing that could be linked to WM load. We had two general predictions related to that. Firstly, we expected to observe an interaction between WM load and DKL direction – i.e. that the differences between DKL conditions will be most pronounced at higher WM loads. The second prediction concerned the earliest visual components we looked at in this experiment; the visual P1 and N1. We looked at whether these two early components will be modulated by WM load, and we expected that the P1 will show such modulation in response to luminance shapes.

In the next section, I will summarise ERP effects that can be linked to perceptual processing. These are likely to reflect changes in response to low-level visual properties of the stimuli, rather than working memory.

16.3.1. Perceptual effects

In accordance with the previous literature (Crognale, 2002; Gerth et al., 2003), the early visual component P1 could be reliably evoked by luminance-defined stimuli at both encoding and retrieval WM stages. There was no reliable P1 in response to isoluminant shapes. N1 was the first component that was elicited by all stimuli classes. The P1 in response to S-cone isolating and L – M shapes would have occurred if a consistent luminance artifact was present in otherwise isoluminant stimuli. As this was not the case, we concluded that the stimulus

design was appropriate. NI in response to luminance was smaller than in response to isoluminant shapes, which is also consistent with the literature (Gerth et al., 2003).

Low contrast stimuli, in general, elicited smaller amplitudes and longer latencies for all components, with the exception of the slow wave. Despite our efforts to increase the signal-to-noise ratio by using scaled thresholds, we hypothesise that reduced amplitudes for the ERP components might be related to decreased signal-to-noise ratio in response to low contrast shapes. Notably, components cannot be measured reliably if they are small (Luck, 2014). This would explain why – for the P1 and N1 – most of the WM-related effects or differences between ERPs elicited by different DKL directions were often significant at high contrast, but not at low contrast (see next section).

At the same time, there were no clear differences between low and high contrast ERPs recorded during the maintenance period (the slow wave); this waveform demonstrated a WM load-related modulation that was not contrast-dependent. This might simply reflect the fact that this component is more sensitive to cognitive modulation rather than to low-level factors, such as contrast.

Alternatively, it could also be a result of the way the amplitude was measured for this particular component. We extracted the mean amplitude within a specified time window for the slow wave, while for the other components a local peak measurement was used. Using a mean over a time window is less prone to noise than the peak amplitude (Luck, 2014). It is possible that we achieved better signal-to-noise ratio for this component at low contrast, which gave us enough statistical power to observe load-dependent effects. However, for the component P3a measured with peak amplitudes, we reported an overall effect of load during WM encoding. This effect did not appear to be contrast-dependent, similarly to the slow wave during maintenance. Therefore, it appears that components sensitive to cognitive factors can be modulated by WM processing even at low contrast levels. On the other hand, since both P1 and N1 components have been shown to be modulated by low-level stimulus properties, including contrast (Luck, 2014), demonstrating WM-related modulation requires good signal-to-noise ratio in this case.

Using only high contrast data to draw our conclusions about the P1 and N1 effects is not without its problems. As mentioned in the introduction, ERP responses to low contrast stimuli are dominated by inputs from the magnocellular pathway. At high contrast, however, inputs from both magno and parvocellular pathway seem to contribute to the signal if the spatial frequency of the stimuli exceeds a specific frequency (i.e. 3 cycles per degree; Souza, 2007). Indeed, it has been suggested in the past that the parvocellular pathway is involved in carrying luminance information as well (De Valois & De Valois, 1975; Ingling & Martinez-Uriegas, 1985; Shapley, 1990; Schiller and Colby, 1983). One cannot, therefore, assume that ERP waveforms in our study reflect responses to signals originating predominantly from the magnocellular pathway. However, it needs to be emphasized that the aim of our study was to investigate the contribution of luminance signals to WM. Therefore, even if part of the signal contributing to a given ERP component was transmitted through the parvocellular pathway, this would not necessarily invalidate our conclusions about the specific role of luminance. Still, one can make inferences about the relative role of either pathway, since the stimuli were carefully designed to be purely achromatic, therefore biasing stimulus processing towards non-chromatic, magnocellular pathway, as opposed to the chromatic parvocellular pathway. A lack of reliable P1 component in response to isoluminant, chromatic stimuli even in high contrast condition strongly supports this notion, as this component is largely attenuated for purely chromatic stimuli (Crognale, 2002; Gerth, Delahunt, Crognale, & Werner, 2003).

In summary, we suggest that future studies interested in cognitive effects related to stimuli presented at low contrast should ensure a sufficient number of trials and use of appropriate, noise-resistant measurements in order to reliably demonstrate the existence of such effects (or lack thereof) in the early visual components.

In the next section, I will summarise ERP effects that appear to be related to WM processing, rather than perception and low-level factors (as described above). One of the hypotheses in this thesis was that processing taking place at WM

encoding is related to task performance; hence, I will also summarise the results of these correlations.

16.3.2. ERP modulations related to working memory load

Both PI and NI components in our experiment were modulated by low-level factors, consistently with previous literature (Luck, 2014). Hence, we found that amplitudes were generally smaller and delayed for low contrast shapes and – for the PI – isoluminant stimuli did not elicit a reliable PI (Gerth et al., 2003).

However, it has been shown previously that beyond such low-level visual properties, the PI, as well as NI, are also sensitive to cognitive factors such as attention (Fu et al., 2010; Hillyard et al., 1998) and perceptual load (Handy & Mangun, 2000; Rose et al., 2004).

Our study adds to the existing literature by showing that the PI can also be modulated by WM, consistently with previous studies (Haenschel et al., 2007). In particular, we show that PI can index the interaction of both low-level visual properties (i.e. using stimuli exciting the luminance channel) and WM. The PI demonstrates a characteristic magnocellular response, while the NI demonstrates parvocellular properties (Elleberg & Hammarrenger, 2001). Thus it is not surprising that the PI was evident only in our luminance condition, given that magnocellular pathway receives predominantly achromatic, luminance inputs. By showing that the PI was modulated by WM load but the NI was not, we support our hypothesis that perception interacts with WM and that this interaction is driven predominantly by luminance inputs.

We found that, during stimulus encoding, the early visual component PI in response to luminance – shapes was modulated by WM load when the stimuli were presented at high contrast. Most importantly, the PI amplitude at high contrast correlated with behavioural performance, thus supporting confirming previous findings (Haenschel et al., 2007) that early encoding WM stages are important for WM. Importantly, load-dependent modulation of component PI in response to luminance might be related signal amplification. Previous studies

suggested that the modulation of the PI amplitude reflects amplification of neural response, which results in increased signal-to-noise ratio (Hanslmayr et al., 2007; Hawkins et al., 1990; Klimesch et al., 2004; Reinitz, 1990). In line with this account, increased amplitude of the PI in response to luminance at high WM load in our study might reflect better fidelity of stimulus encoding, achieved through such signal amplification.

In terms of processing of isoluminant stimuli, the first ERP component that can be reliably elicited by these stimuli is NI. At low and high contrast during the encoding stage of WM, there was no significant load-related modulation of this component in response to isoluminant as well as luminance-defined shapes. Moreover, NI amplitude did not correlate with behavioural performance.

Another component modulated by WM load at encoding was the P3a recorded at central electrodes. Interestingly, however, load modulation appeared to be specific for luminance shapes presented at high contrast. The component's amplitude decreased linearly with increasing WM load, while for the isoluminant conditions it remained similar across different WM loads.

In addition, while at lower WM loads P3a amplitude was similar across DKL directions, at higher WM load luminance amplitude diverged, driving the significant load effects. Notably, this is a similar pattern to the behavioural results, where the differences in accuracy between task performance for luminance and isoluminant shapes were pronounced at higher WM loads as well. This is in line with our predictions. As outlined in the introduction, amplitude of component P3a has been linked to frontal attentional mechanisms related to stimulus processing. The pattern of our results suggests that attentional resources during WM encoding are working differently for the DKL directions tested. The difference seems to arise at high WM load for luminance, suggesting more efficient processing of luminance signals under high load conditions.

The slow wave recorded during the stimulus maintenance stage at occipital and frontal sites appeared to be sensitive to WM load for all DKL conditions. There was some indication that the amplitude of the slow wave recorded from occipital

electrodes in response to luminance diverged from S-cone and L – M at the highest WM load. However, this observation yielded no statistically significant effects. While this could be due to a lack of power, there are no strong conclusions that can be drawn from this observation. Slow wave recorded at frontal sites did not show any differential influence of luminance on amplitude. Therefore, with a degree of caution, we suggest that interactions between WM load and DKL directions are more pronounced during the encoding stage at occipital electrodes, while during the maintenance, waveforms behave similarly across DKL conditions at both occipital and frontal sites.

During the retrieval stage, load effects were not significant for the P1 component. Interestingly, however, the P1 amplitude at retrieval did correlate with behavioural accuracy calculated for mismatch condition. This pattern of results is reminiscent of the behavioural results, where luminance advantage have shown to be present at higher WM loads, but only when the probe mismatched one remembered during the encoding stage. It appears that the memory-probe comparison can be indexed early during probe encoding and that luminance is especially important for discriminating the mismatch between the memory representation and currently encoded test stimulus. Crucially, the memory comparison-related ERPs reported here occurred earlier than in the previous studies (Agam & Sekuler, 2007; Yin et al., 2012). This might suggest that the memory-probe comparison is tightly related to initial perceptual processing also at the retrieval stage.

The P3b component at retrieval was modulated by WM load, along with the P3a component. Interestingly, the load effect at P3b was not present during the encoding; however, such modulation was present at retrieval (in addition to modulation by the DKL direction). As mentioned in the introduction (see Section 9.1.3), it has been suggested that the P3b component reflects a completion of cognitive operations related to a task-relevant stimulus (Desmedt, Bourguet, Huy, & Delacuvellerie, 1984; Desmedt & Debecker, 1979; Desmedt, 1980; Tomberg & Desmedt, 1998; Verleger, 1988). Further, it can be used as an index of a decision mechanism performed during stimulus comparison during a delayed discrimination task (Croizé et al., 2004). Based on that, Croizé et al. suggest that

the P3b is not crucial for WM processing during encoding, and its modulation is related to processes taking place at the retrieval. The presence of WM load-related modulation of the P3b during the retrieval in our study, but not encoding, supports this view.

WM load influenced the NI amplitudes at the retrieval, in particular in response to high contrast shapes. At higher WM loads, DKL directions were more differentiated, with luminance showing lower amplitude than S-cone and L – M. It is important to point out at this point a specific shortcoming of the analysis of ERPs at the retrieval stage. As mentioned above, in terms of behavioural accuracy, the luminance advantage was most pronounced at mismatch condition. However, our ERP analysis did not differentiate between match and mismatch responses due to an insufficient amount of trials. Thus, our ERPs reflect both match and mismatch processing, which in light of our behavioural results is not ideal, as these processes appear to be substantially different. It would be beneficial for the future studies to ensure that sufficient amount of trials is available to probe the effects of match/mismatch comparisons on ERP waveforms.

16.4. What mechanism underlies luminance advantage?

The exact mechanism through which luminance benefits encoding and performance in WM task warrants further investigation. We hypothesize that the luminance benefit can be either low-level, i.e. related to low-level visual processing, or it has to do more with high-level cortical processing, or both. In this view, WM can benefit from luminance signals because the sustained representation is less noisy throughout the maintenance stage, resulting in more accurate memory-probe comparison. On the other hand, our findings might be also interpreted in relation to Bar's (2003) model. Bar proposed that perception (or, more specifically, object recognition) benefits from fast luminance inputs to the cortex, providing frontal areas with a "rough outline" of currently perceived stimuli. Based on the initial shape information, top-down signals would facilitate

further processing and subsequent recognition. Empirical findings were consistent with this model (Bar, et al., 2006; Kveraga et al., 2007; Martinovic, Mordal & Wuerger, 2011). A more comprehensive interpretation of the findings and the mechanisms behind them will be provided more extensively in the General Discussion (see Chapter 6).

16.5. Further directions and general shortcomings

The results of the current study might be invalidated if the stimuli across different classes were not equalized in terms of saliency. We have obtained same/different thresholds from each participant before they completed the delayed match-to-sample WM task to achieve just that. However, it was necessary to ensure that the EEG signal had sufficient signal-to-noise ratio so that individual ERP components could be readily isolated. We have achieved that by scaling same/different discrimination thresholds upwards (see Section 11.2.3). The crucial part of the procedure was to maintain the relative distance between the contrasts for each DKL direction.

However, there is a possibility that the scaling procedure might have violated the saliency. More specifically, the slope of the psychometric function underlying discrimination performance at thresholds could be considerably different between stimuli classes.

Our results suggest that the saliency procedure was appropriate. This conclusion is based on the results which showed that luminance stimuli produced better performance than chromatic stimuli in trials where the probe mismatched remembered stimuli. If the luminance stimuli were simply more salient than the chromatic stimuli, the differences should be general and apply to all experimental conditions. In other words, we should expect to find a similar pattern of results for both match and mismatch conditions. However, this was not the case.

Nevertheless, it would be beneficial to verify the procedure further by measuring slope differences between luminance and chromatic conditions in detection and

discrimination tasks. This was one of the aims of the next experiment, described in Chapter 4.

16.6. Summary

In summary, the findings of the current experiment are consistent with the hypothesis that luminance provides special inputs to working memory over isoluminant signals. In terms of ERP responses, luminance-defined shapes tended to elicit greater amplitudes than isoluminant shapes. Most importantly, however, ERP waveforms in response to luminance-defined stimuli were additionally affected by the number of items stored in memory.

This conclusion is further strengthened by the fact that the PI amplitude at encoding correlated with working memory performance, while the NI amplitude in response to isoluminant items did not. Furthermore, the results also suggested that later components recorded during the encoding stage – namely, the P3a – also appeared to be modulated by WM load, albeit only in response to luminance-defined shapes. This would suggest that luminance inputs interact with working memory already during initial stimulus encoding, and these interactions have an effect on WM performance. Hence, our behavioural results could be successfully linked to ERP modulation, suggesting that higher accuracy seen in behavioural responses most likely results from processes taking place during the encoding stages of working memory, rather than the later stages. However, other WM stages also proved to contribute to performance. More specifically, we found that the luminance advantage was more pronounced when the probe mismatched the remembered shapes; furthermore, the amplitude of the component PI during retrieval correlated with behavioural performance in response to mismatching probe, but not in response to matching shape.

More generally, the above findings suggest that the mechanism behind the interaction between perception and working memory differs depending on the stage of working memory processing. At encoding, we are looking into processes that “write” the stimuli into WM for later maintenance and retrieval. In this sense, perception/WM interaction will be related to creating a WM

representation based on the currently perceived stimuli. On the other hand, no memory encoding is needed at the retrieval stage. Any ERP modulation at this stage will therefore likely reflect the comparison process between currently perceived stimuli (perception) and memory representations encoded earlier. Therefore, even though we analysed the same components at encoding and retrieval (namely, P1 and N1), they might not reflect the same underlying neural processing. This highlights the importance of distinguishing between different working memory stages when investigating neural processing that underlies it.

Chapter 4

Psychophysical experiments on visual working memory

This chapter describes psychophysical experiments that extend the findings outlined in the preceding chapter as well as address some of its potential limitations.

As detailed in the previous chapter, encoding luminance-defined as opposed to isoluminant shapes led to better performance in a delayed match-to-sample WM task. To ensure that our results could be explained in terms of differences between post-receptoral mechanisms, stimuli had to be matched for saliency across different DKL conditions. We have achieved that by estimating same/different discrimination thresholds for each condition using a same/different task. Participants were presented with two stimuli (shown consecutively) and had to respond whether they were the same or different. Same/different discrimination thresholds were estimated using an adaptive procedure for chromatic and achromatic visual channels and reflected a level of intensity at which the probability of individual's correct answer was 75% (derived from a logistic psychometric function fitted to the data; see General Methods chapter). Since we were also interested in EEG measurements, we scaled these thresholds up to make sure that stimuli had a sufficiently high contrast to elicit reliable ERPs. This was done while making sure that the relative difference between each condition was maintained so that they were still matched in saliency.

While this approach enabled us to assess WM task performance as well as obtain EEG recordings, thresholds can be used to directly assess WM and not merely as a control measurement. Threshold estimation, as well as fitting a psychometric function to the data to obtain other measures (such as slope) is the core of psychophysical methods. Since the foundation of the psychophysics (and experimental psychology in general), thresholds have been effectively used to probe sensory function and perception.

In the following section, I will introduce a brief history of psychophysics. The aim of doing so is to demonstrate that psychophysical methods were originally developed to study sensations, but they soon began to be used effectively to study complex perceptual functions and cognition. Importantly, this means that these methods can be used to study visual working memory as well.

17. Psychophysical measurements and sensory perception.

The pioneering experiments of Ernst Weber (1795/1878) investigating the sensation of touch and pressure (Weber, 1834) demonstrated that before any stimulus can be detected by the senses, it needs to pass a “threshold of sensation”. Weber referred to the amount of increase needed to elicit a sensation – or, a ratio between the detected stimulus and a baseline – as “just-noticeable difference”, otherwise known as detection threshold (Weber, 1905). Early psychophysical work focused on senses, such as a sense of touch, vision, hearing and others (Fechner, 1860). The ideas laid foundations for new scientific field, later formalised by Gustav Fechner and since referred to as experimental psychophysics (1801/1887). In more general terms, psychophysical methods (with the threshold being one of the central measures) were used to describe and quantify the relationship between the physical world and the “mind”, i.e. the subjective experience (Ehrenstein & Ehrenstein, 1999).

With the advance in the methodology, thresholds began to be used not to merely describe the detection or discrimination of a given stimulus, but they enabled for a more detailed investigation of visual processing beyond sensation. The contribution of psychophysics to this line of research will be discussed in the next section.

17.1. Insights into visual perception

Threshold measurements, coupled with physiological recordings, helped to break-down visual processing and correlate different aspects of vision with its subdivisions. For example, psychophysics and thresholds measurements helped to establish that magno and parvocellular visual channels are not only separated anatomically but also functionally (De Valois & Kooi, 1991; for a review, see Livingstone & Hubel, 1987). The problem was approached by using stimuli that were designed to be processed predominantly by magno or parvocellular visual channels and comparing how thresholds are affected when engaging one channel

in isolation. It was demonstrated that some aspects of vision are achieved more efficiently by different channels. For example, depth and movement seem to be derived from luminance signals carried by the magnocellular pathway, while colour information is carried predominantly by the parvocellular system. Regarding motion processing, it was demonstrated that the perceived velocity of luminance gratings decreased with added chromatic information, suggesting that the luminance-driven, magnocellular stream is specialised in motion detection (Cavanagh, Tyler, & Favreau, 1984).

Despite this apparent segregation, the two streams interact, and – at some point – an integration of information from both streams must be achieved to come up with a coherent percept of the visual world. A specific example of this would involve working out the basis of object recognition. Psychophysical experiments using discrimination thresholds have proved again to be useful in addressing this issue. For example, it was demonstrated that observer's judgments about the relative position of two components within visual patterns are accurate despite changes in size, orientation or overall spatial profile of the pattern (De Valois et al., 1990). These results supported the notion that the visual system can utilize spatial relations and relative positions of visual features for object recognition.

17.2. Studying memory and cognition with psychophysics

It can be argued that object recognition goes beyond “simple” perception and begins to enter the territory of higher cognitive function. Indeed, psychophysics has been successfully applied to different domains, which exceed the sensory-perceptual domain. One of such domains of particular interest here is memory research. Although the contemporary literature suggests that visual perception and visual memory (specifically, working memory) are not so easily separated (Harrison & Tong, 2009; see Chapter 1), traditionally memory was associated with cognition rather than perception, and thus used to be discussed separately.

The idea of using psychophysics to study memory rather than perceptual representations can be traced back almost to the very origins of the field. As

Algom (2001) points out, the notion was first considered by Fechner in 1882 (translated in Fechner, 1987). It was only later, however, that the focus shifted towards verifying whether some findings from sensory psychophysics – e.g. Weber’s law – hold for memory representations. In other words, researchers began to be interested in whether perceptual psychophysics can be applied to memory as well (Björkman, Lundberg, & Tärnblom, 1960; Hubbard, 1994). In a first systematic attempt to study this issue, Björkman et al. (1960) described the relationship between stimulus intensity and perceived magnitude while also adding another dimension into play: the memory magnitude.

In their experiments, observers were judging the size of the circles or weight of various objects and were later required to recall the magnitude of remembered objects in relation to currently perceived ones. This was used as a basis to estimate the ratio between perceptual and memory amplitude – similarly as it was done in classic Weber’s experiments. Their experiments showed that the magnitude of the memory representation tended to increase with the magnitude of the perceived one, displaying the characteristics of a positively accelerated function – i.e. one where the rate of increase of one variable (memory magnitude) increases with the rate of another variable (perceived magnitude). The rate of the increase is initially characterised by a shallow function, which becomes increasingly steeper. Later experiments additionally suggested that the rate of memory decay is not equal across different visual features, such as height or size (Algom, Wolf, & Bergman, 1985; Hubbard, 1988). It is important to note that short-term memory was not always the focus of the investigation, as researchers were equally interested in estimating the magnitude of memory representations also after longer retention delays, such as 24-hour delay (Moyer, Bradley, Sorensen, Whiting, & Mansfield, 1978).

How does the efficiency of discriminating between memory and perceptual (ongoing) representations compares with perceptual detection and discrimination, where no memory is involved? Generally speaking, detection and discrimination of visual features in the human visual system is very efficient (Salmela & Saarinen, 2013). For example, discrimination thresholds for spatial frequencies are low (Hirsch & Hylton, 1982; Itti, Koch, & Braun, n.d.; Wilson &

Gelb, 1984). Similarly, orientation discrimination is very accurate (Vogels & Orban, 1986; Westheimer, 1998). These findings indicate that perceptual system is able to encode visual stimuli with high fidelity.

However, introducing a delay between encoding and probe, and thus engaging working memory, increases discrimination thresholds and reduces the slope of the psychometric function. This suggests that the ability to store representations for extended periods of time is possible at the expense of precision and fidelity of the representation. As mentioned above, previous studies have mostly investigated the memory for single stimulus features, such as contrast, orientation and spatial frequency. Later experiments confirmed that memory representations for different visual features do not decay at the same rate (Magnussen & Greenlee, 1999; Magnussen et al., 1991; Magnussen, Idås, & Myhre, 1998; Pasternak & Greenlee, 2005). It has been shown that, generally, thresholds for most visual features increase with increasing inter-stimulus interval, although some features, such as spatial frequency (Magnussen, Greenlee, & Thomas, 1996) can be retained with high precision even with long stimulus intervals. Other features, notably orientation, are subject to a more rapid decay (Vogels & Orban, 1986).

Thresholds for single stimulus features are modulated not only by the length of the inter-stimulus interval but also by increasing the number of items that are encoded into memory (Bays & Husain, 2008). For example, orientation discrimination becomes less precise with increasing working memory load, which is reflected in a shallower slope of the psychometric function (Bays & Husain, 2008; Palmer, 1990; Salmela & Saarinen, 2013).

In addition to memory for single stimulus features, these findings also apply to memory for shapes (Salmela, Lähde, & Saarinen, 2012). Salmela et al. used radial frequency patterns (RF shapes) – i.e. contoured shapes that are created from a base circle stimuli by adjusting its radius, amplitude and spatial frequency. They used two tasks: a delayed discrimination task and delayed recall. In the delayed discrimination task, participants were required to discriminate between a set of memorised RF shapes and a probe presented after a blank retention interval. To

manipulate WM load, observers were required to remember from 1 to 6 shapes presented simultaneously. The results showed that discrimination thresholds increased linearly with increasing WM load. The delayed recall followed a similar procedure, except the observers were required to adjust the amplitude of the probe so that it matched one of the remembered shapes in the cued location. Their results showed that thresholds increased linearly with increasing WM load. The same was the case for standard deviations, which were used as a measure of recall error in the delayed recall task, signifying a loss of precision of the stored representations.

17.3. Summary: studying memory and cognition with psychophysics

To summarise, psychophysical measurements of thresholds were at the centre of investigating the relationship between the physical world and perception. It is, therefore, a long-established method, which is also being applied to answer questions that go beyond the perceptual processing and concern cognitive functions, including memory⁸.

Current studies suggest that perception and cognition are inherently linked. This idea was already put forward in the past (Barsalou, 1999; Kosslyn, Thompson, Kim, & Alpert, 1995; Kosslyn, 1994; Kosslyn, Ganis, & Thompson, 2001; Shepard & Metzler, 1971; Shepard & Podgorny, 1978) and has recently enjoyed much attention thanks to advances in neuroimaging and other methods (see Harrison & Tong, 2009 and Chapter 1). The main implication of such view is that cognition can be seen as a continuum to low-level perception, and thus some of the principles of the latter should be applicable to higher-level cognition as well (Nieder & Miller, 2003). Such a view, as argued in Chapter 1, is also adopted in this thesis.

⁸ In fact, psychophysical methods are today employed in various different contexts, including social cognition and emotions (see, for example, MacLin, MacLin, Peterson, Chowdhry, & Joshi, 2009; Roesch, Sander, Mumenthaler, Kerzel, & Scherer, 2010).

Since psychophysical measurements have been successfully applied to investigate memory processing in the past, applying these methods to investigate working memory in this thesis is warranted. In our experiments, we take a similar approach to probe the memory efficiency of different visual channels (e.g. De Valois et al., 1990).

18. Current experiment: visual working memory thresholds

In this experiment, we set to measure thresholds using a delayed match-to-sample task (i.e. the same task design used in Experiment 1). Therefore, we introduce a memory component to same/different discrimination threshold by delaying presentation of the probe, which resembles the delayed-discrimination designs described above (additionally, see General Methods for more detailed description of simple discrimination and same/different thresholds). However, this task also varies the number of stimuli the observers are required to remember (encode). We are going to refer to a threshold measured using this task as *visual working memory thresholds* (vWM thresholds) to emphasize the goal-oriented, working memory component of the task and to discriminate it from delayed discrimination tasks which do not manipulate working memory load.

Building on the findings of our previous study, we aim to compare WM thresholds for chromatic and luminance stimuli, in order to establish how inputs from the chromatic and achromatic visual channels interact with working memory. As previously, we are defining the stimuli in the DKL colour space to excite the appropriate post-receptoral mechanisms. We defined WM thresholds as stimulus contrast level at which the probability of responding correctly is 75%. Hence, we assume that the thresholds will provide a measure of the efficiency of chromatic vs achromatic, luminance mechanism in encoding stimuli to WM. Additionally, we are again recruiting a “*mixed signal*” condition as a control measure. In this condition, stimuli are designed to excite both chromatic mechanisms as well as the luminance mechanism (See Chapter 3 for details on this condition).

Based on the previous studies cited above (e.g. Bays & Husain, 2008), we expected that WM thresholds in the current study will increase with the increased number of shapes stored in memory. However, we do not expect this decrease to be of equal degree for luminance and chromatic shapes. This will be reflected in smaller threshold increase for the luminance-defined shapes.

The prediction that WM thresholds will not be the same for luminance and chromatic stimuli is based on studies showing that global shape discrimination thresholds for chromatic and achromatic mechanisms have been shown to differ (Mullen & Beaudot, 2002). We would expect this pattern to hold even if a retention period is introduced between encoding and recall, given that the same mechanisms are responsible for visual encoding and working memory (Harrison & Tong, 2009).

In their study, Mullen & Beaudot (2002) used stimuli that biased stimuli processing towards chromatic (L – M and S-cone) and achromatic, luminance mechanisms. In the task, participants were shown a circular and a non-circular stimulus and asked to discriminate between them, i.e. respond which of the two stimuli was circular. To allow for a direct comparison between achromatic and chromatic stimuli, their contrasts were equated in terms of multiples of detection threshold. The authors showed that the performance was best for the achromatic stimuli, followed by L – M and S-cone, with the latter associated with the worst performance. Authors note, however, that this relative impairment was mild and all channels appeared to be to some extent efficient at this task. Nevertheless, while the impairment might not have been dramatic, the differences between chromatic and achromatic stimuli were still evident.

Notably, this pattern of results resembles findings from our previous experiment (Chapter 3), where we showed that behavioural performance in a delayed match-to-sample task was also the worst for the S-cone condition (equivalent of the blue-yellow direction in Mullen & Beaudot, 2002), followed by L – M (red-green) and luminance (achromatic). Therefore, we expected that this pattern will be also evident using WM thresholds as a measure of performance.

Salmela et al. (2012) suggest that visual working memory resources are continuous and that the stimulus discriminability determines the fidelity of the stored representations. This conclusion is relevant to our predictions. Our previous study (see Chapter 3) showed that behavioural performance in a delayed match-to-sample task decreases with increasing number of shapes retained in memory. However, loss in accuracy was less severe for luminance-defined shapes

compared to chromatic shapes. Our results and the results of Salmela et al.'s study speak to our interpretation that the luminance channel enables more precise encoding of stimuli into working memory. Based on these results, we expect that WM thresholds in the current study will also show a linear increase with increasing number of encoded shapes. However, we also expect that the loss of accuracy will not be uniform across DKL directions. In particular, we expected the luminance condition to preserve the accuracy (reflected in lower threshold values) even when the number of the items in memory is high. In other words, thresholds in response to chromatic should show a linear increase; in case of luminance-defined stimuli, we predict that the thresholds will remain more uniform across working memory loads (i.e. increase in thresholds will be less steep with increasing load).

An additional reason why it is important to compare the efficiency of chromatic and achromatic mechanisms at near-threshold levels is that the results of our EEG experiment are based on remembering stimuli presented at suprathreshold levels. The contrast was increased (scaled-up) to ensure sufficient signal-to-noise ratio. Separation of chromatic and achromatic mechanisms is not necessarily clear-cut at suprathreshold levels, as they are subject to non-linear interactions (Kulikowski, 2003). It is implied that “mixed detectors” in vision – i.e. mechanisms that are responsible for processing both chromatic and achromatic (luminance) information – are less sensitive than those dedicated to chromatic-only and luminance-only mechanisms (Kulikowski, 2003), and thus cannot operate at near-threshold levels. One of the core conclusions of our previous experiment is that luminance mechanism has special and apparently exclusive contributions to WM encoding. However, one possible objection to this conclusion is that luminance and chromatic mechanisms are likely to interact at contrast levels used in the experiment. Thus, providing data derived from the observer's performance in response to near-threshold stimuli will help to strengthen our conclusions about the special role of luminance inputs into WM.

18.1. Summary – visual working memory threshold experiment

To summarise, we expected that participants will show lower visual working memory thresholds for luminance-defined shapes, as opposed to chromatic and mixed signals shapes. We anticipated that this pattern will be evident at all WM load levels. In addition, we predicted an interaction between WM load and DKL direction. More specifically, we expected that thresholds will increase with increasing number of items held in memory. Importantly, however, if luminance inputs indeed better efficiency, load-related increase in thresholds would be less pronounced for this mechanism.

Lower WM thresholds for luminance channel would imply that WM processing in this channel is facilitated. Higher thresholds would be on the other hand associated with less efficient WM processing. We compare thresholds between the visual channels and additionally contrast them at different WM loads, to assess whether the increase in the number of items stored in memory will affect four mechanisms differently.

We also expected that S-cone contributions to WM will be less effective than other conditions. In previous experiments that included S-cone mechanism to assess its efficiency in mid and high-level vision (Martinovic et al., 2011; Kosilo et al., 2013; Jennings & Martinovic, 2014) performance on various tasks was worse for S-cone. In addition, in our previous experiment (see Chapter 3) we also found that WM performance suffered when to-be remembered shapes isolated S-cone mechanism. Thus, in the current experiment, we expected S-cone condition to elicit higher thresholds.

19. Experiment 1: working memory thresholds

19.1. Methods

19.1.1. Participants

Twenty participants were recruited for the study. Sixteen participants have completed the experiment and were included in the analysis. Four participants were excluded as their thresholds could not be reliably estimated (see Procedure for details).

All participants have reported having normal or corrected-to-normal visual acuity and colour vision. This was confirmed using Acuity Plus and City University Colour test (CAD; Barbur, Rodriguez-Carmona & Harlow, 2006). No participants were rejected based on these measurements.

Participants took part in two separate experimental sessions. The first session consisted of vision tests (AcuityPlus and CAD, mentioned above) and working memory threshold measurements. The latter took place in EEG laboratory (for the experimental setup and display characteristics, see Chapter 2). During the second session, stimulus detection thresholds for the same experimental conditions were estimated. As mentioned above, four participants could not be brought back for this session and their data were also excluded; overall, 16 datasets ended up in the main analysis.

Participants were reimbursed financially or with course credits.

19.1.2. DKL colour space & stimuli

The stimuli used in the experiment differed in terms of their chromatic and achromatic properties. As in the previous experiment, we used DKL colour space to define these properties (Derrington et al., 1984). The DKL space was implemented in the Colour Toolbox (CRS, UK; Westland, Ripamonti, & Cheung, 2012) using measurements of the spectra of the monitor phosphors

taken by a SpectroCAL (CRS, UK) and cone fundamentals (Stockman & Sharpe, 2000; Stockman, Sharpe, & Fach, 1999). See Chapter 2 for details.

For clarity, I reproduce the table from Chapter 2 (general methods) to provide a summary of conditions tested in the current experiment (see Table 10 below).

As mentioned in chapter 2 (general methods), any point in the DKL colour space is defined using the following coordinates: a radius (r), the angle of rotation (ϕ_{DKL}), and angle of elevation (θ_{DKL}).

We used the same three classes of stimuli as in the previous experiment (two chromatic, one achromatic/luminance) plus a “mixed signals” condition.

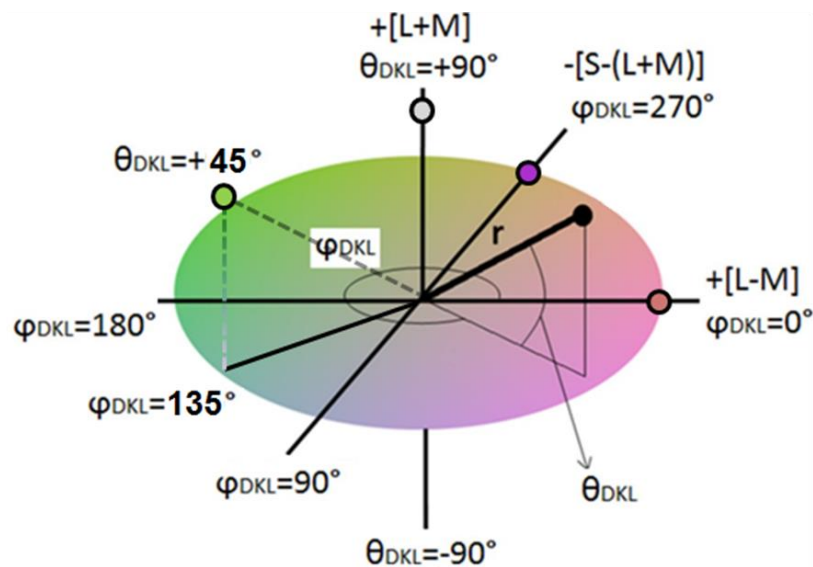
Opponent mechanisms corresponding to chromatic stimuli were L – M ($\phi_{DKL} = 0^\circ$) and S – [L – M] ($\phi_{DKL} = 270^\circ$). Luminance elevation was determined using heterochromatic flicker photometry procedure (see Procedure for details).

Achromatic/luminance mechanism was defined as L+M ($\phi_{DKL} = 0^\circ$) and the elevation was fixed at $\theta_{DKL} = 90^\circ$. For the mixed – signal condition, luminance signal was added to otherwise isoluminant stimuli. This condition excited both isoluminant mechanisms: [L – M] and S – [L – M] as well as the achromatic mechanism [L+M] ($\phi_{DKL} = 135^\circ$). Luminance elevation was fixed ($\theta_{DKL} = 45^\circ$).

For all conditions, radius r (i.e. distance from the white point, equivalent to stimulus intensity) served as the dependent variable and was varied during the staircase procedure.

Table 10 Psychophysical mechanisms of interest and their corresponding DKL coordinates. Only angle and elevation are provided as r is either fixed at individuals' discrimination threshold (Experiment 1, chapter 3) or serves as the dependent variable in threshold experiments (experiment 2 and 3, chapter 4). *The elevation of $L - M$ and S -cone is not 0° , but is determined from the HCFP procedure to adjust for individual's point of isoluminance. Signs in brackets corresponds to the polarity of the angle or luminance elevation (+ for increment and - for decrement). A rough appearance of the stimuli as it could appear on the display is provided, along with a position inside the DKL space (radius r is given only arbitrarily for presentation purposes).

Label	Mechanism	Angle	Elevation	Approx. appearance
Chromatic blue-yellow (S-cone)	$S - (L + M)$	270 (+)	x^*	 
Chromatic red-green	$L - M$	0 (+)	x^*	 
Achromatic luminance	$L + M$	0	90 (+)	 
Mixed signals	$L - M$ & $S - (L + M)$ & $L + M$	135 (-)	45 (+)	 



19.1.3. Threshold normalisation

In our task, the stimulus contrast is expressed in radii (i.e. the distance from the “white point” in the colour space). The axes for each direction in this space are not in same units. Therefore, comparing thresholds simply based on the measures of radiuses is inappropriate. To overcome this problem and to be able to meaningfully compare results from each DKL direction, detection thresholds were additionally measured using a two interval forced-choice task for each individual using the same set of stimuli that were used in the in the delayed match-to-sample task. The details on the detection threshold procedure and normalisation will be described in Section 19.1.4 below.

19.1.4. Procedure

After initial vision tests that ensured normal colour vision and normal, or corrected-to-normal acuity (CAD and AcuityPlus test, respectively), participants completed a Heterochromatic Flicker Optometry tests (HCFP). For the design, procedure and rationale of this test, see Chapter 2, Section 7.3. Participants adjusted the flicker for stimuli chosen randomly from the experimental set. In total, 8 – 10 reliable measurements were recorded (after the outliers were discarded) and averaged to use as an elevation angle for the next task.

After the procedure, the threshold task commenced.

Threshold measurements were obtained using a delayed match-to-sample task (the same design used in the EEG experiment; see Chapter 3).

There were 12 experimental conditions overall, with three WM load levels for each stimulus class (see Table II). Twelve staircases, one for each condition, controlled through Palamedes toolbox (Kingdom & Prins, 2009) were interleaved in the procedure. Each staircase controlled the stimulus intensity for a given condition. The intensity was defined as the DKL radius (r).

Table II Summary of experimental conditions. Numbers in the table (1 – 12) correspond to condition numbers. There were 3 levels of WM load for each of the 4 DKL conditions.

WM load	S-(L+M)	L-M	L+M (luminance)	Mixed signals S-(L+M) & L-M & (L+M)
Load 1	1	4	7	10
Load 2	2	5	8	11
Load 3	3	6	9	12

Each staircase was terminated after 35 trials. Participants were instructed to remember one, two or three abstract shapes shown sequentially, one at a time. After a blank interval (maintenance delay), a probe that either matched the remembered items (a match probe) or one that was different to the remembered shapes (a mismatch probe) was presented. Participants responded whether the probe was the same or different from previously presented shapes (see Figure 39 for trial outline). Participants were told to guess if they were not sure of the answer, forgot the stimuli, or did not see well due to low contrast. This task design probes working memory by requiring participants to hold presented stimuli in memory and later prompting them to make a comparison between the memory of the stimulus with currently perceived shape.

Stimulus intensity was adjusted based on participants responses in an adaptive fashion. Same intensities were applied to all shapes presented in the trial (i.e. intensity of every shape in the encoding array was the same as that of the probe). Every intensity level at which the stimuli were presented during the staircase were recorded in a file, separately for each staircase.

The second experimental session involved estimating detection thresholds for the stimuli used in the previous session. As mentioned above, this was done so that we could normalise WM thresholds to enable a meaningful comparison between different DKL directions. Four participants could not be brought back for the second session; their data were thus discarded.

Detection threshold procedure followed a two interval forced-choice paradigm (2IFC; see Chapter 2 for details on different psychophysical paradigms). A fixation cross was displayed for 1000 ms; it disappeared for the first interval, lasting 600 ms; an 800 ms delay with fixation cross was next, followed by another interval lasting 600 ms. One of the two 600 ms intervals contained a BORT shape. Participants were required to respond whether the shape appeared in the first or the second interval using a button box. They were also instructed to guess if they were not sure of the answer. The control of the stimulus intensity was based on participants' responses and was adjusted adaptively, just like in the WM threshold procedure.

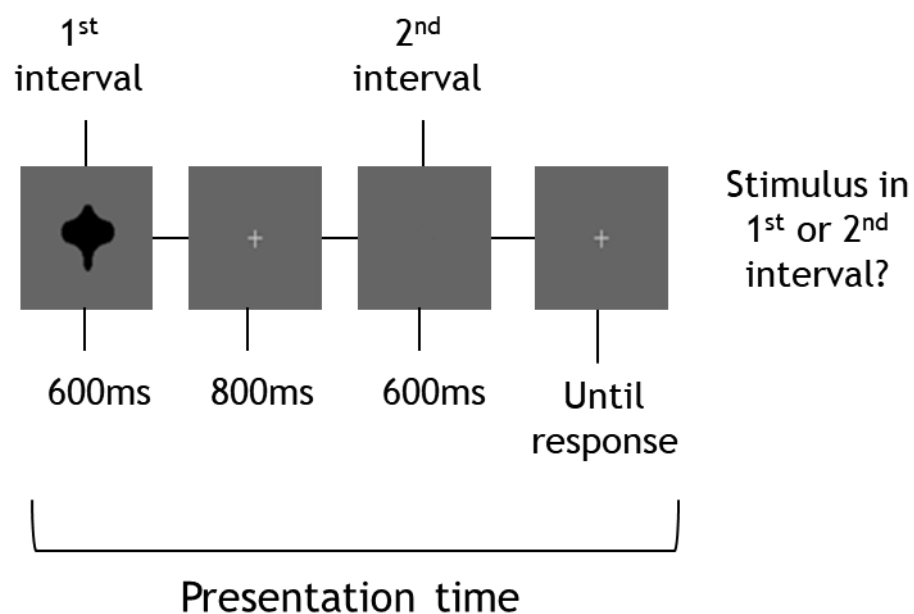


Figure 39 Two interval forced-choice procedure (2IFC) used to measure stimulus detection thresholds.

After all staircases were finished, logistic functions were fitted to data to obtain detection thresholds, i.e. the stimulus intensity (expressed in DKL radius r) at which the probability of correct answer for that individual was 75%. The detection threshold of each DKL direction was then used to normalise staircases obtained in the previous section. This was done as follows: each staircase step was divided by the detection threshold value of the corresponding DKL direction. Subsequently, the logistic function was fitted to these normalised staircases to obtain normalised WM threshold, i.e. the stimulus intensity (expressed in DKL

radius r) at which the probability of correct answer for that individual was 75%. In other words, WM thresholds that we are discussing after they are normalised are expressed in multiples of detection threshold.

Additionally, the second session also served as an opportunity to obtain “correcting” threshold measurements for each participant. For every participant, some WM thresholds could not be estimated during the first session, or the threshold was likely to be a result of incorrect sampling. In the former case, there were instances where for certain conditions participants did not reach 75% accuracy threshold. In the latter case, upon inspection of the logistic fits, it was apparent that for certain conditions contrast limits set prior to the experiment were either too low or too high for a given individual. For example, if the upper contrast limit was too low for a given participant, staircase procedure would end up sampling intensities close to the upper limit. As a result of this, it was likely that the threshold value was underestimated and should have been higher. Stimulus limits would be thus adjusted for that participant in the correcting session.

On average, 6 out of 12 conditions had to be repeated per participant. WM threshold estimation proved to be therefore problematic practically, at least with the adaptive procedure used here. This qualitative observation can be perhaps attributed to considerable individual differences between participants in terms of WM thresholds. Using a common set of contrast limits within which the experimenter expected the threshold to be was counterproductive and led to the problems described above. Note that estimating detection thresholds using 2IFC task did not produce similar problems. It is therefore apparent that WM thresholds might be more variable due to more cognitive nature of the task, as the source of individual differences might lie beyond perceptual factors alone.

For 6 participants, even after running the second session, reliable WM threshold estimates for some conditions could not be achieved. This was usually the case for load 3 condition, especially when defined by $S - [L+M]$ (S-cone) signals. These participants were omitted from the ANOVA analysis due to these missing values. Notably, Jennings and Martinovic (2014) also had to reject a number of

participants due to a difficulty estimating discrimination thresholds for this DKL direction. However, as noted above, other conditions were also problematic in our task.

19.1.5. Analysis

Normalised thresholds were analysed using within-subject, repeated measures ANOVA with factors: DKL direction (4 levels: S-cone, L – M, Luminance, mixed signals) and WM load (3 levels: Load 1, Load 2, Load 3). Greenhouse-Geisser corrections were applied where necessary.

20. Results

Overall results are presented in Figure 40 below.

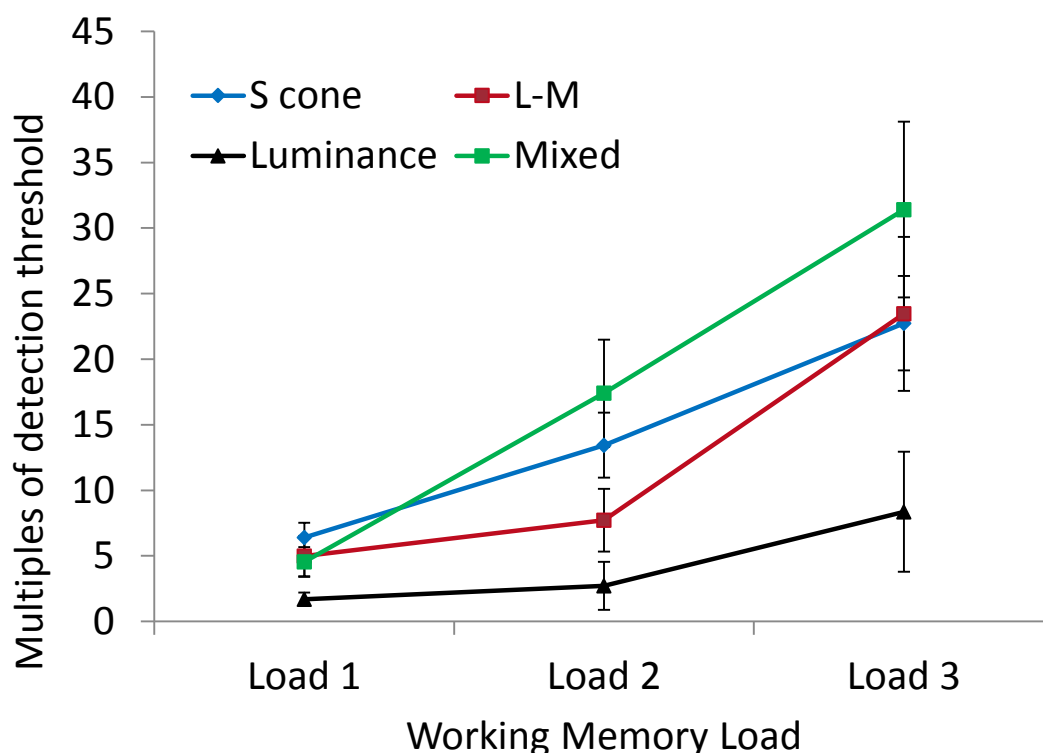


Figure 40 Multiples of detection thresholds plotted for 4 DKL conditions, at 3 levels of WM load. Error bars are 95% confidence intervals.

There was a main effect of DKL direction ($F(1.38, 11)=14.8$, $p=.002$, $\eta^2=.65$). Post-hoc tests using Bonferroni correction indicated that luminance WM thresholds were lower than S-cone ($p<.001$), L - M ($p=.005$) and mixed signal thresholds ($p=.002$). There was no significant difference between S-cone, L - M or mixed signal conditions.

Thresholds were overall lower for luminance than for S-cone, L - M and mixed signal conditions ($F(1.38)=14.8$, $p=.002$, $\eta^2=.65$). Thresholds also increased with increasing WM load ($F(2, 16)=136$, $p<.001$, $\eta^2=.94$). These effects were qualified by an interaction between the DKL direction and WM load ($F(2.12, 17)=9.76$, $p=.001$, $\eta^2=.55$). Post-hoc tests using Bonferroni correction indicated that thresholds increased with WM load for all DKL directions. It appears that thresholds measured for luminance were, however, lower than the chromatic and mixed

conditions at all WM loads, with the exception of load 1, suggesting that luminance thresholds remained to be relatively low despite an increase in WM load. This difference was most pronounced at WM load 3 (see Figure 41 below).

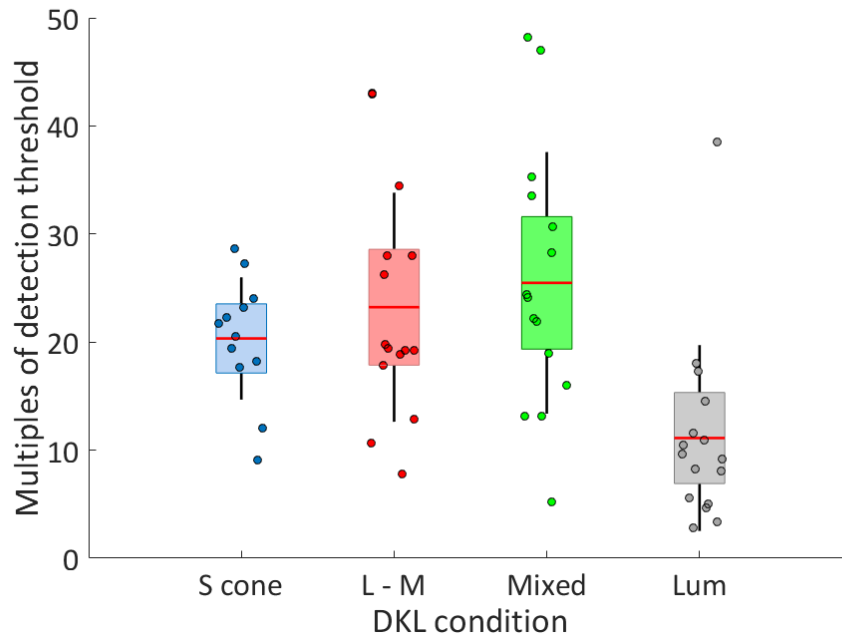


Figure 41 WM thresholds at Load 3, for each DKL condition. Red lines are mean WM thresholds across observers, coloured shaded areas are 95% confidence intervals, and error bars on top and bottom of the shaded area correspond to 1 SD. Each dot represents observer's WM threshold, estimated using the QUEST procedure and normalised to multiples of detection threshold for that participant.

21. Control experiments

As mentioned above, in order to obtain a sufficient signal-to-noise ratio while controlling for stimulus saliency, same/different discrimination thresholds were obtained for the EEG experiment and the resulting contrasts were subsequently scaled up. A possible shortcoming of this approach is that we did not estimate slopes of the psychometric function. During the fitting procedure to obtain the thresholds, it was assumed that the slopes did not differ between the conditions. However, if psychometric functions underlying the performance in our WM task have different slopes for different conditions, there is a possibility that by increasing contrast, the assumption of equivalent saliency of the stimuli was violated. Therefore, we decided to perform additional, control experiments to investigate how the slope of the psychometric function differs depending on the stimulus type (chromatic vs achromatic) as well as the task type (detection vs same/different discrimination task). In line with the previous research, we expected that the slope will be steeper for luminance-defined shapes than for L – M and S-cone directions (Eskew, McLellan & Giulianini, 1990). While the slope measurements vary for the chromatic stimuli, luminance tends to have consistently higher (steeper) slope at detection (See Eskew et al., 1999 for a review). In relation to Experiment 1, it is important to demonstrate that the slopes do not differ between different visual channels in the same/different discrimination task using our stimuli. Showing otherwise could potentially undermine the claim that the stimuli in our task were matched for saliency. For example, if same/different discrimination for luminance-defined stimuli was characterised by a steeper slope of the psychometric function than chromatic condition, this difference could be magnified due to the scaling procedure, thus making the luminance-defined shapes much easier to discriminate.

22. Experiment 2 – shape detection thresholds

22.1. Methods

3 participants (two naïve to the experiment and one author of the study) performed a 2IFC task. Testing conditions were the same as in other experiments. We used Psychtoolbox routines to control the flow of the experiment and Visage Toolbox to control stimulus properties. Shapes were again defined in different directions of DKL colour space to create shapes isolating the luminance mechanism and two opponent-chromatic mechanisms (L – M and S-cone). The additional mixed signal condition, which excited both luminance and chromatic pathways, was also used.

The task used a method of constant stimuli: each visual input condition was presented at 10 stimulus levels, with 100 trials per stimulus level (1000 trials per visual input condition or 4000 trials overall). Stimulus intensity was varied by varying DKL radius, while other DKL parameters remained unchanged.

The condition and stimulus level presented in each trial was randomized. The task followed the same procedure as in detection threshold measurement in experiment 1, i.e. the 2IFC task (see section 19). After the second interval finished (which was signified by the fixation cross changing colour from white to black), participants responded with a button press whether the shape was present in the first or second interval.

As explained before (see section 19), it is impossible to compare thresholds across different DKL directions directly as they do not share a common metric. To allow such comparison, we have normalised detection thresholds in the following manner: once the task has finished, we fitted a logistic PF to individual conditions using Palamedes Toolbox routines to obtain DKL radius that led to 75% performance level. We then divided stimulus level units by these detection thresholds and fitted logistic function again individually to each condition to get the threshold and slope value in converted units.

Once the stimulus levels were normalised for each DKL direction, a combined fit to all conditions was performed.

To reduce the number of free parameters (which is required to perform a combined fit to more than one condition), threshold and guess rates were fixed to the value obtained from individual fits, while the lapse rates were constrained (i.e. the fit was performed, but it would fit the same value to all conditions). Only slope values were unconstrained (i.e. we fit different value to each condition).

Bootstrap analysis was performed to estimate errors of the parameter estimates in the fit. 400 simulations were performed.

To formally check whether the observed differences were significant, we performed a statistical model comparison, again using Palamedes toolbox routines. The routine is based on comparing two models (fuller and lesser) to see which one better fits the data. The fuller model assumed that the thresholds, as well as the lapse rates, are identical between conditions and that the guess rate equals 0.5 for all conditions. The lesser model was identical, except it made an additional assumption that slopes are identical between conditions. The assumptions of the model that turned out to be the best fit for the experimental data were verified using a goodness-of-fit test.

22.2. Results

The results indicate that in two out of three participants' slope of PF for luminance-defined shapes differed significantly from other conditions (see Figure 42 below).

Participant	Model comparison p-value	Goodness-of-fit	Number of converged fits to simulation
MXKM	0.0338 *	0.83	3997 of 4000
CXKF	0.0038 *	0.2910	4000 of 4000
SXPF	0.1105	0.3348	3987 of 4000

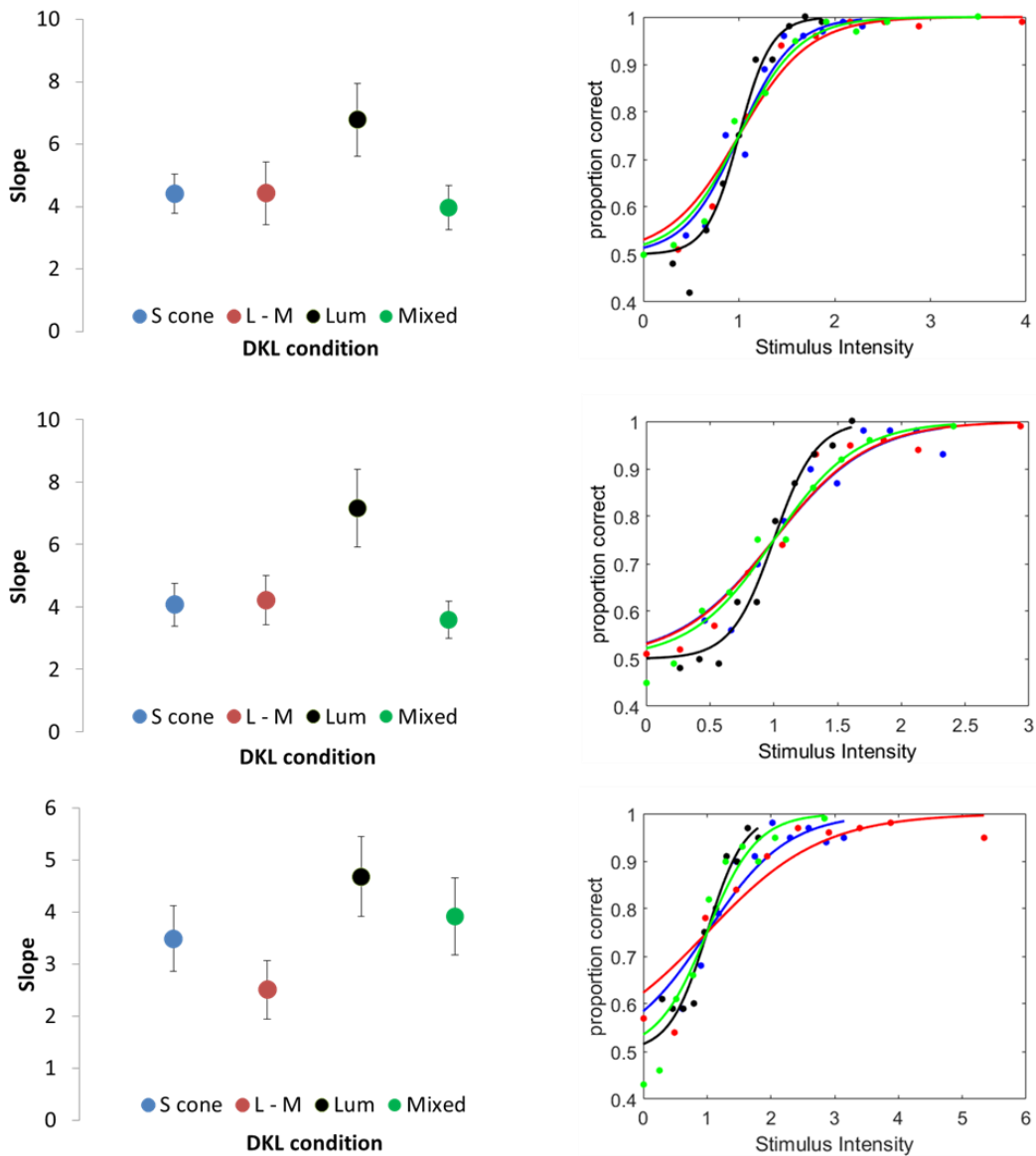


Figure 42 Table at the top shows results of model fits for the 2IFC detection threshold task. Figure below depicts a comparison of slopes of the psychometric function for different post-receptor mechanisms (left) fitted to data derived from shape detection task (right).

23. Experiment 3: Same/different shape discrimination thresholds

23.1. Methods

Additional same/different discrimination threshold task with one participant was performed to see if slopes are similar to those obtained from detection threshold data.

All procedures, routines and analyses are the same as above. The paradigm itself differs however in that this time participants are presented with two shapes in a succession, which could be either two identical shapes or two different shapes. As soon as the second shape disappears, the participant responded whether the shapes were same or different using a button press.

23.2. Results

The model comparison indicated that slopes did not significantly differ between conditions. Although not significant, S-cone tended to have a steeper slope than other DKL conditions. Interestingly, if scaling the contrast up would exaggerate differences between DKL conditions and thus violating the saliency, we should expect S-cone performance to be superior in comparison to other conditions, which was not the case.

Observer	Model comparison p-value	Goodness-of-fit	Number of converged fits to simulation
MXKM	0.635	0.18025	3992 of 4000

MXKM

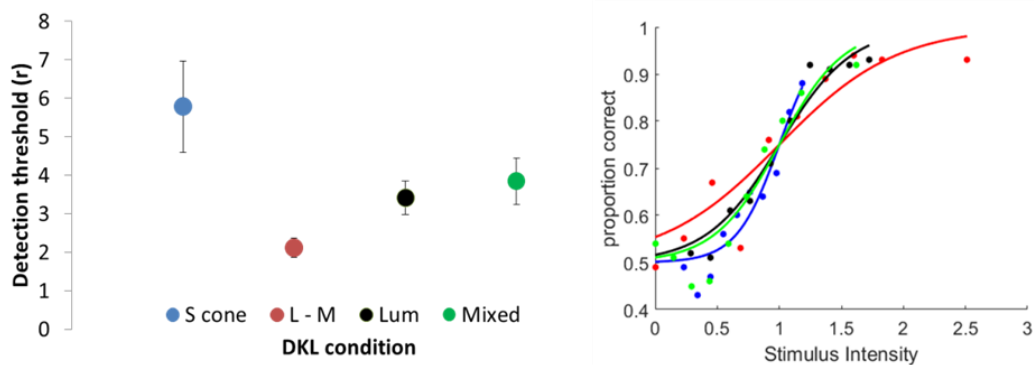


Figure 43 Comparison of slopes of the psychometric function for different post-receptoral mechanisms (left) fitted to data derived from shape discrimination task (right).

24. Discussion

The current set of experiments aimed to explore contributions of chromatic and achromatic channels to visual WM using psychophysical methods. We used a delayed match-to-sample task with varying WM load in order to measure visual working memory thresholds in response to chromatic and achromatic (luminance) shapes. We predicted that encoding of luminance shapes into WM will be more efficient than chromatic shapes, reflected in lower WM thresholds.

The results confirmed our predictions. Encoding of luminance shapes produced lower thresholds than achromatic stimuli. Importantly, thresholds in response to both chromatic and achromatic stimuli increased with increasing WM load, but despite this, threshold increase for luminance was less severe. This suggests that WM representation remains robust even at higher WM loads.

Mullen & Beaudot (2002) reported lower discrimination thresholds for achromatic compared to chromatic stimuli. We report similar pattern in our task, suggesting that similar mechanisms are responsible for perceptual as well as working memory comparisons (Hyun et al., 2009). Mullen & Beadot (2002) note that global shape perception is only moderately worse when performed by the chromatic system. Our study shows, however, that at higher WM loads the difference between chromatic and achromatic mechanisms is becoming more pronounced. In other words, while at perceptual level (and low WM loads), chromatic stimuli perform only moderately worse than luminance, chromatic signals seem less efficient in sustaining multiple memory representations for a prolonged period.

Unlike Mullen and Beadot, we did not find that the two chromatic mechanisms tested (S-cone and L – M) differed in terms of thresholds. In their experiment, the blue-yellow mechanism (which is roughly equivalent to our S-cone condition) performed worse than the red-green mechanism (L – M). There was an indication that at L – M performed better than S-cone at load 2, but, unlike luminance, both chromatic mechanisms performed equally at higher WM loads. This suggests that

L – M and S – (L+M) cone-opponent mechanisms are similarly efficient in terms of WM processing.

Our study is in line with previous literature showing that increasing WM load is associated with an increase in delayed discrimination thresholds and shallower slope of the psychometric function in response to single stimulus features as well as shapes (Bays & Husain, 2008; Palmer, 1990; Salmela, Lahde, & Saarinen, 2012; Salmela & Saarinen, 2013). We extend these previous findings by showing that while this is true for all post-receptoral mechanisms, the luminance channel remains comparatively more efficient than chromatic mechanisms despite the increase in a number of shapes encoded.

Importantly, the pattern of results in the current experiment is analogical to performance in a WM task in conditions where the memory probe was different than stimuli in the encoding array (i.e. mismatch condition; see Chapter 3; see also Figure 44 below for replotted results of the previous experiment).

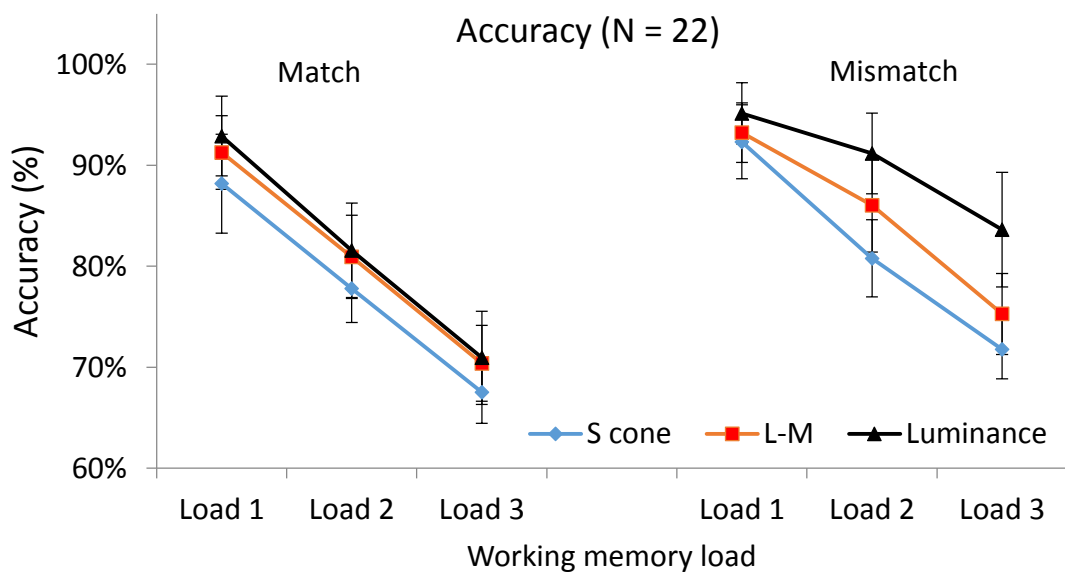


Figure 44 Results from a delayed match-to-sample task with fixed stimulus contrast from the previous experiment (see Chapter 3). Error bars represent 95% confidence intervals.

For mismatch, performance dropped with increasing WM load, however, the loss of accuracy was less severe for luminance-defined stimuli compared to L – M and S – (L+M) conditions. One of the shortcomings of the EEG experiment was that the stimuli used in the main experiment were presented at suprathreshold levels.

While at the level of detection thresholds the contribution of different channels is largely independent, at suprathreshold levels these mechanisms interact in a non-linear fashion (Kulikowski, 2003). Showing similar behavioural effects at a near-threshold level further strengthens our conclusions regarding the special nature of luminance inputs in WM. In summary, the results complement findings from the delayed match-to-sample task with fixed thresholds (see Chapter 3), suggesting that the smaller decrease in accuracy for luminance at higher loads could be explained in terms of better efficiency of luminance inputs to working memory.

One shortcoming of the current experiment is that we did not discriminate between match and mismatch probes like it was done in the EEG experiment. The fact that the threshold data closely follows the pattern found for mismatch condition might suggest that the luminance advantage for higher WM loads is present at near-threshold level. At suprathreshold, the pattern can be also observed at mismatch. Future experiments should discriminate between match and mismatch to support this conclusion.

The current experiment also addresses another potential shortcoming of the EEG experiment. Specifically, using suprathreshold contrasts obtained by scaling same/different discrimination thresholds might have violated the saliency between stimuli classes. This would be the case if the slope of the psychometric function underlying discrimination performance at thresholds was considerably different between stimuli classes. While we concluded that the saliency procedure was appropriate based on the results of the previous experiment (different effects for match and mismatch conditions – see Chapter 3), this study aimed to verify the procedure further by measuring slope differences between luminance and chromatic conditions in detection and discrimination tasks.

As expected, we found that luminance produced steeper function than chromatic stimuli in the detection task, which is consistent with previous findings (Eskew, McLellan & Giulianini, 1990). However, slopes in the discrimination task did not differ between the conditions. This provides support for the use of scaled same/different discrimination thresholds to match stimuli in saliency. The main

problem with this interpretation, however, is that it is based on the data from one participant only. Therefore, more data is needed to confirm this observation and warrant firm conclusions.

The current results do not imply that the interactions between luminance and chromatic mechanisms are unimportant to WM performance. Further experiments might explore the nature of interactions between the channels in WM task. Recently, the focus of vision research shifted to the exploration of these complex interactions, with some interesting results (Shevell & Kingdom, 2008; Clery et al., 2013; Jennings & Martinovic, 2014). Despite this, however, our experiment provides evidence that, when considered separately, chromatic and achromatic mechanisms do not contribute to WM in a symmetric fashion.

Insights into interactions between the mechanisms can be explored at near-threshold levels as well (Jennings & Martinovic, 2014). In our study, we attempted to do so by introducing a “mixed” stimuli in this experiment (which was designed to excite chromatic as well as luminance mechanisms). However, the interpretation of the result is currently limited. The “mixed” condition produced results similar to S-cone and L – M conditions, also revealing higher thresholds than luminance, especially at higher WM loads. This would suggest that performance for this condition was driven predominantly by chromatic, rather than luminance information. Indeed, contrasts calculated for chromatic and achromatic mechanisms for each condition (averaged over all participants and WM load levels) confirm this observation (see Table 12). For the mixed condition, luminance L+M contrast was -0.0157 and chromatic L – M contrast was -0.0621 , making it similar to red-green isoluminant condition, which was -0.007 for luminance (L+M) and 0.0569 for L – M contrast. The luminance condition, on the other hand, had 0.1455 luminance contrast, and -0.0002 L – M contrast. In other words, the luminance contrast in the mixed condition was at similar levels as in the isoluminant red-green condition, supporting the interpretation that performance in response to this class of stimuli was driven predominantly by chromatic information.

Table 12 Weber contrasts for achromatic and chromatic mechanisms for each condition, derived from L, M and S contrasts.

	Mechanism		
	S-(L+M)	L-M	L+M
S cone	0.2975	0.0008	-0.0060
L-M	0.0064	0.0569	-0.0070
Mixed	0.0767	-0.0621	-0.0157
Luminance	-0.0723	-0.0002	0.1455

Previous studies showed that addition of luminance information benefits object recognition over chromatic-only stimuli (Kosilo et al., 2013; Martinovic et al., 2011). It is difficult to compare this design with our experiment, as their study introduced high-level factor by asking participants to discriminate between objects and non-objects. Interestingly, however, performance between mixed and chromatic stimuli produced equivalent results in response to non-objects. This would mean that addition of luminance information to chromatic stimuli interacts with high-level cognition (here, object recognition), but in a task without such high-level factors, the simple addition of luminance signal does not appear to benefit shape discrimination.

Our mixed signal stimuli only tested a single luminance elevation angle. It is possible that luminance benefits can become apparent only at certain luminance levels. An approach adopted by Jennings & Martinovic (2014) might be more appropriate to address this question. Jennings and Martinovic tested several levels of luminance elevation and showed that luminance and chromatic mechanisms interact in a complex fashion. To find out more about the interactions between luminance and chromatic mechanisms in a delayed match-to-sample task and their contribution to WM processing, we suggest that the future studies should incorporate stimuli with varying levels of chromatic and achromatic component (e.g. Jennings & Martinovic, 2014).

In summary, threshold measurements suggested that luminance signals carry an advantage during WM processing over chromatic signals. This is especially pronounced when more stimuli have to be kept in memory. Thus, despite the

increase in task difficulty, the threshold increase expected to occur with increasing WM load is less evident for shapes isolating luminance mechanism. Importantly, these results also complement the finding from the delayed match-to-sample task with fixed, scaled-up same/different discrimination thresholds (see Chapter 3), suggesting that the smaller decrease in accuracy for luminance at higher loads could be explained in terms of better efficiency of luminance inputs to working memory. More broadly, the study further confirms that interactions between perceptual processing and working memory have an impact on performance (Haenschel et al., 2007). Furthermore, isolating post-receptoral mechanisms to study working memory encoding is a fruitful strategy, helping to extend the scope of approaches to working memory. This study also demonstrates that using methods traditionally reserved for vision science can be effectively applied to study cognitive functions, especially in the light of a recently established link between perception and memory (Pasternak & Greenlee, 2005).

Chapter 5

A pilot study of luminance processing and visual working memory in schizophrenia

Schizophrenia is a chronic disorder with a prevalence of about 1% worldwide (Bromet & Fennig, 1999). It is caused by a collection of complex factors interacting with typical brain development, including genetic, environmental and developmental factors (Lewis & Lieberman, 2000; Millan et al., 2016a). The history of psychiatric diagnosis of schizophrenia can be traced back to a Jewish Czech psychiatrist Arnold Pick (1851 – 1924), who was first to use the term “dementia praecox” to describe his patient (Hoenig, 1995). The term became popular and regularly used as a diagnosis after German psychiatrist Emil Kraepelin (1856 – 1926) included it in his famous psychiatry textbook published in 1899 (Greene, 2007; Kraepelin, 1902). The later work by Eugen Bleuler (1857 – 1939) helped to crystallise the clinical definition of the disorder (Berrios, Lague & Villagran, 2003). Bleuler also helped to establish the term “*schizophrenia*”, which replaced the “dementia praecox” (Bleuler, 1908; Bleuler, 1911). Later work by Kurt Schneider further contributed to characterising the disorder, mostly by his attempts to differentiate schizophrenia more clearly from other conditions by developing a list of symptoms typical of the disorder (so-called “first-rank symptoms”; Schneider, 1959). Currently, symptoms that characterise the disorder are categorised as positive and negative symptoms. The former include hallucinations, delusions, thought disorders and other perceptual abnormalities, while the latter refers to social withdrawal and emotional bluntness.

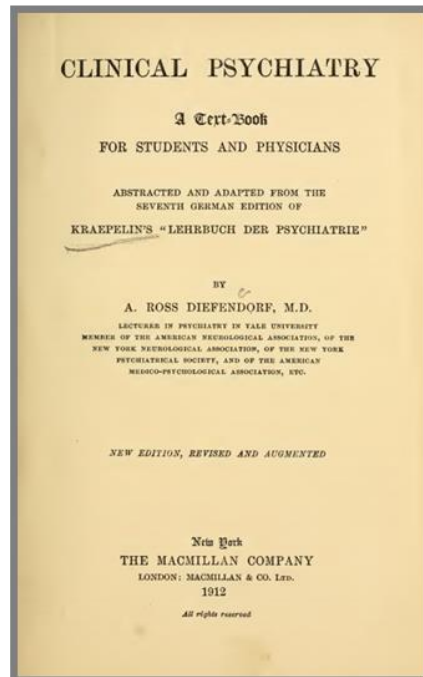
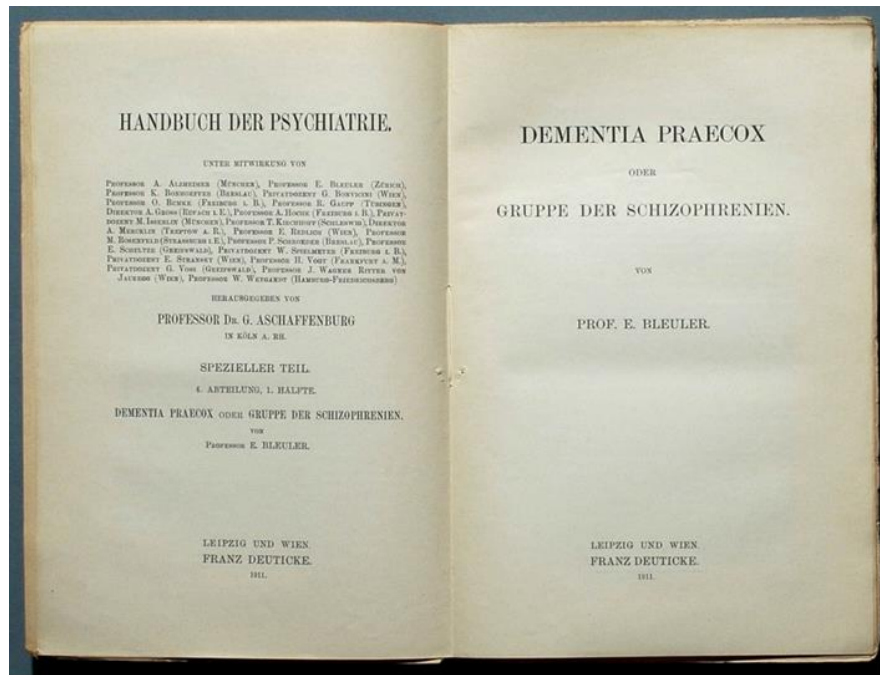


Figure 45 Top: title page of Bleuler’s 1911 article on dementia praecox, where he referred to the disorder as “group of schizophrenias”. Image: H. P.Haack, under Creative Commons licence (CC BY – SA 3.0). Bottom: title page of the 1912’s translation of Kraepelin’s “*Lehrbuch der Psychiatrie*”, originally published in 1899 (Image: <https://ia802703.us.archive.org>).

Central to this thesis are findings that demonstrate a range of deficits in visual perception (Butler, Silverstein, & Dakin, 2008) as well as cognitive impairments (Millan et al., 2016a), including working memory (Goldman-Rakic, 1994). These appear to occur in addition to positive and negative symptoms described above.

It has been suggested that low-level perceptual deficits can actually contribute to some cognitive impairments (Javitt, 2009b). In this chapter, I will describe both cognitive and perceptual deficits in more detail. In terms of cognition, I will focus on visual working memory. In terms of perception, I will mostly focus on the apparent deficits in processing luminance information and – more generally – on magnocellular deficit theory of schizophrenia (Butler et al., 2005). Further, I will argue that the perceptual deficits can be linked to WM deficits (Haenschel et al., 2007); more specifically, impaired luminance processing might explain diminished visual working memory performance in patients.

25. Cognitive deficits in schizophrenia

While cognitive deficits are widely recognised and reported (Javitt, 2009b), they are not regarded as a clinical feature of the disorder (Barch et al., 2013; Tandon et al., 2013). Furthermore, they are not currently a target for medication development (Millan et al., 2016b)⁹. Nevertheless, several deficits have been identified, including working memory, attention, memory, and speed of processing (see Nuechterlein et al., 2004 for a review).

WM memory dysfunction is regarded as one of the most prominent features of the disorder, which adversely affects day-to-day functioning (Forbes, Carrick, McIntosh, & Lawrie, 2009; Goldman-Rakic, 1994; Lee & Park, 2005; Silver et al., 2003). A meta-analysis showed that this deficit cannot be explained by IQ differences between patients and healthy controls (Forbes et al., 2009). It also appears that there is no clear link between WM and the use of antipsychotic medication or illness duration, although, as Forbes et al. note, this interpretation is limited by the heterogeneity of the studies included in the analysis.

Importantly, however, a number of studies demonstrating impairment in WM in patients versus controls included in Forbes' meta-analysis did not show evidence of publication bias. There is also some indication that visuospatial WM deficits are more consistent across studies than verbal working memory (Lee & Park, 2005), though a later meta-analysis did not find a difference between impairments of WM from different domains, including phonological, visuospatial and central executive working memory (Forbes et al., 2009). At the same time, impairments in spatial working memory compared to healthy controls appear to be consistent (Piskulic, Olver, Norman, & Maruff, 2007). Taken together, working memory deficits in schizophrenia can be regarded as a core feature of the disorder. This impairment extends to different modalities, including visual working memory, which is of particular interest to this thesis. In the next section,

⁹ This is not to say that there are no initiatives that attempt to change the current state of affairs – for example, the CNTRICS initiative (Carter & Barch, 2007) aims to identify cognitive impairments that can become a target for treatment development, as well as devise measures that will test cognitive functioning in individuals with schizophrenia using methods derived from cognitive neuroscience.

I will outline perceptual deficits, and I will further argue that they might contribute to the reported impairments in visual working memory.

25.1. Perceptual and sensory deficits in schizophrenia

In addition to cognitive impairments, perceptual deficits received a great deal of attention in the recent years (Butler, Silverstein, & Dakin, 2008). While one of the most prominent symptoms of schizophrenia-related to perception involves visual hallucinations, much less “dramatic” visual impairments in the visual domain have been documented over the years. Interestingly, Bleuler in the 1950’s explicitly stated that sensory processing is intact in schizophrenia, and any self-reported impairments stem from altered top-down processing. More specifically, Bleuler believed that patients would “complain” about their disturbances, but he attributed these complaints to the emotional state of the individual. This view has been highly influential, however, eventually it was challenged by research showing that perception is not as intact as previously thought. A clear example of this are case studies described by (McGhie & Chapman, 1961). McGhie and Chapman quote a number of patients who describe their experiences that point to abnormalities in vision and hearing:

(Patient 17) – Colours seem to be brighter now, almost as if they are luminous. When I look around me it’s like a luminous painting (...)

(Patient 23) – Sometimes I feel alright then the next minute I feel that everything is coming towards me. I see things more than what they really are. Everything’s brighter and louder and noisier.

(Patient 15) – I seem to be noticing colour more than before (...)

The colours of things seem much clearer and yet at the same time there is something missing. The things I look at seem to be flatter as if you were looking just at a surface (...)

- McGhie & Chapman, 1961, p. 105

Other case studies have also listed similar disturbances in the visual domain, including disturbances in the perception of size, seeing things as if they were flat or even apparent need to bind individual elements to form a coherent percept:

Case 22

I have to put things together in my head. If I look at my watch I see the watch, watchstrap, face, hands and so on, then I have got to put them together to get it into one piece.

- Chapman, 1966, p.229

Such first-person accounts contributed to questioning the traditionally held view that perception is intact in the disorder. Javitt (2009) argues that another factor that brought perceptual impairments into focus were new advances in cognitive sciences. For example, Baddeley and Hitch's model of working memory (Baddeley & Hitch, 1974) emphasized the role of the central executive system, but at the same time, he recognised that the low-level, bottom-up aspects of the memory system are capable of independently storing sensory information. Such conceptualisation of cognitive function helped to provide a framework that proved to be influential on cognitive theories in schizophrenia as well (Javitt, 2009b).

A number of disturbances in visual processing have been recognised by contemporary research. Individuals with schizophrenia demonstrate decreased sensitivity to contrast (Butler et al., 2005, 2009; Calderone et al., 2013; Kéri, Szamosi, Benedek, & Kelemen, 2012; Slaghuis, 1998), spatial frequency (Khosravani & Goodarzi, 2013; Antígona Martínez et al., 2008; O'Donnell et al., 2002) and motion (Chen, Nakayama, Levy, Matthyse, & Holzman, 2003; Yue Chen, Levy, Sheremata, & Holzman, 2004; Kim, Wylie, Pasternak, Butler, & Javitt, 2006). Moreover, as pointed out by Yoon, Sheremata, Rokem, and Silver (2013), post-mortem studies have also indicated abnormalities in brain structures related to visual processing, though the findings are not always consistent. More specifically, one study has indicated an increased neuronal density in occipital Brodmann's area 17 (Selemon, Rajkowska, & Goldman-Rakic, 1995). However, this was not confirmed by later post-mortem studies. Although they did demonstrate

a reduction in a total number of neurons and a smaller cortical area allocated to visual perception, however, the overall neural density was not affected (Dorph-Petersen, Pierri, Wu, Sampson, & Lewis, 2007).

Importantly, there is some evidence suggesting that visual impairments might be clinically relevant. For example, Klosterkötter et al. (2001) assessed a sample of patients with prodromal symptoms and found that disturbances in visual perception were among factors that strongly predicted progression to the disorder. Such perceptual disturbances, which include sensitivity to light and changes in face perception of one's own face among others, are considered to be linked to sensory processing (Huber & Gross, 1989; Schultze-Lutter et al., 2007). Similarly, visual disturbances in children of parents with schizophrenia or even disturbances in children in the general population also appear to be associated with later development of schizophrenia (Schiffman et al., 2006; Schubert, Henriksson, & McNeil, 2005; Silverstein et al., 2015). Such deficits impact functional outcome of the affected individuals, i.e. their everyday functioning is impaired as well (Green, Helleman, Horan, Lee, & Wynn, 2012; Rassovsky, Horan, Lee, Sergi, & Green, 2011).

In summary, cognitive as well as perceptual disturbances appear to be prevalent in schizophrenia. Researchers are currently emphasizing that the schizophrenia-related changes in visual processing are especially worth pursuing, given our advanced understanding of the human visual system, from anatomy, neural circuitry and functional assemblies to behaviour (Silverstein & Keane, 2011; Yoon et al., 2013). In other words, visual impairments might provide a window into some of the brain mechanisms involved in the disorder. Interestingly, visual deficits seem to impact other cognitive functions. Studied examples include reading (Revheim et al., 2006), object processing (Doniger, Foxe, Murray, Higgins, & Javitt, 2002) emotional processing (Butler et al., 2009; Turetsky et al., 2007), as well as working memory (Haenschel et al., 2007). In subsequent sections, I will focus on the relationship between early visual processing and working memory. The aim of this approach is to establish whether impairments in visual working memory can be a consequence of altered perceptual processing.

25.2. Interaction between visual perception and working memory in schizophrenia

As outlined above, it is evident that perceptual deficits in the visual domain, as well as WM impairments, are both core features of the disorder. It has been suggested that perception can contribute to WM impairments (Haenschel et al., 2007; Haenschel & Linden, 2011; Tek et al., 2002; Lee & Park, 2002; Park, Swisher, & Knurek, 2001).

One of the consequences of this view is that the research must focus on the earliest, encoding stages of WM as well as on perceptual processing of the stimulus in general (Haenschel et al., 2007). This marks a diversion from earlier research. Typically, studies have focused on cognitive processing supposedly mediated by activity in the prefrontal cortex and differences between patients and controls. Consequently, WM impairments tended to be mainly attributed to dysfunctional prefrontal (Barch et al., 2001; Callicott et al., 2000; Manoach, 2003), rather than sensory networks. Consequently, it was the maintenance and retrieval stages of WM that received the most attention. However, as Lee & Park (2005) suggested, subdividing WM into three, temporally-defined stages can potentially help to elucidate processes that are contributing to successful performance. Indeed, such approach turned out to be beneficial. Studies that did differentiate between WM stages found that the interaction with perceptual processing most likely takes place during early encoding. For example, Haenschel et al. (2007) recorded EEG during WM at all stages from controls and participants with early-onset schizophrenia. They found that modulation of the early event-related components (in particular, P1 component) was sensitive to the number of stimuli kept in memory (i.e. WM load). Importantly, modulation of these components correlated with better WM performance in control group. On the other hand, the P1 in the patient group was largely attenuated, and no correlation with behaviour could be demonstrated.

Another study (Tek et al., 2002) demonstrated that perceptual processing is the main culprit behind WM impairments. They suggested that perceptual deficits manifest themselves during WM encoding, which was demonstrated using a

delayed match-to-sample task. Participants were presented with two shapes, shown consecutively. A probe was presented after a varying time delay. In one condition participants had to respond whether the probe matched one of the presented shapes, thus testing object-based working memory. In other condition, they responded whether the location was the same or different, thus testing spatial working memory. Tek et al. showed that increasing stimulus presentation for patients allowed for more efficient encoding, thus improving performance on the task. At the same time, memory for the spatial location was insensitive to stimulus presentation length. This finding is line with other studies (e.g. Hartman, Steketee, Silva, Lanning, & McCann, 2003) which also showed that longer stimulus presentation allows individuals with schizophrenia to overcome some impairments in WM performance. In their study, control and patient groups were matched in terms of stimulus presentation time needed to reach optimal performance levels. Such manipulation resulted in lack of group differences between patients and participants. Further, a meta-analysis (Lee & Park, 2005) found that the length of WM delay (i.e. time period between the end of stimulus presentation and memory retrieval) does not appear to influence effect size in studies reporting WM deficits in schizophrenia patients. According to Lee and Park (2005), it is important to bear in mind however that demonstrating the importance of encoding does not necessarily indicate that maintenance and retrieval stages of WM are not affected in schizophrenia. In other words, these studies highlight the importance of accurate perceptual encoding in working memory and they suggest that impaired perceptual processing likely contributes to WM impairment in patients compared to controls.

Importantly, this is in line with studies advocating the view that perception and working memory share similar mechanisms (Harrison & Tong, 2009; Pasternak & Greenlee, 2005) since such view implies that close interactions between the two systems must be taking place (Gao et al., 2011). One way of testing such interactions is to take advantage of visual science methods to investigate how early perceptual mechanisms contribute to working memory. In the last two experiments described in this thesis, it was demonstrated that luminance

information appears to contribute to working memory, resulting in better behavioural performance. In the next section, I will argue that this approach might also be used when studying working memory processing in schizophrenia to pin down the mechanisms through which perception interacts with working memory in this disorder.

25.3. Luminance processing in schizophrenia: relevance to working memory performance

In our previous study, it was established that perception contributes to WM performance in a healthy sample of participants. We investigated whether luminance and colour-opponent channels differentially contribute to WM performance. We showed that encoding of luminance-defined shapes led to better performance over isoluminant shapes, suggesting that luminance signals are beneficial for WM performance, possibly through interactions with WM processing during early encoding. In the current study, we aimed to see whether a similar pattern will be evident in patients with schizophrenia. Investigating luminance processing in schizophrenia is interesting for a number of reasons. Firstly, as mentioned above, perceptual deficits in schizophrenia are widely reported; since in a previous experiment, we showed that luminance-defined stimuli are beneficial for WM encoding, investigating whether this aspect of WM processing in schizophrenia is intact is warranted.

Secondly, some studies attribute perceptual deficits in schizophrenia to impairments in the dorsal visual stream (Foxye, Doniger, & Javitt, 2001), while others argue that the impairment might be traced even further back, to a subcortical level, namely the magnocellular visual pathway (Butler et al., 2001; Kéri, 2008; Antígona Martínez et al., 2008; Schechter et al., 2005). Notably, magnocellular pathway receives predominantly luminance inputs. If the luminance processing via magnocellular pathway indeed contributes to perceptual abnormalities in schizophrenia, then one would expect that the luminance – advantage that we demonstrated in healthy participants during a

WM task will be affected in schizophrenia. I will now describe the research suggesting specific magnocellular impairment in the disorder.

To support the claim of impaired magnocellular processing in schizophrenia, a number of studies have shown that the processing of stimuli designed to preferentially stimulate magnocellular pathway appears to be impaired in the disorder (Butler et al., 2001, 2008; Butler & Javitt, 2005; Javitt, 2009a; Kim, Zemon, Saperstein, Butler, & Javitt, 2005; Antígona Martínez et al., 2008). One study (Butler et al., 2005) used a combination of EEG, psychophysics and behavioural measures to provide evidence for impaired magnocellular function. In respect to the EEG, this study has used a steady state visual-evoked potential method (ssVEP). This method allows for isolation of stimulus-related EEG signal by extracting activity constrained only to frequency range at which the stimulus is continuously modulated (Butler & Javitt, 2005). The luminance contrast was manipulated to differentially engage magno and parvocellular pathways. Their study took advantage of the fact that magnocellular pathway is most sensitive to low-frequency stimuli and it saturates at higher contrast levels, while the parvocellular response does not saturate (Tootell, Hamilton, et al., 1988; Tootell, Silverman, et al., 1988). Hence, presenting stimuli at different spatial frequency and contrasts can be used to study the differential contribution of these two pathways in perceptual processing in schizophrenia (Butler et al., 2001). Thus, to isolate magnocellular response, Butler et al. (2005) used a low frequency, low contrast stimuli. On the other hand, for the parvo-biased condition, stimulus contrast was manipulated around a high contrast level (a contrast “pedestal”), which is meant to saturate magnocellular response and thus isolate parvocellular responses. The results showed that the evoked potentials recorded from individuals with schizophrenia in response to magno-biased stimuli were significantly reduced when compared to responses elicited by parvo-biased stimuli. This was not the case in the control group. In terms of behavioural responses, the researchers have biased processing of the stimuli to the magnocellular pathway by manipulating spatial frequency and contrast of the stimuli. Butler et al. (2005) analysed contrast gain in both groups (among other measures). As expected, the magnocellular contrast gain response was

characterised by an initial steep increase, reaching a saturation point at higher contrast levels (Tootell, Hamilton, et al., 1988; Tootell, Silverman, et al., 1988). This was true for both groups. However, the schizophrenia group was characterised by a shallower slope of the contrast gain function compared to controls, indicating impairment in this domain.

These findings were further supported by later studies using VEPs to test magno-biased stimuli (Butler et al., 2007; Schechter et al., 2005). Butler et al. (2007) used high – density recordings while participants viewed stimuli of varying contrast in experiment one and sinusoidal gratings of varying spatial frequency in experiment 2. Contrast and spatial frequency were adapted so that stimuli would be magno or parvo-biased (see above). The authors looked at the amplitudes of the early visual components C1, P1 and N1. They found that the amplitude of these components was significantly reduced in response to magno-biased conditions in patients, but not in controls.

Other EEG studies have also suggested magno-specific impairment (Javitt, 2009b). The P1 component is thought to reflect mostly processing in the dorsal stream which receives predominantly magnocellular inputs (Livingstone & Hubel, 1988). Therefore, decreased P1 amplitude might be taken as an indirect evidence of magnocellular deficit. In line with this, studies showed reduced P1 response in patients compared to controls in object recognition (Doniger et al., 2002), WM tasks (Haenschel et al., 2007) and in response to line drawings (Foxye, Murray, & Javitt, 2005; Foxye & Simpson, 2002; Foxye et al., 2001; Foxye et al., 2008). Similar evidence came from the non-clinical population, e.g. with people who are at increased risk of schizophrenia (i.e. first-degree relatives of diagnosed individuals; Yeap et al., 2006). Furthermore, individuals with a variation of dysbindin gene (associated with increased risk of developing schizophrenia; Norton, Williams, & Owen, 2006) also demonstrate reduced P1 component (Donohoe et al., 2008).

Another suggestion that the functionally-defined magnocellular pathway is impaired in schizophrenia can be inferred from the effects of NMDA antagonists on V1 and LGN (Javitt, 2009b). In the 1950's – 60's, it was observed that a (then

newly discovered) chemical compound phencyclidine (PCP, known also as the “angel dust”), as well as ketamine, induce symptoms that resemble both positive and negative symptoms of schizophrenia. Both compounds work by acting as NMDA antagonists. As Javitt (2009a) points out in his review, NMDA receptors mediate non-linear gain, which is characteristic for magnocellular neurons. More specifically, magnocellular neurons are characterised by a nonlinear contrast response – they start firing at low contrast levels but saturate at higher contrast levels. Infusion of NMDA receptor antagonist into primary visual area V1 affect this nonlinearity. On the other hand, NMDA antagonists infused into the LGN affects the firing of neurons that are likely to be responsible for mediating motion detection, thought to be carried by magnocellular neurons as well. In short, NMDA seems to affect responses of neurons linked to magnocellular functions (Javitt, 2009b). Interestingly, these observations led to a development of an alternative hypothesis to the well – known and dominant model of schizophrenia which suggested a hyperactivity of dopamine systems contributes to the development of the disorder (for a historical overview of the model, see Baumeister & Francis, 2002). This alternative model proposed that symptoms of schizophrenia are related to dysfunction of NMDA receptors in affected individuals rather than overactivity of dopamine systems as such (Javitt & Zukin, 1991). In line with that, the observation that contrast gain function is affected in schizophrenia (for example, Butler et al., 2005, described earlier) might be thus accounted for by the NMDA dysfunction.

To summarise, low-level perceptual deficits have been widely researched in the past. The magnocellular theory of schizophrenia attempts to systemise these deficits and provide a link between them. However, the theory has been met with some criticism (Skottun & Skoyles, 2008a). In the next session, a brief criticism of the magnocellular account will be provided and I will try to specify how our hypothesis fits into the magnocellular deficit narrative, and how it relates to the criticisms that have been put forward.

25.4. Investigating luminance – processing in schizophrenia in the context of magnocellular theory and its criticism

The question whether we can speak of a specific magnocellular deficit in schizophrenia is still (often fiercely) debated. In particular, Skottun and colleagues (Skottun, 2013; Skottun & Skoyles, 2008b; Skottun & Skoyles, 2011) raise concerns whether the stimuli used in previous studies can separate magno and parvocellular responses using variations in contrast and spatial frequency. While others disagree with such criticism (Kéri, 2008; Kéri & Benedek, 2007), the discussion seems to be ongoing (Skottun & Skoyles, 2008a, 2013). The design of our study can overcome these concerns, however, as it is not relying on the spatial frequency or contrast levels to engage luminance processing (which in turn maps onto magnocellular pathway). Rather, our stimuli are defined using the DKL colour space, which allows one to create stimuli that excite post-receptoral mechanisms of interest (Derrington et al., 1984).

On the other hand, while not directly critical of the magnocellular hypothesis in schizophrenia as such, researchers are suggesting a more generalised visual deficit. Such explanation would account for magnocellular-specific impairments, without making strong assumptions about an impairment constrained to magnocellular functioning (Yoon, Sheremata, Rokem, & Silver, 2013). A similar view is also adopted by Skottun & Skoyles (2013), who argue that a general deficit related to diminished attention and medication effects accounts for the apparent magnocellular dysfunction.

It is important to note that a magnocellular deficit does not imply that neurons that form the magnocellular pathway are lost, which the critics of magnocellular impairments in schizophrenia assume should be the case (Skottun & Skoyles, 2008a). The deficit is related to their function, rather than anatomy¹⁰. Indeed, a

¹⁰ Interestingly, some anatomical changes in schizophrenia patients related to visual processing have been suggested to exist, but at the earlier, retinal level (Silverstein & Rosen, 2015). However, there is currently very little direct evidence for these changes, and the research on the topic is ongoing.

post-mortem study of a schizophrenia brain revealed no such loss in the LGN (Selemon & Begovic, 2007). Further, although the deficit seems to be related mostly to the magnocellular pathway, some studies have shown that impairments in the parvocellular pathway are also present (Butler & Javitt, 2005; Javitt, 2009a).

It is perhaps important to note that throughout our study, the stimuli were designed to specifically target post-receptoral mechanisms, namely chromatic and luminance mechanisms. It is well documented that magnocellular pathway takes luminance inputs preferentially. It is, therefore, reasonable to interpret our studies as supporting the magnocellular theory of schizophrenia, although the author of this thesis believes that it is possible to make claims about preferential luminance inputs without making strong arguments for or against the magnocellular theory of schizophrenia; indeed, the critics of the magnocellular theory of schizophrenia take a similar stand while discussing visual search studies that use magno-biased stimuli (Skottun & Skoyles, 2008b).

Moreover, such bottom-up accounts of the disorder are not the only explanations that have been put forward. The next session will outline top-down accounts of some of the deficits in schizophrenia. I will also specify how – and why – investigating luminance processing in the disorder can also inform top-down accounts (in addition to bottom-up ones).

25.5. Top-down accounts of perceptual deficits in schizophrenia and the potential role of luminance signals

Other accounts of perceptual deficits in schizophrenia emphasize the role of top-down in addition bottom-up processing (Dima, Dietrich, Dillo, & Emrich, 2010; Silverstein et al., 2006). For example, Dima et al. used dynamic causal modelling of fMRI (Dima et al., 2009) as well as ERP (Dima et al., 2010) to explain the observation that patients are less prone to some visual illusions, including the hollow mask illusion (Gregory, 1973). In the hollow mask illusion, healthy observers perceive features of a concave mask as convex, while individuals with schizophrenia appear to be less susceptible to this illusion (Emrich, Leweke, & Schneider, 1997; Schneider et al., 2002; Schneider, Leweke, Sternemann, Weber, & Emrich, 1996). In healthy controls, it is the top-down signals that are suspected to be responsible for the illusion. Dima et al. (2009, 2010) demonstrated that in schizophrenia top-down processing might be impaired, while the bottom-up processing is strengthened, thus leading to “correct” perception of the illusion.

Some studies have suggested that perceptual processing is not different in patients and in controls. For example, one study failed to find differences between patients and controls in early visual components during various tasks (van der Stelt et al., 2004). More specifically, using a visual as well as auditory oddball task, van der Stelt et al. (2004) found that patient and control group did not differ significantly in terms of the visual P1 and N1 components (and auditory P2) in response to visual stimuli paired with auditory distractors. They did find, however, differences in the P3 component, which occurs much later than the P1 and is indicative of cognitive rather than low-level sensory processing. The authors thus argued that, while low-level vision (and hearing) are unimpaired, abnormalities in schizophrenia can be explained by general attentional deficits. Another study (Oribe et al., 2015) looked at both early and late visual ERPs in the first episode schizophrenia with a one-year follow-up. The study found reduced P3 in patients compared to controls at both time points; interestingly, P3 was the only component to show a reduction at follow-up. N2 also had reduced

amplitude, though with no sign of reduction at a follow-up; additionally, N1 latency was also delayed compared to controls at both time points. The authors also note that the P1 component appeared to be somewhat reduced at both times, although this effect was not statistically significant.

The results cited above go in line with accounts emphasizing the role of top-down effects on vision in schizophrenia. However, reduced P1 amplitude does not necessarily go against the top-down account of deficits. As outlined in the previous chapter, the P1 component is also sensitive to high-level processing, such as attention. In fact, some studies (Zanto et al., 2011) showed that disrupting the prefrontal cortex using TMS during a WM task not only diminished performance but also reduced the P1 amplitude during stimulus processing. Gazzaley (2011) further suggested that early top-down, attentional modulation impacts WM performance; importantly, they suggested that such modulation must be initiated early enough in order to facilitate WM processing. Fast luminance signals seem to be a good candidate to provide such head-start. As suggested by (Bar, 2003; Kveraga et al., 2007), object recognition is enhanced thanks to fast luminance projections reaching frontal areas, which provide a trigger for top-down modulation, leading to improved performance. Therefore, luminance signals have the potential to impact both bottom-up and top-down processing during WM in schizophrenia. Regardless of which one it is, one can expect that WM processing will not benefit from luminance, as it did for healthy participants in our previous study.

25.6. Summary and aims

In the previous study (see Chapter 3), the luminance benefit was manifested in increased behavioural accuracy in a delayed match-to-sample working memory task. The results showed evidence for perception-working memory interaction mediated by luminance signals. This conclusion was derived from the finding that decreased performance associated with increasing working memory load was less severe when participants remembered luminance-defined, as opposed to isoluminant-chromatic stimuli. The ERP results suggested that luminance

influences working memory processing at early encoding stages. Additionally, luminance signals seemed to also benefit memory-probe comparison at later stages as well, which was reflected in the fact that luminance – advantage was present in conditions where the probe mismatched remembered shapes.

The main aim of the current experiment was to examine whether luminance processing is predominantly impaired in schizophrenia. Based on previous research suggesting early visual deficits (e.g. Javitt, 2009a; Silverstein et al., 2015) and their magnocellular deficit account (Kéri & Benedek, 2007), we predict that the luminance benefit will not be apparent in the behavioural data. More specifically, we do not expect to find that, at higher WM load levels, luminance-defined stimuli will elicit better performance than isoluminant stimuli for patients. In this case, one would expect a general reduction in accuracy across all DKL directions compared to controls, not specific to encoding luminance-defined shapes.

An alternative prediction would be that luminance processing is not affected in schizophrenia and the luminance benefit is preserved despite the overall decrease in accuracy. While it would go against our predictions regarding altered luminance processing in schizophrenia, it would further strengthen our previous finding that luminance leads to better WM encoding by showing that this is not restricted only to healthy participants.

In terms of ERP responses, we expect a reduction of ERPs during early stimulus encoding, i.e. the P1 component. (Haenschel et al., 2007). In their study, Haenschel et al. found that while there were group differences in the early visual components, this was not the case for the family of P3 components (P3a, P3b). Other studies did show that the P3 component is affected in schizophrenia (Oribe et al., 2015). However, we expected to demonstrate a similar pattern as in Haenschel et al. (2007), as we are using the same task design.

Similarly, as in the previous experiment, another aim of the current study is to determine whether the load-related modulation of the early visual components (P1 for luminance, and N1 for isoluminant stimuli) will be present.

We also measured contrast sensitivity to luminance stimuli, and colour sensitivity thresholds using CAD and AcuityPlus (Barbur, Rodriguez-Carmona & Harlow, 2006), the same as in previous experiments (see Chapters 3 and 4). We expect to find reduced contrast sensitivity in patients compared to controls, a pattern that would be indicative of impaired luminance processing. A previous study (Cadenhead, Dobkins, McGovern, & Shafer, 2013) also looked at contrast sensitivity in patients and controls. Participants were presented with chromatic and luminance stimuli in a 2-alternative forced choice task. They found that patients demonstrated lower contrast sensitivity compared to controls. However, the finding was not specific to luminance stimuli, as it also occurred for the chromatic stimuli. On the other hand, another study (Butler et al., 2005) showed impaired contrast gain as well as lower contrast sensitivity in patients compared to controls. By using a standardized luminance and chromatic contrast sensitivity tests, we aimed to verify these results. We expected that patients will show a reduced functional contrast sensitivity, but their colour thresholds will remain within typical levels.

An additional aim of the current study was to replicate results demonstrated in our previous studies, in particular supporting the general conclusion that luminance inputs are beneficial to WM encoding and performance on visual WM tasks (see Chapters 3 and 4). We thus expected that the luminance benefit will be manifested especially at higher working memory loads, and at mismatch condition. Moreover, we were expecting to find an ERP evidence for a luminance-working memory interaction at encoding stage of working memory.

Lastly, we introduced some changes to the study design used in the previous experiment, in order to adapt the study for testing with the patient population by reducing the testing time. Details of the applied changes are highlighted in the methods section below.

26. Methods

26.1. Participants

Patients were recruited from the East London NHS Trust, following NHS ethics approval. Initially, 21 participants were recruited. Three (two patients and one control) were rejected as they did not meet the colour test criteria and were suspected to have colour vision deficiency (see Result subsection 27.1, Vision Tests). This left 18 participants in total used in the behavioural data analysis.

For the ERP analysis, further two participants (one control and one patient) were rejected due to noisy EEG data, i.e. there was an insufficient amount of trials left after the artifact rejection procedure. Hence, 16 participants were analysed in the ERP analysis across two groups (8 patients and 8 controls).

Controls were recruited through adverts in shops local to the university and through word of mouth. Controls and patients were matched in terms of age and educational level. Mean age of patients and controls was 26 and 28.44 years old, respectively. The education level was coded from 1 (lowest educational level) to 4 (highest educational level) and was 3.1 for control and 2.6 for schizophrenia group, on average. See Table 13 for coding key and age/educational level summary for both groups and for a summary of patient and control details.

Table B3 Coding of educational level (A) and a summary of age/qualifications for control (B) and schizophrenia (C) group.

A) Assigned qualification values

Value	Last obtained qualification
1	Disploma
2	GCSE/SATS/GNVQ
3	College/high school
4	Bsc/Post-graduate training

B) Control group

N	Age	Education code	Education level
1	31	4	Bsc
2	34	3	College Level
3	36	4	Bsc
4	25	4	Training
5	26	2	High School
6	25	2	High School
7	28	3	College
8	26	3	College
9	25	3	College
Average:		28.4	3.1

C) Schizophrenia group

N	Age	Education code	Education level
1	33	2	GCES (left at age 16)
2	41	2	GCSE (left at age 18)
3	28	1	diploma (left at age 16)
4	38	2	GNVQ (left at age 19)
5	27	4	Bsc (left age 21)
6	40	4	Bsc (left age 25)
7	31	4	Bsc (left age 21)
8	26	4	Bsc (left age 21)
9	38	2	GVNQ (left age 17)
10	55	1	school-level (left age 16)
Average:		35.7	2.6

26.2. Procedure

The experimental design of the previous experiment was modified to decrease the length of the experiment so that it is better suited for use in a clinical population. The previous experiment could take around 9h to complete over two experimental sessions. We aimed to decrease the testing time so that our hypotheses could be tested in one experimental session lasting around 4h. In order to do that, we decided to drop some of the experimental conditions – refer to the methods section below for details. One of the major changes concerned the use of averaged discrimination thresholds obtained in the previous experiment, rather than estimating thresholds for each individual (again, details on the procedure can be found in the methods section). A secondary aim of this pilot study is to verify whether these changes are not negatively impacting conclusions that can be derived from the results.

Prior to being invited to the laboratory, patients were screened on a variety of measures in day care centres. These included The Manchester Short Assessment of Quality of Life (MANSA), Social Contact Assessment, Edinburgh Handedness Inventory, as well as the digit span and letter-number test.

The rest of the experimental procedures were identical for patients and controls and were conducted in a single session (on a separate day to the screening measures in case of patients). Due to time constraints and to avoid excessive fatigue, some participants performed the vision tests also on a separate day.

The experimental procedure shared the experimental setup and equipment as in the ERP experiment (see Chapter 2: general methods and Chapter 3). The difference between the current task and the previous experiment was the number of conditions and abandonment of the discrimination procedure. These will be described in more detail below.

26.3. Averaged thresholds and Weber contrasts

The difference between the current experiment and the previous experiment (see Chapter 3) was that here participants did not perform the HCFP tests and discrimination threshold tests and went straight to working memory task. In an attempt to maintain equal saliency between DKL conditions, we have used averaged thresholds from the ERP experiment ($N = 22$; see Chapter 3). It was assumed that the average thresholds would be sufficient to achieve that. The main rationale was to significantly reduce overall testing time to avoid excessive fatigue and accommodate patients.

We averaged scaled thresholds in the low contrast conditions and high contrast conditions, obtaining a value for each DKL direction at low and high contrast levels. Similarly, we used averaged luminance elevation for L – M and S-cone condition obtained through the HCFP task in the ERP experiment (for task design, timings and implementation, see Chapter 3). Although the final sample size in the previous experiment was 22, for the averaged thresholds we only used participants that were tested on the same display calibration, i.e. 19 (as outlined in Chapter 3, three participants completed the experiment under different display calibration).

Table 14 shows individual thresholds as well as averaged values that were used in the current experiment. Weber contrasts of the averaged thresholds are provided in Table 15.

Table 14 Individual discrimination thresholds for all DKL directions obtained in the previous experiment (see Chapter 3). Averaged thresholds used in the current study are at the bottom of the table

N	L-M elevation	S cone elevation	low S cone	low L-M	low Lum	high S cone	high L-M	high Lum
1	-11.40	1.20	0.06	0.01	0.05	0.13	0.01	0.11
2	-20.75	2.50	0.12	0.01	0.05	0.24	0.02	0.11
3	-8.00	3.80	0.12	0.01	0.05	0.23	0.02	0.11
4	-15.00	0.75	0.07	0.01	0.05	0.14	0.02	0.11
5	-6.75	-0.25	0.08	0.01	0.05	0.16	0.01	0.11
6	-27.75	2.00	0.07	0.01	0.05	0.14	0.02	0.11
7	-23.75	-0.25	0.11	0.01	0.05	0.22	0.02	0.11
8	-17.43	1.43	0.09	0.01	0.05	0.18	0.02	0.11
9	-29.43	1.75	0.07	0.01	0.05	0.13	0.02	0.11
10	-35.00	0.60	0.09	0.01	0.05	0.18	0.03	0.11
11	-34.25	3.71	0.15	0.01	0.05	0.30	0.03	0.11
12	-5.25	2.44	0.06	0.01	0.05	0.12	0.01	0.11
13	-38.44	4.22	0.11	0.01	0.05	0.22	0.02	0.11
14	-33.75	0.25	0.08	0.01	0.05	0.17	0.02	0.11
15	-22.86	2.00	0.10	0.01	0.05	0.21	0.02	0.11
16	-20.25	3.00	0.11	0.01	0.05	0.22	0.02	0.11
17	-10.00	1.40	0.08	0.01	0.05	0.17	0.01	0.11
18	-2.50	-2.20	0.10	0.01	0.05	0.20	0.02	0.11
19	-19.25	2.29	0.10	0.01	0.05	0.19	0.02	0.11
Averaged radius	-20.09519632	1.612907268	0.09	0.01	0.05	0.19	0.02	0.11
	L-M elevation	S cone elevation	low S cone	low L-M	low Lum	high S cone	high L-M	high Lum

Table 15 Weber contrast values for all post-receptoral mechanisms tested in the experiment, based on averaged thresholds.

	Low contrast	High contrast
S-cone (S-[L+M])	0.18	0.37
L - M	0.03	0.05
Luminance (L+M)	0.10	0.19

26.4. Task design

The same task design was used as in Experiment 1, i.e. the delayed match-to-sample task. Refer to Chapter 3 for details.

In contrast to the previous experiment (see Chapter 3), we dropped several conditions in order to make the study shorter and more suited for the clinical population. In particular, we decided to drop load 2 condition (see Table 16). The inclusion of three load levels allowed us to demonstrate a mostly linear decline of performance with increasing WM load. This time we are focusing on DKL effects

on low (one item to memorize) versus high WM load (three items to memorize). Since the previous study suggested that differences between DKL conditions are most pronounced at load 3, we decided that we can drop load 2 condition to increase the number of trials and shorten the study length while still being able to look at DKL-specific effects at high WM loads.

Table 16 Conditions in the current study.

	Load 1	Load 3	
DKL condition	1. S cone	7. S cone	Low contrast
	2. L-M	8. L-M	
	3. Luminance	9. Luminance	
DKL condition	4. S cone	10. S cone	High contrast
	5. L-M	11. L-M	
	6. Luminance	12. Luminance	
	Load 1	Load 3	

26.5. EEG data acquisition, pre-processing and analysis

EEG data were acquired using a 64-channel ActiCap, with an in-built reference electrode at location FCz. FT7 electrode was placed below participant’s left eye and served as a vertical ocular electrode. Recording and digitization were performed using a BrainAmp amplifier and the BrainVision Recorder software (Brain Products, Munich, Germany). The EEG was recorded at a 1000Hz sampling rate with an on-line bandpass filter between 0.1 and 1000 Hz.

Data were pre-processed using Brain Vision Analyzer software (Brain Products, Germany). Further data analysis, including averaging, was done using custom routines as well as functions from EEGLAB (Delorme & Makeig, 2004) and FieldTrip (Oostenveld et al., 2011) toolboxes developed for Matlab (Mathworks, Natick, Massachusetts), incorporated into custom scripts.

We applied the following pre-processing steps:

Step 1: Data were filtered with a low-pass filter (0.01 Hz) to remove low-frequency drifts.

Step 2: Noisy electrodes were interpolated.

Step 3: An ocular correction was performed using ICA algorithm (Infomax Restricted).

Step 4: The data were re-referenced to an average of all electrodes.

Step 5: Continuous EEG data was segmented into epochs. Epochs ranged from -100 ms before stimulus onset and to 600 ms for analysis of encoding stage; longer epochs were used for the maintenance stage (-100 ms to 1700 ms); shorter epochs were again used for the retrieval stage (-100 ms to 600 ms). We chose not to use longer epochs for the encoding stage to increase the number of trials available for analysis; extracting longer epochs results in the decreased amount of trials due to artifacts occurring after 600 ms.

Epochs were time-locked to the onset of the last item in the memory array (i.e. single item for load 1, second item from the two presented for load 2 and third item from the three presented for load 3).

Step 6: Baseline correction was applied (100 ms prior to stimulus onset)

Step 7: Automatic artifact rejection procedure was applied. Epochs were removed if they met the following criteria:

- The maximum voltage exceeded 100 μ V
- If the difference between maximum and minimum values in an epoch exceeded 100 μ V;
- If the gradient (i.e. voltage step) exceeded 30 μ V.
- If the activity was below 0.5 μ V for at least 50 ms.

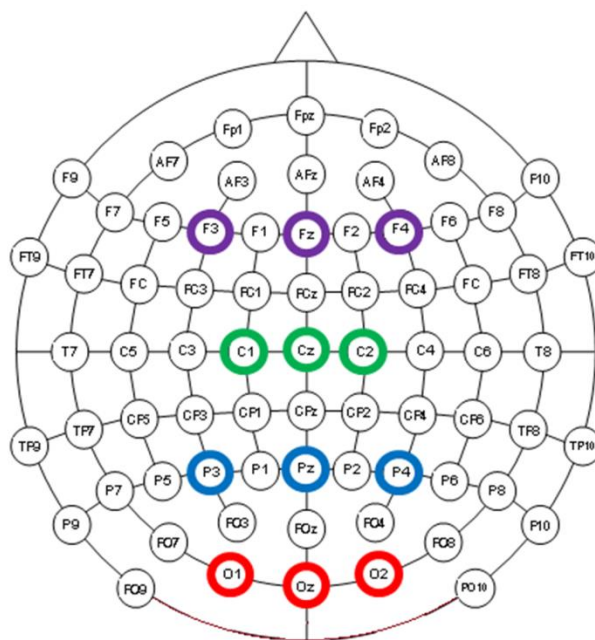
Step 8: Pre-processed data was exported to MATLAB and further processing/data analysis was done using EEGLAB and FieldTrip routines. These are outlined below.

Peak ERP component amplitudes were extracted from the predefined time intervals within the epochs. Details on extracting peak amplitudes are provided

in Chapter 3. For the slow wave, mean amplitude was extracted, rather than local peak. Statistical analysis was performed using SPSS. Local (or mean) amplitudes for each component were analysed using a mixed ANOVA with between-subject factor (group: control or patient group), and the following within-subject factors: contrast level (2 levels: low and high contrast), electrode location (2 lateral electrodes plus 1 central electrode, specified in each section) and WM load (2 levels: Load 1 and Load 3). Greenhouse-Geisser corrections were applied where necessary.

Table 17 Analysed ERP components, electrode sites and time intervals used to define and extract components. The map at the bottom shows electrode setup used in the experiment, with electrodes of interest marked with coloured circles.

ERP component	Time interval	Electrodes	
P1	80 – 160 ms	O1, Oz, O2	○
N1	130 – 300 ms	O1, Oz, O2	○
P3a	200 – 400 ms	C1, Cz, C2	○
P3b	200 – 500 ms	P3, Pz, P4	○
Slow wave (occipital)	1000 – 1600 ms	O1, Oz, O2	○



ERP components and time intervals used for peak extraction in this study were the same as in Experiment 1 (see Chapter 3) and are summarised in Table 17 above. We decided not to include the negative peak occurring at the stimulus offset and the frontal slow wave in the current analysis, as both were not informative in terms of the tested hypotheses in the previous experiment (see Chapter 3).

26.6. Vision tests and behavioural data analysis

We compared the red-green and yellow-blue colour contrast thresholds (as measured by CAD), as well as visual acuity and functional contrast sensitivity (measured using Acuity+) between the groups using a between-subject one way ANOVA.

Accuracy (defined as proportion of correct answers) and reaction times were analysed using a mixed ANOVA with between-subject factor (group: control or patient group), and the following within-subject factors: contrast level (2 levels: low and high contrast), DKL direction (3 levels: Luminance, isoluminant L – M, isoluminant S-cone), WM load (2 levels: Load 1 and Load 3) and probe type (2 levels: match or mismatch). Greenhouse-Geisser corrections were applied where necessary.

27. Behavioural results

27.1. Vision tests

Results of the vision tests are summarised in the figure below. Based on the CAD, we excluded six participants (including three patients) due to deficient colour vision. These participants did not take part in further tests and were discharged after the vision tests were completed.

There was a significant difference between controls and patients in terms of acuity, as measured with luminance-increment stimuli ($F(1,12)=5.95$, $p=.033$, $\eta^2=.35$). See Figure 46 for the summary of results for both groups.

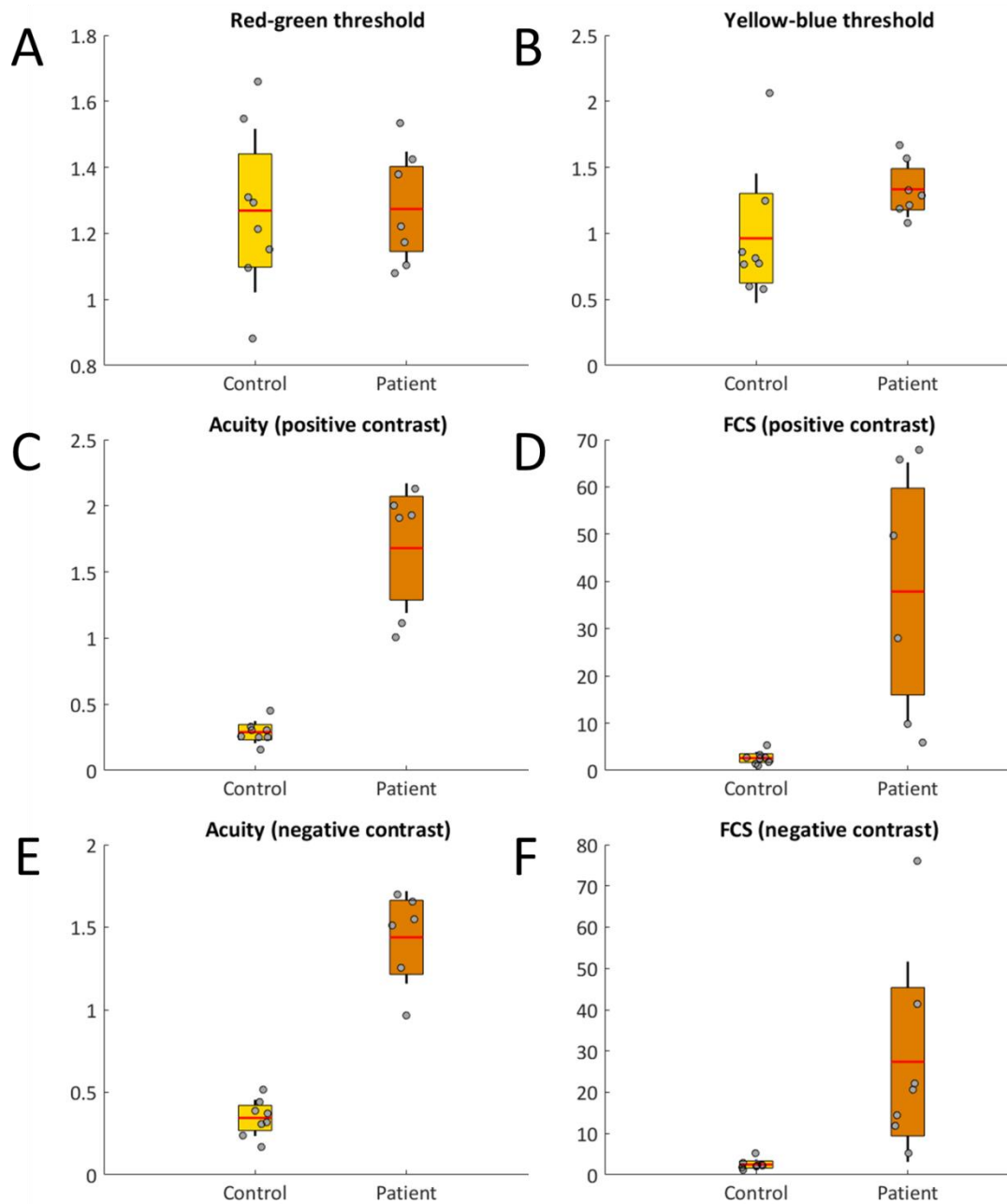


Figure 46 Results of the vision tests for patients and controls shown in box plots. Each dot represents contrast threshold value for an individual participant. Red line in the middle represents the mean, red shading is the 95% confidence interval, and blue shading is 1 standard deviation. A) red-green colour threshold B) yellow – blue threshold C) Acuity (increment, or positive contrast) D)Functional contrast sensitivity (increment, or positive contrast) E) Acuity (decrement, or negative contrast) F)Functional contrast sensitivity (decrement, or negative contrast).

27.2. Accuracy

27.2.1. Between-subject effects

Overall controls outperformed patients ($F(1, 16)=8.25$, $p=.011$, $\eta^2=.34$; see Figure 47 below). Load and DKL factors did not interact with group type.

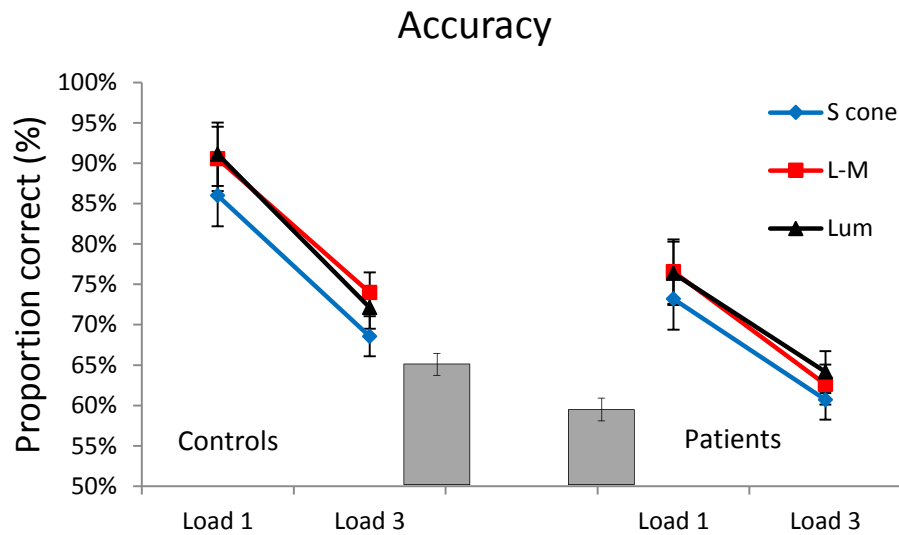


Figure 47 Overall mean accuracy for control and patient group (middle bar graph), and control/patient group mean accuracy shown at WM load 1 and load 3, separately for DKL directions (line graphs). Patients performed worse than controls on average, though group type did not interact with other factors. Error bars represent standard error of the mean.

27.2.2. Within-subject effects

There was a main effect of DKL direction ($F(2, 32)=11.8$, $p<.001$, $\eta^2=.42$); post-hoc Bonferroni-corrected tests indicated that responses to luminance and L – M shapes were more accurate than to S-cone shapes (difference significant at $p=.003$ for Lum/S-cone and $p=.001$ for L – M/S-cone).

We found higher accuracy for load 1 than load 3 ($F(1, 16)=64.2$, $p<.001$, $\eta^2=.80$) as well as higher accuracy for high contrast than low contrast shapes ($F(1, 16)=12.0$, $p=.003$, $\eta^2=.43$).

There was a significant three-way interaction between probe type (match/mismatch), load and DKL direction ($F(2, 32)=5.64$, $p=.008$, $\eta^2=.26$).

We conducted three separate ANOVAs (probe type x contrast x load x group) for each DKL direction to account for this interaction.

Patients demonstrated lower accuracy than controls at each DKL direction (significant effect of group for S-cone: $F(1,16)=7.09$, $p=.017$, $\eta^2=.31$; L - M: $F(1,16)=8.92$, $p=.009$, $\eta^2=.36$; Luminance: $F(1,16)=7.19$, $p=.016$, $\eta^2=.31$).

Additionally, accuracy dropped with increased WM load for each DKL direction (main effects of Load for S-cone: $F(1,16)=40.3$, $p<.001$, $\eta^2=.72$; L - M: $F(1,16)=58.3$, $p<.001$, $\eta^2=.78$; Luminance: $F(1,16)=56.7$, $p<.001$, $\eta^2=.78$). While S-cone and luminance accuracy did not differ significantly for low and high contrast condition, the difference was significant for L - M, with participants performing better at high contrast level (main effect of contrast: $F(1,16)=5.12$, $p=.038$, $\eta^2=.24$).

Interestingly, an interaction between probe type and WM Load was significant for L - M direction ($F(1,16)=5.48$, $p=.032$, $\eta^2=.25$) and Luminance ($F(1,16)=6.51$, $p=.021$, $\eta^2=.29$), but not for S-cone ($F(1,16)=.108$, $p=.747$, $\eta^2=.007$, n.s.). Post-hoc tests using Bonferroni correction did not point to significant differences that could explain this interaction; however, visual inspection of the data suggests that for S-cone performance decreased with load for match and mismatch equally, while for L - M and Luminance the decrease was sharper for match condition (see Figure 48 and Figure 49). Also of note is apparent lack of difference between match and mismatch accuracy data in patients, although (as noted above), the group by probe type interaction was not significant.

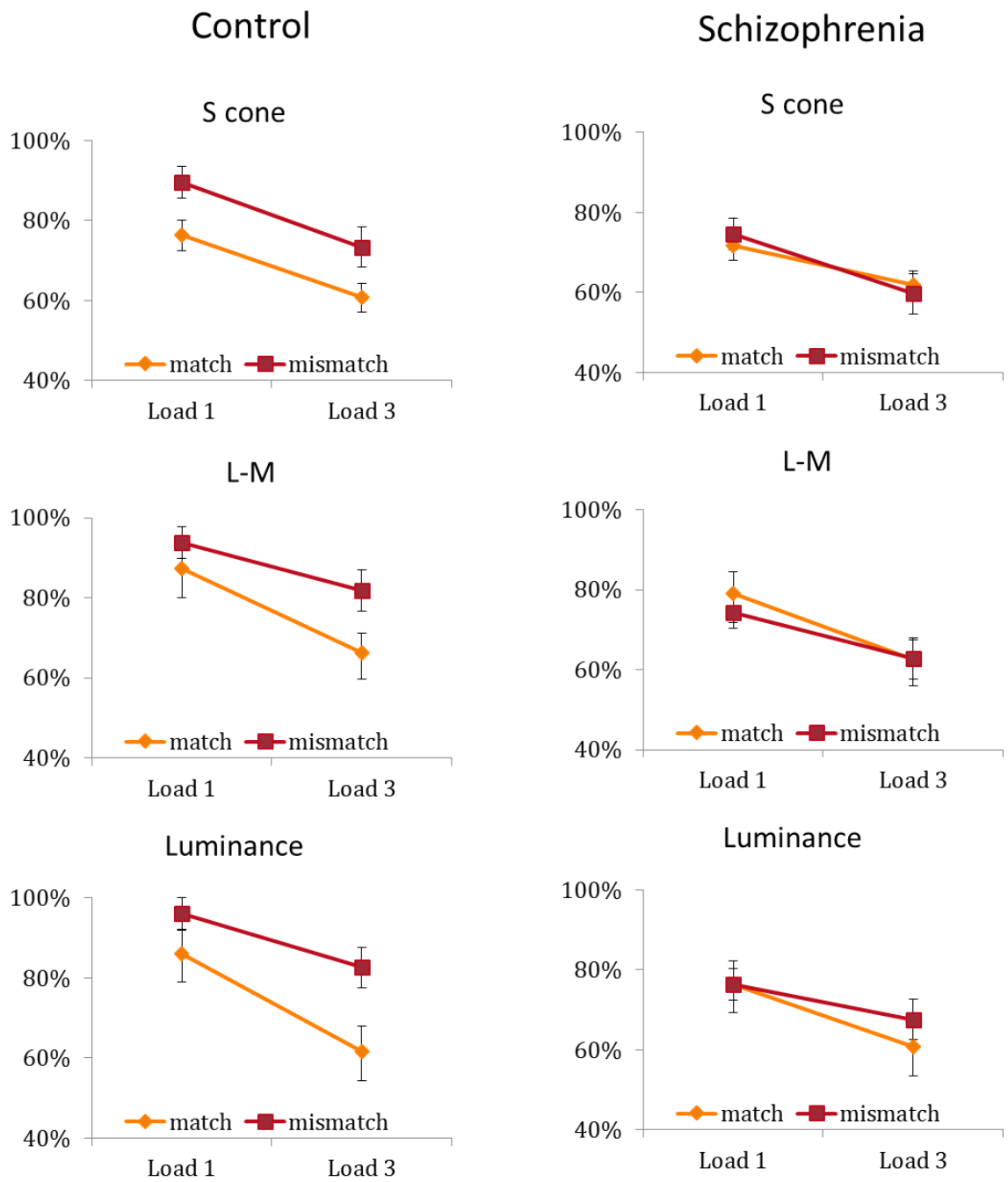


Figure 48 Accuracy at load 1 and load 3 for matching and mismatching memory probe, shown for each DKL direction and control/patient group separately. Error bars represent standard error of the mean.

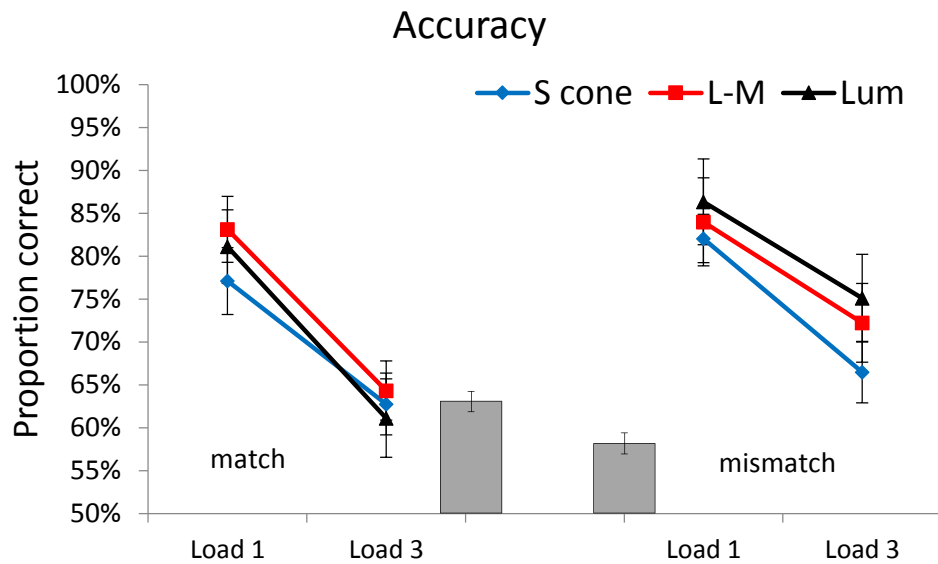


Figure 49 Overall match & mismatch accuracy (patients + controls) for the different DKL directions at low and high WM load. The bar graph in the middle shows an average of match (left) and mismatch (right). Error bars represent standard error of the mean.

27.3. Reaction times

27.3.1. Between-subject effects

Overall reaction times did not differ significantly between control and the patient group ($F(1,15)=97.7$, $p=.214$, $\eta^2=.10$, n.s.; see Figure 50).

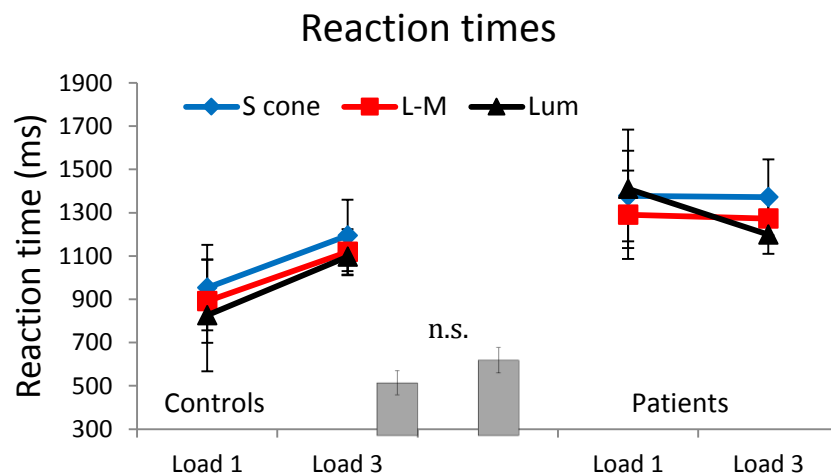


Figure 50 Overall reaction times for control and patient group (middle bar graph), and control/patient group reaction times are shown at WM load 1 and load 3, separately for DKL directions (line graphs). RTs did not differ significantly between the groups and there were no group interactions with other conditions. Error bars represent standard error of the mean.

27.3.2. Within-subject effects

There was a main effect of DKL condition ($F(2, 30)=5.56, p=.009, \eta^2=.27$).

Responses to S-cone stimuli were slower than L – M ($p=.045$) and Luminance stimuli ($p=.030$). L – M and luminance did not differ significantly (see Figure 51).

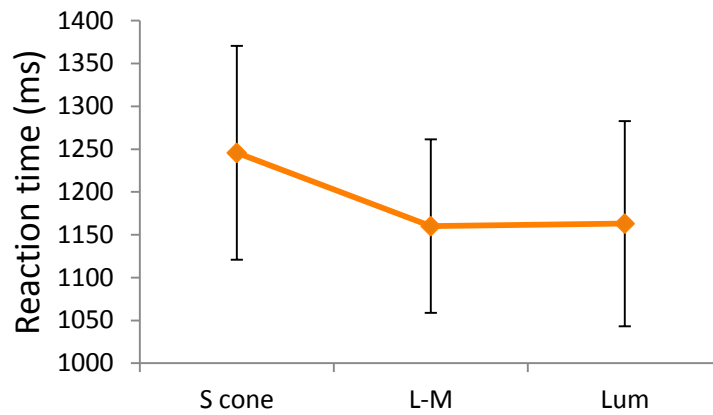


Figure 51 Reaction times for S-cone, L – M and Luminance conditions. Error bars represent standard error of the mean.

An interaction between probe type and WM load was not significant

($F(1,15)=4.42, p=.053, \eta^2=.29, n.s.$). Responses to high contrast stimuli were faster

($F(1,15)=9.97, p=.007, \eta^2=.40$). Responses to matching probes were also on

average quicker ($F(1,15)=10.3, p=.006, \eta^2=.41$) than mismatching probes (see

Figure 52).

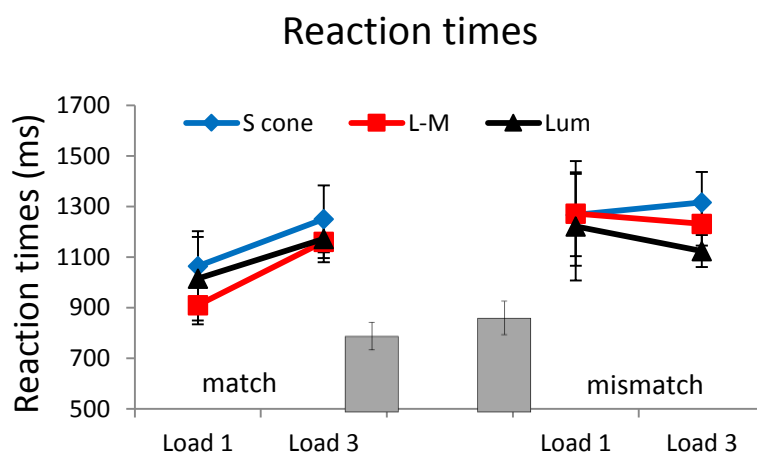


Figure 52 Overall match & mismatch reaction times (patients + controls; middle bar graph) and RTs for different DKL directions at low and high WM load for match and mismatch (red and left line graphs, respectively). Error bars represent standard error of the mean.

28. Event-related potential (ERP) results

After the pre-processing steps were complete, we compared the number of resulting trials for each condition and group (see Figure 53). This was done using a mixed ANOVA with between-subject factor (group) and the following within-subject factors: contrast (low/high), WM load (Load 1/Load 3) and DKL direction (S-cone/L - M/Luminance). We found that there were no significant differences between groups ($F(1, 14)=.592$, $p=.592$, $\eta^2=.04$, n.s.) or interactions with the group factor. A number of trials differed between WM load levels ($F(1, 14)=8.25$, $p=.012$, $\eta^2=.37$), with more trials for Load 1 condition (25.4 on average) than Load 3 (21 on average).

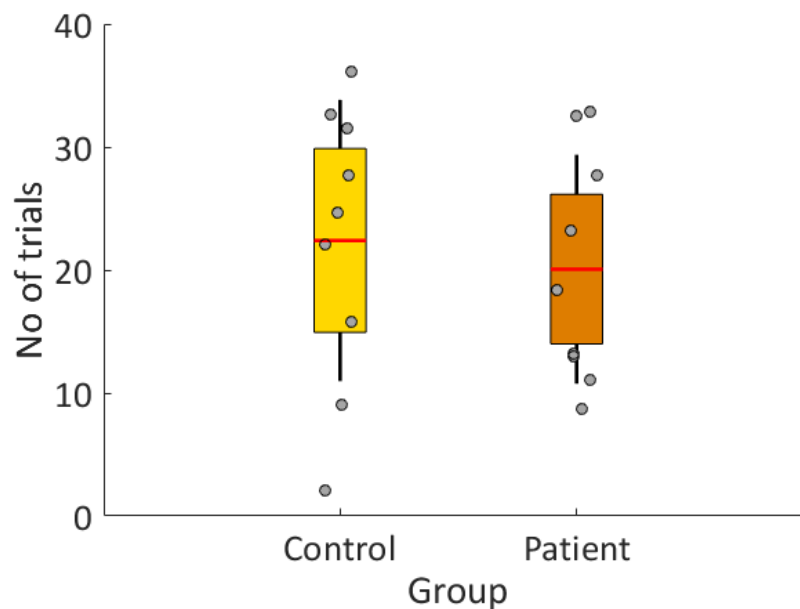


Figure 53 Comparison between the number of trials for patients and controls. Each dot represents average no of trials across all conditions for each individual participant. Red line in the middle represents the mean, red shading is the 95% confidence interval, and blue shading is 1 standard deviation.

28.1. Encoding stage

28.1.1. P1 Amplitude (Oz, O1, O2; 80-160 ms)

There was no significant effect of group ($F(1, 14)=2.38$, $p=.145$, $\eta^2=.14$, n.s.). A three-way interaction between contrast, electrode location and group was significant ($F(2, 28)=4.15$, $p=.026$, $\eta^2=.23$) as well as a three-way interaction between contrast, electrode location and WM load ($F(2, 28)=4.82$, $p=.016$, $\eta^2=.26$). To disentangle this interaction, we performed 2 mixed ANOVAs separately for each contrast level, with between-subject factor (controls vs patients) and the following within-subject factors: electrode location (O1, O2, Oz) and WM load (2 levels: Load 1 and Load 3).

28.1.2. Low contrast

At low contrast, there were no significant differences between patients and controls ($F(1, 14)=.338$, $p=.570$, $\eta^2=.02$, n.s.); there were no within-subject effects overall (see Figure 54). The averaged waveforms suggested that component P1 was largely attenuated in both groups compared to high contrast responses. We suggest that this is due to low signal-to-noise ratio in response to low contrast stimuli, a pattern observed in the previous experiment (see Chapter 3).

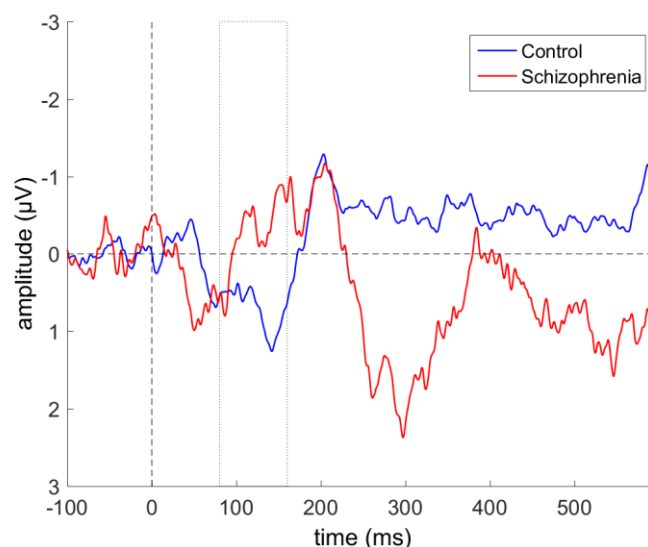


Figure 54 ERP waveforms during the encoding of low contrast luminance shapes are shown for control group (blue trace) and schizophrenia group (orange trace). The waveforms represent an

average over two WM loads and over three electrodes (O1, O2, Oz). Time 0 is the onset of the to-be-remembered stimulus. There were no differences in terms of P1 amplitude in the time – window of interest (80 ms – 160 ms)

28.1.3. High contrast

Overall, the P1 amplitude at high contrast was greater for controls than patients ($F(1, 14)=5.44, p=.035, \eta^2=.28$; see figure Figure 55).

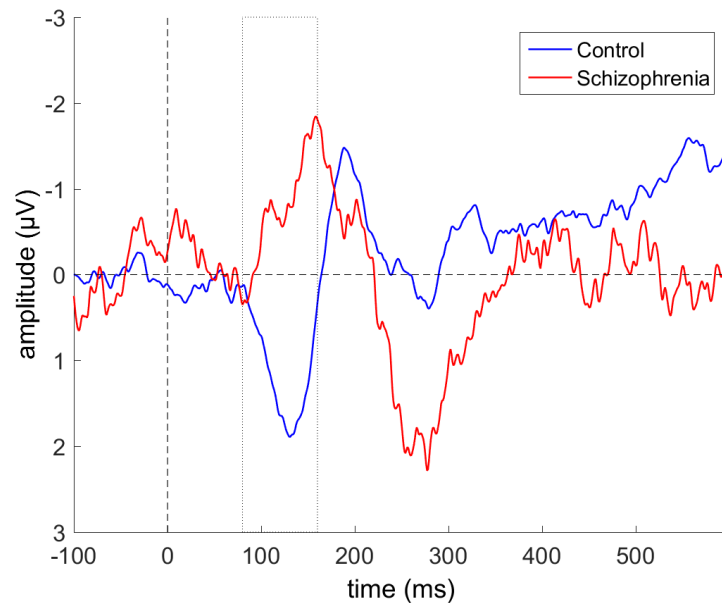


Figure 55 ERP waveforms during the encoding of high contrast luminance shapes are shown for control group (blue trace) and schizophrenia group (orange trace). The waveforms represent an average over two WM loads and over three electrodes (O1, O2, Oz). Time 0 is the onset of the to-be-remembered stimulus. P1 amplitude was greater for control group than patients.

There was a significant interaction between electrode locations and WM load ($F(2, 28)=3.57, p=.041, \eta^2=.20$). Post-hoc, Bonferroni-corrected tests indicated that P1 amplitude for load 3 encoding was greater than that for load 1 at electrode O2 ($p=.014$), which was not the case for electrode O1 ($p=.419, n.s.$) nor for the Oz ($p=.770, n.s.$).

There was no interaction between group and electrode location or WM load.

28.1.4. Latency

A separate repeated measures ANOVA was conducted for latency measures.

There was a significant three-way interaction between contrast level, electrode location and WM load ($F(2, 18)=6.73$, $p=.007$, $\eta^2=.43$). To understand this interaction, we performed 2 mixed ANOVAs separately for each contrast level, with between-subject factor (controls vs patients) and the following within-subject factors: electrode location (O1, O2, Oz) and WM load (2 levels: Load 1 and Load 3). There were no effects for high contrast reaction time data. At low contrast, an interaction between electrode location and WM load was significant ($F(2, 24)=3.73$, $p=.039$, $\eta^2=.24$). Post-hoc tests using Bonferroni correction did not point to significant comparisons, however, latencies tended to be somewhat shorter for load 1 than load 3 at electrode O2 ($p=.087$, n.s.).

28.2. N1 Amplitude (Oz, O1, O2; 130-300 ms)

There was no significant effect of group ($F(1, 14)=1.00$, $p=.333$, $\eta^2=.07$, n.s.). There was a main effect of DKL direction ($F(2, 28)=20.4$, $p=.018$, $\eta^2=.25$; see Figure 56 below). Post-hoc Bonferroni-corrected tests revealed that luminance shapes elicited lower N1 amplitude than L – M shapes ($p=.041$). The difference between luminance and S-cones was not significant ($p=.141$, n.s.).

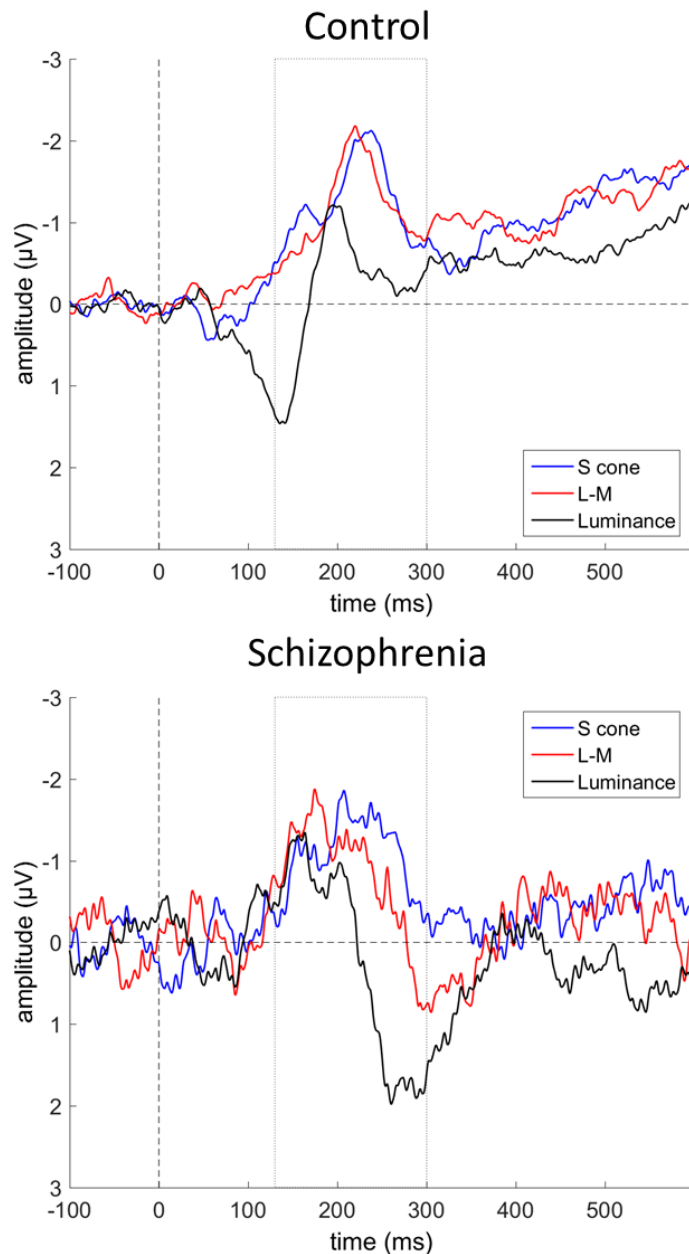


Figure 56 ERP waveforms during encoding of S-cone (blue trace), L – M (red trace) and luminance shapes (black trace). Waveforms were collapsed across WM load, contrast levels, electrode locations and groups to show a significant main effect of DKL direction.

A number of interactions involving contrast level was significant. There was an interaction between contrast level and electrode location ($F(2, 28)=4.03$, $p=.029$, $\eta^2=.22$) as well as an interaction between contrast and load was also significant ($F(2, 28)=5.00$, $p=.042$, $\eta^2=.26$). Further, a three-way interaction between contrast, electrode location and DKL was significant ($F(4, 56)=2.68$, $p=.041$, $\eta^2=.16$) as well as a four-way interaction between contrast, electrode location, DKL direction and group ($F(4, 56)=4.20$, $p=.005$, $\eta^2=.23$). To disentangle these

interactions, we performed separate ANOVAs for low and high contrast levels separately.

28.2.1. Low contrast

The NI amplitude for patients and controls was not significantly different ($F(1, 14)=1.37$, $p=.261$, $\eta^2=.09$, n.s.). There was a main effect of DKL ($F(2, 28)=3.78$, $p=.035$, $\eta^2=.21$), though pairwise comparisons were not significant. There was a three-way interaction between electrode locations, DKL condition and group ($F(4, 56)=3.32$, $p=.017$, $\eta^2=.19$).

A separate ANOVA for control and the patient group was performed. There were no significant results for the patient group. For controls, the main effect of DKL direction was significant ($F(2, 14)=3.88$, $p=.046$, $\eta^2=.36$). Post-hoc tests using Bonferroni correction did not point to significant differences, although it appears that the amplitude was the most negative for S-cone, then L – M, then luminance. There was a trend for a significant linear contrast which is in line with this interpretation, although it was not significant ($F(1, 7)=5.10$, $p=.058$, $\eta^2=.42$, n.s.; see Figure 57 NI amplitude in response to different DKL directions at low contrast level for control and schizophrenia group below).

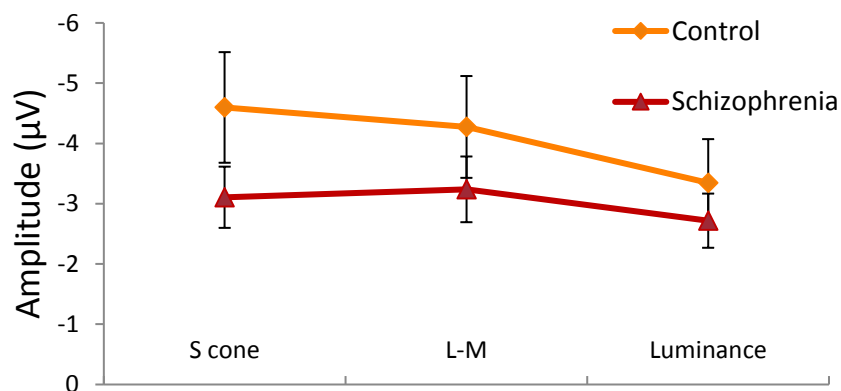


Figure 57 NI amplitude in response to different DKL directions at low contrast level for control and schizophrenia group. Error bars represent standard error of the mean.

28.2.2. High contrast

There were no significant group or within-subject effects for high contrast. Groups did not appear to differ, and there were no differences between DKL conditions within groups.

28.2.3. Latency

A separate repeated measures ANOVA was conducted for latency measures.

NI component in response to high contrast shapes peaked earlier than in response to low contrast shapes ($F(1, 8)=32.3$, $p<.001$, $\eta^2=.80$). There was a main effect of DKL condition ($F(2, 16)=3.81$, $p=.044$, $\eta^2=.32$). Post-hoc Bonferroni-corrected tests did not show significant pairwise comparisons, however, it appeared that the latency was the shortest in response to luminance-defined shapes, followed by the L – M, and the slowest for S-cone condition. This observation was confirmed with significant linear effect for DKL direction ($F(1, 8)=5.61$, $p=.045$, $\eta^2=.41$; see Figure 58 below).

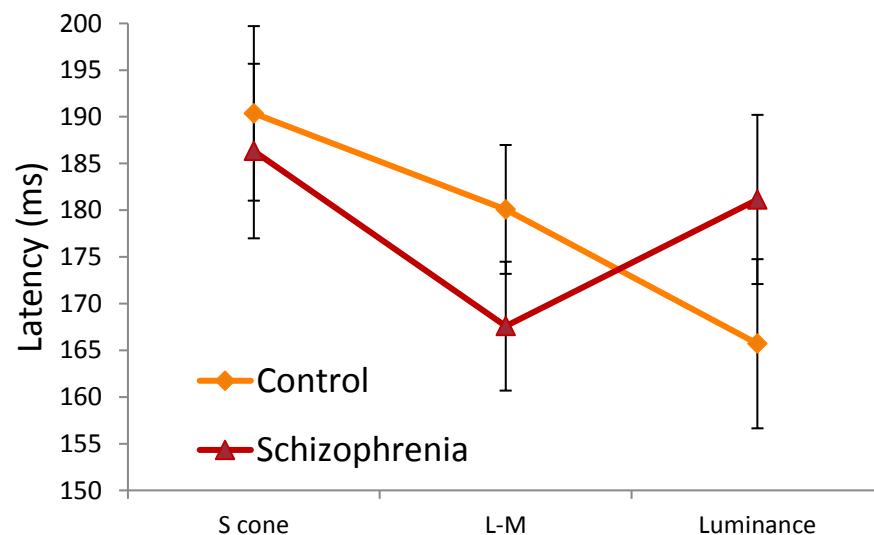


Figure 58 NI component latencies for control (blue) and schizophrenia group (red), for the three DKL directions. Group factor did not interact with DKL direction. There was an overall effect of DKL. Error bars represent standard error of the mean.

There was a significant three-way interaction between contrast level, electrode location and WM load ($F(2, 16)=3.85$, $p=.043$, $\eta^2=.32$). Post-hoc, Bonferroni-

corrected tests showed that there was a trend at low contrast at channel O2, for load 1 had shorter N1 latency than Load 3 ($p=.05$).

28.3. P3a Amplitude (C1, C2, Cz; 200-400 ms)

There were no significant results for P3a amplitude.

28.3.1. Latency

A separate repeated measures ANOVA was conducted for latency measures.

There was a trend towards a significant interaction between electrode location and group ($F(2, 14)=3.74$, $p=.050$, $\eta^2=.35$, n.s.). There was a main effect of DKL direction ($F(2, 14)=4.65$, $p=.028$, $\eta^2=.40$). Post-hoc Bonferroni-corrected tests did not show significant pairwise comparisons, however, it appeared that the latency was the shortest in response to luminance-defined shapes, followed by the L – M, and the slowest for S-cone condition. This observation was confirmed with significant linear effect for DKL direction ($F(1, 7)=7.36$, $p=.030$, $\eta^2=.51$). Further, an interaction between group and DKL direction was significant ($F(2, 14)=3.92$, $p=.044$, $\eta^2=.36$), suggesting that the above pattern was evident in schizophrenia but not in the control group (see Figure 59). Additionally, post-hoc, Bonferroni-corrected tests showed that component P3a peaked earlier for patients than controls for luminance condition ($p=.015$).

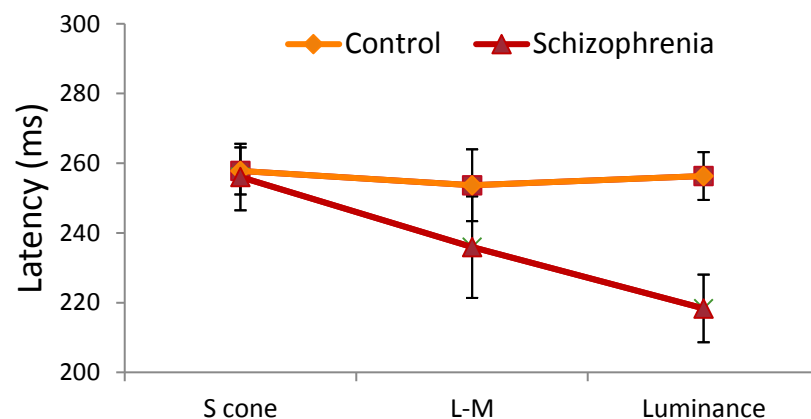


Figure 59 N1 component latencies for control and schizophrenia group during encoding luminance-defined shapes. Error bars represent standard error of the mean.

28.4. P3b Amplitude (P3, P4, Pz; 200-500 ms)

P3b amplitude differed between DKL directions ($F(2, 28)=5.72$ $p=.008$, $\eta^2=.29$; see Figure 60). Post-hoc tests using Bonferroni correction showed that there was a lower amplitude in response to S-cone shapes than in response to luminance ($p=.018$).

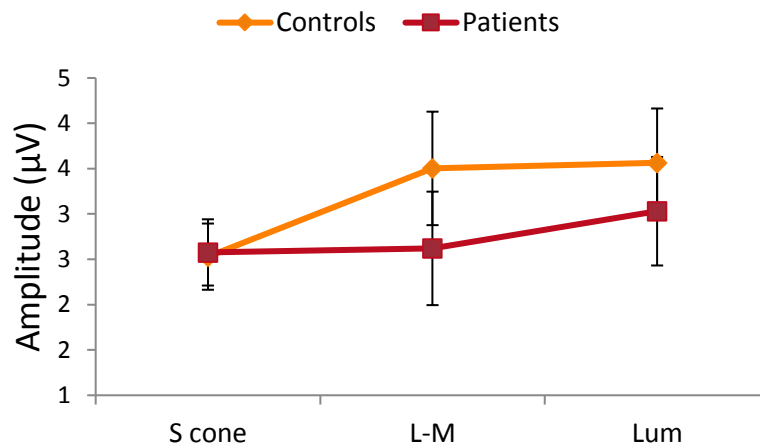


Figure 60 P3b amplitude in response to S-cone, L – M and Luminance shapes. The amplitude at each DKL direction did not differ significantly between control and patient group. Error bars represent the standard error of the mean.

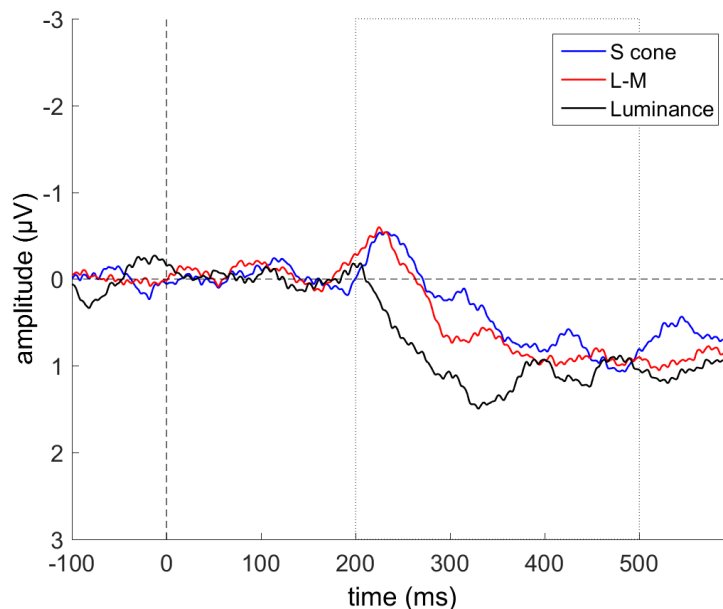


Figure 61 ERP waveforms during encoding of S-cone (blue trace), L – M (red trace) and luminance shapes (black trace). Waveforms were collapsed across WM load, contrast levels, electrode locations (P3, P4, Pz) and groups to show a significant main effect of DKL direction.

There was an interaction between contrast level and WM load ($F(1,14)=18.5$, $p=.001$, $\eta^2=.57$). Post-hoc tests using Bonferroni correction showed that Load 1 had a lower amplitude than load 3 only at low contrast ($p=.002$).

A three-way interaction between electrode location, WM load and DKL direction was also significant ($F(4, 56)=3.20$, $p=.020$, $\eta^2=.18$).

There was a trend for an interaction between contrast, electrode location, WM load, DKL direction and group ($F(4, 56)=2.54$, $p=.050$, $\eta^2=.15$, n.s.).

To disentangle this and previous interactions, we performed separate ANOVAs for control and patient group.

28.4.1. Control group

28.4.1.1. Low contrast

There was a marginal main effect of load for the control group ($F(1, 7)=5.67$, $p=.049$, $\eta^2=.45$). Load 1 elicited lower amplitude than load 3.

28.4.1.2. High contrast

There was an interaction between electrode location, WM load and DKL direction ($F(4, 28)=3.83$, $p=.013$, $\eta^2=.35$). Post-hoc tests using the Bonferroni correction did not yield significant pairwise comparisons. Inspection of the plots (see Figure 60 below) suggests that differences in amplitudes between DKL directions had different patterns on each electrode, although generally, luminance tended to demonstrate lower amplitude than S-cone and L – M.

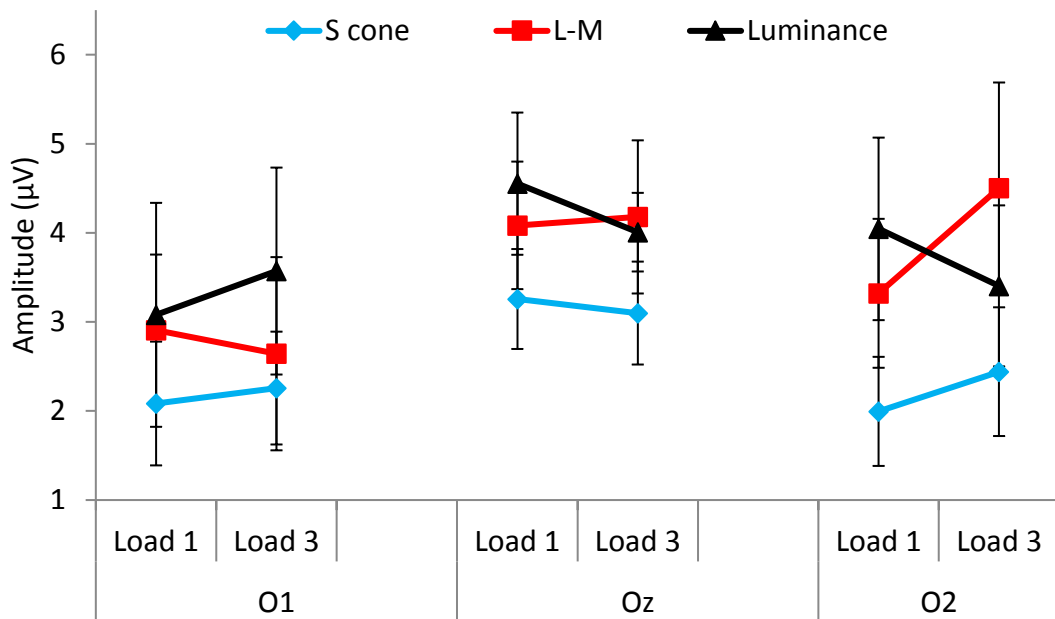


Figure 62 P3b amplitudes at electrode O1, O2 and Oz, at two levels of load, for each DKL direction. Error bars are the standard error of the mean.

28.4.2. Patient group

28.4.2.1. Low contrast

There was a main effect of WM load ($F(1, 7)=12.3$, $p=.010$, $\eta^2=.64$). Load 1 elicited lower amplitude than load 3.

28.4.2.2. High contrast

There were no main effects or interactions.

28.4.3. Latency

A separate repeated measures ANOVA was conducted for latency measures.

There was a main effect of DKL direction ($F(2, 14)=6.99$, $p=.008$, $\eta^2=.50$); luminance demonstrated shorter latencies than S-cone ($p=.049$).

An interaction between electrode location, load and group was in trend significant ($F(2, 14)=3.60$, $p=.055$, $\eta^2=.34$, n.s.).

29. Maintenance stage

29.1. Slow wave (1000-1600 ms) – occipital (O1, O2, Oz).

Controls were characterised by a larger mean amplitude of the slow wave compared to patients ($F(1, 14)=5.07$, $p=.041$, $\eta^2=.27$). Group factor interacted with contrast level and electrode location $F(2, 28)=3.44$, $p=.046$, $\eta^2=.20$; see Figure 63 below). Post-hoc, Bonferroni corrected tests showed that the amplitude difference between patients and controls was significant at low contrast at electrode Oz only (the difference between groups had $p=.008$). The difference at the Oz at high contrast showed a non-significant effect at $p=.055$.

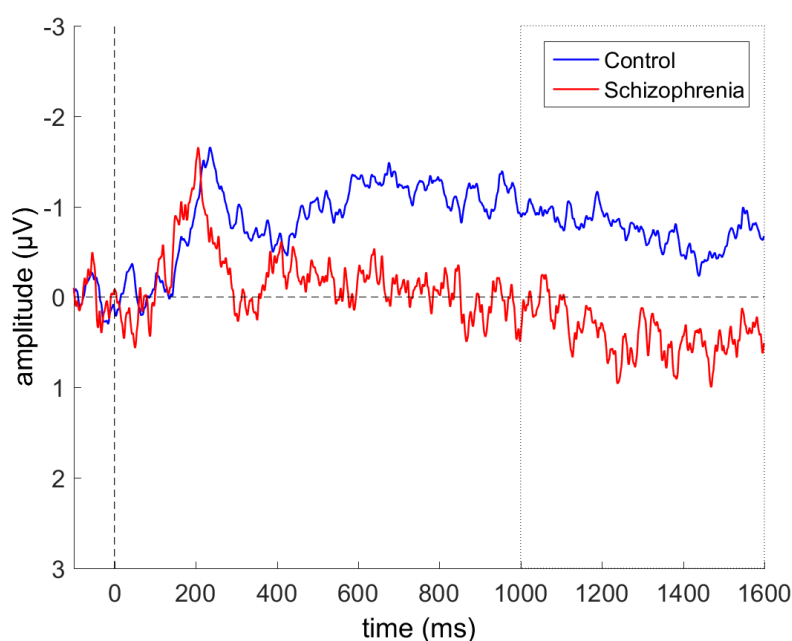


Figure 63 Late, slow wave for controls (blue trace) and patients (red trace), presented at low contrast, at electrode Oz; data were collapsed across 3 DKL directions and 2 load levels to illustrate the significant group by contrast by electrode position interaction.

There was a significant four-way interaction between group, contrast level, WM load and DKL direction ($F(2, 28)=3.44$, $p=.046$, $\eta^2=.20$). A separate ANOVA was conducted for each group.

For controls, there was a trend towards contrast by load interaction ($F(1, 7)=5.04$, $p=.060$, $\eta^2=.42$). No main effects or interactions were significant.

For patients, there was a significant three-way interaction between contrast level, WM load and DKL direction ($F(2, 14)=7.39$, $p=.006$, $\eta^2=.51$). Post-hoc, Bonferroni-corrected t-tests did not point to pairwise differences. Inspection of Grand averaged waveforms (see Figure 64 below) suggested that at low contrast, the amplitude at load 3 was higher than load 1 for luminance. At high contrast, for S-cone, Load 1 elicited higher amplitude than Load 3.

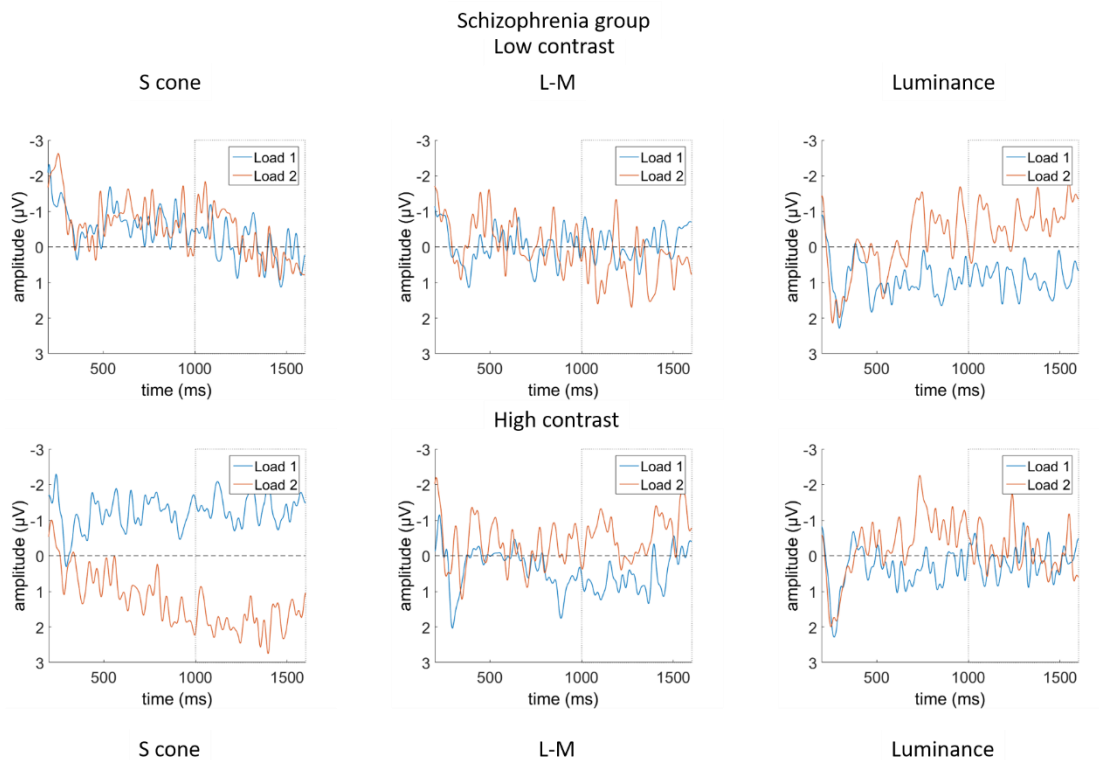


Figure 64 Slow wave for the patient group, presented at low and high contrast, for separate DKL directions and load levels. Data were collapsed across channels to demonstrate an interaction between contrast, WM load and DKL direction. The data was filtered using a 20Hz low-pass filter for presentation purposes.

30. Retrieval stage

30.1. P1 Amplitude (Oz O1 O2; 80-160 ms)

There was no overall difference between groups ($F(1, 14)=1.06$, $p=.320$, $\eta^2=.071$, n.s.). There was a trend towards contrast by group interaction ($F(1, 14)=3.58$, $p=.079$, $\eta^2=.20$), suggesting that at high contrast, the P1 amplitude for the control group was greater than that for the patient group.

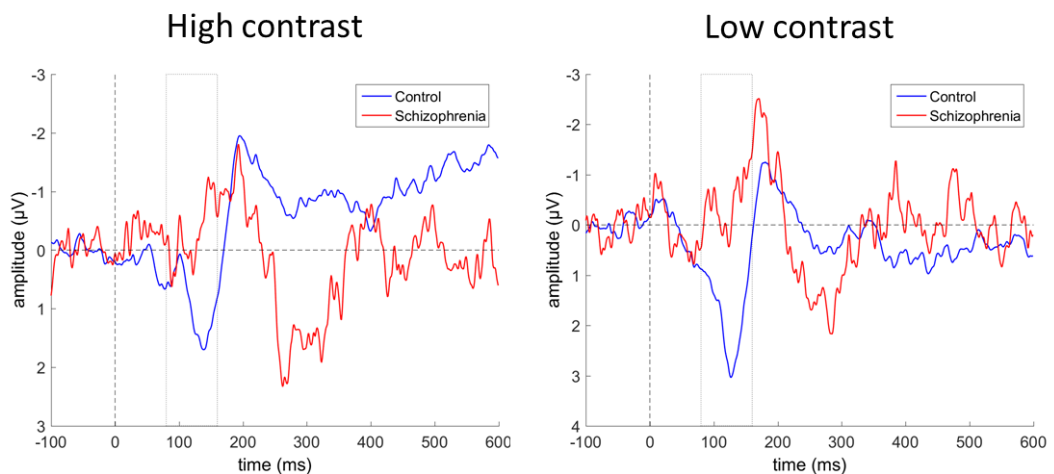


Figure 65 ERP waveforms collapsed across load contrasting patient and control luminance data at retrieval at low and high levels of contrast.

30.2. Latency

A separate ANOVA for latency measures was conducted. There was a significant interaction between contrast level and group ($F(1, 9)=7.31$, $p=.024$, $\eta^2=.45$) as well as a three-way interaction between contrast, electrode location and group ($F(2, 18)=4.15$, $p=.033$, $\eta^2=.31$). Post hoc, Bonferroni-corrected tests showed that at high contrast, control participants demonstrated shorter latencies than patients at electrode O2 ($p=.017$). At low contrast, controls demonstrated shorter latencies than patients as well ($p=.028$).

30.3. N1 Amplitude (Oz O1 O2; 130 ms – 300 ms)

There was no overall difference between groups ($F(1, 14)=.372, p=.552, \eta^2=.026, n.s.$). There was a main effect of DKL direction ($F(2, 28)=4.42, p=.021, \eta^2=.24$). Post-hoc Bonferroni corrected tests did not point to any significant pairwise comparisons.

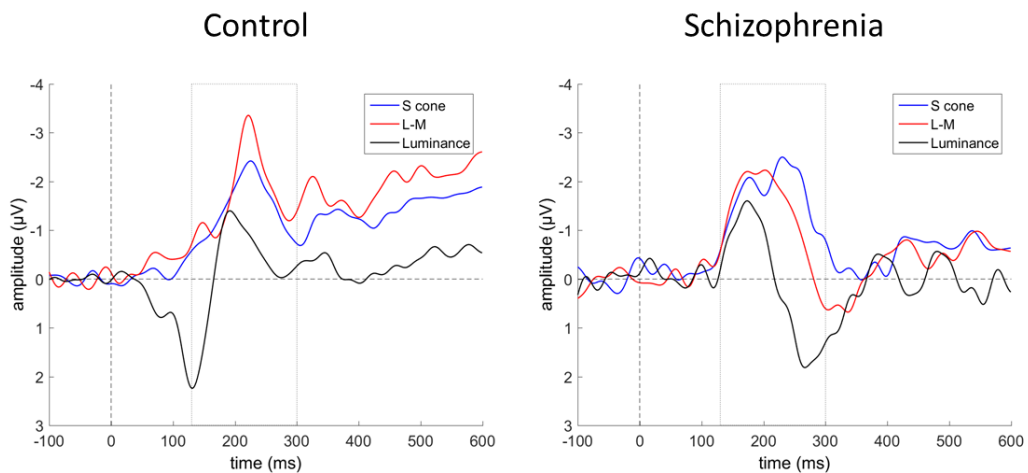


Figure 66 Waveforms collapsed across WM load, electrode location & contrast to show differences between DKL directions, for controls and patients separately. Waveforms were low-pass filtered at 20Hz for presentation.

30.3.1. Latency

A separate ANOVA for latency measures was conducted. There was a main effect of contrast ($F(1, 9)=7.48, p=.023, \eta^2=.45$), with shorter latencies for high contrast shapes. There was a main effect of load ($F(1, 9)=650, p=.031, \eta^2=.42$), with shorter latencies for load 1 than load 3. A main effect of DKL ($F(1.29, 11.6)=12.7, p=.003, \eta^2=.59$) showed that luminance shapes were characterised by shorter NI latencies than S-cone ($p=.005$) and L – M ($p=.014$). There was a four-way interaction between contrast, load, DKL direction and group ($F(2, 18)=5.79, p=.011, \eta^2=.39$) as well as between electrode location, load, DKL and group ($F(4, 36)=2.68, p=.047, \eta^2=.23$). A separate ANOVA for each group was conducted to disentangle these interactions. Controls showed significant effect of load ($F(1, 4)=8.14, p=.046, \eta^2=.67$), with load 1 eliciting shorter NI latencies, and main effect of DKL direction ($F(2, 8)=5.87, p=.027, \eta^2=.59$); post-hoc, Bonferroni corrected tests did

not point to any significant differences, although latencies for S-cone appeared to be longer than for L – M and luminance. Patients showed only DKL-related modulation ($F(2, 10)=7.35, p=.011, \eta^2=.59$). Luminance elicited shorter NI latencies than L – M ($p=.015$), though the difference between luminance and S-cone was not significant ($p=.078, n.s.$).

30.4. P3aAmplitude (C1, C2, Cz; 200-400 ms)

There was no overall difference between groups ($F(1, 14)=2.46, p=.139, \eta^2=.15, n.s.$). There was a significant interaction between group and DKL direction ($F(2, 28)=4.29, p=.024, \eta^2=.23$). Post-hoc tests showed that the P3a amplitude was higher for controls for isoluminant L – M condition ($p=.025, Bonferroni-corrected$). For luminance and S-cone, amplitudes were not statistically different between controls and patients.

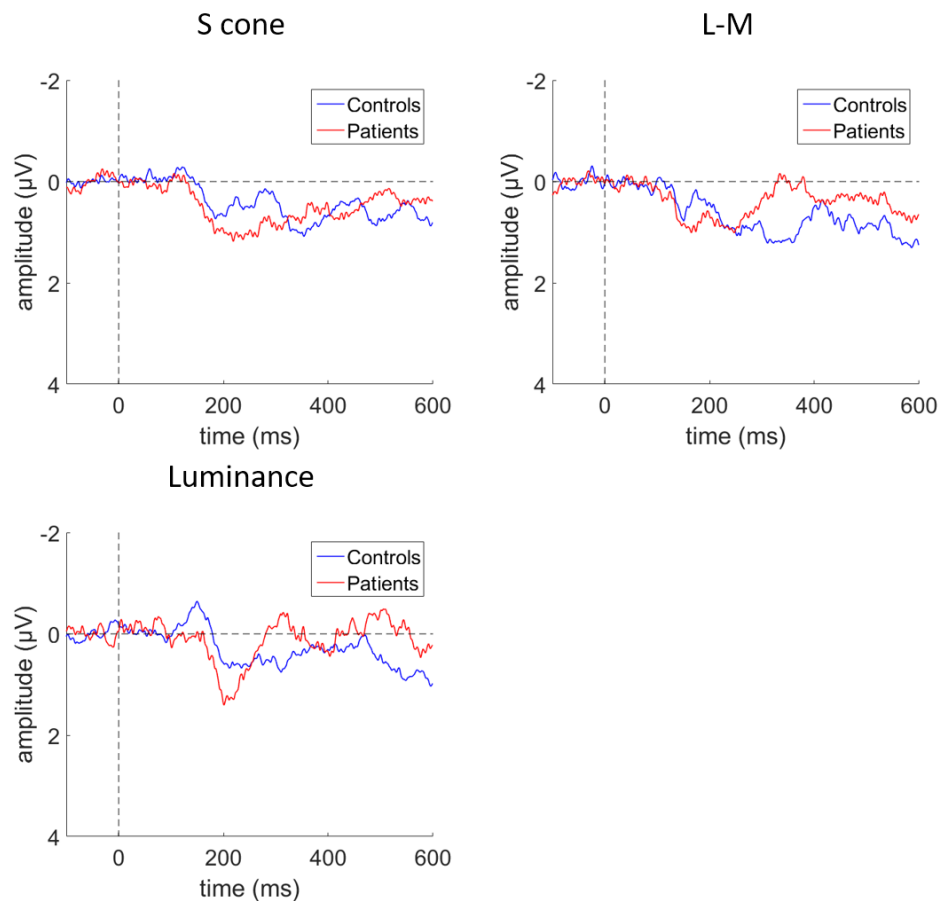


Figure 67 ERP waveforms collapsed across contras levels, WM load and electrode locations (C1, C2 & Cz), presented at each DKL direction separately to demonstrate differences between control and patient group for component P3a (200-400 ms).

30.4.1. Latency

A separate ANOVA for latencies was conducted. High contrast shapes elicited shorter latencies than low contrast shapes ($F(1, 10)=5.30$, $p=.044$, $\eta^2=.35$). There was a main effect of DKL ($F(2, 20)=4.00$, $p=.035$, $\eta^2=.29$); L – M shapes elicited shorter latencies than S-cone shapes ($p=.048$).

There was a trend for DKL effect ($F(2, 16)=3.39$, $p=.059$, $\eta^2=.30$, n.s.); luminance appeared to elicit somewhat shorter latencies than l – M and S-cone.

An interaction between electrode location, DKL direction and group was significant ($F(4, 40)=2.85$, $p=.036$, $\eta^2=.22$). We conducted separate ANOVAs for each group.

30.4.2. Control group

Latencies were shorter for high than low contrast stimuli ($F(1, 5)=8.55$, $p=.033$, $\eta^2=.63$). There was a main effect of load ($F(1, 5)=27.7$, $p=.003$, $\eta^2=.85$), showing that latencies were shorter for load 3. Load interacted with electrode location ($F(2, 10)=5.76$, $p=.022$, $\eta^2=.53$). Post-hoc tests using Bonferroni correction showed that load 1 differed from load 3 at electrode P4 ($p=.007$). An interaction between contrast level, electrode location and DKL direction was significant ($F(4, 20)=3.19$, $p=.035$, $\eta^2=.39$). Post-hoc tests using Bonferroni correction did not show significant effects.

30.4.3. Patient group

There was a main effect of DKL direction ($F(2, 10)=7.52$, $p=.010$, $\eta^2=.60$).

Latencies decreased linearly ($F(1, 5)=17.7$, $p=.008$, $\eta^2=.78$), with longest latencies for S-cone, then L – M, and shortest for luminance stimuli. Post-hoc tests using Bonferroni correction showed that luminance had significantly different latencies than S-cone ($p=.025$). Electrode location interacted with DKL direction ($F(4, 20)=3.90$, $p=.017$, $\eta^2=.44$). Post-hoc tests using Bonferroni correction showed that the differences between DKL directions were most evident at electrode P3, where luminance was significantly different than both S-cone ($p=.018$) and L – M

($p=.001$). At electrode P4, luminance was different only from S-cone ($p=.002$), while there were no differences in latencies at electrode Pz.

30.5. P3b Amplitude (P3, P4, Pz; 200-500 ms)

There was no overall difference between groups ($F(1, 14)=.825$, $p=.379$, $\eta^2=.056$, n.s.). Low contrast shapes elicited lower P3b amplitude ($F(1, 14)=6.00$, $p=.028$, $\eta^2=.30$). There was a trend towards significant group by electrode location interaction ($F(2, 28)=3.18$, $p=.057$, $\eta^2=.18$, n.s.), with somewhat higher amplitude for controls compared to patients at electrode Pz.

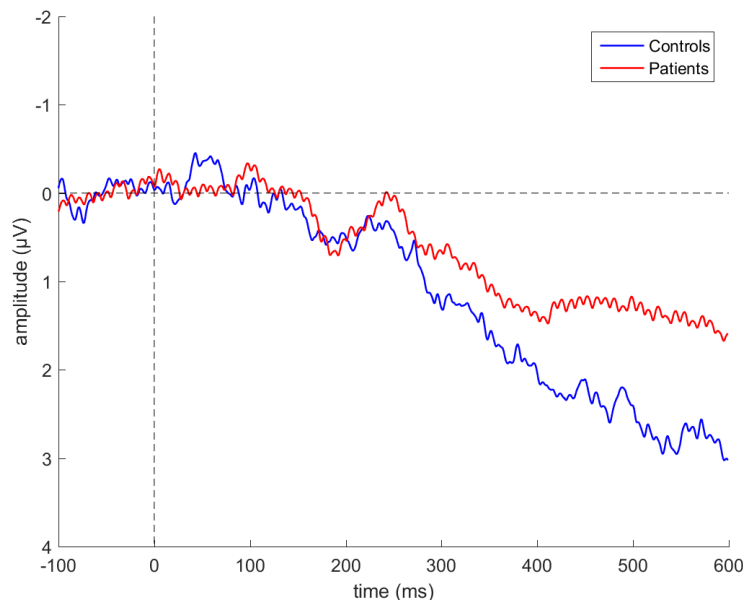


Figure 68 Waveforms collapsed across DKL directions, load and contrast levels at electrode Pz for controls (blue trace) and patients (red trace).

There was a main effect of DKL direction ($F(2, 28)=8.65$, $p=.001$, $\eta^2=.38$); luminance had a higher amplitude than S-cone ($p=.013$); L – M also had a higher amplitude than S-cone ($p=.015$). There was a trend towards channel by load interaction ($F(1.26, 17.7)=3.6$, $p=.066$, $\eta^2=.20$, n.s.); load 1 elicited somewhat higher amplitude than Load 3 at the central electrode Pz. Finally, there was a three-way interaction between contrast level, WM load and DKL direction ($F(2, 28)=4.75$, $p=.017$, $\eta^2=.25$). We run a separate ANOVA for each contrast level. At low contrast, group interacted with electrode location ($F(2, 28)=4.51$, $p=.020$,

$\eta^2=.24$). Post hoc tests using Bonferroni correction showed that P3b amplitude for patient group was lower than for controls at electrode Pz ($p=.023$). There was a main effect of DKL at low contrast was significant ($F(2, 28)=4.94, p=.015, \eta^2=.26$). There was a linear increase in amplitude ($F(1, 14)=8.24, p=.0127, \eta^2=.37$) across the three DKL directions, with the smallest amplitude for S-cone, then L – M, then luminance. Post-hoc tests using Bonferroni correction showed that the difference in amplitude between luminance and S-cone was significant ($p=.037$). DKL factor interacted with electrode location ($F(4, 56)=2.78, p=.035, \eta^2=.17$). Post-hoc tests using Bonferroni correction suggested that differences in amplitudes between DKL directions were most pronounced at electrode P4, where luminance had significantly greater amplitude than L – M ($p=.014$) and marginally greater than S-cone ($p=.05$). There was also a trend for a significant load by DKL direction interaction, although it was not significant ($F(2, 28)=3.20, p=.056, \eta^2=.19$). This interaction would suggest that differences between DKL directions were most pronounced at higher WM load (see Figure 69 below). There were no effects or interaction at high contrast

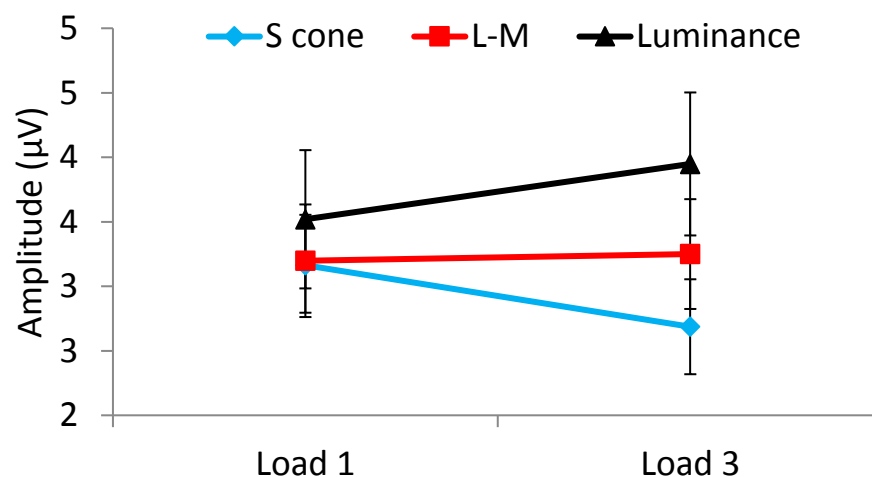


Figure 69 P3b amplitude during retrieval for 3 DKL directions, at load 1 and load 3. Although the interaction between load and DKL was significant, differences between DKL directions could be more pronounced at higher WM load levels. Error bars represent standard error of the mean.

30.5.1. Latency

A separate ANOVA for latencies was conducted. High contrast shapes elicited shorter latencies than low contrast shapes ($F(1, 8)=5.91, p=.041, \eta^2=.42$).

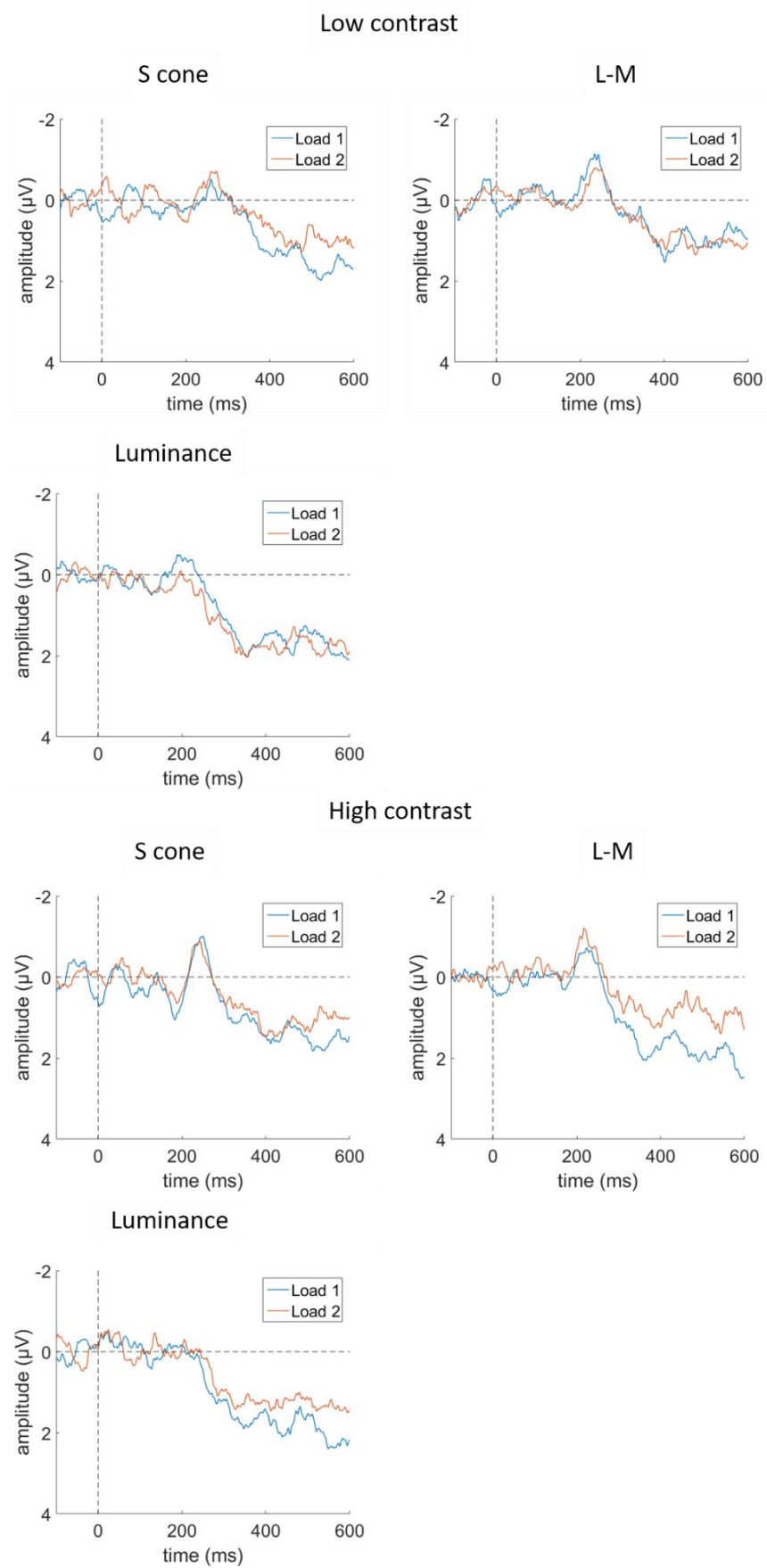


Figure 70 Waveforms collapsed across groups and electrodes and presented at low and high contrast separately, for each DKL direction, to demonstrate the three-way interaction between contrast, WM load and DKL direction.

31. Discussion

In this experiment, we compared WM performance on a delayed match-to-sample task between schizophrenia and control group (matched for age and educational level). We expected that performance of the schizophrenia group will be overall worse than that of controls on this task (Haenschel et al., 2009; Haenschel, Linden, Bittner, Singer, & Hanslmayr, 2010; Haenschel, Bittner, Haertling, Rotarska-Jagiela, Maurer, Singer, Linden, et al., 2007; Nuechterlein et al., 2004; Nuechterlein, Ventura, Subotnik, & Bartzokis, 2014),

We predicted that given apparent visual deficits in schizophrenia (e.g. Javitt, 2009a; Silverstein et al., 2015)) and magnocellular deficit account of these impairments (Kéri & Benedek, 2007), luminance-defined shapes will not provide a memory advantage over isoluminant shapes.

Another aim of the current study was to replicate the main behavioural finding of the previous EEG and psychophysics experiment – that is, that luminance benefits visual WM. More specifically, we looked whether, in the control group data, the advantage of luminance over isoluminant conditions will be reflected in better accuracy in response to luminance shapes at higher working memory loads. In the previous study, this was the case for the probes that mismatched remembered shapes.

In terms of ERP responses for the control group, we were mostly interested whether the amplitude of the early visual component P1 in response to luminance shapes will be modulated by WM load (Haenschel et al., 2007). For patients, we expected no such modulation of the component P1, along with the overall reduction of this component in response to our stimuli (Haenschel et al., 2007).

We also looked at N1 in response to isoluminant shapes – our hypothesis was that the N1 will not be modulated by WM load in either group.

The interaction between WM load, DKL direction and probe type was one of the major findings in the previous study. In particular, we showed that the luminance benefit was manifested in the behavioural accuracy data especially at higher WM

loads and in the mismatch condition (i.e. when the memory probe was different to the remembered stimuli).

We did not show a clear indication of luminance benefit in control participants. Participants' accuracy levels were indeed higher for luminance than S-cone, but this was also the case for L – M condition. Accuracy in response to all DKL directions was reduced in patients compared to controls, however, there was no specific reduction for luminance-defined shapes.

We also expected to see the luminance benefit to manifest at higher WM load for mismatching probes, as we have shown in the previous experiment.

Consistently with the previous study, we found that the probe type interacted with WM load for luminance. The results suggested that a higher WM level, the decrease in accuracy was more severe for a match than it was at the mismatch. While no such interaction could be seen in S-cone condition, L – M condition displayed a similar pattern.

While there were no significant interactions with group type, the pattern of results (see Figure 48) suggests that in the schizophrenia group, accuracy was similar in response to match and mismatch probes, i.e. it decreased with increasing WM load. On the other hand, while in the control group both conditions also suffered from increasing WM load, mismatch probes tended to produce higher accuracy than in the match condition, suggesting that the benefit of luminance at mismatch could be lost in the schizophrenia group. However, more data is needed to confirm this interpretation.

The modulation of the early visual component in control and schizophrenia group was in line with our predictions. Based on previous findings (e.g. Heanschel et al., 2007) we expected to see a reduced P1 amplitude for patients compared to controls, which was the case with our data. It is worth noting that P1 component was reduced for both patients and controls in low contrast condition. As discussed in the previous chapter, we attribute this to the low signal-to-noise ratio for low contrast condition. A similar pattern was also observed at retrieval, although the difference was not statistically significant.

Additionally, we also found that the P1 component was modulated by WM load in controls, reflected in higher amplitude in high WM load condition. However, in the current study, the effect was confined to electrode O2. It is worth noting that in the previous study load effects were most evident at lateral electrodes (O1 and O2), while such pattern was less clear at electrode Oz. In the future studies, it would be reasonable to focus on lateral electrodes, as it appears that load effects are lateralised. Averaging across multiple electrode sites might be also beneficial to increase the signal-to-noise ratio, as load effects in the previous and in the current study were small.

N1 was the first component that was reliably elicited by isoluminant shapes, as the P1 was absent in response to this class of stimuli (Crognale, 2002; Gerth et al., 2003). Similarly to the experiment one, this pattern suggests that the isoluminant stimuli were not contaminated by luminance artifact, thus validating the design of our stimuli.

As previously, we did not find clear load-related modulation of this component, neither for isoluminant or luminance condition, confirming that the P1 component was the first to be modulated by WM load. Luminance elicited overall less negative amplitude than isoluminant conditions. There was no clear differentiation between control and patient group in terms of N1 amplitude. However, at low contrast, the difference between luminance and isoluminant conditions seemed to be more pronounced for controls.

There was also no clear distinction between controls and patients for the P3a and P3b components, which was in line with previous studies (Haenschel, Bittner, Haertling, Rotarska-Jagiela, Maurer, Singer, Linden, et al., 2007). This finding (together with P1 effects discussed above) suggests that, in terms of WM encoding, early visual processing is especially affected in schizophrenia.

The maintenance period also appeared to play a role, however, as the occipital slow wave differentiated between patients and controls. At retrieval, on the other hand, there were no specific group or WM load-related effects.

Taken together, the findings suggest that WM is affected in schizophrenia compared to controls. This was reflected in lower behavioural accuracy. A

reduction of ERP component P1 in patients but not in controls suggests that early visual processing is altered in schizophrenia. Slow wave recorded from occipital sites could also differentiate between controls and patients during the maintenance. One interpretation of this finding could be that the impaired perceptual processing (as indicated by reduced P1) has effects on the maintenance of the stimulus in later WM stages, which in turn impacts behavioural performance. It would be beneficial in future studies to establish how the neural activity at one stage affects the next.

The overall pattern of results also suggests that in controls, responding to mismatching memory probes produced better performance than when the memory matches previously presented item at high WM load. This suggests that the process which compares memory representation with the ongoing perceptual representation is different for match and mismatch (Hyun et al., 2009) and is in line with other studies that showed that mismatch probes are accurately rejected by participants in a WM task regardless of WM load (Bledowski et al., 2011). This interpretation was also put forward while discussing the similar pattern of results in experiment one (see Chapter 3).

Interestingly, this pattern is less evident in the patient sample (see Figure 5). For patients, accuracy in response to different DKL directions was similar at low and high WM load, and at match and mismatch condition. Even with the confound introduced by the use of averaged thresholds, these results might suggest that accuracy in response to luminance behaves differently than in controls.

However, while the previous study showed that this mismatch-specific effect was demonstrated for luminance-defined stimuli, in the current study the pattern was similar in L – M condition. Moreover, the overall accuracy did not seem to benefit from luminance, although it was reduced for the isoluminant S-cone condition. Furthermore, the current study failed to show a luminance-specific impairment in the patient group, showing instead a generalised reduction in accuracy.

The failure to observe the difference between luminance and isoluminant L – M could suggest that our earlier finding was a false positive. However, it could as well be the case that there was a significant luminance artifact in the L – M data

that would essentially make these two classes of stimuli similar. Inspection of the ERP waveforms does not seem to support this interpretation as there is no clear P1 in response to L – M shapes, which should be the case if a substantial luminance artifact was present in the data. An alternative explanation for this pattern is that it was due to the decision to use average thresholds instead of measuring individual thresholds prior to the main WM experiment.

At this point, we cannot rule out the possibility that in some participants averaged thresholds could contribute to unequal stimulus saliency between different DKL directions. This could lead, for example, to overestimated L – M contrast and/or underestimated Luminance contrast, which, on average, would cancel out any differences between these two conditions that would be otherwise observable.

However, even if we would be able to replicate the results of the previous study, they would be not free from the same criticism – mainly that using averaged thresholds could make it more likely to invalidate our efforts to make stimuli isosalient. Moreover, one could also argue that by using averaged thresholds we have biased the patients to perform worse than controls. If magnocellular deficits are actually present in our sample of patients, and if (as we claim), luminance processing is casually tied to WM performance, then the luminance discrimination thresholds must be higher than those of controls. This would be consistent with vision test results; in our sample, patients tended to perform worse on acuity measures, and somewhat worse on functional contrast sensitivity measures (although in the latter case the results were not significant). Using thresholds that are based on non-clinical population can, therefore, introduce a major bias. In conclusion, any strong conclusions derived from our data are therefore prone to criticism, should the pattern replicated that of the previous experiment or not (as it is the case currently). In summary, the use of individual thresholds should be preferable.

Currently, we are collecting more data to address those shortcomings. Should we find that the pattern of results still does not replicate the first experiment, we

would know that our design choice was not at fault. However, this is beyond the scope of this thesis.

The results of the pilot study are mostly promising. We have replicated the accuracy advantage in the behavioural data; luminance-defined shapes led to better accuracy than S-cone and L – M conditions, although this effect did not correlate with the group. Nevertheless, patients performed worse than controls overall.

Interestingly, besides the overall group differences, the data showed that patients performed somewhat worse than controls in the mismatch condition. This finding is promising for the future study – it would partially support the conclusion of our previous experiment that the luminance advantage manifests itself when the probe mismatches remembered stimuli and that this advantage might be less pronounced in patients. This conclusion is, of course, limited by the three-way interaction between probe type, WM load and DKL direction – it occurred regardless of the group type. However, it is important to bear in mind that the sample size of this study is small (8 participants per group), and thus the study was likely underpowered to detect a four-way interaction with the group. Visual inspection of the box plots (see figure) indicates that this conclusion is likely. The pattern of results for controls resembles the one we reported in the previous experiment; namely, accuracy for luminance at mismatch appears to be somewhat higher than S-cone; although luminance and L – M do not appear to differ in this case (see above for a discussion on the apparent lack of dissociation between responses to L – M and luminance shapes). For patients, accuracy in response to S-cone, L – M and luminance at mismatch seems to be uniform across these conditions, resembling the match condition pattern that we found in both the previous and in the current study as well.

While our study highlighted the importance of perceptual processing, there is a number of other factors that could contribute to WM performance (Lee & Park, 2005), or even interact with perceptual processing at encoding. For example, attention might be a relevant factor. Failure to select information relevant to the task, or a failure to direct attention to the relevant feature could result in worse

performance via lack of encoding precision (Adler et al., 1998; Braver, Barch, & Cohen, 1999).

While our study is not testing these factors directly, it would be useful for future research to identify top-down factors that can interact with perception at the encoding stage.

Other low-level factors might be also at play. For example, performance in patients versus controls could stem from slower encoding (Hartman et al., 2003). It would be interesting to see whether increasing the timing of stimulus presentation would increase performance in patients, as was the case in previous studies (Tek et al., 2002).

Given that visual impairments in schizophrenia have been widely reported (Silverstein et al., 2015), studies attempting to assess visual WM in schizophrenia would be wrong to assume intact perceptual processing (Tek et al., 2002). However, it is unclear what the precise nature of this perceptual impairment is and how it contributes to WM performance. Results of our study go in line with a growing number of studies that recognise the role of sensory and perceptual processing at the encoding stage of WM (e.g. Haenschel, Bittner, Haertling, Rotarska-Jagiela, Maurer, Singer, Linden, et al., 2007). It also sheds light on the potential perceptual mechanism contributing to impaired WM performance – namely, an impaired processing of luminance signals. While more data is needed to confirm this interpretation, current results suggest that this is a direction worth pursuing.

As mentioned above, a study by (Haenschel et al., 2007) recorded EEG from patients and controls during WM task. More specifically, they were looking at ERP component P1, which is related to perceptual processing (see Chapter 3). They found that this component was sensitive to WM load in the control group. More specifically, while WM load was inversely correlated with performance (participants in both groups found it harder to remember more items), the amplitude of P1 component increased with increasing WM load in controls. Moreover, the amplitude of this component successfully predicted performance on the task, but again, only in the control group. If component P1 is mainly

associated with perceptual processing, this study supports the notion of an impairment in perceptual processing during WM encoding. Other EEG and studies have also indicated impairment in early visual processing (Butler et al., 2001, 2005; Uhlhaas et al., 2006)

Interestingly, amplitudes of the NI components did not differ between patients and controls; we also did not report a load-dependent modulation of this component for luminance or isoluminant conditions. This would suggest that, in correspondence to our hypothesis, the interaction between perception and WM appears to occur early and can be indexed using a PI component.

In summary, the results of the pilot study provide a partial support for the luminance advantage hypothesis; although the pattern of behavioural results is similar to the previous study, luminance elicited similar accuracy to L – M isoluminant condition. At the same time, visual component PI at encoding seems to be modulated by WM load, while component NI was not; this could suggest perception/WM interactions at the level of PI component, which suggests the role of luminance.

At this point, it is also difficult to establish whether the luminance advantage is not present in the patient population. It does appear, however, that patients have reduced component PI, and that the component seems not to be modulated by load. It is important to note however that overall, patient data appeared to be noisier than that of controls. Additionally, it is assumed that using average thresholds in an attempt to equate stimuli in terms of saliency is not a viable approach, and it has likely contributed to unclear results of the current study.

Chapter 6

General discussion

Sensory areas have been shown to play a crucial role in both encoding and maintaining information in WM (Harrison & Tong, 2009; Pasternak & Greenlee, 2005). This has considerably changed the long-held view that perception and working memory are separate systems (D'Esposito & Postle, 2015).

Neuroscientific studies, ranging from single-cell recordings in primates to EEG and fMRI in humans indicated the importance of frontoparietal network in working memory, with the dorsolateral prefrontal cortex implied as the location of the memory storage (Levy & Goldman-Rakic, 2000). While it was acknowledged that working memory relies on a distributed network of closely interacting brain areas (Eriksson, Vogel, Lansner, Bergström, & Nyberg, 2015), the sensory cortex, together with perceptual processing mediated by it, played a considerably lesser role (Linden et al., 2003; Munk et al., 2002). In light of the new findings, however, it became clear that we should pay closer attention to how perception and working memory interact (Haenschel et al., 2007; Lara & Wallis, 2012).

In this thesis, it was argued that the problem of the interaction between perception and working memory can be approached using tools derived from vision science. The visual system is thoroughly described and a detailed description of its hierarchy exists, from the retina and subcortical structures to the primary visual cortex and beyond. In the past, using stimuli that selectively excited post-retinal mechanisms helped to elucidate how the visual information is “put together” to form a perceptual representation of the visual world (De Valois & Kooi, 1991; Crognale, 2002; Gegenfurtner & Kiper, 2003; McKeefry,

Murray, & Kulikowski, 2001; Vidyasagar, Kulikowski, Lipnicki, & Dreher, 2002). This approach has since been used to refine some of the early conclusions regarding perception, including high-level aspects of vision such as object recognition (Martinovic et al., 2011). Given the current evidence suggesting that perception and working memory are closely linked (D'Esposito & Postle, 2015; Lara & Wallis, 2012; Postle, 2006; Zimmer, 2008), we decided to apply this strategy to visual working memory.

This thesis presented a number of experiments that aimed to verify the utility of this approach. Specifically, we looked at how the achromatic, luminance mechanism (L+M) and two chromatic mechanisms (S - [L+M], or S-cone, and L - M) compare in terms of encoding, maintaining and the retrieval of the visual information in WM. We showed that processing of luminance-defined items indeed leads to better WM performance over isoluminant shapes. In particular, in two separate behavioural experiments, we demonstrated an interaction between the number of items stored in memory and the stimulus type. Although memory accuracy decreased with increasing WM load, this drop was less severe for luminance. This was reflected in better behavioural accuracy in the ERP experiment (Chapter 3) and lower WM thresholds in the psychophysics experiment (Chapter 4).

Our studies are novel in that the differential contribution of the psychophysical channels in visual working memory has not been investigated before. The results are in line with earlier findings that showed that luminance signals are especially suitable for processing and integration of edges and contours, and thus are important for the perception of form (Beaudot & Mullen, 2005; Gregory & Heard, 1989; Lu & Fender, 1972; Gregory, 1977; Livingstone & Hubel, 1987, 1988; Mullen, Beaudot, & McIlhagga, 2000). Other studies also implicated that luminance plays a special role in object recognition (Bar, 2003; Kveraga et al., 2007; Martinovic et al., 2011). Our experiments extend these findings and suggest that luminance and chromatic channels provide differential contribution WM, with the luminance information being especially important for performance.

Looking only at behavioural data cannot answer the question at which WM stage luminance has the greatest benefit for the behavioural accuracy. Hence, it is important to differentiate between encoding, maintenance and retrieval using appropriate study design paired with a technique that provides an insight into processing taking place at each stage. To that end, we have used a delayed match-to-sample working memory task (Haenschel et al., 2009; Haenschel et al., 2007; Linden et al., 2003) and recorded the EEG.

Our ERP experiment demonstrated that the PI component in response to luminance shapes at encoding was indeed modulated by WM load; further, the component peak correlated with behavioural performance. Interestingly, we did not find NI to be reliably modulated by load in response to isoluminant items; this component also did not correlate with performance. We suggest that this observation corroborates our conclusion that luminance poses a benefit for WM performance and that this benefit may stem from early encoding stages of WM. However, the results also show that luminance plays an important role during the retrieval stage of WM. This conclusion is based on the finding that retrieving luminance-defined shapes led to better performance if the probe was different from the remembered shapes. Such mismatch-specific effect might indicate that luminance contributes to a successful comparison between the memory representation and currently perceived stimuli. This was further supported by a significant interaction between the PI component during retrieval with behavioural performance.

Although our experiments manipulated low-level properties of the stimuli (i.e. their luminance and chromaticity in order to stimulate different visual channels), the results do not exclude the possibility of the top-down signals impacting performance on the task. Notably, in addition to being sensitive to low-level features, the component PI can be modulated by attention as well (Gazzaley & Nobre, 2012; Taylor, 2002). As attentional load increases, the PI amplitude and latency increase as well (Fu et al., 2010). Thus, one should avoid implying a strong dichotomy between these two cognitive processes, especially in studies that do not attempt to dissociate between these two by design. It has been suggested that because WM and attention have to actively interact, they might as

well share a common mechanism (e.g. Chun, 2011; Gazzaley & Nobre, 2012), although this view is facing some criticism (Tas, Luck, & Hollingworth, 2016). It would be interesting to address this issue in future studies by separating attention from WM with the appropriate experimental design. If the mechanism behind luminance advantage reported here works through the facilitation of top-down modulation, attention could be the modulating factor triggered by luminance.

In the next section, I will describe the nature of the reported “luminance advantage” in more detail and consider different mechanisms through which luminance signals might contribute to better WM performance.

32. The underlying mechanism(s) behind the luminance advantage in visual working memory

If the luminance indeed benefits WM as our results seem to indicate, it is important to consider what the specific mechanism behind this advantage is. Based on previous research, there are a number of possibilities. I will now outline each them and argue that, although our study did not test these mechanisms directly, the current evidence favours the interpretation that luminance benefits WM by improving the fidelity of memory representation as well as facilitating memory-probe comparison.

32.1. Is luminance advantage mediated by a top-down or bottom-up mechanism?

Bar (2003) proposed a mechanism of object recognition in which luminance information serves as a trigger for a top-down facilitation. According to the model, luminance rapidly provides frontal areas with low-resolution information, which is then used as a basis to form an initial prediction about the object identity. Such “prediction” then serves as a top-down facilitator for object recognition, improving task performance (Kveraga et al., 2007). Specifically, they argue that magnocellular projections enable fast connections between early visual areas and inferotemporal regions (linked to object recognition) with orbitofrontal cortex.

We reasoned that object recognition does not have to be the only process that can benefit from enhanced communication between visual areas and frontal regions, and therefore hypothesised that luminance can benefit WM via similar interactions.

There is a large body of evidence for feedforward and feedback connections between the prefrontal cortex and sensory areas (Pasternak & Greenlee, 2005). Importantly, these connections appear to be important for WM (Fuster et al., 1985; Miller & Cohen, 2001; Tomita, Ohbayashi, Nakahara, Hasegawa, & Miyashita, 1999).

Indeed, it has been shown that WM performance is facilitated by top-down interactions with frontal areas (e.g. see Gazzaley, 2011). Furthermore, a study using dynamic causal modelling (Friston, Harrison, & Penny, 2003) showed that increased WM load in a verbal N-back task increased connection from the left posterior parietal cortex to the left inferior frontal cortex (Ma et al., 2012). At the same time, lower WM load inhibited connection between right posterior parietal cortex to the left anterior cingulate cortex. Since the benefit of luminance demonstrated in our studies was most pronounced at higher WM load, we suggest that luminance information may enhance the connection between posterior and frontal areas. Because Ma et al. (2012) interpreted the enhanced posterior-frontal connection as an evidence for PPC's involvement with early visual processing stages, this further supports the notion that WM encoding is crucial for WM performance. This interpretation can be further supported by the fact that posterior parietal cortex forms part of the dorsal visual stream, which receives predominantly magnocellular inputs (which, in turn, carry predominantly luminance information). The posterior parietal cortex has been shown to be connected to visual areas (Baizer, Ungerleider, & Desimone, 1991). Moreover, this region plays an important role in the processing of early visual signals (Andersen, 1989; Nakashita et al., 2008).

Additionally, Gazzaley (2011) argues that top-down modulation must be initiated sufficiently early for the facilitation to take place. Such “head start”, could be achieved via fast luminance projections (Bar, 2003). The modulation early visual component P1 by luminance-defined stimuli in our experiment might support this view. It is important to note that by “facilitation”, Gazzaley and his colleagues usually mean improving the “fidelity” of memory representation. They define fidelity as the ability to distinguish memory representations from irrelevant signals and overcoming “undesired processing” (Gazzaley, 2011). To support this hypothesis, Rutman, Clapp, Chadick, & Gazzaley (2010) used a design in which a distractor is superimposed with a target. Thus, to perform correctly on the task, an appropriate stimulus selection must take place. According to Rutman et al. (2010), WM facilitation is achieved both via suppression of irrelevant information (or processing) and facilitation of attended

information. Even though our design does not introduce distractors, sustained attention on correct trials is nevertheless important for correct performance (Pessoa et al., 2002). As Bays (2014) argues, the neural noise is the main culprit behind errors in WM performance. The result from our psychophysical experiments would argue for this interpretation: lower WM thresholds for luminance-defined items would imply more efficient processing of the stimuli and higher precision of the stored representations. In other words, luminance could effectively “amplify” activity related to stimulus representation, through a top-down control, in consequence allowing for better extraction and later storage of relevant features (Gazzaley, Cooney, McEvoy, Knight, & D’Esposito, 2005; Hillyard et al., 1998).

However, another possibility is that a more efficient representation and better signal-to-noise ratio can be achieved because of the way luminance is used in perception to build a perceptual representation of the stimulus, without necessarily invoking top-down influences.

Within this framework, the studies on visual binding using luminance and isoluminant stimuli are of particular interest. As mentioned in the introduction (see Chapter 1), Lehky (2000) showed that participants produce more feature binding errors when the stimuli are isoluminant. They argue that the errors are a result of poor form processing, and that feature binding of isoluminant features is less efficient and possibly slower (Leonards & Singer, 1998). Efficient feature integration might be especially important in WM tasks, where the relevant stimuli must be accurately (and quickly) encoded before they disappear from view, as is the case in the delayed match-to-sample task used in our experiments. It is possible that the luminance advantage might be therefore better explained not by top-down facilitation via luminance, but through less efficient isoluminant signals, which (on their own) cannot sufficiently support adequate stimulus encoding and representation, especially over time.

Analysis and task design utilised in our experiments cannot directly test which one of the two mechanisms (top-down facilitation versus low-level inefficiency of isoluminant encoding) would be a better explanation for the results presented in

this thesis. It is, of course, plausible that WM performance would not depend only on one mechanism, and both factors contribute to successful performance. Nevertheless, a way to provide a support (or undermine) the top-down account of our results would be to analyse the time-frequency dynamics of the EEG signal during WM encoding from our ERP experiment. By applying connectivity measures, such as time-frequency coupling, we could establish whether visual areas and frontal areas were reciprocally engaged in WM encoding; additionally, we could also assess the direction of causality by using more advanced connectivity techniques, such as DCM (which can also be successfully applied to EEG signals – e.g. see Dima et al., 2010). Additionally, modelling the source of the PI elicited by our stimuli might also be informative. As earlier source localisation studies have indicated, the PI is characterised by two neural generators; component's early portion (peak latency at 98 – 110 ms, as measured by Di Russo et al. (2002) seems to be localised in the dorsal extrastriate cortex, while its later portion (136 – 146 ms) is localised in the ventral extrastriate cortex. It was suggested that this early portion corresponds to spatial selection, while the later portion is related to attention-enhanced processing taking place in the ventral stream (Di Russo et al., 2003). Hence, tracking down the neural generators of the ERPs shown to be selectively modulated by luminance would help to clarify whether attention contributed to this modulation as well.

We also hypothesise that the encoding of luminance-defined stimuli results in better fidelity of the memory/perceptual representation, and hence better behavioural performance. This issue is related to the signal-to-noise ratio of the neural signals representing the encoded stimuli. With no time delay, detection and discrimination between visual stimuli is highly efficient. However, introducing a time delay between stimuli has a negative impact on discrimination performance (Wilken & Ma, 2004; Najima, Doshier, Chu, & Lu, 2011; Salmela, 2012). Furthermore, the representation of the majority of visual features (such as orientation or contrast) decays over time (Pasternak & Greenlee, 2005). It has been argued (Bays, 2014; Bays et al., 2011) that increasing the number of stimuli held in memory increases the neural noise, and that such noise is the main source of errors in WM. It is also conceivable that the neural noise accumulates

over time, also contributing to less precise working memory representations, and thus leading to errors (Salmela et al. 2012). In line with this accounts, the results of our psychophysical experiments (see Chapter 4) showed that the observers needed less stimulus contrast to perform a delayed match-to-sample task with luminance-defined stimuli than with isoluminant shapes, even if the number of remembered items was high. This suggests that WM system is more efficient in processing luminance-defined stimuli, which could be the result of better fidelity and reduced noise.

This leads to an interesting conclusion. Even if perception and working memory share similar mechanisms and the underlying neural architecture (Harrison & Tong, 2009; Pasternak & Greenlee, 2005), the efficiency of the visual working memory system seems to be inferior to that of perception (Salmela et al., 2012). In other words, even though the recently proposed sensory recruitment hypothesis (D'Esposito & Postle, 2015) emphasizes that the same areas are involved in encoding and storage of visual information, one should remember that this does not imply that the fidelity and neural noise is invariant to time delay and a number of encoded stimuli. Thus, it is important to compare the efficiency of both systems under such conditions, as well as to contrast new findings with our extensive knowledge of the nuts and bolts of the visual system.

The above considerations point to an obvious direction which future studies should undertake in order to follow up on our experiments. More specifically, it is important to note that we did not measure fidelity or neural noise as such directly. In other studies, good fidelity (also referred to as resolution and precision) is defined with respect to irrelevant stimuli (e.g. Gazzaley & Nobre, 2012). In other words, if the target stimuli are clearly distinguishable from non-targets or distractors, it means that it is represented with a very good resolution. Other studies attempted to directly test the precision of WM by using a task where participants are required to adjust the test stimulus in order to match stimulus held in memory. For example, Bays et al. (2011) used a task where participants were required to remember orientations of coloured bars. After a memory delay, participants would adjust the orientation of the final bar to try to

reproduce target's orientation. Difference between target's and probe's orientation served as a measure of recall error and precision.

To directly test the assertion that luminance has a considerable impact on fidelity, it would be useful to employ a similar task. For now, our interpretation of the data remains somewhat indirect, based on available literature and the properties of the visual system. A more direct fidelity measure would be certainly beneficial.

32.2. Contribution of luminance signals to memory-probe comparison

Interestingly, we found that the luminance advantage in the match-to-sample task was pronounced in trials where the memory probe mismatched the remembered items. This finding seems to be replicated in healthy controls in the pilot schizophrenia study (See Chapter 5) and in an unpublished study performed in a different lab, but using similar design (Haenschel, Kosilo & Martinovic, 2012). To understand this result, we need to appreciate that successful comparison between memory representation and incoming/currently perceived stimuli is achieved differently in the match and mismatch conditions. This deserves a more detailed discussion, which will be presented in the section below.

32.3. Comparison between WM representation and currently-perceived stimuli – insights from WM literature.

Episodic and long-term memory is generally considered to be specially tuned to detection of familiarity (Davelaar, Tian, Weidemann, & Huber, 2011b). The distinction between detecting familiarity or novelty is analogical to our match and mismatch conditions, respectively. Notably, however, the process behind the comparison between memory representation and incoming stimuli, and the consequences for the memory performance, has also received less attention over

the years (Hyun et al., 2009)¹¹. The current available empirical evidence and theoretical accounts highlight however that these processes are not equivalent. For example, Bledowski, Kaiser, Wibral, Yildiz-Erzberger, & Rahm (2011) report that mismatch-dissimilar probes were accurately rejected regardless of memory load. On the other hand, rejecting match probes or probes similar to sample stimuli was worse with increasing WM load. Bledowski et al. (2011) regard the results as evidence that working memory comparisons share similar mechanisms to long-term memory comparisons, and that these are based on similarity summation.

As mentioned at the beginning of this chapter, top-down signals from the prefrontal cortex to sensory areas are important for WM. Interestingly, evidence for this came from primate studies looking at the function of inferotemporal cortex in the absence of inputs from prefrontal cortex (e.g. Tomita et al., 1999). Inferotemporal cortex forms a final stage in the dorsal visual stream and is considered crucial to object recognition (e.g. Tanaka, 1996). Neurons in the IT areas (in monkeys) are also responsive to aspects of shapes that are already segregated from the background (Baylis & Driver, 2001). Crucially to our findings, neurons in this area demonstrate match suppression as well as novelty enhancement; more specifically, nonmatching stimulus evokes larger responses than the same stimuli presented as a match (Constantinidis & Procyk, 2004; Miller, Li, & Desimone, 1991).

This, by itself, does not provide an answer as to how the luminance signals provide an advantage over isoluminant signals. However, there are a few interesting, loosely connected clues.

More specifically, based on the match-suppression and novelty-enhancement properties of the IT neurons, Miller, Li, & Desimone (1993) suggested that one can think of the comparison between memory representation and currently

¹¹ Perhaps with the exception of studies related to change blindness (Simons, Levin, & Haber, 1997; Simons & Rensink, 2005), where much more attention is drawn to these comparisons due to the nature of this phenomenon.

perceived stimuli as a process analogical to figure-ground segmentation, but in a *temporal*, rather than *spatial*, domain. Miller et al. (1993) build this analogy by pointing out that the visual system is highly responsive to contrasts, in the sense that two opposing features are compared. According to this analogy, memory representation (or, as Miller et al. put it more broadly, “the past”) functions as a surround, with which the incoming, currently perceived stimuli is contrasted. This analogy is especially attractive given that detection of luminance contours is an important step in figure-ground segmentation process (Peterson & Gibson, 1993; Peterson & Gibson, 1994; Rubin, 2001)¹². Furthermore, as mentioned above, it is the early luminance projections from the inferotemporal cortex that form the basis for luminance advantage in object recognition (Bar, 2003; Kveraga et al., 2007). It is tempting to explore the nature of such temporal figure-ground segmentation further, although it is not clear to what extent this is indeed a good analogy for memory-perception comparisons in WM, and whether luminance would indeed be somehow beneficial in this instance.

To further draw on how match and mismatch WM comparisons are achieved, and how luminance could enhance mismatch comparisons, in particular, we can turn towards the perceptual literature. I will now describe how match/mismatch comparison is achieved in perceptual comparison studies and how this may inform memory-percept comparisons in WM in general, and luminance advantage in particular.

32.4. Insights from perceptual comparison studies

According to Hyun et al. (2009), in order to describe the processes behind comparing memory representations with currently perceived stimuli, one can turn to the literature on perceptual comparisons. Studies in this field use a

¹² Although contour recognition alone is not enough for separating figure from the background, as a simple contour do not, by itself, carry information as to which side of the contour is the “figure”, and which one is the “background” – a problem referred to as *Zusammengehörigkeit* (“belonging together”) by Edward Rubin in his classic work (Rubin, 2001).

similar methodology as WM experiments, i.e. they require participants to make same/different decisions during change detection or match-to-sample tasks. Therefore, perceptual comparison literature can provide a step towards the conceptualization of comparison processes in WM. This approach is sensible considering the already described overlap between WM and perception (Harrison & Tong, 2009; see Chapter 1).

Hyun et al. (2009) proposed, for instance, that mechanisms of change detection, and thus comparison, can be regarded as equivalent to visual search. According to this view, the presence of change is detected using unlimited – capacity comparison process, which is analogical to responses to salient features during visual search tasks. Also, targets defined by the presence of a feature are detected more efficiently than the targets defined by the absence of a feature (Treisman, 1998). In other words, detection of change can be more efficient.

In one study, Davelaar et al. (2011b) attempted to establish whether change detection is made based on the strength of the match signal (detection of familiarity), or on the magnitude of the mismatch signal (detection of novelty). Using MEG, they presented participants with a same/different judgement task. In terms of neural responses, they failed to detect different patterns of activity for the match or mismatch responses, interpreting this as an evidence for a common neural source of such comparison. At the same time, the activity was larger for mismatch responses. Behaviourally, they showed that, when participants were cued with targets in trials preceding the same/different judgement, their responses were slower. At the same time, when participants were primed with the non-target cue, their response times improved. Together, the data presented in their study is taken as an evidence for change detection, rather than familiarity detection, as the driver for same/different judgements.

The authors propose a habituation account to explain their findings on a neural level (Davelaar et al., 2011b). When the target prime is salient, it causes the given stimuli to be habituated; when the response probe appears, the habituation state is still persistent. As a result, a subject is able to detect novel stimuli more effectively. At a neural level, it is hypothesised that neurons which were

habituated to a given stimulus (i.e. ones that have been active recently) do not have enough neurotransmitters available to effectively transmit activation to other neurons. On the other hand, inactive neurons will have enough neurotransmitters available to transmit its activation to other neurons. Thus, same/judgement task would be based on response to novelty, rather than similarity. Similar conclusions were drawn from other experiments (Huber, 2008). They showed that, if the exposure to the stimuli matching the target presented prior to judgement was sufficiently long, behavioural performance was worse unless the final target represented a change. Again, these results can be explained in terms of habituation.

Another model described by Johnson et al. (2009) model draws on the similar assumption in relation to same/different judgements. However, their model is applied explicitly to WM, rather than perceptual judgement. Johnson et al. described the neural architecture that underlies WM encoding and maintenance as well as possible mechanisms behind the comparison of current perceptual input with memory representations (inspired by canonical cortical circuit by Douglas & Martin, 2004 and Douglas, Martin, & Whitteridge, 1989). According to this model, there are two excitatory fields (perceptual field and working memory field), and one inhibitory field. Current input enters the perceptual field while working memory field receives excitatory input primarily from the perceptual field. Sustained activation occurs due to excitatory and inhibitory interactions between neurons in those fields.

The model adds another layer to account for responses in change detection tasks – the response field. For instance, when presented colour is the same as a colour currently stored in memory, activation in the perceptual field remains below a threshold. This is due to neurons in this field being inhibited as a result of the previous exposure to that colour. Therefore, the input to the response layer comes from the working memory field – and a ‘same’ response is made. If on the other hand, a colour enters an uninhibited perceptual field, it generates an activation which is relayed to the response field, and ‘different’ judgement ‘wins the competition’.

In short, Johnson's model suggests that the "match" response is a default one since the activation of the change-detection node in their model remains below the threshold due to inhibition; if the threshold is not reached, the system produces a "match/same" response. As Johnson et al. note, the "match" response comes from WM mode, while the "mismatch" response is driven by perceptual field. Incoming stimuli that mismatches the stored WM representation enters an uninhibited perceptual field, allowing for an activity peak exceeding the judgment threshold.

An interesting and, at first, counterintuitive behavioural prediction of this model is that the change detection will be enhanced if the mismatch stimuli have similar features. According to their model, WM representations excite the inhibitory field; if the inhibition is strong, the perceptual field is strongly inhibited; this raises the threshold needed for the system to reach a "mismatch" decision (and if such threshold is not exceeded, the system produces the default "match" response). In line with this, similar representations in WM field would interact and inhibit one another; as a result, their excitation of the inhibitory field is weaker; which, in turn, makes the perceptual field less inhibited, meaning a lower threshold is needed to reach a mismatch response.

This prediction could be relevant to our study. Even though similarity was not tested in our experiment directly, the stimuli that we have used are (at least qualitatively) similar. Moreover, the stimuli that participants remember are always presented at the same DKL direction as the probe; thus, it could be argued that the shapes must produce similar representations (even if the shape outline might be different). Indeed, our results show that responses to mismatch probes produce more accurate results than match probes in general. However, the main question is why would luminance pose an advantage over isoluminant shapes at match, and especially at higher WM loads?

If we were to use Johnson et al.'s model to explain this results, one could say that luminance-driven WM representations are "sharper" and thus produce weaker excitatory inputs to the inhibitory field, leaving the perceptual field receptive to incoming, mismatching stimuli (as outlined in the example above). This can be

linked to a better signal-to-noise ratio achieved with luminance inputs, as discussed earlier in the discussion; less noisy neural representations could drive weaker excitatory inputs to the inhibitory field. This would explain why luminance produced better mismatch responses than mismatching isoluminant stimuli. While isoluminant mismatch stimuli also result in better responses due to the uninhibited perceptual field, luminance would be superior due to sharper representation in memory.

Another possibility is that isoluminant and luminance shapes provide a similarly weak excitatory input to the inhibitory field, but due to a less noisy perceptual representation of the incoming stimuli it is easier for luminance inputs to exceed the threshold, leading to fewer errors. On the other hand, isoluminant inputs are noisy and thus they would more often than not stay below the threshold, producing more errors. To directly test these two predictions against each other, it would be useful to quantify errors in response to mismatching stimuli for luminance and isoluminant conditions (as already discussed above). If the magnitude of errors is higher for the isoluminant conditions, this would indicate that indeed the neural representation is far noisier than for luminance stimuli.

Johnson et al.'s model is of course not the only one that attempts to account for memory or perceptual comparison process. Since Hyun et al. (2009) suggested that the perceptual comparison literature can be as well used to explain comparisons between incoming stimuli with existing WM representations, this opens a path to a broad perceptual decision – making literature; dwelling deeper into this topic is however outside the scope of this thesis (although it does indicate one possible direction where our research question can lead us). Some of the models, similar to Johnson's, also discuss repetition suppression phenomenon, citing it as a driving factor behind more optimal match versus mismatch responses (e.g. Engel & Wang, 2011; Hussar & Pasternak, 2012) ¹³.

¹³ Notably, the relative advantage of mismatch responses (manifested behaviourally in better accuracy and/or faster reaction times) can be overridden by top – down inputs, for example, in tasks that require the subject to specifically respond to match trials.

Of note are the experiments by Hussar & Pasternak (2012), who recorded the activity of prefrontal cortex neurons from monkeys performing a delayed motion direction comparison. Among other findings, they also observed that the activity signalling different trials (equivalent to our mismatch) emerged earlier than the activity signalling same (match trials). They hypothesised that this difference is due to local origins of the more optimal “different” responses in the middle temporal area MT (V5). Better responses to “same” trials would, on the other hand, originate via slower, top-down inputs (Lui & Pasternak, 2011). According to this view, a comparison between sensory representations would take place in MT, and thus would be achieved quicker. Although we did not observe a specific advantage in terms of RT for mismatching luminance stimuli, Lui and Pasternak’s account is an attractive one due to the fact that area MT forms part of the dorsal visual stream, which receives predominant magnocellular inputs. It is, of course, hardly surprising, given that this area is dedicated to motion detection; it is also problematic to directly relate that to the findings of our study, given that our experiment does not involve motion detection and thus cannot be localised to the area MT specifically. Nevertheless, it is, to an extent, sensible to hypothesise that efficient feed-forward signalling from this area may produce a more optimal behavioural performance for luminance stimuli over isoluminant stimuli. The lack of reaction time advantage for luminance over isoluminant stimuli does not necessarily exclude that possibility; Lui and Pasternak also acknowledge that the late mismatch- over-match advantage would be also driven by slower top-down signals. It is conceivable that the reaction time advantage was overridden, but the accuracy advantage achieved by more efficient top-down signalling has been preserved.

33. Summary and implications for future research

Overall, the psychophysical, behavioural, and ERP data presented in this thesis support the notion that encoding luminance-defined shapes into WM results in relatively better performance than encoding isoluminant shapes. Although the exact mechanism behind this advantage cannot be directly inferred from the current data, we propose that the general factor behind the luminance advantage is a better signal-to-noise ratio of the stored representations and enhanced communication between sensory and frontal areas. Because the luminance advantage is most pronounced at higher WM loads, it supports the notion that WM and perception are intrinsically linked. Furthermore, our ERP data suggests that this benefit might manifest itself already during the early WM stages.

To fully understand factor contributing to successful WM performance, we argue that is necessary to focus on the encoding stage of WM when the dynamic interactions between perception and WM are likely to take place. Luminance benefit was also pronounced in cases when the probe did not match the previously presented stimuli. This also points to the possible importance of memory/perception interaction, but at the retrieval stage as well, when the processes behind contrasting the memory representation with currently perceived stimuli are taking place. This opens up new possibilities. In particular, it emphasizes the importance of studying how the memory/percept comparison is achieved, and how it is linked to the fidelity of encoding at earlier stages. In addition to encoding, retrieval might be another WM stage where interaction between WM and perception is especially important for performance. Findings from the perceptual comparison literature might prove to be relevant here (Hyun et al., 2009), and establishing whether WM comparisons work analogically to perceptual comparisons might be a good starting point.

Crucially, the results of the current study emphasize the need to consider the validity of collapsing responses across match and mismatch conditions. It appears that it might not be the best strategy, as match and mismatch appear to be tapping into different processes which might impact performance in a different manner.

Conclusion

Vision starts from detecting spots of light and advances further through computing edges, contours, colours, segmenting objects from the background, and finally combining elemental visual features into meaningful representations. A classical approach in vision science would be to compare the performance of luminance and chromatic channels to determine whether they are equally efficient in sustaining different aspects of vision. Our experiments show that it is possible to use this approach to investigate the capability of visual channels not only during the on-line vision but also when the visual input is no longer present in the visual field. Achieving this requires working memory. Working memory processing involves encoding and sustaining the representation of the visual stimulus over time. Subsequently, the representation needs to be accessed to meet current task demands, such as comparison of the memory representation with a newly presented stimulus. Consequently, it is important to consider how the different visual channels are contributing to these processes. The results presented in this thesis suggest that the visual channels do not perform equally in working memory tasks, with the luminance providing a benefit over isoluminant signals. This finding adds to the growing body of literature concerned with mechanisms behind working memory performance in health and disease.

References

- Adler, L. E., Olincy, A., Waldo, M., Harris, J. G., Griffith, J., Stevens, K., ... Freedman, R. (1998). Schizophrenia, sensory gating, and nicotinic receptors. *Schizophrenia Bulletin*, 24(2), 189–202. <http://www.ncbi.nlm.nih.gov/pubmed/9613620>
- Agam, Y., Hyun, J. – S., Danker, J. F., Zhou, F., Kahana, M. J., & Sekuler, R. (2009). Early neural signatures of visual short-term memory. *NeuroImage*, 44(2), 531–6. <http://doi.org/10.1016/j.neuroimage.2008.09.018>
- Agam, Y., & Sekuler, R. (2007). Interactions between working memory and visual perception: an ERP/EEG study. *NeuroImage*, 36(3), 933–42. <http://doi.org/10.1016/j.neuroimage.2007.04.014>
- Algom, D. (2001). Theories and methods of memory psychophysics: Links to cognitive psychology. In E. Sommerfield, R. Kompass & T. Lachman (Eds.), *Fechner Day 2001* (pp. 69 – 74), Leipzig: International Society for Psychophysics.
- Algom, D., Wolf, Y., & Bergman, B. (1985). Integration of stimulus dimensions in perception and memory: composition rules and psychophysical relations. *Journal of Experimental Psychology. General*, 114(4), 451–71. <http://www.ncbi.nlm.nih.gov/pubmed/2934498>
- Andersen, R. A. (1989). Visual and Eye Movement Functions of the Posterior Parietal Cortex. *Annual Review of Neuroscience*, 12(1), 377–403. <http://doi.org/10.1146/annurev.ne.12.030189.002113>
- Awh, E., Vogel, E. K., & Oh, S. H. (2006). Interactions between attention and working memory. *Neuroscience*, 139(1), 201–208. <http://doi.org/10.1016/j.neuroscience.2005.08.023>
- Baddeley, A. (2003). Working memory: looking back and looking forward. *Nature Reviews. Neuroscience*, 4(10), 829–39. <http://doi.org/10.1038/nrn1201>
- Baddeley, A. D., & Hitch, G. (1974). Working Memory (pp. 47–89). [http://doi.org/10.1016/S0079-7421\(08\)60452-1](http://doi.org/10.1016/S0079-7421(08)60452-1)
- Baizer, J. S., Ungerleider, L. G., & Desimone, R. (1991). Organization of visual inputs to the inferior temporal and posterior parietal cortex in macaques. *The Journal of Neuroscience : The Official Journal of the Society for Neuroscience*, 11(1), 168–90. <http://www.ncbi.nlm.nih.gov/pubmed/1702462>
- Bar, M. (2003). A cortical mechanism for triggering top-down facilitation in visual object recognition. *Journal of Cognitive Neuroscience*, 15(4), 600–9. <http://doi.org/10.1162/089892903321662976>
- Barcelo, F., Suwazono, S., & Knight, R. T. (2000). Prefrontal modulation of visual processing in humans. *Nature Neuroscience*, 3(4), 399–404.
- Barceló, F., Martín-Loeches, M., & Rubia, F. J. (1997). Event-related potentials during memorization of spatial locations in the auditory and visual modalities. *Electroencephalography and Clinical Neurophysiology*, 103(2), 257–267. [http://doi.org/10.1016/S0013-4694\(97\)96610-4](http://doi.org/10.1016/S0013-4694(97)96610-4)
- Barch, D. M., Bustillo, J., Gaebel, W., Gur, R., Heckers, S., Malaspina, D., ... Carpenter, W. (2013). Logic and justification for dimensional assessment of symptoms and related clinical phenomena in psychosis: Relevance to DSM-5. *Schizophrenia Research*. <http://doi.org/10.1016/j.schres.2013.04.027>
- Barch, D. M., Carter, C. S., Braver, T. S., Sabb, F. W., MacDonald, A., Noll, D. C., & Cohen, J. D. (2001). Selective Deficits in Prefrontal Cortex Function in Medication-Naive Patients With Schizophrenia. *Archives of General Psychiatry*, 58(3), 280. <http://doi.org/10.1001/archpsyc.58.3.280>
- Barsalou, L. W. (1999). Perceptual symbol systems. *The Behavioral and Brain Sciences*, 22(4), 577 – 609–60. <http://www.ncbi.nlm.nih.gov/pubmed/11301525>
- Baumeister, A. A., & Francis, J. L. (2002). Historical Development of the Dopamine Hypothesis of Schizophrenia. *Journal of the History of the Neurosciences*, 11(3), 265–277. <http://doi.org/10.1076/jhin.11.3.265.10391>
- Baylis, G. C., & Driver, J. (2001). Shape-coding in IT cells generalizes over contrast and mirror reversal, but not figure-ground reversal. *Nature Neuroscience*, 4(9), 937–942. <http://doi.org/10.1038/nn0901-937>
- Bays, P., & Husain, M. (2008). Dynamic shifts of limited working memory resources in human vision. *Science*, 321(5890), 851–854. <http://doi.org/10.1126/science.1158023>
- Bays, P. M. (2014). Noise in Neural Populations Accounts for Errors in Working Memory. *Journal of Neuroscience*, 34(10), 3632–3645. <http://doi.org/10.1523/JNEUROSCI.3204-13.2014>

- Bays, P. M., Marshall, L., & Husain, M. (2011). Temporal dynamics of encoding, storage, and reallocation of visual working memory, *II*, 1-15. <http://doi.org/10.1167/11.10.6>.
- Beaudot, W. H. a, & Mullen, K. T. (2005). Orientation selectivity in luminance and color vision assessed using 2-d bandpass filtered spatial noise. *Vision Research*, *45*(6), 687-96. <http://doi.org/10.1016/j.visres.2004.09.023>
- Beaudot, W. H., & Mullen, K. T. (2003). How long range is contour integration in human color vision? *Vis Neurosci*, *20*(1), 51-64.
- Behrmann, M., Geng, J. J., & Shomstein, S. (2004). Parietal cortex and attention. *Current Opinion in Neurobiology*, *14*(2), 212-217. <http://doi.org/10.1016/j.conb.2004.03.012>
- Berrios, G. E., Luque, R., & Villagrán, J. M. (2003). Schizophrenia: a conceptual history. *International Journal of Psychology and Psychological Therapy*, *3*(2).
- Bisley, J. W., Zaksas, D., Droll, J., & Pasternak, T. (2003). Activity of Neurons in Cortical Area MT During a Memory for Motion Task. *J Neurophysiol*, 286-300. <http://doi.org/10.1152/jn.00870.2003>
- Björkman, M., Lundberg, I., & Tärnblom, S. (1960). On the relationship between percept and memory: a psychophysical approach. *Scandinavian Journal of Psychology*, *1*(1), 136-144. <http://doi.org/10.1111/j.1467-9450.1960.tb01292.x>
- Bledowski, C., Cohen Kadosh, K., Wibrál, M., Rahm, B., Bittner, R. A., Hoehstetter, K., ... Linden, D. E. J. (2006). Mental Chronometry of Working Memory Retrieval: A Combined Functional Magnetic Resonance Imaging and Event-related Potentials Approach. *Journal of Neuroscience*, *26*(3), 821-829. <http://doi.org/10.1523/JNEUROSCI.3542-05.2006>
- Bledowski, C., Kaiser, J., Wibrál, M., Yildiz-Erzberger, K., & Rahm, B. (2011). Separable Neural Bases for Subprocesses of Recognition in Working Memory. *Cerebral Cortex (New York, N.Y. : 1991)*, 1-9. <http://doi.org/10.1093/cercor/bhr276>
- Bleuler, E. (1908). Die Prognose der Dementia Praecox - Schizophreniegruppe. *Allgemeine Zeitschrift für Psychiatrie*, *65*, 436 - 464.
- Bleuler, E. (1911). *Dementia Praecox oder Gruppe der Schizophrenien*. Leipzig: Deuticke.
- Bosch, V., Mecklinger, A., & Friederici, A. D. (2001). Slow cortical potentials during retention of object, spatial, and verbal information. *Cognitive Brain Research*, *10*(3), 219-237. [http://doi.org/10.1016/S0926-6410\(00\)00040-9](http://doi.org/10.1016/S0926-6410(00)00040-9).
- Brainard, D. H., Pelli, D. G., & Robson, T. (2002). Display characterization. In *Encyclopedia of imaging science and technology* (pp. 172 - 188).
- Brass, M., & Von Cramon, D. Y. (2004). Decomposing components of task preparation with functional magnetic resonance imaging. *Journal of Cognitive Neuroscience*, *16*(4), 609-620. <http://doi.org/10.1162/089892904323057335>
- Braver, T. S., Barch, D. M., & Cohen, J. D. (1999). Cognition and control in schizophrenia: a computational model of dopamine and prefrontal function. *Biological Psychiatry*, *46*(3), 312-328. [http://doi.org/10.1016/S0006-3223\(99\)00116](http://doi.org/10.1016/S0006-3223(99)00116)
- Brewster, D., & Newton, I. (1855). *Memoirs of the life, writings and discoveries of Sir Isaac Newton (Vol. 2)*. Constable.
- Broadbent, A. D. (2004). A critical review of the development of the CIE1931 RGB color-matching functions. *Color Research & Application*, *29*(4), 267-272. <http://doi.org/10.1002/col.20020>
- Bromet, E. J., & Fennig, S. (1999). Epidemiology and natural history of schizophrenia. *Biological Psychiatry*, *46*(7), 871-81. <http://www.ncbi.nlm.nih.gov/pubmed/10509170>
- Bullier, J., & Nowak, L. G. (1995). Parallel versus serial processing: New vistas on the distributed organization of the visual system. *Current Opinion in Neurobiology*, *5*(4), 497-503. [http://doi.org/10.1016/0959-4388\(95\)80011-5](http://doi.org/10.1016/0959-4388(95)80011-5)
- Butler, P. D., Abeles, I. Y., Weiskopf, N. G., Tambini, A., Jalbrzikowski, M., Legatt, M. E., ... Javitt, D. C. (2009). Sensory contributions to impaired emotion processing in schizophrenia. *Schizophrenia Bulletin*, *35*(6), 1095-107. <http://doi.org/10.1093/schbul/sbp109>
- Butler, P. D., & Javitt, D. C. (2005). Early-stage visual processing deficits in schizophrenia. *Current Opinion in Psychiatry*, *18*(2), 151-7. <http://www.ncbi.nlm.nih.gov/pubmed/16639168>
- Butler, P. D., Martinez, A., Foxe, J. J., Kim, D., Zemon, V., Silipo, G., ... Javitt, D. C. (2007). Subcortical visual dysfunction in schizophrenia drives secondary cortical impairments. *Brain : A Journal of Neurology*,

130(Pt 2), 417–30. <http://doi.org/10.1093/brain/awl233>

- Butler, P. D., Schechter, I., Zemon, V., Schwartz, S. G., Greenstein, V. C., Gordon, J., ... Javitt, D. C. (2001). Dysfunction of Early – Stage Visual Processing in Schizophrenia. *American Journal of Psychiatry*, 158(7), 1126–1133. <http://doi.org/10.1176/appi.ajp.158.7.1126>
- Butler, P. D., Silverstein, S. M., & Dakin, S. C. (2008). Visual Perception and Its Impairment in Schizophrenia. *Biological Psychiatry*, 64(1), 40–47. <http://doi.org/10.1016/j.biopsych.2008.03.023>
- Butler, P. D., Zemon, V., Schechter, I., Saperstein, A. M., Hoptman, M. J., Lim, K. O., ... Javitt, D. C. (2005). Early-stage visual processing and cortical amplification deficits in schizophrenia. *Archives of General Psychiatry*, 62(5), 495–504. <http://doi.org/10.1001/archpsyc.62.5.495>
- Buzsáki, G., Anastassiou, C. A., & Koch, C. (2012). The origin of extracellular fields and currents — EEG, ECoG, LFP and spikes. *Nature Reviews Neuroscience*, 13(6), 407–420. <http://doi.org/10.1038/nrn3241>
- Buzsáki, G., & Draguhn, A. (2004). Neuronal oscillations in cortical networks. *Science (New York, N.Y.)*, 304(5679), 1926–9. <http://doi.org/10.1126/science.1099745>
- Buzsáki, G., & Wang, X. – J. (2012). Mechanisms of Gamma Oscillations. *Annual Review of Neuroscience*, 35(1), 203–225. <http://doi.org/10.1146/annurev-neuro-062111-150444>
- Cadenhead, K. S., Dobkins, K., McGovern, J., & Shafer, K. (2013). Schizophrenia spectrum participants have reduced visual contrast sensitivity to chromatic (red/green) and luminance (light/dark) stimuli: New insights into information processing, visual channel function, and antipsychotic effects. *Frontiers in Psychology*, 4(AUG), 535. <http://doi.org/10.3389/fpsyg.2013.00535>
- Calderone, D. J., Martinez, A., Zemon, V., Hoptman, M. J., Hu, G., Watkins, J. E., ... Butler, P. D. (2013). Comparison of psychophysical, electrophysiological, and fMRI assessment of visual contrast responses in patients with schizophrenia. *NeuroImage*, 67, 153–162. <http://doi.org/10.1016/j.neuroimage.2012.11.019>
- Callicott, J. H., Bertolino, A., Mattay, V. S., Langheim, F. J. P., Duyn, J., Coppola, R., ... Weinberger, D. R. (2000). Physiological Dysfunction of the Dorsolateral Prefrontal Cortex in Schizophrenia Revisited. *Cerebral Cortex*, 10(11), 1078–1092. <http://doi.org/10.1093/cercor/10.11.1078>
- Canolty, R. T., Edwards, E., Dalal, S. S., Soltani, M., Nagarajan, S. S., Kirsch, H. E., ... Knight, R. T. (2006). High gamma power is phase-locked to theta oscillations in human neocortex. *Science (New York, N.Y.)*, 313(5793), 1626–1628. <http://doi.org/10.1126/science.1128115>
- Carter, C. S., & Barch, D. M. (2007). Cognitive Neuroscience-based Approaches to Measuring and Improving Treatment Effects on Cognition in Schizophrenia: The CNTRICS Initiative. *Schizophrenia Bulletin*, 33(5), 1131–1137. <http://doi.org/10.1093/schbul/sbm081>
- Cavanagh, P., Tyler, C. W., & Favreau, O. E. (1984). Perceived velocity of moving chromatic gratings. *Journal of the Optical Society of America. Optics and Image Science*, 1(8), 893–9. <http://www.ncbi.nlm.nih.gov/pubmed/6470841>
- Chapman, J. (1966). The Early Symptoms of Schizophrenia. *The British Journal of Psychiatry*, 112(484).
- Chatterjee, S., & Callaway, E. M. (2002). S-cone Contributions to the Magnocellular Visual Pathway in Macaque Monkey. *Neuron*, 35(6), 1135–1146. [http://doi.org/10.1016/S0896-6273\(02\)00874-7](http://doi.org/10.1016/S0896-6273(02)00874-7)
- Chaumon, M., Bishop, D. V. M., & Busch, N. A. (2015). A practical guide to the selection of independent components of the electroencephalogram for artifact correction. *Journal of Neuroscience Methods*, 250, 47–63. <http://doi.org/10.1016/j.jneumeth.2015.02.025>
- Chen, Y., Levy, D. L., Sheremata, S., & Holzman, P. S. (2004). Compromised late – stage motion processing in schizophrenia. *Biological Psychiatry*, 55(8), 834–841. <http://doi.org/10.1016/j.biopsych.2003.12.024>
- Chen, Y., Nakayama, K., Levy, D., Matthyse, S., & Holzman, P. (2003). Processing of global, but not local, motion direction is deficient in schizophrenia. *Schizophrenia Research*, 61(2–3), 215–27. [http://doi.org/10.1016/S0920-9964\(02\)00222-0](http://doi.org/10.1016/S0920-9964(02)00222-0)
- Christensen, A. R. (2014). Media, Hot & Cold. Making Sense of Temperature in Early Psychophysics. *International Journal of Communication*, 8, 5.
- Christophel, T. B., Klink, P. C., Spitzer, B., Roelfsema, P. R., & Haynes, J. – D. (2017). The Distributed Nature of Working Memory. *Trends in Cognitive Sciences*, 21(2), 111–124. <http://doi.org/10.1016/j.tics.2016.12.007>
- Chun, M. M. (2011). Visual working memory as visual attention sustained internally over time. *Neuropsychologia*, 49(6), 1407–1409. <http://doi.org/10.1016/j.neuropsychologia.2011.01.029>

- CIE (1932). Commission internationale de l'Eclairage proceedings, 1931. Cambridge: Cambridge University Press.
- Clery, S., Bloj, M., & Harris, J. M. (2013). Interactions between luminance and color signals: Effects on shape. *Journal of Vision*, 13(5), 16–16. <http://doi.org/10.1167/13.5.16>
- Constantinidis, C., & Procyk, E. (2004). The primate working memory networks. *Cognitive, Affective & Behavioral Neuroscience*, 4(4), 444–65. <http://www.ncbi.nlm.nih.gov/pubmed/15849890>
- Cooper, B., Sun, H., & Lee, B. B. (2012). Psychophysical and physiological responses to gratings with luminance and chromatic components of different spatial frequencies. *Journal of the Optical Society of America. A, Optics, Image Science, and Vision*, 29(2), A314 – 23. <http://www.ncbi.nlm.nih.gov/pubmed/22330395>
- Corbetta, M., & Shulman, G. L. (2002). Control of goal-directed and stimulus-driven attention in the brain. *Nature Reviews Neuroscience*, 3(3), 215–229. <http://doi.org/10.1038/nrn755>
- Crognale, M. a. (2002). Development, maturation, and aging of chromatic visual pathways: VEP results. *Journal of Vision*, 2(6), 438–450. <http://doi.org/10.1167/2.6.2>
- Croizé, A. C., Ragot, R., Garnero, L., Ducorps, A., Péligrini – Issac, M., Dauchot, K., ... Burnod, Y. (2004). Dynamics of parietofrontal networks underlying visuospatial short-term memory encoding. *NeuroImage*, 23(3), 787–799. <http://doi.org/10.1016/j.neuroimage.2003.10.052>
- D'Esposito, M. (2007). From cognitive to neural models of working memory. *Philosophical Transactions of the Royal Society of London. Series B, Biological Sciences*, 362(1481), 761–72. <http://doi.org/10.1098/rstb.2007.2086>
- D'Esposito, M., & Postle, B. R. (2015). The Cognitive Neuroscience of Working Memory. *Annual Review of Psychology*, 66(1), 115–142. <http://doi.org/10.1146/annurev-psych-010814-015031>
- D'Esposito, M., Postle, B. R., & Rypma, B. (2000). Prefrontal cortical contributions to working memory: evidence from event-related fMRI studies. *Experimental Brain Research*, 133(1), 3–11. <http://doi.org/10.1007/s002210000395>
- da Silva, F. L. (2009). EEG: Origin and Measurement. In *EEG – fMRI* (pp. 19–38). Berlin, Heidelberg: Springer Berlin Heidelberg. http://doi.org/10.1007/978-3-540-87919-0_2
- Dacey, D. M., & Lee, B. B. (1994). The “blue – on” opponent pathway in primate retina originates from a distinct bistratified ganglion cell type. *Nature*, 367(6465), 731–5. <http://doi.org/10.1038/367731a0>
- Davelaar, E. J., Tian, X., Weidemann, C. T., & Huber, D. E. (2011a). A habituation account of change detection in same/different judgments. *Cognitive, Affective, & Behavioral Neuroscience*, 11(4), 608–626. <http://doi.org/10.3758/s13415-011-0056-8>
- Davelaar, E. J., Tian, X., Weidemann, C. T., & Huber, D. E. (2011b). A habituation account of change detection in same/different judgments. *Cognitive, Affective & Behavioral Neuroscience*, 11(4), 608–26. <http://doi.org/10.3758/s13415-011-0056-8>
- De Valois, K. K., & Kooi, F. (1991). Functional classification of parallel visual pathways. In *From pigments to perception* (pp. 165 – 171). Springer US.
- De Valois, K. K., Lakshminarayanan, V., Nygaard, R., Schluskel, S., & Sladky, J. (1990). Discrimination of relative spatial position. *Vision Research*, 30(11), 1649–1660. [http://doi.org/10.1016/0042-6989\(90\)90150-J](http://doi.org/10.1016/0042-6989(90)90150-J)
- De Valois, R. L. & De Valois, K. K. (1975) Neural coding of color. In *Handbook of Perception*, Vol 5, Seeing (Edited by Carterette E. C. and Friedman M. P.), pp. 117–166. Academic Press, New York
- Delorme, A., & Makeig, S. (2004). EEGLAB: an open source toolbox for analysis of single-trial EEG dynamics including independent component analysis. *Journal of Neuroscience Methods*, 134(1), 9–21. <http://doi.org/10.1016/j.jneumeth.2003.10.009>
- DeMarco, P., Pokorny, J., & Smith, V. C. (1992). Full-spectrum cone sensitivity functions for X – chromosome-linked anomalous trichromats. *Journal of the Optical Society of America. A, Optics and Image Science*, 9(9), 1465–76. <http://www.ncbi.nlm.nih.gov/pubmed/1527649>
- Derrington, M., Krauskopf, J., & Lennie, P. (1984). Chromatic mechanisms in lateral geniculate nucleus of macaque. *The Journal of Physiology*, 357, 241–265. <http://doi.org/10.1113/jphysiol.1984.sp015499>
- Desmedt, J. ., & Debecker, J. (1979). Wave form and neural mechanism of the decision P350 elicited without pre-stimulus CNV or readiness potential in random sequences of near-threshold auditory clicks and finger stimuli. *Electroencephalography and Clinical Neurophysiology*, 47(6), 648–670.

[http://doi.org/10.1016/0013-4694\(79\)90293-1](http://doi.org/10.1016/0013-4694(79)90293-1)

- Desmedt, J. E. (1980). P300 in Serial Tasks: an Essential Post-decision Closure Mechanism (pp. 682–686). [http://doi.org/10.1016/S0079-6123\(08\)61690-8](http://doi.org/10.1016/S0079-6123(08)61690-8)
- Desmedt, J. E., Bourget, M., Huy, N. T., & Delacuvellerie, M. (1984). The P40 and P100 Processing Positivities That Precede P300 Closure in Serial Somatosensory Decision Tasks. *Annals of the New York Academy of Sciences*, 425(1), 188–193. <http://doi.org/10.1111/j.1749-6632.1984.tb23531.x>
- Di Russo, F., Martínez, A., & Hillyard, S. A. (2003). Source Analysis of Event-related Cortical Activity during Visuospatial Attention. *Cerebral Cortex*, 13(5), 486–499. <http://doi.org/10.1093/cercor/13.5.486>
- Di Russo, F., Martínez, A., Sereno, M. I., Pitzalis, S., & Hillyard, S. A. (2002). Cortical sources of the early components of the visual evoked potential. *Human Brain Mapping*, 15(2), 95–111. <http://doi.org/10.1002/hbm.10010>
- Dima, D., Dietrich, D. E., Dillo, W., & Emrich, H. M. (2010). Impaired top-down processes in schizophrenia: A DCM study of ERPs. *NeuroImage*, 52(3), 824–832. <http://doi.org/10.1016/j.neuroimage.2009.12.086>
- Dima, D., Roiser, J. P., Dietrich, D. E., Bonnemann, C., Lanfermann, H., Emrich, H. M., & Dillo, W. (2009). Understanding why patients with schizophrenia do not perceive the hollow – mask illusion using dynamic causal modelling. *NeuroImage*, 46(4), 1180–1186. <http://doi.org/10.1016/j.neuroimage.2009.03.033>
- Dixon, W. J., & Mood, A. M. (1948). A Method for Obtaining and Analyzing Sensitivity Data. *Journal of the American Statistical Association*, 43(241), 109–126. <http://doi.org/10.1080/01621459.1948.10483254>
- Donchin, E. (1981). Surprise!... Surprise? *Psychophysiology*, 18(5), 493–513. <http://doi.org/10.1111/j.1469-8986.1981.tb01815.x>
- Doniger, G. M., Foxe, J. J., Murray, M. M., Higgins, B. A., & Javitt, D. C. (2002). Impaired Visual Object Recognition and Dorsal/Ventral Stream Interaction in Schizophrenia. *Archives of General Psychiatry*, 59(11), 1011. <http://doi.org/10.1001/archpsyc.59.11.1011>
- Donohoe, G., Morris, D. W., De Sanctis, P., Magno, E., Montesi, J. L., Garavan, H. P., ... Foxe, J. J. (2008). Early Visual Processing Deficits in Dysbindin – Associated Schizophrenia. *Biological Psychiatry*, 63(5), 484–489. <http://doi.org/10.1016/j.biopsych.2007.07.022>
- Dorph-Petersen, K. A., Pierri, J. N., Wu, Q., Sampson, A. R., & Lewis, D. A. (2007). Primary visual cortex volume and total neuron number are reduced in schizophrenia. *The Journal of Comparative Neurology*, 501(2), 290–301. <http://doi.org/10.1002/cne.21243>
- Douglas, R. J., & Martin, K. A. C. (2004). Neuronal circuits of the neocortex. *Annual Review of Neuroscience*, 27(1), 419–451. <http://doi.org/10.1146/annurev.neuro.27.070203.144152>
- Douglas, R. J., Martin, K. A. C., & Whitteridge, D. (1989). A Canonical Microcircuit for Neocortex. *Neural Computation*, 1(4), 480–488. <http://doi.org/10.1162/neco.1989.1.4.480>
- Drew, T. W., McCollough, A. W., & Vogel, E. K. (2006). Event-related potential measures of visual working memory. *Clinical EEG and Neuroscience : Official Journal of the EEG and Clinical Neuroscience Society (ENCS)*, 37(4), 286–91. <http://www.ncbi.nlm.nih.gov/pubmed/17073166>
- Duncan, J. (2001). An adaptive coding model of neural function in prefrontal cortex. *Nature Reviews Neuroscience*, 2(11), 820–829. <http://doi.org/10.1038/35097575>
- Ebmeier, K. P., Steele, J. D., MacKenzie, D. M., O'Carroll, R. E., Kydd, R. R., Glabus, M. F., ... Goodwin, G. M. (1995). Cognitive brain potentials and regional cerebral blood flow equivalents during two – and three – sound auditory “oddball tasks.” *Electroencephalography and Clinical Neurophysiology*, 95(6), 434–443. [http://doi.org/10.1016/0013-4694\(95\)00173-5](http://doi.org/10.1016/0013-4694(95)00173-5)
- Ehrenstein, W. H., & Ehrenstein, A. (1999). Psychophysical Methods. In *Modern Techniques in Neuroscience Research* (pp. 1211–1241). Berlin, Heidelberg: Springer Berlin Heidelberg. http://doi.org/10.1007/978-3-642-58552-4_43
- Elleberg, D., & Hammarrenger, B. (2001). Contrast dependency of VEPs as a function of spatial frequency : the parvocellular and magnocellular contributions to human VEPs. *Spatial Vision*, 15(1), 99–111.
- Emrich, H. M., Leweke, F. M., & Schneider, U. (1997). Towards a cannabinoid hypothesis of schizophrenia: cognitive impairments due to dysregulation of the endogenous cannabinoid system. *Pharmacology, Biochemistry, and Behavior*, 56(4), 803–7. <http://www.ncbi.nlm.nih.gov/pubmed/9130308>
- Emrich, S. M., Riggall, A. C., LaRocque, J. J., & Postle, B. R. (2013). Distributed patterns of activity in sensory cortex reflect the precision of multiple items maintained in visual short-term memory. *The Journal of*

- Neuroscience*, 33(15), 6516–6523. <http://doi.org/10.1523/JNEUROSCI.5732-12.2013>
- Engel, T. a, & Wang, X. – J. (2011). Same or different? A neural circuit mechanism of similarity-based pattern match decision making. *The Journal of Neuroscience : The Official Journal of the Society for Neuroscience*, 31(19), 6982–96. <http://doi.org/10.1523/JNEUROSCI.6150-10.2011>
- Eriksson, J., Vogel, E. K., Lansner, A., Bergström, F., & Nyberg, L. (2015). Neurocognitive Architecture of Working Memory. *Neuron*, 88(1), 33–46. <http://doi.org/10.1016/j.neuron.2015.09.020>
- Ester, E. F., Sprague, T. C., & Serences, J. T. (2015). Parietal and Frontal Cortex Encode Stimulus-specific Mnemonic Representations during Visual Working Memory. *Neuron*, 87(4), 893–905. <http://doi.org/10.1016/j.neuron.2015.07.013>
- Ester, E., Serences, J., & Awh, E. (2010). Global mechanisms of sensory recruitment during working memory maintenance. *Journal of Vision*, 9(8), 597–597. <http://doi.org/10.1167/9.8.597>
- Evers, A., Muñoz, J., Bartram, D., Boben, D., Egeland, J., Fernández – Hermida, J. R., ... Urbánek, T. (2012). Testing Practices in the 21st Century. *European Psychologist*, 17(4), 300–319. <http://doi.org/10.1027/1016-9040/a000102>
- Fallon, S. J., Zokaei, N., & Husain, M. (2016). Causes and consequences of limitations in visual working memory. *Annals of the New York Academy of Sciences*, n/a – n/a. <http://doi.org/10.1111/nyas.12992>
- Fechner, G. Elemente der Psychophysik (Breitkopf und Hartel, Leipzig, 1860)
- Fechner, G. T. (1987). Some thoughts on the psychophysical representation of memories (1882). By Gustav Theodor Fechner (translation). *Psychological Research*, 49(4), 209–12. <http://www.ncbi.nlm.nih.gov/pubmed/3327075>
- Forbes, N. F., Carrick, L. A., McIntosh, A. M., & Lawrie, S. M. (2009). Working memory in schizophrenia: a meta-analysis. *Psychological Medicine*, 39(6), 889. <http://doi.org/10.1017/S0033291708004558>
- Foxe, J. J., Doniger, G. M., & Javitt, D. C. (2001). Early visual processing deficits in schizophrenia: impaired P1 generation revealed by high – density electrical mapping. *Neuroreport*, 12(17), 3815–20. <http://www.ncbi.nlm.nih.gov/pubmed/11726801>
- Foxe, J. J., Murray, M. M., & Javitt, D. C. (2005). Filling – in in Schizophrenia: a High – density Electrical Mapping and Source – analysis Investigation of Illusory Contour Processing. *Cerebral Cortex*, 15(12), 1914–1927. <http://doi.org/10.1093/cercor/bhi069>
- Foxe, J. J., Strugstad, E. C., Sehatpour, P., Molholm, S., Pasioka, W., Schroeder, C. E., & McCourt, M. E. (2008). Parvocellular and magnocellular contributions to the initial generators of the visual evoked potential: high – density electrical mapping of the “C1” component. *Brain Topography*, 21(1), 11–21. <http://doi.org/10.1007/s10548-008-0063-4>
- Foxe, J., & Simpson, G. (2002). Flow of activation from V1 to frontal cortex in humans. *Experimental Brain Research*, 142(1), 139–150. <http://doi.org/10.1007/s00221-001-0906-7>
- Friston, K. J., Harrison, L., & Penny, W. (2003). Dynamic causal modelling. *NeuroImage*, 19(4), 1273–302. <http://www.ncbi.nlm.nih.gov/pubmed/12948688>
- Fu, S., Fedota, J. R., Greenwood, P. M., & Parasuraman, R. (2010). Dissociation of visual C1 and P1 components as a function of attentional load: an event-related potential study. *Biological Psychology*, 85(1), 171–8. <http://doi.org/10.1016/j.biopsycho.2010.06.008>
- Fukuda, K., & Vogel, E. K. (2009). Human variation in overriding attentional capture. *The Journal of Neuroscience : The Official Journal of the Society for Neuroscience*, 29(27), 8726–33. <http://doi.org/10.1523/JNEUROSCI.2145-09.2009>
- Fuster, J. M. (2008). *The Prefrontal Cortex*. Oxford, U.K.: Elsevier.
- Fuster, J. M., Bauer, R. H., & Jervey, J. P. (1985). Functional interactions between inferotemporal and prefrontal cortex in a cognitive task. *Brain Research*, 330(2), 299–307. [http://doi.org/10.1016/0006-8993\(85\)90689-4](http://doi.org/10.1016/0006-8993(85)90689-4)
- Fuster, J. M., & Jervey, J. P. (1982). Neuronal firing in the inferotemporal cortex of the monkey in a visual memory task. *The Journal of Neuroscience : The Official Journal of the Society for Neuroscience*, 2(3), 361–75. <http://www.ncbi.nlm.nih.gov/pubmed/7062115>
- Gao, T., Gao, Z., Li, J., Sun, Z., & Shen, M. (2011). The perceptual root of object-based storage: an interactive model of perception and visual working memory. *Journal of Experimental Psychology. Human Perception and Performance*, 37(6), 1803–23. <http://doi.org/10.1037/a0025637>
- Gazzaley, A. (2011). Influence of early attentional modulation on working memory. *Neuropsychologia*, 49(6),

1410-1424. <http://doi.org/10.1016/j.neuropsychologia.2010.12.022>

- Gazzaley, A., Cooney, J. W., McEvoy, K., Knight, R. T., & D'Esposito, M. (2005). Top-down enhancement and suppression of the magnitude and speed of neural activity. *Journal of Cognitive Neuroscience*, *17*(3), 507-17. <http://doi.org/10.1162/0898929053279522>
- Gazzaley, A., & Nobre, A. C. (2012). Top-down modulation: bridging selective attention and working memory. *Trends in Cognitive Sciences*, *16*(2), 129-35. <http://doi.org/10.1016/j.tics.2011.11.014>
- Gegenfurtner, K. R., & Rieger, J. (2000). Sensory and cognitive contributions of color to the recognition of natural scenes. *Current Biology*, *10*(13), 805-808. [http://doi.org/10.1016/S0960-9822\(00\)00563-7](http://doi.org/10.1016/S0960-9822(00)00563-7)
- Gerth, C., Delahunt, P. B., Crognale, M. A., & Werner, J. S. (2003). Topography of the chromatic pattern - onset VEP. *Journal of Vision*, *3*(2), 171-182. <http://doi.org/10.1167/3.2.5>
- Goldman-Rakic, P. S. (1992). Working memory and the mind. *Scientific American*, *267*(3), 110-7. <http://www.ncbi.nlm.nih.gov/pubmed/1502513>
- Goldman-Rakic, P. S. (1995). Cellular basis of working memory. *Neuron*, *14*(3), 477-85. <http://www.ncbi.nlm.nih.gov/pubmed/7695894>
- Goldman-Rakic, P. S. (2011). Circuitry of Primate Prefrontal Cortex and Regulation of Behavior by Representational Memory. In *Comprehensive Physiology*. Hoboken, NJ, USA: John Wiley & Sons, Inc. <http://doi.org/10.1002/cphy.cp010509>
- Goldman-Rakic, P. S. (1994). Working memory dysfunction in schizophrenia. *The Journal of Neuropsychiatry and Clinical Neurosciences*, *6*(4), 348-357. <http://doi.org/10.1176/jnp.6.4.348>
- Golz, J., & MacLeod, D. I. A. (2003). Colorimetry for CRT displays. *Journal of the Optical Society of America A*, *20*(5), 769. <http://doi.org/10.1364/JOSAA.20.000769>
- Gregory, R. L. (1973). The confounded eye. Illusion in nature and art, 49 - 95.
- Gregory, R.L. and P. Heard (1989) "Some Phenomena and Implications of Isoluminance." In Seeing Contour and Colour (eds.) J.J. Kulikowski and C.M. Dickinson and I.J. Murray. (p. 725 - 728).
- Green, M. F., Helleman, G., Horan, W. P., Lee, J., & Wynn, J. K. (2012). From Perception to Functional Outcome in Schizophrenia. *Archives of General Psychiatry*, *69*(12), 1216. <http://doi.org/10.1001/archgenpsychiatry.2012.652>
- Greene, T. (2007). The Kraepelinian dichotomy: the twin pillars crumbling? *History of Psychiatry*, *18*(3), 361-379. <http://doi.org/10.1177/0957154X07078977>
- Groos, K. (1896). "Die Spiele der Thiere." Fischer, Jena
- Guild, J. (1932). The Colorimetric Properties of the Spectrum. *Philosophical Transactions of the Royal Society of London A: Mathematical, Physical and Engineering Sciences*, *230*(681-693). <http://rsta.royalsocietypublishing.org/content/230/681-693/149>
- Haenschel, C., Bittner, R. a, Haertling, F., Rotarska-Jagiela, A., Maurer, K., Singer, W., & Linden, D. E. J. (2007). Contribution of impaired early-stage visual processing to working memory dysfunction in adolescents with schizophrenia: a study with event-related potentials and functional magnetic resonance imaging. *Archives of General Psychiatry*, *64*(11), 1229-40. <http://doi.org/10.1001/archpsyc.64.11.1229>
- Haenschel, C., Bittner, R. a, Waltz, J., Haertling, F., Wibrall, M., Singer, W., ... Rodriguez, E. (2009). Cortical oscillatory activity is critical for working memory as revealed by deficits in early-onset schizophrenia. *The Journal of Neuroscience: The Official Journal of the Society for Neuroscience*, *29*(30), 9481-9. <http://doi.org/10.1523/JNEUROSCI.1428-09.2009>
- Haenschel, C., & Linden, D. (2011). Exploring intermediate phenotypes with EEG: working memory dysfunction in schizophrenia. *Behavioural Brain Research*, *216*(2), 481-95. <http://doi.org/10.1016/j.bbr.2010.08.045>
- Haenschel, C., Linden, D. E., Bittner, R. a., Singer, W., & Hanslmayr, S. (2010). Alpha Phase Locking Predicts Residual Working Memory Performance in Schizophrenia. *Biological Psychiatry*, *68*(7), 595-598. <http://doi.org/10.1016/j.biopsych.2010.06.013>
- Haenschel, Kosilo & Martinovic (2012). Influence of colour and luminance contrast on working memory performance. Unpublished manuscript.
- Hall, J. L. (1968). Maximum-Likelihood Sequential Procedure for Estimation of Psychometric Functions. *The Journal of the Acoustical Society of America*, *44*(1), 370-370. <http://doi.org/10.1121/1.1970490>

- Han, S., Jiang, Y., Gu, H., Rao, H., Mao, L., Cui, Y., & Zhai, R. (2003). The role of human parietal cortex in attention networks. *Brain*, *127*(3), 650–659. <http://doi.org/10.1093/brain/awh071>
- Handy, T. C., & Mangun, G. R. (2000). Attention and spatial selection: Electrophysiological evidence for modulation by perceptual load. *Perception & Psychophysics*, *62*(1), 175–186. <http://doi.org/10.3758/BF03212070>
- Hanslmayr, S., Klimesch, W., Sauseng, P., Gruber, W., Doppelmayr, M., Freunberger, R., ... Birbaumer, N. (2007). Alpha Phase Reset Contributes to the Generation of ERPs. *Cerebral Cortex* (January), 1–8. <http://doi.org/10.1093/cercor/bhj129>
- Harrison, S. A., & Tong, F. (2009). Decoding reveals the contents of visual working memory in early visual areas. *Nature*, *458*(7238), 632–635. <http://doi.org/10.1038/nature07832>.Decoding
- Hartman, M., Steketee, M. C., Silva, S., Lanning, K., & McCann, H. (2003). Working memory and schizophrenia: evidence for slowed encoding. *Schizophrenia Research*, *59*(2–3), 99–113. <http://www.ncbi.nlm.nih.gov/pubmed/12414067>
- Hawkins, H. L., Hillyard, S. A., Luck, S. J., Mouloua, M., et al, C. J., & Woodward, D. P. (1990). Visual attention modulates signal detectability. *Journal of Experimental Psychology: Human Perception and Performance*, *16*(4), 802–811. <http://doi.org/10.1037/0096-1523.16.4.802>
- Helmholtz, H. (1866). *Handbuch der Physiologischen Optik*, 1st ed. Leipzig: Voss.
- Hesse, G. S., & Georgeson, M. A. (2005). Edges and bars: Where do people see features in 1 – D images? *Vision Research*, *45*(4), 507–525. <http://doi.org/10.1016/j.visres.2004.09.013>
- Hicks, T. P., Lee, B. B., & Vidyasagar, T. R. (1983). The responses of cells in macaque lateral geniculate nucleus to sinusoidal gratings. *The Journal of Physiology*, *337*(1), 183–200. <http://doi.org/10.1113/jphysiol.1983.sp014619>
- Hillyard, S. A., & Münte, T. F. (1984). Selective attention to color and location: an analysis with event-related brain potentials. *Perception & Psychophysics*, *36*(2), 185–98. <http://www.ncbi.nlm.nih.gov/pubmed/6514528>
- Hillyard, S. A., Vogel, E. K., & Luck, S. J. (1998). Sensory gain control (amplification) as a mechanism of selective attention: electrophysiological and neuroimaging evidence. *Philosophical Transactions of the Royal Society of London. Series B, Biological Sciences*, *353*(1373), 1257–70. <http://doi.org/10.1098/rstb.1998.0281>
- Hirsch, J., & Hylton, R. (1982). Limits of spatial – frequency discrimination as evidence of neural interpolation. *Journal of the Optical Society of America*, *72*(10), 1367–74. <http://www.ncbi.nlm.nih.gov/pubmed/7143125>
- Hoenig, J (1995). "Schizophrenia: clinical section". In Berrios, German E.; Porter, Roy. *A History of Clinical Psychiatry: The Origin and History of Psychiatric Disorders*. London.
- Hollingworth, A., Matsukura, M., Luck, S. J. (2013). Visual working memory modulates low-level saccade target selection: Evidence from rapidly generated saccades in the global effect paradigm. *Journal of Vision*, *13*(13), 4–4. <http://doi.org/10.1167/13.13.4>
- Holmes, G., & Khazipov, R. (2007). Basic neurophysiology and the cortical basis of EEG. *The clinical neurophysiology primer*, 19–33. Hopf, J., Vogel, E., Woodman, G., Heinze, H. – J., & Luck, S. J. (2002). Localizing Visual Discrimination Processes in Time and Space. *Journal of Neurophysiology*, *88*(4), 2088–2095. <http://doi.org/10.1152/jn.00860.2001>
- Hopf, J., Vogel, E., Woodman, G., Heinze, H., Steven, J., & Luck, S. J. (2013). Localizing Visual Discrimination Processes in Time and Space Localizing Visual Discrimination Processes in Time and Space, 2088–2095.
- Hubbard, T. L. (1988). *Temporal aspects of mental representation: A psychophysical approach*. Doctoral dissertation, Dartmouth College, Hanover, New Hampshire.
- Hubbard, T. L. (1994). Memory psychophysics. *Psychological Research*, *56*(4), 237–250. <http://doi.org/10.1007/BF00419654>
- Hubel, D. H., & Wiesel, T. N. (1959). Receptive fields of single neurones in the cat's striate cortex. *The Journal of Physiology*, *148*, 574–591. <http://doi.org/10.1113/jphysiol.2009.174151>
- Huber, D. E. (2008). Immediate priming and cognitive aftereffects. *Journal of Experimental Psychology. General*, *137*(2), 324–47. <http://doi.org/10.1037/0096-3445.137.2.324>
- Huber, D. E., Tian, X., Curran, T., O'Reilly, R. C., & Worocho, B. (2008). The dynamics of integration and

- separation: ERP, MEG, and neural network studies of immediate repetition effects. *Journal of Experimental Psychology. Human Perception and Performance*, 34(6), 1389–416. <http://doi.org/10.1037/a0013625>
- Huber, G., & Gross, G. (1989). The concept of basic symptoms in schizophrenic and schizoaffective psychoses. *Recenti Progressi in Medicina*, 80(12), 646–52. <http://www.ncbi.nlm.nih.gov/pubmed/2697899>
- Hussar, C. R., & Pasternak, T. (2012). Memory – guided sensory comparisons in the prefrontal cortex: contribution of putative pyramidal cells and interneurons. *The Journal of Neuroscience: The Official Journal of the Society for Neuroscience*, 32(8), 2747–61. <http://doi.org/10.1523/JNEUROSCI.5135-11.2012>
- Hyun, J., Woodman, G., & Vogel, E. (2009). The comparison of visual working memory representations with perceptual inputs. : *Human Perception*, 35(4), 1140–1160. <http://doi.org/10.1037/a0015019>
- Ingling, C. R. & Martinez-Uriegas, E. (1985) The spatio-temporal properties of the r – g X – cell channel. *Vision Research* 25, 33–38.
- Itti, L., Koch, C., & Braun, J. (n.d.). Revisiting spatial vision: toward a unifying model. <http://authors.library.caltech.edu/5881/1/ITTjosaa00.pdf>
- Ivanov, I. V, & Mullen, K. T. (2012). The role of local features in shape discrimination of contour – and surface-defined radial frequency patterns at low contrast. *Vision Research*, 52(1), 1–10. <http://doi.org/10.1016/j.visres.2011.10.002>
- Jackson, A. F., & Bolger, D. J. (2014). The neurophysiological bases of EEG and EEG measurement: A review for the rest of us. *Psychophysiology*, 51(11), 1061–1071. <http://doi.org/10.1111/psyp.12283>
- James, William. (1890). *Principles of psychology*. New York: Holt.
- Javitt, D. C. (2009a). Sensory processing in schizophrenia: neither simple nor intact. *Schizophrenia Bulletin*, 35(6), 1059–64. <http://doi.org/10.1093/schbul/sbp110>
- Javitt, D. C. (2009b). When doors of perception close: bottom-up models of disrupted cognition in schizophrenia. *Annual Review of Clinical Psychology*, 5, 249–75. <http://doi.org/10.1146/annurev.clinpsy.032408.153502>
- Javitt, D. C., & Zukin, S. R. (1991). Recent advances in the phencyclidine model of schizophrenia. *The American Journal of Psychiatry*, 148(10), 1301–8. <http://doi.org/10.1176/ajp.148.10.1301>
- Jennings, B. J., & Martinovic, J. (2014). Luminance and color inputs to mid-level and high-level vision. *Journal of Vision*, 14(2), 9. <http://doi.org/10.1167/14.2.9>
- Johannes, S., Münte, T. F., Heinze, H. J., & Mangun, G. R. (1995). Luminance and spatial attention effects on early visual processing. *Cognitive Brain Research*, 2(3), 189–205. [http://doi.org/10.1016/0926-6410\(95\)90008-X](http://doi.org/10.1016/0926-6410(95)90008-X)
- Johnson, J. S., Spencer, J. P., Luck, S. J., & Schöner, G. (2009). A dynamic neural field model of visual working memory and change detection. *Psychological Science*, 20(5), 568–77. <http://doi.org/10.1111/j.1467-9280.2009.02329.x>
- Jonides, J., Smith, E. E., Koeppe, R. A., Awh, E., Minoshima, S., & Mintun, M. A. (1993). Spatial working memory in humans as revealed by PET. *Nature*, 363(6430), 623–625. <http://doi.org/10.1038/363623a0>
- Kafaligonul, H., Breitmeyer, B. G., & Ögmen, H. (2015). Feedforward and feedback processes in vision. *Frontiers in Psychology*, 6(March), 279. <http://doi.org/10.3389/fpsyg.2015.00279>
- Kandel, E. R. (2014). Republication of The Journal of Physiology (2009) 587, 2733 – 2741 : An introduction to the work of David Hubel. *J Physiol*, 1, 1–11. <http://doi.org/10.1113/jphysiol.2013.268060>
- Kang, M. – S., Hong, S. W., Blake, R., & Woodman, G. F. (2011). Visual working memory contaminates perception. *Psychonomic Bulletin & Review*, 18(5), 860–9. <http://doi.org/10.3758/s13423-011-0126-5>
- Kaplan, E., & Shapley, R. M. (1982). X and Y cells in the lateral geniculate nucleus of macaque monkeys. *The Journal of Physiology*, 330(1), 125–143. <http://doi.org/10.1113/jphysiol.1982.sp014333>
- Kéri, S. (2008). The magnocellular pathway and schizophrenia. *Vision Research*, 48(9), 1181–1182. <http://doi.org/10.1016/j.visres.2007.11.021>
- Kéri, S., & Benedek, G. (2007). Visual contrast sensitivity alterations in inferred magnocellular pathways and anomalous perceptual experiences in people at high – risk for psychosis. *Visual Neuroscience*, 24(2), 183–9. <http://doi.org/10.1017/S0952523807070253>

- Kéri, S., Szamosi, A., Benedek, G., & Kelemen, O. (2012). How does the hippocampal formation mediate memory for stimuli processed by the magnocellular and parvocellular visual pathways? Evidence from the comparison of schizophrenia and amnesic mild cognitive impairment (aMCI). *Neuropsychologia*, 50(14), 3193–3199. <http://doi.org/10.1016/j.neuropsychologia.2012.10.010>
- Khorsand, P., Moore, T., & Soltani, A. (2015). Combined contributions of feedforward and feedback inputs to bottom-up attention. *Frontiers in Psychology*, 6(March), 155. <http://doi.org/10.3389/fpsyg.2015.00155>
- Khosravani, N., & Goodarzi, M. A. (2013). Patients with schizophrenia show deficits on spatial frequency doubling. *Vision Research*, 93, 49–53. <http://doi.org/10.1016/j.visres.2013.10.007>
- Kiesel, A., Miller, J., Jolicœur, P., & Brisson, B. (2008). Measurement of ERP latency differences: A comparison of single-participant and jackknife-based scoring methods. *Psychophysiology*, 45(2), 250–274.
- Kim, D., Wylie, G., Pasternak, R., Butler, P. D., & Javitt, D. C. (2006). Magnocellular contributions to impaired motion processing in schizophrenia. *Schizophrenia Research*, 82(1), 1–8. <http://doi.org/10.1016/j.schres.2005.10.008>
- Kim, D., Zemon, V., Saperstein, A., Butler, P. D., & Javitt, D. C. (2005). Dysfunction of early-stage visual processing in schizophrenia: harmonic analysis. *Schizophrenia Research*, 76(1), 55–65. <http://doi.org/10.1016/j.schres.2004.10.011>
- Kirino, E., Belger, A., Goldman-Rakic, P., & McCarthy, G. (2000). Prefrontal activation evoked by infrequent target and novel stimuli in a visual target detection task: an event-related functional magnetic resonance imaging study. *The Journal of Neuroscience : The Official Journal of the Society for Neuroscience*, 20(17), 6612–8. <http://www.ncbi.nlm.nih.gov/pubmed/10964966>
- Klaver, P., Talsma, D., Wijers, A. A., Heinze, H. J., & Mulder, G. (1999). An event-related brain potential correlate of visual short-term memory. *Neuroreport*, 10(10), 2001–5. <http://www.ncbi.nlm.nih.gov/pubmed/10424664>
- Klimesch, W., Freunberger, R., Sauseng, P., & Gruber, W. (2008). A short review of slow phase synchronization and memory: evidence for control processes in different memory systems? *Brain Research*, 1235, 31–44. <http://doi.org/10.1016/j.brainres.2008.06.049>
- Klimesch, W., Schack, B., Schabus, M., Doppelmayr, M., Gruber, W., & Sauseng, P. (2004). Phase – locked alpha and theta oscillations generate the P1-N1 complex and are related to memory performance. *Cognitive Brain Research*, 19(3), 302–316. <http://doi.org/10.1016/j.cogbrainres.2003.11.016>
- Klosterkötter, J., Hellmich, M., Steinmeyer, E. M., Schultze-Lutter, F., K, M., CM, C., ... (eds.), G. W. (2001). Diagnosing Schizophrenia in the Initial Prodromal Phase. *Archives of General Psychiatry*, 58(2), 158. <http://doi.org/10.1001/archpsyc.58.2.158>
- Knudsen, E. I. (2007). Fundamental Components of Attention. *Annual Review of Neuroscience*, 30(1), 57–78. <http://doi.org/10.1146/annurev.neuro.30.051606.094256>
- Kok, A. (2001). On the utility of P3 amplitude as a measure of processing capacity. *Psychophysiology*, 38(3), 557–577. [http://doi.org/10.1016/S0167-8760\(98\)90168-4](http://doi.org/10.1016/S0167-8760(98)90168-4)
- König, A. & Dieterici, C. (1886). Die Grundempfindungen und ihre Intensitäts – Vertheilung im Spektrum. *Siz. Akad. Wiss. Berlin*, 1886, 805 – 829.
- König, A. & Dieterici, C. (1893). Die Grundempfindungen in normalen und anomalen Farbensystemen und ihre Intensitätsverteilung im Spektrum. *Z. Psychol. Physiol. Sinnesorg.* 4, 241 – 347.
- Kosilo, M., Wuergler, S. M., Craddock, M., Jennings, B. J., Hunt, A. R., & Martinovic, J. (2013). Low-level and high-level modulations of fixational saccades and high-frequency oscillatory brain activity in a visual object classification task. *Frontiers in Psychology*, 4, 948. <http://doi.org/10.3389/fpsyg.2013.00948>
- Kosslyn, S. M. *Image and Brain: The Resolution of the Imagery Debate*, MIT Press, Cambridge, MA (1994)
- Kosslyn, S. M., Ganis, G., & Thompson, W. L. (2001). Neural foundations of imagery. *Nature Reviews Neuroscience*, 2(9), 635–642. <http://doi.org/10.1038/35090055>
- Kosslyn, S. M., Thompson, W. L., Kim, I. J., & Alpert, N. M. (1995). Topographical representations of mental images in primary visual cortex. *Nature*, 378(6556), 496–8. <http://doi.org/10.1038/378496a0>
- Kraepelin, E. (1902) *Clinical Psychiatry: A Text – Book for Students and Physicians*, translated and edited by A. R. Diefendorf (New York and London: Macmillan); originally published in 1899 as *Psychiatrie*, 6th edn.
- Kraepelin, E. (1912) *Clinical Psychiatry: A Text – Book for Students and Physicians*, translated and edited by

- A. R. Diefendorf (New York and London: Macmillan); originally published in 1899 as *Psychiatrie*, 7th edn.
- Krauskopf, J., Williams, D. R., & Heeley, D. W. (1982). Cardinal directions of color space. *Vision Research*, 22(9), 1123–31. <http://www.ncbi.nlm.nih.gov/pubmed/7147723>
- Kveraga, K., Boshyan, J., & Bar, M. (2007). Magnocellular projections as the trigger of top-down facilitation in recognition. *The Journal of Neuroscience: The Official Journal of the Society for Neuroscience*, 27(48), 13232–40. <http://doi.org/10.1523/JNEUROSCI.3481-07.2007>
- La Vaque, T. J. (1999). The History of EEG. Hans Berger. Psychophysiological. A Historical Vignette. *Journal of Neurotherapy*, 3(2), 1–9. http://doi.org/10.1300/J184v03n02_01
- Lamme, V. F., & Roelfsema, P. R. (2000). The distinct modes of vision offered by feedforward and recurrent processing. *Trends in Neurosciences*, 23(11), 571–579. [http://doi.org/10.1016/S0166-2236\(00\)01657-X](http://doi.org/10.1016/S0166-2236(00)01657-X)
- Lara, A. H., & Wallis, J. D. (2012). Capacity and precision in an animal model of visual short-term memory. *Methods*, 12, 1–12. <http://doi.org/10.1167/12.3.13.Introduction>
- Lara, A. H., & Wallis, J. D. (2015). The Role of Prefrontal Cortex in Working Memory: A Mini Review. *Frontiers in Systems Neuroscience*, 9, 173. <http://doi.org/10.3389/fnsys.2015.00173>
- Lavie, N., & Tsal, Y. (1994). Perceptual load as a major determinant of the locus of selection in visual attention. *Perception & Psychophysics*, 56(2), 183–97. <http://www.ncbi.nlm.nih.gov/pubmed/7971119>
- Laycock, R., Crewther, D. P., & Crewther, S. G. (2008). The advantage in being magnocellular: a few more remarks on attention and the magnocellular system. *Neuroscience and Biobehavioral Reviews*, 32(8), 1409–15. <http://doi.org/10.1016/j.neubiorev.2008.04.008>
- Laycock, R., Crewther, S. G., & Crewther, D. P. (2007). A role for the “magnocellular advantage” in visual impairments in neurodevelopmental and psychiatric disorders. *Biobehavioral Reviews*, 31, 363–376. <http://doi.org/10.1016/j.neubiorev.2006.10.003>
- Lee, B. B., Martin, P. R., & Valberg, A. (1988). The physiological basis of heterochromatic flicker photometry demonstrated in the ganglion cells of the macaque retina. *The Journal of Physiology*, 404, 323–47. <http://www.ncbi.nlm.nih.gov/pubmed/3253435>
- Lee, B. B., Sun, H., & Valberg, A. (2011). Segregation of chromatic and luminance signals using a novel grating stimulus. *The Journal of Physiology*, 589(Pt 1), 59–73. <http://doi.org/10.1113/jphysiol.2010.188862>
- Lee, H., Simpson, G. V., Logothetis, N. K., & Rainer, G. (2005). Phase locking of single neuron activity to theta oscillations during working memory in monkey extrastriate visual cortex. *Neuron*, 45(1), 147–56. <http://doi.org/10.1016/j.neuron.2004.12.025>
- Lee, J., & Park, S. (2005). Working memory impairments in schizophrenia: a meta-analysis. *Journal of Abnormal Psychology*, 114(4), 599–611. <http://doi.org/10.1037/0021-843X.114.4.599>
- Lehky, S. R. (2000). Deficits in visual feature binding under isoluminant conditions. *Journal of Cognitive Neuroscience*, 12(3), 383–392. <http://doi.org/10.1162/089892900562200>
- Leonards, U., & Singer, W. (1998). Two segmentation mechanisms with differential sensitivity for colour and luminance contrast. *Vision Research*, 38(1), 101–109. [http://doi.org/10.1016/S0042-6989\(97\)00148-X](http://doi.org/10.1016/S0042-6989(97)00148-X)
- Levy, R., & Goldman-Rakic, P. S. (2000). Segregation of working memory functions within the dorsolateral prefrontal cortex. *Experimental Brain Research. Experimentelle Hirnforschung. Expérimentation Cérébrale*, 133(1), 23–32. <http://www.ncbi.nlm.nih.gov/pubmed/10933207>
- Lewis, D. A., & Lieberman, J. A. (2000). Catching Up on Schizophrenia: Natural History and Neurobiology. *Neuron*, 28(2), 325–334. [http://doi.org/10.1016/S0896-6273\(00\)00111-2](http://doi.org/10.1016/S0896-6273(00)00111-2)
- Liebe, S., Hoerzer, G. M., Logothetis, N. K., & Rainer, G. (2012). Theta coupling between V4 and prefrontal cortex predicts visual short-term memory performance. *Nature Neuroscience*, 15(3), 456–62. <http://doi.org/10.1038/nn.3038>
- Linden, D. E. J., Bittner, R. A., Muckli, L., Waltz, J. A., Kriegeskorte, N., Goebel, R., ... Munk, M. H. J. (2003). Cortical capacity constraints for visual working memory: dissociation of fMRI load effects in a frontoparietal network. *NeuroImage*, 20(3), 1518–1530. <http://doi.org/10.1016/j.neuroimage.2003.07.021>
- Linkenkaer-Hansen, K., Palva, J. M., Sams, M., Hietanen, J. K., Aronen, H. J., & Ilmoniemi, R. J. (1998). Face-selective processing in human extrastriate cortex around 120 ms after stimulus onset revealed by magneto- and electroencephalography. *Neuroscience Letters*, 253(3), 147–150.

[http://doi.org/10.1016/S0304-3940\(98\)00586-2](http://doi.org/10.1016/S0304-3940(98)00586-2)

- Livingstone, M., & Hubel, D. (1988). Segregation of form, color, movement, and depth: anatomy, physiology, and perception. *Science (New York, N.Y.)*, 240(4853), 740–9. <http://www.ncbi.nlm.nih.gov/pubmed/3283936>
- Livingstone, M. S., & Hubel, D. H. (1987). Psychophysical evidence for separate channels for the perception of form, color, movement, and depth. *The Journal of Neuroscience: The Official Journal of the Society for Neuroscience*, 7(11), 3416–68. <http://www.ncbi.nlm.nih.gov/pubmed/3316524>
- Löw, A., Rockstroh, B., Cohen, R., Hauk, O., Berg, P., & Maier, W. (1999). Determining Working Memory from ERP Topography. *Brain Topography*, 12(1), 39–47. <http://doi.org/10.1023/A:1022229623355>
- Luck, S. J. (2016). Artifact Rejection in Continuous Data. <https://github.com/lucklab/erplab/wiki/Artifact-rejection-in-a-continuous-data>
- Luck, S. J. (1995). Multiple mechanisms of visual-spatial attention: recent evidence from human electrophysiology. *Behavioural Brain Research*, 71(1–2), 113–123. [http://doi.org/10.1016/0166-4328\(95\)00041-0](http://doi.org/10.1016/0166-4328(95)00041-0)
- Luck, S. J., Heinze, H. J., Mangun, G. R., & Hillyard, S. A. (1990). Visual event-related potentials index focused attention within bilateral stimulus arrays. II. Functional dissociation of PI and NI components. *Electroencephalography and Clinical Neurophysiology*, 75(6), 528–42. <http://www.ncbi.nlm.nih.gov/pubmed/1693897>
- Luck, S. J., & Vogel, E. K. (1997). The capacity of visual working memory for features and conjunctions. *Nature*, 390(6657), 279–81. <http://doi.org/10.1038/36846>
- Luck, S. J., Woodman, & Vogel. (2000). Event-related potential studies of attention. *Trends in Cognitive Sciences*, 4(11), 432–440. <http://www.ncbi.nlm.nih.gov/pubmed/11058821>
- Lui, L. L., & Pasternak, T. (2011). Representation of comparison signals in cortical area MT during a delayed direction discrimination task. *Journal of Neurophysiology*, 106(3), 1260–73. <http://doi.org/10.1152/jn.00016.2011>
- Luria, R., Balaban, H., Awh, E., & Vogel, E. K. (2016). The contralateral delay activity as a neural measure of visual working memory. *Neuroscience and Biobehavioral Reviews*, 62, 100–8. <http://doi.org/10.1016/j.neubiorev.2016.01.003>
- Ma, L., Steinberg, J. L., Hasan, K. M., Narayana, P. A., Kramer, L. A., & Moeller, F. G. (2012). Working memory load modulation of parieto-frontal connections: Evidence from dynamic causal modeling. *Human Brain Mapping*, 33(8), 1850–1867. <http://doi.org/10.1002/hbm.21329>
- MacLeod, D. I., & Boynton, R. M. (1979). Chromaticity diagram showing cone excitation by stimuli of equal luminance. *Journal of the Optical Society of America*, 69(8), 1183–6. <http://www.ncbi.nlm.nih.gov/pubmed/490231>
- MacLin, O. H., MacLin, M. K., Peterson, D., Chowdhry, O., & Joshi, P. (2009). Social psychophysics: Using psychophysics to answer social questions with PsychoPro. *Behavior Research Methods*, 41(3), 623–632. <http://doi.org/10.3758/BRM.41.3.623>
- Magnussen, S. (2000). low-level memory processes in vision. *Trends in Neurosciences*, 23(6), 247–51. <http://www.ncbi.nlm.nih.gov/pubmed/10838593>
- Magnussen, S., & Greenlee, M. W. (1999). The psychophysics of perceptual memory. *Psychological Research*, 62(2–3), 81–92. <http://doi.org/10.1007/s004260050043>
- Magnussen, S., Greenlee, M. W., Asplund, R., & Dyrnes, S. (1991). Stimulus-specific mechanisms of visual short-term memory. *Vision Research*, 31(7), 1213–1219. [http://doi.org/10.1016/0042-6989\(91\)90046-8](http://doi.org/10.1016/0042-6989(91)90046-8)
- Magnussen, S., Greenlee, M. W., & Thomas, J. P. (1996). Parallel processing in visual short-term memory. *Journal of Experimental Psychology. Human Perception and Performance*, 22(1), 202–12. <http://doi.org/10.1037//0096-1523.22.1.202>
- Magnussen, S., Idås, E., & Myhre, S. H. (1998). Representation of orientation and spatial frequency in perception and memory: a choice reaction time analysis. *Journal of Experimental Psychology. Human Perception and Performance*, 24(3), 707–18. <http://www.ncbi.nlm.nih.gov/pubmed/9627410>
- Malhotra, P., Coulthard, E. J., & Husain, M. (2009). Role of right posterior parietal cortex in maintaining attention to spatial locations over time. *Brain*, 132(3), 645–660. <http://doi.org/10.1093/brain/awn350>
- Mangun, G. R. (1995). Neural mechanisms of visual selective attention. *Psychophysiology*, 32(1), 4–18.

<http://doi.org/10.1111/j.1469-8986.1995.tb03400.x>

- Mangun GR, Hillyard SA, Luck SJ (1993) Electrocortical substrates of visual selective attention. In: Attention and performance XIV (Meyer D, Kornblum S, eds), pp 219–243, Cambridge, MA: MIT.
- Manoach, D. S. (2003). Prefrontal cortex dysfunction during working memory performance in schizophrenia: reconciling discrepant findings. *Schizophrenia Research*, 60(2), 285–298. [http://doi.org/10.1016/S0920-9964\(02\)00294-3](http://doi.org/10.1016/S0920-9964(02)00294-3)
- Martin-Loeches, M., Gomez-Jarabo, G., & Rubia, F. J. (1994). Human brain potentials of spatial location encoding into memory. *Electroencephalography and Clinical Neurophysiology*, 91(5), 363–373. [http://doi.org/10.1016/0013-4694\(94\)90121-X](http://doi.org/10.1016/0013-4694(94)90121-X)
- Martin, P. R., & Lee, B. B. (2014). Distribution and specificity of S-cone (“blue cone”) signals in subcortical visual pathways. *Visual Neuroscience*, 31(2), 177–187. <http://doi.org/10.1017/S0952523813000631>
- Martínez, A., Anllo – Vento, L., Sereno, M. I., Frank, L. R., Buxton, R. B., Dubowitz, D. J., ... Hillyard, S. A. (1999). Involvement of striate and extrastriate visual cortical areas in spatial attention. *Nature Neuroscience*, 2(4), 364–369. <http://doi.org/10.1038/7274>
- Martínez, A., Hillyard, S. A., Dias, E. C., Hagler, D. J., Butler, P. D., Guilfoyle, D. N., ... Javitt, D. C. (2008). Magnocellular Pathway Impairment in Schizophrenia: Evidence from Functional Magnetic Resonance Imaging. *Journal of Neuroscience*, 28(30).
- Martinovic, J., Gruber, T., & Mu, M. M. (2008). Coding of Visual Object Features and Feature Conjunctions in the Human Brain. *Trial*, 3(11). <http://doi.org/10.1371/journal.pone.0003781>
- Martinovic, J., Mordal, J., & Wuerger, S. M. (2011). Event-related potentials reveal an early advantage for luminance contours in the processing of objects. *Journal of Vision*, 11, 1–15. <http://doi.org/10.1167/11.7.1>
- Martínez, A., DiRusso, F., Anllo – Vento, L., Sereno, M. I., Buxton, R. B., & Hillyard, S. A. (2001). Putting spatial attention on the map: timing and localization of stimulus selection processes in striate and extrastriate visual areas. *Vision Research*, 41(10–11), 1437–1457. [http://doi.org/10.1016/S0042-6989\(00\)00267-4](http://doi.org/10.1016/S0042-6989(00)00267-4)
- Maunsell, J., Nealey, T., & DePriest, D. (1990). Magnocellular and parvocellular contributions to responses in the middle temporal visual area (MT) of the macaque monkey. *Journal of Neuroscience*, 10(October), 3323–3334. <http://www.jneurosci.org/cgi/content/abstract/10/10/3323>
- McCarthy, G., Blamire, A. M., Puce, A., Nobre, A. C., Bloch, G., Hyder, F., ... Shulman, R. G. (1994). Functional magnetic resonance imaging of human prefrontal cortex activation during a spatial working memory task. *Proceedings of the National Academy of Sciences of the United States of America*, 91(18), 8690–4. <http://www.ncbi.nlm.nih.gov/pubmed/8078943>
- McEvoy, L., Smith, M. E., & Gevins, A. (1998). Dynamic cortical networks of verbal and spatial working memory: effects of memory load and task practice. *Cerebral Cortex*, 8(7), 563–574. <http://doi.org/10.1093/cercor/8.7.563>
- McGhie, A., & Chapman, J. (1961). Disorders of attention and perception in early schizophrenia. *British Journal of Medical Psychology*, 34(2), 103–116. <http://doi.org/10.1111/j.2044-8341.1961.tb00936.x>
- McIlhagga, W. H., & Mullen, K. T. (1996). Contour integration with colour and luminance contrast. *Vision Research*, 36(9), 1265–1279. [http://doi.org/10.1016/0042-6989\(95\)00196-4](http://doi.org/10.1016/0042-6989(95)00196-4)
- Mecklinger, A., & Pfeifer, E. (1996). Event-related potentials reveal topographical and temporal distinct neuronal activation patterns for spatial and object working memory. *Cognitive Brain Research*, 4(3), 211–224. [http://doi.org/10.1016/S0926-6410\(96\)00034-1](http://doi.org/10.1016/S0926-6410(96)00034-1)
- Millan, M. J., Andrieux, A., Bartzokis, G., Cadenhead, K., Dazzan, P., Fusar – Poli, P., ... Weinberger, D. (2016a). Altering the course of schizophrenia: progress and perspectives. *Nature Reviews. Drug Discovery*, 15(7), 485–515. <http://doi.org/10.1038/nrd.2016.28>
- Millan, M. J., Andrieux, A., Bartzokis, G., Cadenhead, K., Dazzan, P., Fusar – Poli, P., ... Weinberger, D. (2016b). Altering the course of schizophrenia: progress and perspectives. *Nature Reviews. Drug Discovery*, 15(7), 485–515. <http://doi.org/10.1038/nrd.2016.28>
- Miller, E. K., & Cohen, J. D. (2001). An Integrative Theory of Prefrontal Cortex Function. *Annual Review of Neuroscience*, 24(1), 167–202. <http://doi.org/10.1146/annurev.neuro.24.1.167>
- Miller, E. K., Li, L., & Desimone, R. (1991). A neural mechanism for working and recognition memory in inferior temporal cortex. *Science (New York, N.Y.)*, 254(5036), 1377–9. <http://www.ncbi.nlm.nih.gov/pubmed/1962197>

- Miller, E. K., Li, L., & Desimone, R. (1993). Activity of neurons in anterior inferior temporal cortex during a short-term memory task. *The Journal of Neuroscience: The Official Journal of the Society for Neuroscience*, *13*(4), 1460–1478.
- Miller, K. M., Price, C. C., Okun, M. S., Montijo, H., & Bowers, D. (2009). Is the N-back task a valid neuropsychological measure for assessing working memory? *Archives of Clinical Neuropsychology: The Official Journal of the National Academy of Neuropsychologists*, *24*(7), 711–7. <http://doi.org/10.1093/arclin/acp063>
- Miyakoshi, M. (2017, August 4). Makoto's preprocessing pipeline. https://sccn.ucsd.edu/wiki/Makoto's_preprocessing_pipeline
- Miyashita, Y., & Chang, H. S. (1988). Neuronal correlate of pictorial short-term memory in the primate temporal cortex Yasushi Miyashita. *Nature*, *331*(6151), 68–70. <http://doi.org/10.1038/331068a0>
- Moyer, R., Bradley, D., Sorensen, M., Whiting, C., & Mansfield, D. (1978). Psychophysical functions for perceived and remembered size. *Science*, *200*(4339). <http://science.sciencemag.org/content/200/4339/330>
- Mullen, K. T., & Beaudot, W. H. a. (2002). Comparison of color and luminance vision on a global shape discrimination task. *Vision Research*, *42*(5), 565–75. <http://www.ncbi.nlm.nih.gov/pubmed/11853774>
- Mullen, K. T., Beaudot, W. H., & McIlhagga, W. H. (2000). Contour integration in color vision: a common process for the blue-yellow, red-green and luminance mechanisms? *Vision Research*, *40*(6), 639–55. <http://www.ncbi.nlm.nih.gov/pubmed/10824267>
- Munk, M. H. J., Linden, D. E. J., Muckli, L., Lanfermann, H., Zanella, F. E., Singer, W., & Goebel, R. (2002). Distributed Cortical Systems in Visual Short-term Memory Revealed by Event-related Functional Magnetic Resonance Imaging. *Cerebral Cortex*, *12*(8), 866–876. <http://doi.org/10.1093/cercor/12.8.866>
- Näätänen, R., Gaillard, A. W. K., & Mäntysalo, S. (1978). Early selective attention effect on evoked potential reinterpreted. *Acta Psychologica*, *42*(4), 313–329. [http://doi.org/10.1016/0001-6918\(78\)90006-9](http://doi.org/10.1016/0001-6918(78)90006-9)
- Näätänen, R., Paavilainen, P., Rinne, T., & Alho, K. (2007). The mismatch negativity (MMN) in basic research of central auditory processing: A review. *Clinical Neurophysiology*, *118*(12), 2544–2590. <http://doi.org/10.1016/j.clinph.2007.04.026>
- Nakashita, S., Saito, D. N., Kochiyama, T., Honda, M., Tanabe, H. C., & Sadato, N. (2008). Tactile–visual integration in the posterior parietal cortex: A functional magnetic resonance imaging study. *Brain Research Bulletin*, *75*(5), 513–525. <http://doi.org/10.1016/j.brainresbull.2007.09.004>
- Natale, E., Marzi, C. A., Girelli, M., Pavone, E. F., & Pollmann, S. (2006). ERP and fMRI correlates of endogenous and exogenous focusing of visual – spatial attention. *European Journal of Neuroscience*, *23*(9), 2511–2521. <http://doi.org/10.1111/j.1460-9568.2006.04756.x>
- Nieder, A., & Miller, E. K. (2003). Coding of Cognitive Magnitude. *Neuron*, *37*(1), 149–157. [http://doi.org/10.1016/S0896-6273\(02\)01144-3](http://doi.org/10.1016/S0896-6273(02)01144-3)
- Norton, N., Williams, H. J., & Owen, M. J. (2006). An update on the genetics of schizophrenia. *Current Opinion in Psychiatry*, *19*(2), 158–164. <http://doi.org/10.1097/01.yco.0000214341.52249.59>
- Nuechterlein, K. H., Barch, D. M., Gold, J. M., Goldberg, T. E., Green, M. F., & Heaton, R. K. (2004). Identification of separable cognitive factors in schizophrenia. In *Schizophrenia Research* (Vol. 72, pp. 29–39). <http://doi.org/10.1016/j.schres.2004.09.007>
- Nuechterlein, K. H., Ventura, J., Subotnik, K. L., & Bartzokis, G. (2014). The early longitudinal course of cognitive deficits in schizophrenia. *The Journal of Clinical Psychiatry*, *75* Suppl 2(0 2), 25–9. <http://doi.org/10.4088/JCP.13065.su1.06>
- O'Callaghan, C., Kveraga, K., Shine, J. M., Adams, R. B., & Bar, M. (2017). Predictions penetrate perception: Converging insights from brain, behaviour and disorder. *Consciousness and Cognition*, *47*, 63–74. <http://doi.org/10.1016/j.concog.2016.05.003>
- O'Donnell, B. F., Potts, G. F., Nestor, P. G., Stylianopoulos, K. C., Shenton, M. E., & McCarley, R. W. (2002). Spatial frequency discrimination in schizophrenia. *Journal of Abnormal Psychology*, *111*(4), 620–5. <http://www.ncbi.nlm.nih.gov/pubmed/12428775>
- Offen, S., Schluppeck, D., & Heeger, D. J. (2009). The role of early visual cortex in visual short-term memory and visual attention. *Vision Research*, *49*(10), 1352–62. <http://doi.org/10.1016/j.visres.2007.12.022>
- Olkkonen, M., Allred, S. R., Shevell, S., Singer, W., & Muckli, L. (2014). Short-term Memory Affects Color Perception in Context. *PLoS ONE*, *9*(1), e86488. <http://doi.org/10.1371/journal.pone.0086488>

- Oostenveld, R., Fries, P., Maris, E., & Schoffelen, J. – M. (2011). FieldTrip: Open source software for advanced analysis of MEG, EEG, and invasive electrophysiological data. *Computational Intelligence and Neuroscience*, 2011, 156869. <http://doi.org/10.1155/2011/156869>
- Oribe, N., Hirano, Y., Kanba, S., del Re, E., Seidman, L., MesholaM-Gately, R., ... Niznikiewicz, M. (2015). Progressive Reduction of Visual P300 Amplitude in Patients With First – Episode Schizophrenia: An ERP Study. *Schizophrenia Bulletin*, 41(2), 460–470. <http://doi.org/10.1093/schbul/sbu083>
- Pajitnov, A. (1984), Tetris [computer software].
- Palmer, J. (1990). Attentional limits on the perception and memory of visual information. *Journal of Experimental Psychology. Human Perception and Performance*, 16(2), 332–50. <http://www.ncbi.nlm.nih.gov/pubmed/2142203>
- Pasternak, T., & Greenlee, M. W. (2005). Working memory in primate sensory systems. *Nature Reviews. Neuroscience*, 6(2), 97–107. <http://doi.org/10.1038/nrn1603>
- Paulesu, E., Frith, C. D., & Frackowiak, R. S. J. (1993). The neural correlates of the verbal component of working memory. *Nature*, 362(6418), 342–345. <http://doi.org/10.1038/362342a0>
- Pelli, D. G., & Farell, B. (1995) Psychophysical methods. In: M. Bass, E. W. Van Stryland, D. R. Williams, & W. L. Wolfe (Eds.), *Handbook of Optics*, 2nd ed., I (pp. 29.21 – 29.13). New York: McGraw – Hill
- Pelli, D. G., & Farell, B. (2010). Psychophysical methods. In M. Bass, C. DeCusatis, J. Enoch, V. Lakshminarayanan, G. Li, C. MacDonald, V. Mahajan & E. V. Stryland (Eds.), *Handbook of Optics, Third Edition, Volume III: Vision and Vision Optics* (pp. 3.1 – 3.12). New York: McGraw – Hill
- Pentland, A. (1980). Maximum likelihood estimation: The best PEST. *Perception & Psychophysics*, 28(4), 377–379. <http://doi.org/10.3758/BF03204398>
- Pessoa, L., Gutierrez, E., Bandettini, P., & Ungerleider, L. (2002). Neural correlates of visual working memory: fMRI amplitude predicts task performance. *Neuron*, 35(5), 975–87. <http://www.ncbi.nlm.nih.gov/pubmed/12372290>
- Peterson, M. A., & Gibson, B. S. (1993). Shape Recognition Inputs To Figure-ground Organization in Three – Dimensional Displays. *Cognitive Psychology*, 25(3), 383–429. <http://doi.org/10.1006/cogp.1993.1010>
- Peterson, M. A., & Gibson, B. S. (1994). Object recognition contributions to figure-ground organization: Operations on outlines and subjective contours. *Perception & Psychophysics*, 56(5), 551–564. <http://doi.org/10.3758/BF03206951>
- Petrides, M., Alivisatos, B., Meyer, E., & Evans, A. C. (1993). Functional activation of the human frontal cortex during the performance of verbal working memory tasks. *Proceedings of the National Academy of Sciences of the United States of America*, 90(3), 878–82. <http://doi.org/10.1073/PNAS.90.3.878>
- Petro, L. S., Vizioli, L., & Muckli, L. (2014). Contributions of cortical feedback to sensory processing in primary visual cortex. *Frontiers in Psychology*, 5(November), 1–8. <http://doi.org/10.3389/fpsyg.2014.01223>
- Pillsbury, W. B. (1908). “Attention.” MacMillan, New York
- Pinal, D., Zurrón, M., & Díaz, F. (2014). Effects of load and maintenance duration on the time course of information encoding and retrieval in working memory: from perceptual analysis to post-categorization processes. *Frontiers in Human Neuroscience*, 8(April), 165. <http://doi.org/10.3389/fnhum.2014.00165>
- Pinal, D., Zurrón, M., Díaz, F., Campbell, W., Bokde, A., & Lai, R. (2015). An Event Related Potentials Study of the Effects of Age, Load and Maintenance Duration on Working Memory Recognition. *PLOS ONE*, 10(11), e0143117. <http://doi.org/10.1371/journal.pone.0143117>
- Piskulic, D., Olver, J. S., Norman, T. R., & Maruff, P. (2007). Behavioural studies of spatial working memory dysfunction in schizophrenia: A quantitative literature review. *Psychiatry Research*, 150(2), 111–121. <http://doi.org/10.1016/j.psychres.2006.03.018>
- Polich J. Overview of P3a and P3b. In: Polich J, editor. *Detection of change: event-related potential and fMRI findings*. Boston, MA: Kluwer; 2003. pp. 83–98.
- Polich, J. (2007). Updating P300: an integrative theory of P3a and P3b. *Clinical Neurophysiology: Official Journal of the International Federation of Clinical Neurophysiology*, 118(10), 2128–48. <http://doi.org/10.1016/j.clinph.2007.04.019>
- Postle, B. (2006). Working memory as an emergent property of the mind and brain. *Neuroscience*, 139(1), 23–38. <http://www.sciencedirect.com/science/article/pii/S0306452205006202>

- Prins, N & Kingdom, F. A. A. (2009) Palamedes: Matlab routines for analyzing psychophysical data. <http://www.palamedestoolbox.org>
- Raghavachari, S., Kahana, M. J., Rizzuto, D. S., Caplan, J. B., Kirschen, M. P., Bourgeois, B., ... Lisman, J. E. (2001). Gating of human theta oscillations by a working memory task. *The Journal of Neuroscience : The Official Journal of the Society for Neuroscience*, 21(9), 3175–3183. <http://doi.org/21/9/3175> [pii]
- Rämä, P., Kesseli, K., Reinikainen, K., Kekoni, J., Hämäläinen, H., & Carlson, S. (1997). Visuospatial mnemonic load modulates event-related slow potentials. *Neuroreport*, 8(4), 871–6. <http://www.ncbi.nlm.nih.gov/pubmed/9141055>
- Rassovsky, Y., Horan, W. P., Lee, J., Sergi, M. J., & Green, M. F. (2011). Pathways between early visual processing and functional outcome in schizophrenia. *Psychological Medicine*, 41(3), 487–497. <http://doi.org/10.1017/S0033291710001054>
- Regan, D. (2000). Human Perception of Objects. Sunderland, MA: Sinauer Associates Inc.
- Reid, R. C., & Shapley, R. M. (2002). Space and time maps of cone photoreceptor signals in macaque lateral geniculate nucleus. *The Journal of Neuroscience : The Official Journal of the Society for Neuroscience*, 22(14), 6158–75. <http://doi.org/20026444>
- Reinitz, M. T. (1990). Effects of spatially directed attention on visual encoding. *Perception & Psychophysics*, 47(5), 497–505. <http://doi.org/10.3758/BF03208183>
- Revheim, N., Butler, P. D., Schechter, I., Jalbrzikowski, M., Silipo, G., & Javitt, D. C. (2006). Reading impairment and visual processing deficits in schizophrenia. *Schizophrenia Research*, 87(1–3), 238–45. <http://doi.org/10.1016/j.schres.2006.06.022>
- Richardson, J. T. E. (2007). Measures of Short-term Memory: A Historical Review. *Cortex*, 43(5), 635–650. [http://doi.org/10.1016/S0010-9452\(08\)70493-3](http://doi.org/10.1016/S0010-9452(08)70493-3)
- Ritter, W., Simson, R., Vaughan, H. G., & Friedman, D. (1979). A brain event related to the making of a sensory discrimination. *Science (New York, N.Y.)*, 203(4387), 1358–61. <http://www.ncbi.nlm.nih.gov/pubmed/424760>
- Rodriguez, J. S., & Paule, M. G. (2009). *Working Memory Delayed Response Tasks in Monkeys. Methods of Behavior Analysis in Neuroscience*. CRC Press/Taylor & Francis. <http://www.ncbi.nlm.nih.gov/pubmed/21204334>
- Roesch, E. B., Sander, D., Mumenthaler, C., Kerzel, D., & Scherer, K. R. (2010). Psychophysics of emotion: The QUEST for Emotional Attention. *Journal of Vision*, 10(3), 1–9. <http://doi.org/10.1167/10.3.4>
- Rolke, B., Heil, M., Hennighausen, E., Häussler, C., & Rösler, F. (2000). Topography of brain electrical activity dissociates the sequential order transformation of verbal versus spatial information in humans. *Neuroscience Letters*, 282(1–2), 81–84. [http://doi.org/10.1016/S0304-3940\(00\)00891-0](http://doi.org/10.1016/S0304-3940(00)00891-0)
- Rose, M., Schmid, C., Winzen, A., Sommer, T., & Büchel, C. (2004). The Functional and Temporal Characteristics of Top-down Modulation in Visual Selection. *Cerebral Cortex*, 15(9), 1290–1298. <http://doi.org/10.1093/cercor/bhi012>
- Rubin, N. (2001). Figure and ground in the brain. *Nature Neuroscience*, 4(9), 857–8. <http://doi.org/10.1038/nn0901-857>
- Ruchkin, D. ., Johnson, R., Grafman, J., Canoune, H., & Ritter, W. (1997). Multiple visuospatial working memory buffers: Evidence from spatiotemporal patterns of brain activity. *Neuropsychologia*, 35(2), 195–209. [http://doi.org/10.1016/S0028-3932\(96\)00068-1](http://doi.org/10.1016/S0028-3932(96)00068-1)
- Ruchkin, D. S., Canoune, H. L., Johnson, R., & Ritter, W. (1995). Working memory and preparation elicit different patterns of slow wave event-related brain potentials. *Psychophysiology*, 32(4), 399–410. <http://doi.org/10.1111/j.1469-8986.1995.tb01223.x>
- Ruchkin, D. S., Johnson, R., Canoune, H., & Ritter, W. (1990). Short-term memory storage and retention: an event-related brain potential study. *Electroencephalography and Clinical Neurophysiology*, 76(5), 419–39. <http://www.ncbi.nlm.nih.gov/pubmed/1699736>
- Ruchkin, D. S., Johnson, R., Grafman, J., Canoune, H., & Ritter, W. (1992). Distinctions and similarities among working memory processes: an event-related potential study. *Brain Research. Cognitive Brain Research*, 1(1), 53–66. <http://www.ncbi.nlm.nih.gov/pubmed/15497435>
- Ruppertsberg, A. I., Wuergler, S. M., & Bertamini, M. (2003). The chromatic input to global motion perception. *Visual Neuroscience*, 20(4), 421–428. <http://doi.org/10.1017/S0952523803204077>
- Rutman, A. M., Clapp, W. C., Chadick, J. Z., & Gazzaley, A. (2009). Early top-down control of visual

- processing predicts working memory performance. *Journal of Cognitive Neuroscience*, 22, 1224–34. <http://doi.org/10.1162/jocn.2009.21257>
- Salmela, V. R., Lahde, M., & Saarinen, J. (2012). Visual working memory for amplitude – modulated shapes. *Journal of Vision*, 12(6), 2–2. <http://doi.org/10.1167/12.6.2>
- Salmela, V. R., Lähde, M., & Saarinen, J. (2012). Visual working memory for amplitude – modulated shapes. *Journal of Vision*, 12(6), 2. <http://doi.org/10.1167/12.6.2>
- Salmela, V. R., & Saarinen, J. (2013). Detection of small orientation changes and the precision of visual working memory. *Vision Research*, 76, 17–24. <http://doi.org/10.1016/j.visres.2012.10.003>
- Sarnthein, J., Petsche, H., Rappelsberger, P., Shaw, G. L., & Von Stein, a. (1998). Synchronization between prefrontal and posterior association cortex during human working memory. *Proceedings of the National Academy of Sciences of the United States of America*, 95(12), 7092–7096. <http://doi.org/10.1073/pnas.95.12.7092>
- Sauseng, P., Klimesch, W., Schabus, M., & Doppelmayr, M. (2005). Frontoparietal EEG coherence in theta and upper alpha reflect central executive functions of working memory. *International Journal of Psychophysiology*, 57(2), 97–103. <http://doi.org/10.1016/j.ijpsycho.2005.03.018>
- Schechter, I., Butler, P. D., Zemon, V. M., Revheim, N., Saperstein, A. M., Jalbrzikowski, M., ... Javitt, D. C. (2005). Impairments in generation of early-stage transient visual evoked potentials to magno – and parvocellular – selective stimuli in schizophrenia. *Clinical Neurophysiology*, 116(9), 2204–2215. <http://doi.org/10.1016/j.clinph.2005.06.013>
- Schiffman, J., Maeda, J. A., Hayashi, K., Michelsen, N., Sorensen, H. J., Ekstrom, M., ... Mednick, S. A. (2006). Premorbid childhood ocular alignment abnormalities and adult schizophrenia – spectrum disorder. *Schizophrenia Research*, 81(2–3), 253–260. <http://doi.org/10.1016/j.schres.2005.08.008>
- Schiller, P. H. & Colby, C. L. (1983). The responses of single cells in the lateral geniculate nucleus of the rhesus monkey to color and luminance contrast. *Vision Research* 23, 1631–1641.
- Schneider, K. *Clinical Psychopathology*. New York: Grune and Stratton. 1959.
- Schneider, U., Borsutzky, M., Seifert, J., Leweke, F. M., Huber, T. J., Rollnik, J. D., & Emrich, H. M. (2002). Reduced binocular depth inversion in schizophrenic patients. *Schizophrenia Research*, 53(1–2), 101–8. <http://www.ncbi.nlm.nih.gov/pubmed/11728843>
- Schneider, U., Leweke, F. M., Sternemann, U., Weber, M. M., & Emrich, H. M. (1996). Visual 3D illusion: a systems – theoretical approach to psychosis. *European Archives of Psychiatry and Clinical Neuroscience*, 246(5), 256–60. <http://www.ncbi.nlm.nih.gov/pubmed/8863004>
- Schubert, E. W., Henriksson, K. M., & McNeil, T. F. (2005). A prospective study of offspring of women with psychosis: visual dysfunction in early childhood predicts schizophrenia – spectrum disorders in adulthood. *Acta Psychiatrica Scandinavica*, 112(5), 385–393. <http://doi.org/10.1111/j.1600-0447.2005.00584.x>
- Schubotz, R., & Friederici, A. D. (1997). Electrophysiological correlates of temporal and spatial information processing. *Neuroreport*, 8(8), 1981–6. <http://www.ncbi.nlm.nih.gov/pubmed/9223089>
- Schultze-Lutter, F., Ruhrmann, S., Pickler, H., von Reventlow, H. G., Brockhaus-Dumke, A., & Klosterkotter, J. (2007). Basic symptoms in early psychotic and depressive disorders. *The British Journal of Psychiatry*, 191(51), s31–s37. <http://doi.org/10.1192/bjp.191.51.s31>
- Scocchia, L., Cicchini, G. M., & Triesch, J. (2013). What’s “up”? Working memory contents can bias orientation processing. *Vision Research*, 78, 46–55. <http://doi.org/10.1016/j.visres.2012.12.003>
- Selemon, L. D., & Begovic, A. (2007). Stereologic analysis of the lateral geniculate nucleus of the thalamus in normal and schizophrenic subjects. *Psychiatry Research*, 151(1–2), 1–10. <http://doi.org/10.1016/j.psychres.2006.11.003>
- Selemon, L. D., Rajkowska, G., & Goldman-Rakic, P. S. (1995). Abnormally High Neuronal Density in the Schizophrenic Cortex. *Archives of General Psychiatry*, 52(10), 805. <http://doi.org/10.1001/archpsyc.1995.03950220015005>
- Shallice, T. (1982). Specific impairments of planning. *Philosophical Transactions of the Royal Society of London. Series B, Biological Sciences*, 298(1089), 199–209. <http://www.ncbi.nlm.nih.gov/pubmed/6125971>
- Shapley, R. (1990). Visual sensitivity and parallel retinocortical channels. *Annual Review of Psychology*, 41, 635–658. <http://doi.org/10.1146/annurev.psych.41.1.635>

- Shapley, R., & Hawken, M. J. (2011). Color in the cortex: single – and double-opponent cells. *Vision Research*, 51(7), 701–17. <http://doi.org/10.1016/j.visres.2011.02.012>
- Shepard, R. N., & Metzler, J. (1971). Mental rotation of three – dimensional objects. *Science (New York, N.Y.)*, 171(3972), 701–3. <http://www.ncbi.nlm.nih.gov/pubmed/5540314>
- Shepard, R. N., & Podgorny, P. (1978). Cognitive processes that resemble perceptual processes. Lawrence Erlbaum. <http://psycnet.apa.org/psycinfo/1978-19902-007>
- Siegelbaum, S. A., & Hudspeth, A. J. (2000). Principles of neural science (Vol. 4, pp. 1227 – 1246). E. R. Kandel, J. H. Schwartz, & T. M. Jessell (Eds.). New York: McGraw – hill.
- Silver, H., Feldman, P., Bilker, W., & Gur, R. C. (2003). Working Memory Deficit as a Core Neuropsychological Dysfunction in Schizophrenia. *American Journal of Psychiatry*, 160(10), 1809–1816. <http://doi.org/10.1176/appi.ajp.160.10.1809>
- Silverstein, D. N. (2015). A computational investigation of feedforward and feedback processing in metacontrast backward masking. *Frontiers in Psychology*, 6(February), 1–14. <http://doi.org/10.3389/fpsyg.2015.00006>
- Silverstein, S., Hatashita – Wong, M., Schenkel, L., Wilkniss, S., Kovács, I., Fehér, A., ... Savitz, A. (2006). Reduced top-down influences in contour detection in schizophrenia. *Cognitive Neuropsychiatry*, 11(2), 112–132. <http://doi.org/10.1080/13546800444000209>
- Silverstein, S., Keane, B. P., Blake, R., Giersch, A., Green, M., & Kéri, S. (2015). Vision in schizophrenia: why it matters. *Frontiers in Psychology*, 6, 41. <http://doi.org/10.3389/fpsyg.2015.00041>
- Silverstein, S. M., & Keane, B. P. (2011). Vision Science and Schizophrenia Research: Toward a Review of the Disorder Editors' Introduction to Special Section. *Schizophrenia Bulletin*, 37(4), 681–689. <http://doi.org/10.1093/schbul/sbr053>
- Silverstein, S. M., & Rosen, R. (2015). Schizophrenia and the eye. *Schizophrenia Research: Cognition*, 2(2), 46–55. <http://doi.org/10.1016/j.scog.2015.03.004>
- Simons, D. J., Levin, D. T., & Haber, R. N. (1997). Change blindness. *Trends in Cognitive Sciences*, 1(7), 261–7. [http://doi.org/10.1016/S1364-6613\(97\)01080-2](http://doi.org/10.1016/S1364-6613(97)01080-2)
- Simons, D. J., & Rensink, R. A. (2005). Change blindness : Past, present, and future. *Psychology*, 9(1).
- Skottun, B. C. (2013). On using isoluminant stimuli to separate magno – and parvocellular responses in psychophysical experiments—A few words of caution. *Behavior Research Methods*, 45(3), 637–645. <http://doi.org/10.3758/s13428-012-0290-1>
- Skottun, B. C., & Skoyles, J. R. (2008a). Reply to Kéri, S. The magnocellular system and schizophrenia. *Vision Research*, 48(9), 1183–1185. <http://doi.org/10.1016/j.visres.2008.02.010>
- Skottun, B. C., & Skoyles, J. R. (2008b). Visual Search: Magno – and Parvocellular Systems or Color and Luminance Processes? *International Journal of Neuroscience*, 118(9), 1259–1267. <http://doi.org/10.1080/00207450701239434>
- Skottun, B. C., & Skoyles, J. R. (2011). On identifying magnocellular and parvocellular responses on the basis of contrast – response functions. *Schizophrenia Bulletin*, 37(1), 23–6. <http://doi.org/10.1093/schbul/sbq114>
- Skottun, B. C., & Skoyles, J. R. (2013). Is vision in schizophrenia characterized by a generalized reduction? *Frontiers in Psychology*, 4, 999. <http://doi.org/10.3389/fpsyg.2013.00999>
- Slaghuis, W. L. (1998). Contrast sensitivity for stationary and drifting spatial frequency gratings in positive – and negative – symptom schizophrenia. *Journal of Abnormal Psychology*, 107(1), 49–62. <http://www.ncbi.nlm.nih.gov/pubmed/9505038>
- Smith, T.; Guild, J.(1931–32). "The C.I.E. colorimetric standards and their use". Transactions of the Optical Society. 33 (3): 73–134. doi:10.1088/1475-4878/33/3/301.
- Smith, V. C., & Pokorny, J. (1975). Spectral sensitivity of the foveal cone photopigments between 400 and 500 nm. *Vision Research*, 15(2), 161–171. [http://doi.org/10.1016/0042-6989\(75\)90203-5](http://doi.org/10.1016/0042-6989(75)90203-5)
- Smithson, H. E. (2014). S-cone psychophysics. *Visual Neuroscience*, 31(2), 211–225. <http://doi.org/10.1017/S0952523814000030>
- Spearman, C. E. (1937). "Psychology Down the Ages." MacMillan, New York.
- Squires, N. K., Squires, K. C., & Hillyard, S. A. (1975). Two varieties of long-latency positive waves evoked by unpredictable auditory stimuli in man. *Electroencephalography and Clinical Neurophysiology*, 38(4),

387–401. <http://www.ncbi.nlm.nih.gov/pubmed/46819>

- Stockman, A., & Brainard, D. H. (2010). Color vision mechanisms. *The Optical Society of America Handbook of Optics* (May), 11.1–11.104. http://www.researchgate.net/publication/228358887_Color_vision_mechanisms
- Stockman, A., & Sharpe, L. T. (2000). The spectral sensitivities of the middle – and long – wavelength – sensitive cones derived from measurements in observers of known genotype. *Vision Research*, 40(13), 1711–1737. [http://doi.org/10.1016/S0042-6989\(00\)00021-3](http://doi.org/10.1016/S0042-6989(00)00021-3)
- Squire, L.R. and Zola-Morgan, E.R. (1991) *Memory. From Mind to Molecules*, Freeman 42
- Sun, H., Smithson, H. E., Zaidi, Q., & Lee, B. B. (2006a). Do magnocellular and parvocellular ganglion cells avoid short-wavelength cone input? *Visual Neuroscience*, 23(3–4), 441–6. <http://doi.org/10.1017/S0952523806233042>
- Sun, H., Smithson, H. E., Zaidi, Q., & Lee, B. B. (2006b). Specificity of cone inputs to macaque retinal ganglion cells. *Journal of Neurophysiology*, 95(2), 837–49. <http://doi.org/10.1152/jn.00714.2005>
- Super, H., Spekrijse, H., & Lamme, V. A. (2001). A Neural Correlate of Working Memory in the Monkey Primary Visual Cortex. *Science*, 293(5527), 120–124. <http://doi.org/10.1126/science.1060496>
- Tailby, C., Szmajda, B. A., Buzás, P., Lee, B. B., & Martin, P. R. (2008). Transmission of blue (S) cone signals through the primate lateral geniculate nucleus. *The Journal of Physiology*, 586(24), 5947–5967. <http://doi.org/10.1113/jphysiol.2008.161893>
- Tanaka, K. (1996). Inferotemporal Cortex and Object Vision. *Annual Review of Neuroscience*, 19(1), 109–139. <http://doi.org/10.1146/annurev.ne.19.030196.000545>
- Tandon, R., Gaebel, W., Barch, D. M., Bustillo, J., Gur, R. E., Heckers, S., ... Carpenter, W. (2013). Definition and description of schizophrenia in the DSM-5. *Schizophrenia Research*, 150(1), 3–10. <http://doi.org/10.1016/j.schres.2013.05.028>
- Tas, A. C., Luck, S. J., & Hollingworth, A. (2016). The relationship between visual attention and visual working memory encoding: A dissociation between covert and overt orienting. *Journal of Experimental Psychology. Human Perception and Performance*, 42(8), 1121–38. <http://doi.org/10.1037/xhp0000212>
- Taylor, M. J. (2002). Non-spatial attentional effects on PI. *Clinical Neurophysiology: Official Journal of the International Federation of Clinical Neurophysiology*, 113(12), 1903–8. <http://www.ncbi.nlm.nih.gov/pubmed/12464327>
- Taylor, M. M., & Creelman, C. D. (1967). PEST: Efficient Estimates on Probability Functions. *The Journal of the Acoustical Society of America*, 41(4A), 782–787. <http://doi.org/10.1121/1.1910407>
- Tek, C., Gold, J., Blaxton, T., Wilk, C., McMahon, R. P., & Buchanan, R. W. (2002). Visual Perceptual and Working Memory Impairments in Schizophrenia. *Archives of General Psychiatry*, 59(2), 146. <http://doi.org/10.1001/archpsyc.59.2.146>
- Tomberg, C., & Desmedt, J. E. (1998). Human perceptual processing: inhibition of transient prefrontal – parietal 40 Hz binding at P300 onset documented in non-averaged cognitive brain potentials. *Neuroscience Letters*, 255(3), 163–166. [http://doi.org/10.1016/S0304-3940\(98\)00740-X](http://doi.org/10.1016/S0304-3940(98)00740-X)
- Tomita, H., Ohbayashi, M., Nakahara, K., Hasegawa, I., & Miyashita, Y. (1999). Top-down signal from prefrontal cortex in executive control of memory retrieval. *Nature*, 401(6754), 699–703. <http://doi.org/10.1038/44372>
- Tootell, R. B., Hamilton, S. L., & Switkes, E. (1988). Functional anatomy of macaque striate cortex. IV. Contrast and magno-parvo streams. *The Journal of Neuroscience: The Official Journal of the Society for Neuroscience*, 8(5), 1594–609. <http://www.ncbi.nlm.nih.gov/pubmed/3367212>
- Tootell, R. B., Silverman, M. S., Hamilton, S. L., Switkes, E., & De Valois, R. L. (1988). Functional anatomy of macaque striate cortex. V. Spatial frequency. *The Journal of Neuroscience: The Official Journal of the Society for Neuroscience*, 8(5), 1610–24. <http://www.ncbi.nlm.nih.gov/pubmed/3367213>
- Treisman, A. (1998). Feature binding, attention and object perception. *Philosophical Transactions of the Royal Society of London. Series B, Biological Sciences*, 353(1373), 1295–306. <http://doi.org/10.1098/rstb.1998.0284>
- Tsotsos, J. K. (2011). *A computational perspective on visual attention*. MIT Press.
- Tsotsos, J. K., Itti, L., & Rees, G. (2005). A brief and selective history of attention. *Neurobiology of attention*.
- Turetsky, B. I., Kohler, C. G., Indersmitten, T., Bhati, M. T., Charbonnier, D., & Gur, R. C. (2007). Facial emotion recognition in schizophrenia: when and why does it go awry? *Schizophrenia Research*, 94(1–

- 3), 253–63. <http://doi.org/10.1016/j.schres.2007.05.001>
- Uhlhaas, P. J., Linden, D. E. J., Singer, W., Haenschel, C., Lindner, M., Maurer, K., & Rodriguez, E. (2006). Dysfunctional Long – Range Coordination of Neural Activity during Gestalt Perception in Schizophrenia. *Journal of Neuroscience*, 26(31), 8168–8175. <http://doi.org/10.1523/JNEUROSCI.2002-06.2006>
- Ullman, S. (1995). Sequence seeking and counter – streams: a model for information flow in the visual cortex. *Cerebral Cortex*, 5(1), 1–11. <http://cercor.oxfordjournals.org/content/5/1/1.long>
- van der Stelt, O., Frye, J., Lieberman, J. A., Belger, A. (2004). Impaired P3 Generation Reflects High-level and Progressive Neurocognitive Dysfunction in Schizophrenia. *Archives of General Psychiatry*, 61(3), 237. <http://doi.org/10.1001/archpsyc.61.3.237>
- Verleger, R. (1988). Event-related potentials and cognition: A critique of the context updating hypothesis and an alternative interpretation of P3. *Behavioral and Brain Sciences*, 11(3), 343. <http://doi.org/10.1017/S0140525X00058015>
- Verleger, R. (1997). On the utility of P3 latency as an index of mental chronometry. *Psychophysiology*, 34(2), 131–156. <http://doi.org/10.1111/j.1469-8986.1997.tb02125.x>
- Vidyasagar, T. R., Kulikowski, J. J., Lipnicki, D. M., & Dreher, B. (2002). Convergence of parvocellular and magnocellular information channels in the primary visual cortex of the macaque, 16(i). <http://doi.org/10.1046/j.1460-9568.2002.02137.x>
- Vogel, E. K., & Luck, S. J. (2000). The visual N1 component as an index of a discrimination process. *Psychophysiology*, 37(2), 190–203. <http://doi.org/10.1111/1469-8986.3720190>
- Vogel, E. K., & Machizawa, M. G. (2004). Neural activity predicts individual differences in visual working memory capacity. *Nature*, 428(6984), 748–751. <http://doi.org/10.1038/nature02447>
- Vogel, E. K., McCollough, A. W., & Machizawa, M. G. (2005). Neural measures reveal individual differences in controlling access to working memory. *Nature*, 438(November). <http://doi.org/10.1038/nature04171>
- Vogels, R., & Orban, G. A. (1986). Decision processes in visual discrimination of line orientation. *Journal of Experimental Psychology. Human Perception and Performance*, 12(2), 115–32. <http://www.ncbi.nlm.nih.gov/pubmed/2940317>
- Watson, A. B., Luck, S. J., MacLeod, D. I. A., Alvarez, G. A., Freeman, R. D., Dolan, R. J. ., & Bestmann, S. (2017). QUEST+: A general multidimensional Bayesian adaptive psychometric method. *Journal of Vision*, 17(3), 10. <http://doi.org/10.1167/17.3.10>
- Watson, A. B., & Pelli, D. G. (1979). The QUEST staircase procedure. *Applied Vision Assoc. Newsletter*, 14, 6–7. Walsh, J. W. T. *Photometry* (3rd edition). London, UK: Constable & Co. Ltd. (1958).
- Watson, A. B., & Pelli, D. G. (1983). Quest: A Bayesian adaptive psychometric method. *Perception & Psychophysics*, 33(2), 113–120. <http://doi.org/10.3758/BF03202828>
- Weber, E. H. (1834). De Tactu [Concerning touch]. In De Pulsu, Resorptione, Auditu, et Tactu. *Annotationes Anatomicae et Physiologicae* [Concerning pulse, respiration, hearing, and touch: Anatomical and physiological notes] (pp. 44–174). Leipzig, Germany: C. F. Koehler.
- Weber, E. H. (1905). Tastsinn und gemeingefühl (No. 149). W. Engelmann.
- Wechsler, D. *The Wechsler Intelligence Scale for Children*. The Psychological Corporation, San Antonio, TX (1949).
- Wechsler D. (1991). *The Wechsler Intelligence Scale for Children—Third Edition (WISC – III)*. The Psychological Corporation, San Antonio, TX (1991)
- Wechsler D. (1997). *WMS – III Administration and Scoring Manual*. San Antonio, TX: The Psychological Corporation. Harcourt Brace & Co.
- Westheimer, G. (1998). Lines and Gabor functions compared as spatial visual stimuli. *Vision Research*, 38(4), 487–91. <http://www.ncbi.nlm.nih.gov/pubmed/9536372>
- Westland, S., Ripamonti, C. & Cheung, V. *Computational colour science using MatLab* (second edition). Wiley. ISBN: 978 – 0 – 470 – 66569 – 5. (2012).
- Whitman, J. C., Ward, L. M., & Woodward, T. S. (2013). Patterns of Cortical Oscillations Organize Neural Activity into Whole – Brain Functional Networks Evident in the fMRI BOLD Signal. *Frontiers in Human Neuroscience*, 7, 80. <http://doi.org/10.3389/fnhum.2013.00080>
- Wilson, H. R., & Gelb, D. J. (1984). Modified line – element theory for spatial – frequency and width

- discrimination. *Journal of the Optical Society of America A*, 1(1), 124. <http://doi.org/10.1364/JOSAA.1.000124>
- Woodman, G. F., & Vogel, E. K. (2005). Fractionating working memory: consolidation and maintenance are independent processes. *Psychological Science*, 16(2), 106–13. <http://doi.org/10.1111/j.0956-7976.2005.00790.x>
- Woods, D. L., Kishiyama, M. M., Lund, E. W., Herron, T. J., Edwards, B., Poliva, O., ... Reed, B. (2011). Improving digit span assessment of short-term verbal memory. *Journal of Clinical and Experimental Neuropsychology*, 33(1), 101–11. <http://doi.org/10.1080/13803395.2010.493149>
- Wright, W. D. (2007). Professor Wright's Paper from the Golden Jubilee Book: The historical and experimental background to the 1931 CIE system of colorimetry. *Colorimetry: Understanding the CIE System*, 9–23. Wright, W. D. (1928). A trichromatic colorimeter with spectral primaries. *Transactions of the Optical Society*, 29(5), 225–242. <http://doi.org/10.1088/1475-4878/29/5/302>
- Wright, W. D. (1929). A re-determination of the trichromatic coefficients of the spectral colours. *Transactions of the Optical Society*, 30(4), 141–164. <http://doi.org/10.1088/1475-4878/30/4/301>
- Wuerger, S. M., Ruppertsberg, A., Malek, S., Bertmini, M., & Martinovic, J. (2011). The integration of local chromatic motion signals is sensitive to contrast polarity. *Visual Neuroscience*, 28(3), 239–246. <http://doi.org/10.1017/S0952523811000058>
- Wyatte, D., Jilk, D. J., & O'Reilly, R. C. (2014). Early recurrent feedback facilitates visual object recognition under challenging conditions. *Frontiers in Psychology*, 5(July), 674. <http://doi.org/10.3389/fpsyg.2014.00674>
- Wyszecki G. Stiles W. S. (2000). *Color science: Concepts and methods, quantitative data and formulae* (2nd ed.). New York: John Wiley & Sons.
- Xing, Y., Ledgeway, T., McGraw, P. V., & Schluppeck, D. (2013). Decoding working memory of stimulus contrast in early visual cortex. *J Neurosci*, 33(25), 10301–10311. <http://doi.org/10.1523/jneurosci.3754-12.2013>
- Yeap, S., Kelly, S. P., Sehatpour, P., Magno, E., Javitt, D. C., Garavan, H., ... SA, H. (2006). Early Visual Sensory Deficits as Endophenotypes for Schizophrenia. *Archives of General Psychiatry*, 63(11), 1180. <http://doi.org/10.1001/archpsyc.63.11.1180>
- Yin, J., Gao, Z., Jin, X., Ding, X., Liang, J., & Shen, M. (2012). The neural mechanisms of percept–memory comparison in visual working memory. *Biological Psychology*, 90(1), 71–79. <http://doi.org/10.1016/j.biopsycho.2012.02.023>
- Yoon, J. H., Sheremata, S. L., Rokem, A., & Silver, M. A. (2013). Windows to the soul: vision science as a tool for studying biological mechanisms of information processing deficits in schizophrenia. *Frontiers in Psychology*, 4, 681. <http://doi.org/10.3389/fpsyg.2013.00681>
- Young, T. (1807). *Lectures on Natural Philosophy*. London: Johnson, Vol. II.
- Zanto, T. P., & Gazzaley, A. (2009). Neural suppression of irrelevant information underlies optimal working memory performance. *The Journal of Neuroscience: The Official Journal of the Society for Neuroscience*, 29(10), 3059–66. <http://doi.org/10.1523/JNEUROSCI.4621-08.2009>
- Zanto, T. P., Rubens, M. T., Thangavel, A., & Gazzaley, A. (2011). Causal role of the prefrontal cortex in top-down modulation of visual processing and working memory. *Nature Neuroscience*, 14(5), 656–61. <http://doi.org/10.1038/nn.2773>
- Zimmer, H. D. (2008). Visual and spatial working memory: from boxes to networks. *Neuroscience and Biobehavioral Reviews*, 32(8), 1373–95. <http://doi.org/10.1016/j.neubiorev.2008.05.016>

